VU Research Portal

Radiotherapy and esophageal cancer; towards novel and improved combination treatments

Goedegebuure, Ruben Sije Adriaan

2022

document version
Publisher's PDF, also known as Version of record

Link to publication in VU Research Portal

citation for published version (APA)
Goedegebuure, R. S. A. (2022). *Radiotherapy and esophageal cancer; towards novel and improved combination treatments*. s.n.

RADIOTHERAPY AND ESOPHAGEAL CANCER;

TOWARDS NOVEL AND IMPROVED COMBINATION TREATMENTS

Ruben Goedegebuure

VRIJE UNIVERSITEIT

RADIOTHERAPY AND ESOPHAGEAL CANCER; TOWARDS NOVEL AND IMPROVED COMBINATION TREATMENTS.

ACADEMISCH PROEFSCHRIFT

ter verkrijging van de graad Doctor aan
de Vrije Universiteit Amsterdam,
op gezag van de rector magnificus
prof.dr. J.J.G. Geurts,
in het openbaar te verdedigen
ten overstaan van de promotiecommissie
van de Faculteit der Geneeskunde
op dinsdag 1 november 2022 om 13.45 uur
in een bijeenkomst van de universiteit,
De Boelelaan 1105
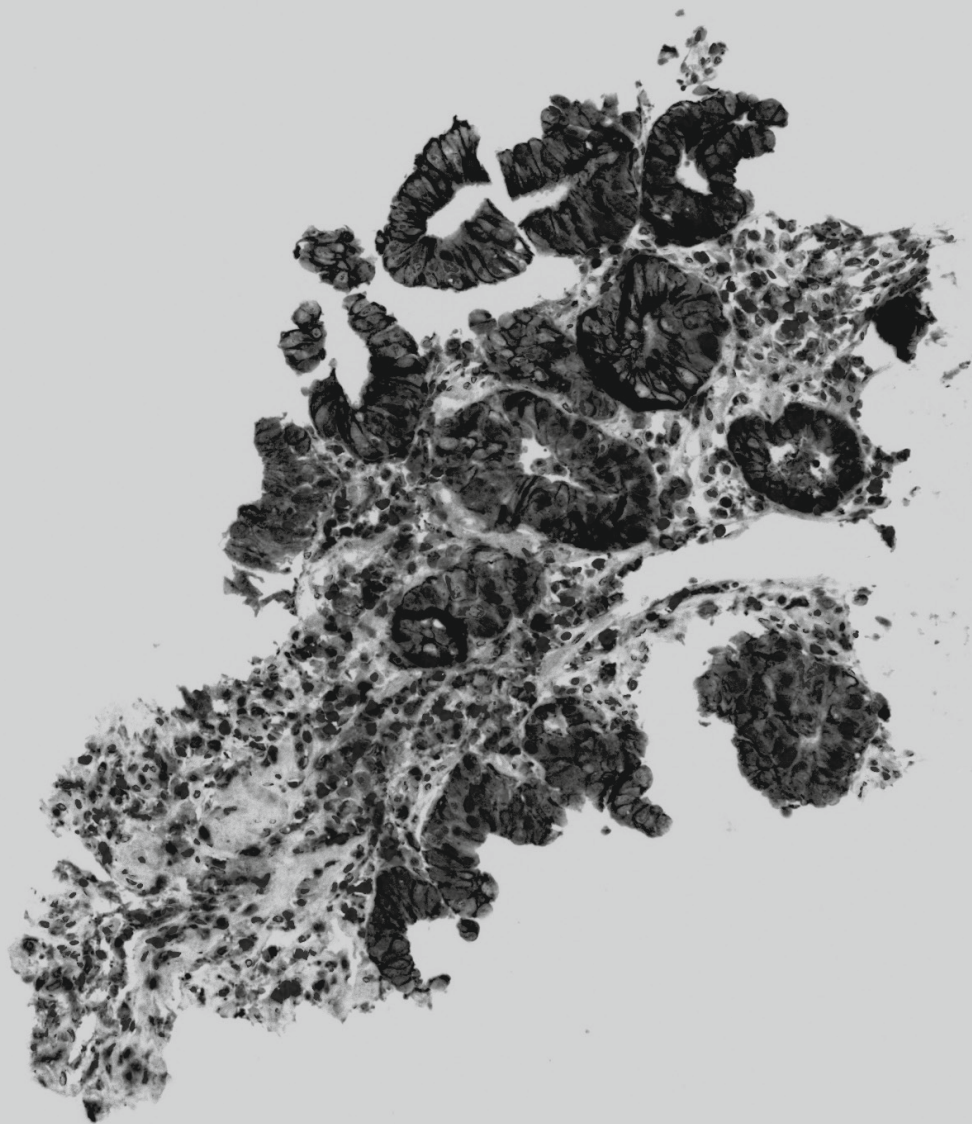
door

Ruben Sije Adriaan Goedegebuure

geboren te Leiden

TABLE OF CONTENTS

Chapter 1

Introduction and thesis outline

INTRODUCTION

Esophageal cancer (EC) is the seventh most common cancer and the sixth most common cause of cancer-associated death worldwide, with 544.000 deaths reported in 2020[1]. The prognosis is poor as diagnosis is often late owing to a lack of early easily identifiable symptoms and because systemic therapy effectiveness is limited[2]. Although the survival rate has tripled over the past 40 years, the 5-year survival of patients with localized disease, locally advanced disease and metastatic disease is only 47.1%, 25.2% and 4.9%, respectively[3].

Etiology, pathogenesis and histological subtypes
EC can be classified in two different histological subtypes, i.e., squamous cell carcinoma (ESCC) and adenocarcinoma (EAC), which have a quite distinct etiology and geographical distribution. ESCC accounts for 90% of all cases of EC globally and is highly prevalent in Asia, East Africa and South America. Heavy alcohol and tobacco use and their synergistic effects are the major risk factors for ESCC in the Western world[4]. In low-income countries suspected additional risk factors include betel quid chewing (on the Indian subcontinent) and drinking very hot mate (in Southern America). The incidence of ESCC is broadly declining in these regions and may have been preceded by economic gains, dietary improvements in certain high-risk areas in Asia and a decline in cigarette smoking. At the same time, incidence rates of EAC are rising rapidly, in part due to increasing gastroesophageal reflux disease (GERD) and obesity[5,6]. EAC also represents the majority of esophageal cancer cases in high-income countries, with advancing age and male sex as key risk factors, next to obesity and GERD. Currently, about two-thirds of patients with EAC are male and by 2030 one in every hundred men in the Netherlands and the United Kingdom is predicted to be diagnosed with EAC during their lifetime[5].

ESCC mostly affects the upper part of the esophagus. Squamous hyperplasia precedes low and high grade squamous dysplasia which then develops into invasive cancer[7]. EAC is normally located in the lower third of the esophagus and GE-junction and is often preceded by Barrett's esophagus (BE). BE is a well-recognized pre-malignant condition characterized by abnormal mucosal cell lining of the lower region of the esophagus[8]. Disrupted p53 signaling plays a central role in the progression of BE to invasive EAC[7]. Although the annual risk of progressing from BE to EAC is around 0.33% (depending on the dysplastic grade)[9], the relative risk of EAC in BE patients was found to be 11.3 (95% CI, 8.8 to 14.4)[10]. This is comparable to the risk of breast cancer in first-degree relatives of breast cancer patients with a BRCA1/BRCA2 mutation[11]. Endoscopic surveillance programs for BE are enrolled in most countries, but under constant discussion given the overall low incidence of neoplastic progression and lack of evidence that it prevents advanced cancer[8,12].

Treatment for gastro-esophageal cancer

Although chemotherapy with platinum and fluoropyrimidines (5-FU) remains the mainstay of first line treatment for metastasized EC[2], targeted therapy has been introduced as a therapeutic option for selected patients as well. For example, overexpression or amplification of HER2 occurs in around 10-15% all gastric and esophageal adenocarcinomas[13,14] and anti-HER2 directed therapy with trastuzumab improves overall survival (OS) from 11.1 to 13.8 months (HR: 0.74; 95% CI: 0.60–0.91; P = 0.0046)[14] when given in combination with first line chemotherapy. In addition, the monoclonal antibody ramucirumab, directed against Vascular Endothelial Growth Factor Receptor-2 (VEGFR-2), improves OS with 2.2 months (7.4 to 9.6 months) in combination with paclitaxel, as compared to paclitaxel alone (HR: 0.81; 95% CI: 0.68-0.96; P = 0.017) in second line treatment of gastric- and gastro-esophageal junction cancer (GC/GEJC)[15]. Despite these advancements, prognosis remains poor and novel treatments are urgently needed for EC patients with advanced disease.

In parallel to improving therapeutic strategies for patients with advanced and metastatic disease, it is important to maximize treatment success in early-stage disease and thereby prevent disease recurrence. In that regard, combination treatment with neoadjuvant chemotherapy or chemoradiotherapy followed by a surgical resection results a clear survival benefit compared to a surgical resection alone[16], and is currently the standard for patients with localized disease, i.e., stage II (T1N1M0 or T2N0M0) and III (T2N1M0 or T3-4aN0-1M0) esophageal cancer. Combinations of 5-fluorouracil, leucovorin and oxaliplatin (FOLFOX) and 5-fluorouracil and cisplatin have been used together with radiotherapy. The combination of paclitaxel (50 mg/m2), carboplatin (AUC 2 mg/ml/min) and concurrent radiotherapy (41.4 Gy in 23 fractions), followed by a surgical resection, significantly improves median OS of patients to 49.4 months compared to 24.0 months with surgery alone, as demonstrated by the Dutch CROSS trial[17,18].

ESCC has been shown to be more sensitive to neoadjuvant CRT than EAC; around 49% of ESCC patients have a complete histopathological response (Mandard tumor regression grade (TRG)[19] of 1) after CRT compared to only 23% of EAC patients[20]. Achieving a complete response is a strong predictor of long-term survival. Conversely, patients with a limited or absent response to neoadjuvant treatment have a comparable survival to patients that underwent a surgical tumor resection without neoadjuvant therapy[21]. Thus, patients with limited response to CRT may not benefit from standard neoadjuvant treatment and alternative neoadjuvant approaches or immediate surgical intervention might be considered. At the same time, if it would be possible to predict a complete histopathological response, consideration can be made to forgo surgery, especially in patients with substantial comorbidities or with tumors in locations where the morbidity of resection is greater. Given the reduced quality of life that people experience after surgery[22] this would be an attractive strategy.

Improving response to chemoradiotherapy

There have been multiple attempts to identify clinical-, histopathological- and molecular biomarkers to predict the response to neoadjuvant CRT in esophageal cancer[23,24]. Nonetheless, most studies have been performed in small cohorts focused on specific biomarkers and validated biomarkers are lacking. Irrespective of treatment, recent studies performed by The Cancer Genome Atlas (TCGA)[13] and the International Cancer Genome Consortium (ICGC)[25] identified large genomic heterogeneity within ECs and underlined that ESCC and EAC have profoundly distinct molecular characteristics, both in patterns of somatic mutations and in copy-number aberrations. ESCCs display similar molecular characteristics as head and neck squamous cell carcinoma (HNSCC), such as amplification of *CCND1*, *SOX2* of *TP63*, whereas EACs shows most resemblance with the gastric cancer chromosome instable (CIN) type. Both EC subtypes also differ significantly in DNA methylation patterns. While ESCCs have low DNA CpG island promoter methylation, EACs can be divided in distinct subtypes with a variable degree of CpG island promoter methylation[26]. Whether these molecular characteristics affect response to neoadjuvant CRT is currently unknown.

The efficacy of (chemo)radiotherapy might also be influenced by the composition of the pre-existing tumor immune microenvironment (TME)[27]. Especially the T cell status was found to be associated with the success or failure of radiotherapy[28]. Already over 30 years ago, it was established that tumor regression upon irradiation is impaired in the absence of a normal T cell repertoire[29]. More recently, it was shown in murine tumor models that intratumoral T cells can survive irradiation up to 20 Gy and show an improved effector function afterwards by mediating tumor growth control without the contribution of newly infiltrating T cells[30]. Transcriptomic analysis of these intratumoral T cells showed genetic reprogramming by the TME and a significant overlap with gene expression patterns of tissue-resident memory T cells, which are also radioresistant[30]. In addition, more immunosuppressive tumor-associated cell types such as Th2-skewed CD4+ T cells, regulatory T-cells, M2 macrophages and MDSCs can induce radiotherapy resistance by hampering CD8+ cytotoxic T cells which are crucial for an effective radiotherapy-induced antitumor immune response[31].

How these findings translate to the response to neoadjuvant CRT in EC patients is currently unknown. Yet, it has been demonstrated that EACs are mostly immune cell excluded, although some degree of T cell infiltration has been identified[32]. EACs typically develop within a chronically inflamed and immunosuppressive TME, caused by chronic gastric acid-mediated irritation. This environment is characterized by PD-L2 expressing tumor cells, PD-L1 expressing immune cells, Th2-skewing, and the presence of tumor-promoting M2 macrophages and MDSCs[33,34]. Such an immunosuppressive environment may hamper chemoradiotherapy efficacy and consequently, additional immunomodulatory strategies may be called for to improve treatment outcome.

1

In the last decades it has become recognized that radiotherapy also influences the local anti-tumor immune response via several mechanisms[35], e.g., enhanced T cell priming through immunogenic cell death and sensitization of cancer cells to T cell killing by upregulation of Fas and MHC-I. Furthermore, increased expression of adhesion molecules on endothelial cells in irradiated tumor tissue results in enhanced immune cell trafficking into the tumor[36]. These findings present a rationale to combine radiotherapy with immunotherapy and perhaps also anti-angiogenic therapy. Deciphering additional molecular, immunological and vascular responses occurring during radiotherapy is key to further improve (chemo)radiotherapy efficacy.

In conclusion, esophageal cancer is a deadly disease with a fast-rising incidence of especially adenocarcinoma in the Western world. A better understanding of the molecular and immunological factors influencing the response to neoadjuvant CRT is important to improve the treatment outcome and to develop patient-tailored treatment strategies. Moreover, insights into the effects of radiotherapy on the tumor microenvironment and the effect of the immune microenvironment on the response to chemoradiotherapy can provide further guidance to optimize treatment strategies and to develop novel combination therapies.

THESIS OUTLINE

The overarching goal of this thesis is to gain insights in biological processes that influence the treatment outcome of patients with localized esophageal cancer. The first aim (**part I**) is to identify molecular and immunological mediators of the response to neoadjuvant chemoradiotherapy (CRT) in EC. Therefore, in **chapter 2** the molecular profiles in tumors of EC patients are studied in relation to the response to neoadjuvant CRT. In addition, in **chapter 3** the tumor immune microenvironment of EAC patients is characterized and linked to treatment outcome. The second aim (**part II**) is to elucidate the molecular and immunological responses occurring upon fractionated radiotherapy that might be exploited for novel treatment strategies, with a focus on immunological and vascular responses. In **chapter 4** the biological principles and outstanding questions for combining radiotherapy with either anti-angiogenic therapy, immunotherapy or both, are discussed based on recent literature. To further improve radiotherapy efficacy, in **chapter 5** the molecular responses in tumor cells upon fractionated radiotherapy are investigated *in vitro*, *in vivo* and in esophageal cancer patients. In **chapter 6** the historical efforts on combining radiotherapy with a specific type of immunotherapy, i.e., interferon alpha or -beta treatment, are reviewed. In **chapter 7** the results of a phase I clinical trial evaluating the safety and efficacy of a novel anti-angiogenic vaccine hVEGF26-104/RFASE are presented. Finally, **chapter 8** summarizes and links key results of both parts of this thesis in the context of recent literature and discusses the implications for future research.

REFERENCES

1. Sung H, Ferlay J, Siegel RL, et al. Global cancer statistics 2020: GLOBOCAN estimates of incidence and mortality worldwide for 36 cancers in 185 countries. *CA Cancer J Clin*. 2021;0(0):caac.21660. doi:10.3322/caac.21660

2. Cunningham D, Starling N, Rao S, et al. Capecitabine and Oxaliplatin for Advanced Esophagogastric Cancer. *N Engl J Med*. 2008;358(1):36-46. doi:10.1056/NEJMoa073149

3. Howlader N, Noone AM, Krapcho M, Miller D, Brest A, Yu M, Ruhl J, Tatalovich Z, Mariotto A, Lewis DR, Chen HS, Feuer EJ CK (eds). SEER Cancer Statistics Review, 1975-2017. *https://seer.cancer.gov/csr/1975_2017*. 2020.

4. Bray F, Ferlay J, Soerjomataram I, Siegel RL, Torre LA, Jemal A. Global cancer statistics 2018: GLOBOCAN estimates of incidence and mortality worldwide for 36 cancers in 185 countries. *CA Cancer J Clin*. 2018;68(6):394-424. doi:10.3322/caac.21492

5. Arnold M, Laversanne M, Brown LM, Devesa SS, Bray F. Predicting the Future Burden of Esophageal Cancer by Histological Subtype: International Trends in Incidence up to 2030. *Am J Gastroenterol*. 2017;112(8):1247-1255. doi:10.1038/ajg.2017.155

6. Rubenstein JH, Shaheen NJ. Epidemiology, Diagnosis, and Management of Esophageal Adenocarcinoma. *Gastroenterology*. 2015;149(2):302-317.e1. doi:10.1053/J.GASTRO.2015.04.053

7. Smyth EC, Lagergren J, Fitzgerald RC, et al. Oesophageal cancer. *Nat Rev Dis Prim*. 2017;3(1):17048. doi:10.1038/nrdp.2017.48

8. Jankowski J, Franklin J. Recent advances in understanding and preventing oesophageal cancer. *F1000Research*. 2020;9:1-9. doi:10.12688/f1000research.21971.1

9. Shaheen NJ, Falk GW, Iyer PG, Gerson LB. ACG Clinical Guideline: Diagnosis and Management of Barrett's Esophagus. *Am J Gastroenterol*. 2016;111(1):30-50; quiz 51. doi:10.1038/ajg.2015.322

10. Hvid-Jensen F, Pedersen L, Drewes AM, Sørensen HT, Funch-Jensen P. Incidence of adenocarcinoma among patients with Barrett's esophagus. *N Engl J Med*. 2011;365(15):1375-1383. doi:10.1056/NEJMoa1103042

11. Rebbeck TR, Domchek SM. Variation in breast cancer risk in BRCA1 and BRCA2 mutation carriers. *Breast Cancer Res*. 2008;10(4):108. doi:10.1186/bcr2115

12. Kastelein F, van Olphen SH, Steyerberg EW, Spaander MCW, Bruno MJ. Impact of surveillance for Barrett's oesophagus on tumour stage and survival of patients with neoplastic progression. *Gut*. 2016;65(4):548-554. doi:10.1136/gutjnl-2014-308802

13. Kim JJ, Bowlby R, Mungall AJ, et al. Integrated genomic characterization of oesophageal carcinoma. *Nature*. 2017;541(7636):169-174. doi:10.1038/nature20805

14. Bang Y-J, Van Cutsem E, Feyereislova A, et al. Trastuzumab in combination with chemotherapy versus chemotherapy alone for treatment of HER2-positive advanced gastric or gastro-oesophageal junction cancer (ToGA): a phase 3, open-label, randomised controlled trial. *Lancet*. 2010;376(9742):687-697. doi:10.1016/S0140-6736(10)61121-X

15. Wilke H, Muro K, Van Cutsem E, et al. Ramucirumab plus paclitaxel versus placebo plus paclitaxel in patients with previously treated advanced gastric or gastro-oesophageal junction adenocarcinoma (RAINBOW): a double-blind, randomised phase 3 trial. *Lancet Oncol*. 2014;15(11):1224-1235. doi:10.1016/S1470-2045(14)70420-6

16. Sjoquist KM, Burmeister BH, Smithers BM, et al. Survival after neoadjuvant chemotherapy or chemoradiotherapy for resectable oesophageal carcinoma: An updated meta-analysis. *Lancet Oncol*. 2011;12(7):681-692. doi:10.1016/S1470-2045(11)70142-5

17. van Hagen P, Hulshof MCCMC, van Lanschot JJBJ, et al. Preoperative chemoradiotherapy for esophageal or junctional cancer. *N Engl J Med*. 2012;366(22):2074-2084. doi:10.1056/NEJMoa1112088

18. Shapiro J, van Lanschot JJB, Hulshof MCCM, et al. Neoadjuvant chemoradiotherapy plus surgery versus surgery alone for oesophageal or junctional cancer (CROSS): long-term results of a randomised controlled trial. *Lancet Oncol*. 2015;16(9):1090-1098. doi:10.1016/S1470-2045(15)00040-6

19. Mandard AM, Dalibard F, Mandard JC, et al. Pathologic assessment of tumor regression after preoperative chemoradiotherapy of esophageal carcinoma. Clinicopathologic correlations. *Cancer*. 1994;73(11):2680-2686. doi:10.1002/1097-0142(19940601)73:11<2680::aid-cncr2820731105>3.0.co;2-c

20. Oppedijk V, Van Der Gaast A, Van Lanschot JJB, et al. Patterns of recurrence after surgery alone versus preoperative chemoradiotherapy and surgery in the CROSS trials. *J Clin Oncol*. 2014;32(5):385-391. doi:10.1200/JCO.2013.51.2186

21. den Bakker CM, Smit JK, Bruynzeel AME, et al. Non responders to neoadjuvant chemoradiation for esophageal cancer: Why better prediction is necessary. *J Thorac Dis*. 2017;9(Suppl 8):S843-S850. doi:10.21037/jtd.2017.06.123

22. Jacobs M, Macefield RC, Elbers RG, et al. Meta-analysis shows clinically relevant and long-lasting deterioration in health-related quality of life after esophageal cancer surgery. *Qual Life Res*. 2014;23(4):1155-1176. doi:10.1007/s11136-013-0576-5

23. Tao C-J, Lin G, Xu Y-P, Mao W-M. Predicting the Response of Neoadjuvant Therapy for Patients with Esophageal Carcinoma: an In-depth Literature Review. *J Cancer*. 2015;6(11):1179-1186. doi:10.7150/jca.12346

24. Hoefnagel SJM, Boonstra JJ, Russchen MJAM, Krishnadath KK. Towards Personalized Treatment Strategies for Esophageal Adenocarcinoma; A Review on the Molecular Characterization of Esophageal Adenocarcinoma and Current Research Efforts on Individualized Curative Treatment Regimens. *Cancers 2021, Vol 13, Page 4881*. 2021;13(19):4881. doi:10.3390/CANCERS13194881

25. Frankell AM, Jammula S, Li X, et al. The landscape of selection in 551 esophageal adenocarcinomas defines genomic biomarkers for the clinic. *Nat Genet*. 2019;51(3):506-516. doi:10.1038/s41588-018-0331-5

26. Jammula S, Katz-Summercorn AC, Li X, et al. Identification of Subtypes of Barrett's Esophagus and Esophageal Adenocarcinoma Based on DNA Methylation Profiles and Integration of Transcriptome and Genome Data. *Gastroenterology*. February 2020. doi:10.1053/j.gastro.2020.01.044

27. Formenti SC, Demaria S. Combining radiotherapy and cancer immunotherapy: A paradigm shift. *J Natl Cancer Inst*. 2013;105(4):256-265. doi:10.1093/jnci/djs629

28. Demaria S, Formenti SC. Role of T lymphocytes in tumor response to radiotherapy. *Front Oncol*. 2012;2. doi:10.3389/FONC.2012.00095

29. Slone HB, Peters LJ, Milas L. Effect of host immune capability on radiocurability and subsequent transplantability of a murine fibrosarcoma. *J Natl Cancer Inst*. 1979;63(5):1229-1235. doi:10.1093/jnci/63.5.1229

30. Arina A, Beckett M, Fernandez C, et al. Tumor-reprogrammed resident T cells resist radiation to control tumors. *Nat Commun*. 2019;10(1). doi:10.1038/s41467-019-11906-2

31. Shiao SL, Ruffell B, DeNardo DG, Faddegon BA, Park CC, Coussens LM. TH2-Polarized CD4+ T Cells and Macrophages Limit Efficacy of Radiotherapy. *Cancer Immunol Res*. 2015;3(5):518-525. doi:10.1158/2326-6066.CIR-14-0232

32. Derks S, de Klerk LK, Xu X, et al. Characterizing diversity in the tumor-immune microenvironment of distinct subclasses of gastroesophageal adenocarcinomas. *Ann Oncol Off J Eur Soc Med Oncol*. 2020;31(8):1011-1020. doi:10.1016/j.annonc.2020.04.011

33. Derks S, Nason KS, Liao X, et al. Epithelial PD-L2 expression marks Barrett's Esophagus and Esophageal Adenocarcinoma. *Cancer Immunol Res*. 2015:1123-1130. doi:10.1158/2326-6066.CIR-15-0046

34. Gao J, Wu Y, Su Z, et al. Infiltration of alternatively activated macrophages in cancer tissue is associated with MDSC and Th2 polarization in patients with esophageal cancer. *PLoS One*. 2014;9(8). doi:10.1371/journal.pone.0104453

35. Spiotto M, Fu Y-X, Weichselbaum RR. The intersection of radiotherapy and immunotherapy: Mechanisms and clinical implications. *Sci Immunol*. 2016;1(3):eaag1266 LP-eaag1266. doi:10.1126/sciimmunol.aag1266

36. Baluna RG, Eng TY, Thomas CR. Adhesion molecules in radiotherapy. *Radiat Res*. 2006;166(6):819-831. doi:10.1667/RR0380.1
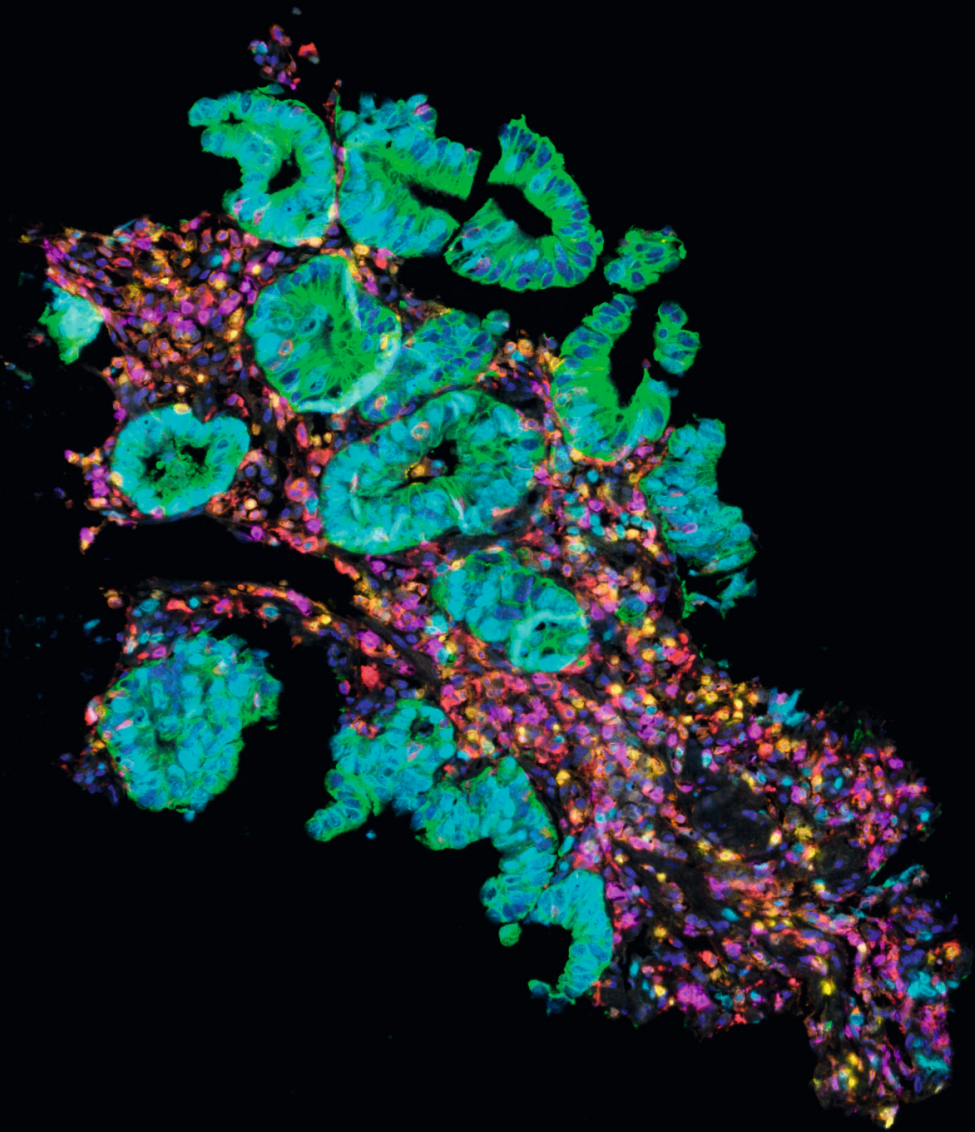
1

PART I

Identifying molecular and immunological mediators of response to neoadjuvant chemoradiotherapy in esophageal cancer

Chapter 2

Molecular profiles of response to neoadjuvant chemoradiotherapy in esophageal cancers to develop personalized treatment strategies

Leonie K. de Klerk*, Ruben S. A. Goedegebuure*, Nicole C. T. van Grieken, Johanna W. van Sandick, Annemieke Cats, Jurrien Stiekema, Rosa T. van der Kaaij, Arantza Farina Sarasqueta, Manon van Engeland, Maarten A. J. M. Jacobs, Roy L. J. van Wanrooij, Donald L. van der Peet, Aaron R. Thorner, Henk M. W. Verheul, Victor L. J. L. Thijssen, Adam J. Bass[†] and Sarah Derks[†]

*[/][†] authors contributed equally to this article

ABSTRACT

Identification of molecular predictive markers of response to neoadjuvant chemoradiation could aid clinical decision-making in patients with localized esophageal cancer. Therefore, we subjected pre-treatment biopsies of 75 adenocarcinoma (EAC) and 16 squamous cell carcinoma (ESCC) patients to targeted next-generation DNA sequencing, as well as biopsies of 85 EAC and 20 ESCC patients to promoter methylation analysis of 8 GI-specific genes, and followingly searched for associations with histopathological response and disease-free (DFS) and overall survival (OS). Thereby we found that in EAC, *CSMD1* deletion (8%) and *ETV4* amplification (5%) were associated with a favorable histopathological response, whereas *SMURF1* amplification (5%) and *SMARCA4* mutation (7%) were associated with an unfavorable histopathological response. *KRAS* (15%) and *GATA4* (7%) amplification were associated with shorter OS. In ESCC, *TP63* amplification (25%) and *TFPI2* (10%) gene methylation were associated with an unfavorable histopathological response and shorter DFS (*TP63*) and OS (*TFPI2*), whereas *CDKN2A* deletion (38%) was associated with prolonged OS. In conclusion, this study identified candidate genetic biomarkers associated with response to neoadjuvant chemoradiotherapy in patients with localized esophageal cancer.
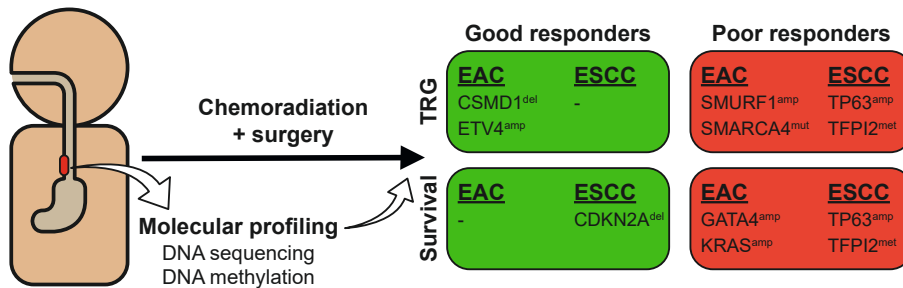
1. INTRODUCTION

Esophageal cancer (EC) is the eighth most common cancer and one of the leading causes of cancer-related death[1]. Five-year survival rates are low, mainly because of late-stage diagnosis and limited effectiveness of systemic therapy[2]. In parallel to developing better therapy for those with more advanced disease, it is important to maximize treatment success in early-stage disease and thereby prevent disease recurrence. When EC is confined to the esophagus and regional lymph nodes, treatment is with curative intent. In case of stage II (T1N1M0 or T2N0M0) and III (T2N1M0 or T3-4aN0-1M0) disease, neoadjuvant chemoradiotherapy (CRT) with paclitaxel (50 mg/m^2), carboplatin (AUC 2 mg/ml/min) and concurrent radiotherapy (41.4 Gy in 23 fractions) followed by a surgical resection is a commonly used treatment regimen that improves median overall survival of patients to 49.4 months compared to 24.0 months with surgery alone[3].

EC is classified in two different histological subtypes, squamous cell carcinoma (ESCC) and adenocarcinoma (EAC). ESCC has been shown to be more sensitive to neoadjuvant CRT than EAC; around 49% of ESCC patients have a complete histopathological response (Mandard tumor regression grade (TRG)[4] of 1) compared to only 23% of EAC patients[5]. A complete histopathological response to neoadjuvant treatment is a strong predictor of long-term survival. Conversely, patients with a limited or absent histopathological response have a comparable survival to patients that underwent a surgical tumor resection without neoadjuvant therapy[6]. As these patients may not benefit from standard neoadjuvant treatment, they may be better treated with alternative neoadjuvant approaches or, alternatively, considered for immediate surgical intervention. At the same time, if it would be possible to predict a complete histopathological response, consideration can be made to forgo surgery, especially in patients with substantial comorbidities or with tumors in locations where the morbidity of resection is higher.

There have been multiple attempts to identify clinical-, histopathological- and molecular biomarkers for response to neoadjuvant treatment in EC[7], but most studies have been performed in small cohorts and in a focused manner. Irrespective of treatment, recent studies performed by The Cancer Genome Atlas[8] and the International Cancer Genome Consortium[9] identified large genomic heterogeneity within ECs and underlined that ESCC and EAC have profoundly distinct molecular characteristics, both in patterns of somatic mutations and in copy-number aberrations. ESCC and EAC also differ significantly in DNA methylation patterns[8]. While ESCCs have low frequent DNA CpG island promoter methylation, EACs can be divided in distinct subtypes with a variable degree of CpG island promoter methylation[10]. Whether these molecular characteristics affect response to CRT in EAC is currently unknown.

2

This study aimed to evaluate whether common molecular characteristics are associated with response to neoadjuvant chemoradiotherapy and subsequent survival in EC patients. Thereby we explore the potential of molecular profiling to complement other clinical and histopathological factors to inform treatment strategies for localized esophageal cancer.

2. MATERIALS AND METHODS

2.1 Patient population
Clinical data and pre-treatment tissue from 131 patients with stage II-III esophageal cancer was retrospectively collected from three hospitals (VU University Medical Center, Netherlands Cancer Institute/Antoni van Leeuwenhoek Hospital and Leiden University Medical Center). The study methodology was approved by the ethical committees of all three hospitals and in accordance with the Declaration of Helsinki. Selected patients had been treated with neoadjuvant chemoradiotherapy consisting of paclitaxel (50 mg/m^2), carboplatin (AUC 2 mg/ml/min) and concurrent radiotherapy (41.4 Gy in 23 fractions) followed by surgical resection. Data on histopathological response, as well as on clinical follow-up was documented.

Histopathological response was assessed by pathologists at Amsterdam UMC (NvG and AFS). Both the ypTNM stage (7th edition), as well as the Tumor Regression Grade (TRG) according to Mandard[4] were scored. Mandard's TRG consists of 5 tiers, which are TRG1 (no residual cancer), TRG2 (rare residual cancer cells), TRG3 (fibrosis outgrowing residual cancer), TRG4 (residual cancer outgrowing fibrosis), and TRG5 (absence of regressive changes). In addition, we calculated the histopathologic prognostic score (PRSC)[11], which is based on ypT stage (ypT0-2 = 1 pt, ypT3-4 = 2 pts), ypN stage (ypN0 = 1 pt, ypN1-3 = 2 pts), and residual tumor per tumor bed (≤ 50% = 1 pt, > 50% = 2 pts), and then divided into three groups (group A: 3 pts total, B: 4-5 pts, C: 6 pts). For the 50% cut-off for residual tumor per tumor bed, a Mandard TRG up to 3 ('fibrosis outgrowing residual cancer') was considered lower than 50%, and a Mandard TRG of 4 ('residual cancer outgrowing fibrosis') or higher was considered higher than 50%.

Clinical response was expressed as overall survival (OS) and disease-free survival (DFS). Survival was defined as time from the date of surgery to death from any cause for OS, and to disease recurrence for DFS. Recurrence was evaluated during standard follow-up post treatment at the surgery department. Recurrent disease was defined as locoregional recurrence or distant metastasis ascertained by radiological or histopathological evaluation. Patients lost to follow-up were censored at the time of their last contact with the outpatient clinic. Median follow-up time was 3.7 years (3.7 years for EAC, 4.7 years for ESCC).

2.2 DNA extraction

Formalin-fixed paraffin-embedded (FFPE) tissue slides were obtained from all patients. An expert pathologist (NvG) reviewed H&E-stained sections in order to confirm the diagnosis and to ensure >50% tumor content in areas for genomic DNA extraction; if necessary macro-dissection was performed. From 30 tumors DNA from adjacent normal esophageal epithelium was also extracted.

Genomic DNA was extracted from tissue sections using the DNeasy FFPE Tissue Kit (Qiagen, Germantown, MD, USA) according to the manufacturer's instructions with a modification of an overnight incubation with proteinase K. Genomic DNA was eluted into 40 μL total volume and quantified with Quant-iT PicoGreen DNA assay kit (Invitrogen, Carlsbad, CA, USA) following the manufacturers' instructions.

2.3 Targeted Sequencing

A total of 200ng of DNA per sample was fragmented (Covaris sonication, Covaris, Woburn, MA, USA) to 250 bp and purified using Agentcourt AMPure XP beads (Beckman Coulter, Brea, CA, USA). Size distribution after fragmentation was checked using the Agilent 2200 TapeStation system (Agilent Technologies, Santa Clara, CA, USA). To determine the amount of each library to add for sequencing, all libraries were then pooled and low-depth sequencing was performed on an Illumina MiSeq Nano flow cell (Illumina, San Diego, CA, USA). Concentrations were normalized for analysis based on the number of reads of each adapter barcode. Normalized libraries were again pooled in batches ranging from 12-15 samples and enriched for the exonic regions of 243 GI-specific target (as previously described[12]) using the Agilent SureSelect Hybrid Capture kit (Agilent, Santa Clara, CA, USA). Samples were combined and pooled to a lane equivalent of 32 samples per lane (HiSeq 2500 Rapid Run Mode) for each sequencing pool.

Mutation analysis for single nucleotide variants (SNV) was performed using MuTect v1.1.4 in paired mode using CEPH as a project normal, or the matched normal where appropriate, and annotated by Oncotator[13,14]. We used the SomaticIndelDetector tool that is part of the GATK for indel calling. Only commonly reported (COSMIC ≥ 3 times), and clear loss-of-function mutations were used for analysis.

Copy number variants were called using the tool ReCapSeg v1.4.4, which is in development by the Cancer Group at the Broad Institute (http://gatkforums. broadinstitute.org/categories/cancer-tools). Within the (+) calls a gene was considered amplified if it had a $\log_2$ ratio of greater than 2. For loss calls, a gene was considered to have a two-copy deletion if the $\log_2$ ratio was less than -0.7.

2.4 Methylation-specific polymerase chain reaction
The methylation status of the CpG island in the promoter region of a GI cancer relevant panel (*CHFR, RASSF1, NDRG4, CDKN2A, MLH1, TFPI2, MGMT, and RUNX3*) was determined by a two-step nested methylation-specific polymerase chain reaction (MSP), as described in detail previously[15]. DNA from normal peripheral lymphocytes from healthy individuals and in vitro methylated DNA were included as negative and positive controls.

The methylation index was calculated by dividing the number of methylated gene promoters (ranging from 0 to 8) by the number of successfully tested gene promoters (usually 8).

2.5 Statistical analysis
Associations between (epi)genetic events and dichotomized Mandard TRG (TRG1-3 vs 4-5), ypN stage (ypN0 vs ypN1-3), and clinical N stage (0 vs 1-3), and associations between histology and baseline characteristics such as gender and completeness of resection were tested with a Fisher's Exact test, or, if assumptions were met, a Pearson Chi-Squared test (indicated in tables). Associations between (epi)genetic events and TRG, PRSC, and clinical N stage, clinical T stage, and between histology and clinical T stage, clinical N stage, ypT stage, ypN stage, TRG and PRSC, and between Mandard TRG and PRSC, were analyzed with a linear-by-linear exact test. To test associations between methylation index dichotomized Mandard TRG (TRG1-3 vs 4-5), ypN stage (ypN0 vs ypN1-3), clinical N stage (0 vs 1-3), and histology, a Wilcoxon rank-sum test was used, and between methylation index and TRG, PRSC, clinical N stage, and ypN stage, a Kruskal-Wallis test. Survival differences between binary predictor variables were analyzed with a log-rank test, and Hazard Ratio's (HR) calculated with univariate Cox regression analysis. Median follow-up time was calculated using the reverse Kaplan Meier approach[16]. The forced entry method was used for both the logistic and Cox multiple regression analyses. *P*-values (two sided) < 0.05 were considered statistically significant. Multiple comparison correction was performed using the two-stage linear step-up procedure of Benjamini, Krieger and Yekutieli, with an FDR (Q) of 5%, using GraphPad Prism (version 8). All other statistical analyses were performed with SPSS version 25 (IBM). Kaplan-Meier survival plots were generated with the survminer package in R (version 1.1.453).

3. RESULTS

3.1 Patient characteristics and response evaluation
In our search for molecular biomarkers to tailor treatment decisions in non-metastatic esophageal cancer (EC) we isolated DNA from a retrospectively collected series of 131 archival pre-treatment tumor biopsies from three different hospitals in the Netherlands. All patients had been clinically diagnosed with stage II or III EC and received treatment

with neoadjuvant chemoradiotherapy (CRT), containing carboplatin and paclitaxel, followed by surgical resection. DNA, meeting requirements for targeted sequencing, could be extracted from formalin-fixed paraffin-embedded biopsies of 92 out of 131 patients, which included 16 esophageal squamous cell carcinoma (ESCC), 75 esophageal adenocarcinoma (EAC) and one undifferentiated carcinoma, and was evaluated using a custom GI-specific hybrid capture 243 gene panel to assess mutations and copy-number status, as described before (**Table S1**)[12]. Baseline patient characteristics are presented in **Table 1** and **Table S2**. The median age at diagnosis was 64 years and patients were predominantly male (78.0%). The majority of patients presented with a ≥ cT3 tumor (82.4%) and/or lymph node positivity (62.6%). Resection of the tumor was complete in 91.2% of cases. ESCC and EAC patients did not differ in pre-treatment characteristics (age, gender, T stage, N stage) and completeness of resection (**Table 1**). Median disease-free survival (DFS) was 3.2 years and median overall survival (OS) 4.3 years; and did not differ significantly between EAC and ESCC (**Figure S1**).

2

Table 1. Baseline characteristics of patients whose biopsies were used for the custom upper gastrointestinal cancer-specific next-generation targeted sequencing.

	Total N = 91 (%)		EAC N = 75 (%)		ESCC N = 16 (%)		P
Age at diagnosis							ns
Median with range	64.0	(37-81)	64.0	(37-81)	65.5	(43-76)	
Gender							ns
Male	71	(78.0%)	61	(81.3%)	10	(62.5%)	
Female	20	(22.0%)	14	(18.7%)	6	(37.5%)	
Clinical T stage							ns
T1	0	(0.0%)	0	(0.0%)	0	(0.0%)	
T2	9	(9.9%)	7	(9.3%)	2	(12.5%)	
T3	67	(73.6%)	57	(76.0%)	10	(62.5%)	
T4	8	(8.8%)	5	(6.7%)	3	(18.8%)	
Missing	7	(7.7%)	6	(8.0%)	1	(6.3%)	
Clinical N stage							ns
N0	28	(30.8%)	25	(33.3%)	3	(18.8%)	
N1	37	(40.7%)	32	(42.7%)	5	(31.3%)	
N2	18	(19.8%)	12	(16.0%)	6	(37.5%)	
N3	2	(2.2%)	2	(2.7%)	0	(0.0%)	
Missing	6	(6.6%)	4	(5.3%)	2	(12.5%)	
Resection							ns
Complete	83	(91.2%)	69	(92.0%)	14	(87.5%)	
Not complete	4	(4.4%)	3	(4.0%)	1	(6.3%)	
Missing	4	(4.4%)	3	(4.0%)	1	(6.3%)	

Table 1. Baseline characteristics of patients whose biopsies were used for the custom upper gastrointestinal cancer-specific next-generation targeted sequencing. (continued)

	Total		EAC		ESCC		
	N = 91 (%)		*N* = 75 (%)		*N* = 16 (%)		*P*
ypT stage							0.021[†]
ypT0	25	(27.5%)	15	(20.0%)	10	(62.5%)	
ypT1	10	(11.0%)	10	(13.3%)	0	(0%)	
ypT2	7	(7.7%)	7	(9.3%)	0	(0%)	
ypT3	46	(50.5%)	40	(53.3%)	6	(37.5%)	
Missing	3	(3.3%)	3	(4.0%)	0	(0%)	
ypN stage							ns
ypN0	54	(59.3%)	43	(57.3%)	11	(68.8%)	
ypN1	20	(22.0%)	17	(22.7%)	3	(18.8%)	
ypN2	11	(12.1%)	9	(12.0%)	2	(12.5%)	
ypN3	4	(4.4%)	4	(5.3%)	0	(0%)	
Missing	2	(2.2%)	2	(2.7%)	0	(0%)	
Mandard's TRG							0.004[†]
TRG 1	25	(27.5%)	15	(20.0%)	10	(62.5%)	
TRG 2	13	(14.3%)	11	(14.7%)	2	(12.5%)	
TRG 3	22	(24.2%)	20	(26.7%)	2	(12.5%)	
TRG 4	27	(29.7%)	26	(34.7%)	1	(6.3%)	
TRG 5	1	(1.1%)	0	(0.0%)	1	(6.3%)	
Missing	3	(3.3%)	3	(4.0%)	0	(0.0%)	
Prognostic Score							ns
PRSC A	30	(33.0%)	22	(29.3%)	8	(50.0%)	
PRSC B	41	(45.1%)	34	(45.3%)	7	(43.8%)	
PRSC C	17	(18.7%)	16	(21.3%)	1	(6.3%)	
Missing	3	(3.3%)	3	(4.0%)	0	(0.0%)	
Recurrence < 1 year	24	(26.4%)	20	(26.7%)	4	(25.0%)	ns
Median OS (yrs (95% CI))	4.29 (2.9-5.7)		4.29 (3.1-5.5)		3.08 (0.0-6.3)		ns
Median DFS (yrs (95% CI))	3.21 (2.3-4.1)		3.53 (2.1-5.0)		2.95 (1.7-4.2)		ns

†: Linear-by-linear, exact text

Response to neoadjuvant CRT was evaluated by histopathological tumor regression grading (TRG) using the post-treatment resection specimen. Tumor regression was graded using the Mandard score, which is a five-tiered TRG ranging from 1 (no residual cancer) to 5 (absence of regressive changes)[4]. As expected[3], a complete histopathological response (TRG 1) was observed more often in ESCC patients (62.5%, 10/16) than in EAC patients (20.0%, 15/75; *P* = 0.002; **Table 1**). The association between higher Mandard TRG scores and shorter disease-free and overall survival was confirmed (**Figure S2A**).

As the Mandard TRG is limited to the response of the primary tumor and does not include response in lymph nodes, we added the Prognostic Score (PRSC)[11] to our

outcome measures. The PRSC is a histopathological response grading system that combines tumor regression (<50% vs >50%) with the presence of residual cancer in lymph nodes (ypN0 vs ypN1-3) and tumor stage (ypT0-2 vs ypT3-4); it ranges from A (favorable prognosis) to C (poor prognosis)[11]. We confirmed a strong association between the PRSC and survival in our series (disease-free survival (DFS): P = 0.0015, overall survival (OS): P = 0.0065; **Figure S2B**). Post-CRT lymph node positivity (ypN) by itself was also a strong predictor of shortened survival as compared to ypN negativity[11] (**Figure S2C**). Within EAC 30.6% had a PRSC A, 47.2% PRSC B, and 22.2% PRSC C; and within ESCC 50.0% had a PRSC A, 43.8% PRSC B, and 6.3% PRSC C.

3.2 Genetic alterations in EAC and ESCC

Targeted sequencing of pre-treatment biopsies confirmed known genetic patterns in EAC and ESCC[8]. As expected, *TP53* was the most frequently mutated gene in both EAC (80%, 60/75) and ESCC (75%, 12/16). Other frequently mutated genes were *CDKN2A* (13.3%, 10/75) and *BRCA2* (10.7%, 8/75) in EAC, and *PIK3CA* in ESCC (25%, 4/16; **Figure 1, Table S3** and **Table S4**).

Copy number variation (CNV) analysis identified amplifications of *ERBB2* (17q12; 20.0%, 15/75), *KRAS* (12p12.1; 14.7%, 11/75), and *GATA6* (18q11.2; 14.7%, 11/75), and deletion of *CDKN2A* (9p21.3; 16.0%, 12/75; **Figure 1** and **Table S3**) mostly in EAC, while *CCND1* amplification was the most prevalent CNV in ESCC (11q13.3; 56.3%, 9/16). Other commonly observed CNVs in ESCC were deletion of *CDKN2A* and/or *CDKN2B* (9p21.3), amplification of *EGFR* (7p11.2), and amplification of *TP63* (3q28; 25%, 4/16 (all cases with *SOX2* amplification co-occurred with TP63 amplification); **Figure 1** and **Table S4**). These alterations are consistent with the histology-specific genomic patterns described by The Cancer Genome Atlas[8] and the International Cancer Genome Consortium[9], thereby confirming the feasibility of using a custom targeted sequencing panel on archival pre-treatment biopsies.

There were no significant associations between any genetic events and clinical N or T stage in both EAC and ESCC. *ATM* mutation was associated with younger age at diagnosis in EAC (median 47 vs 64 years, P = 0.031) and *PIK3CA* mutation was associated with younger age at diagnosis in ESCC (median 56 vs 66.5 years, P = 0.042).
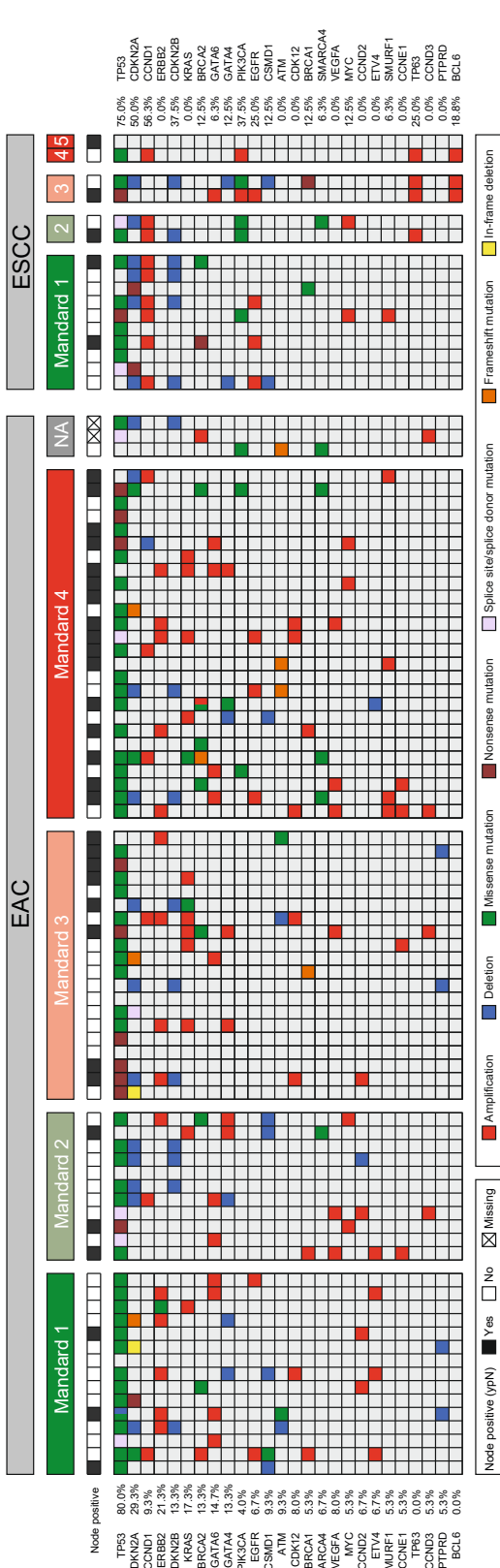
Figure 1. Overview of genomic alterations in relation to histopathological response according to Mandard's tumor regression grade to neoadjuvant chemoradiotherapy in patients with esophageal adenocarcinoma (EAC) and esophageal squamous cell carcinoma (ESCC). Percentages indicate frequency of occurrence within EAC and ESCC, respectively.

3.3 CpG island promoter methylation in EC

Because CpG island promoter methylation is a common feature of EC[8], we performed a multiplex methylation specific PCR on a panel of 8 gene promoters known to be methylated in GI cancers, *CHFR*, *MGMT*, *CDKN2A*, *RASSF1*, *MLH1*, *TFPI2*, *RUNX3*, and *NDRG4*, on 105 formalin-fixed paraffin-embedded tumor samples, among which 85 EACs and 20 ESCCs. The majority of this group (76/105 samples) had sufficient DNA for both custom GI-specific targeted sequencing and methylation analyses (**Figure S3**).

We confirmed that CpG Island promoter methylation is predominantly a characteristic of EAC, with a median methylation index (promoters methylated/promoters tested) of 0.57 (95% CI 0.52-0.62) compared to 0.25 (95% CI 0.16-0.38) in ESCC ($P < 0.0001$; **Figure S4**). CpG island promoter methylation was significantly lower in normal tumor-adjacent epithelium (mean methylation index 0.05 in normal (n = 30) vs 0.51 in tumor; $P < 0.0001$; **Table 2**).

In EAC, CpG island promoter methylation was observed, in descending order, in 85.9% (73/85) for *NDRG4*, 80.0% (65/85) for *TFPI2*, 75.3% (64/85) for *RUNX3*, 72.9% (62/85) for *MGMT*, 55.4% (46/83) for *CHFR*, 31.8% (21/66) for *CDKN2A*, 21.2% (18/85) for *MLH1*, and 12.1% (7/58) for *RASSF1* (**Table 2**). In ESCC, CpG island promoter methylation frequencies were lower than in EAC, which reached statistical significance for *CHFR* (25% vs 55.4%, $P = 0.015$), *TFPI2* (10% vs 80%, $P < 0.001$), *RUNX3* (40% vs 75.3%, $P = 0.002$) and *NDRG4* (5% vs 85.9%, $P < 0.001$). *CDKN2A* methylation was mutually exclusive with *CDKN2A* deletion. There were no significant associations between promoter methylation of these selected genes and clinical N or T stage in both EAC and ESCC. *CHFR* methylation was associated with an older age at diagnosis in ESCC (median 70 vs 65 years, $P = 0.019$).

Table 2. Prevalence of promoter CpG island methylation of selected genes.

Gene	Methylated in normal tissue		Methylated in EAC		Methylated in ESCC		EAC vs. ESCC
	N/total	%	N/total	%	N/total	%	*P*
CDKN2A	0/26	0.00	21/66	31.8	5/12	41.7	ns
CHFR	2/30	6.67	46/83	55.4	5/20	25.0	0.015
MGMT	2/30	6.67	62/85	72.9	12/20	60.0	ns
MLH1	0/30	0.00	18/85	21.2	6/20	30.0	ns
NDRG4	1/30	3.33	73/85	85.9	1/20	5.0	< 0.001
RASSF1	1/30	3.33	7/58	12.1	3/20	15.0	ns
RUNX3	4/30	13.33	64/85	75.3	8/20	40.0	0.002
TFPI2	1/28	3.57	68/85	80.0	2/20	10.0	< 0.001

EAC: esophageal adenocarcinoma, ESCC: esophageal squamous cell carcinoma. CDKN2A: cyclin dependent kinase inhibitor 2A, CHFR: checkpoint with forkhead and ring finger domains, MGMT: O-6-methylguanine-DNA methyltransferase, MLH1: mutL homolog 1, NDRG4: NDRG family member 4, RASSF1: ras association domain family member 1, RUNX3: RUNX family transcription factor 3, TFPI2: tissue factor pathway inhibitor 2, ns: not significant

3.4 Genomic alterations and histopathological response

Since EAC and ESCC are molecularly distinct and respond differently to CRT, we analyzed associations between molecular alterations and therapy response for both histological subtypes separately. The undifferentiated carcinoma was excluded from this analysis. We first evaluated recurring CNVs (≥ 5% of all samples) in relation to histopathological response according to the Mandard TRG. Thereby, we identified that within EAC deletion of *CUB and Sushi multiple domains 1, CSMD1* (8p23.2; 8.0%, 6/75) and amplification of *ETS Variant Transcription Factor 4, ETV4* (17q21.31; 5.3%, 4/75) were associated with a favorable Mandard TRG (P = 0.039 and P = 0.006, respectively; **Figure 2A** and **Table S3**). Five out of six patients with *CSMD1* deletion had a Mandard TRG of 1 or 2; and all four patients with *ETV4* amplification had a Mandard TRG of 1 or 2. Amplification of *SMAD Specific E3 Ubiquitin Protein Ligase 1, SMURF1* (7q22.1; 5.3%, 4/75) on the other hand, was associated with an unfavorable Mandard TRG (P = 0.035); all patients with *SMURF1* amplification had a TRG 4. Due to the low frequency of *ETV4* amplifications and *CSMD1* deletions (and their co-occurrence in one patient), they could not be confirmed as independent predictors of Mandard TRG by multiple regression analysis. In addition to the association with an unfavorable Mandard TRG, amplification of *SMURF1* was also associated with an unfavorable PRSC (P = 0.027; **Figure 2B**).

With regard to gene mutation, only *SMARCA4* mutation (5.3%, 4/75; all missense) was associated with an unfavorable PRSC in EAC (P = 0.027; **Figure 2B, Table S1**) but not unfavorable Mandard's TRG, which can be explained by the difference in ypN positivity (80% vs. 38%) between EAC patients with mutant *SMARCA4* compared to wildtype *SMARCA4*, which is not included in the Mandard's TRG.

In ESCC, amplification of chromosomal region 3q27.3-28, harboring *TP63* (25.0%, 4/16) and *BCL6* (18.8%, 3/16)*,* was associated with an unfavorable Mandard TRG (P = 0.034 and P = 0.036, respectively; **Figure 2C** and **Table S4**). There were no significant associations between gene mutation and histopathological response in ESCC.

For CpG island promoter methylation, we observed a trend towards an unfavorable Mandard TRG for *NDRG4* promoter methylation in EAC (P = 0.050; **Table S5**). In ESCC, *TFPI2* promoter methylation (10%, 2/20) was associated with an unfavorable PRSC (P = 0.042; **Figure 2D, Table S6**), which was mostly due to all patients with *TFPI2* promoter methylation having ypN positivity (P = 0.032).

We did not find significant associations between histopathological response (Mandard TRG and PRSC) and disruption of specific pathways such as the RTK/RAS/PI(3)K pathway, chromatin remodeling, cell cycle, cell differentiation, and proliferation; or potentially targetable genes (**Figure S5**).
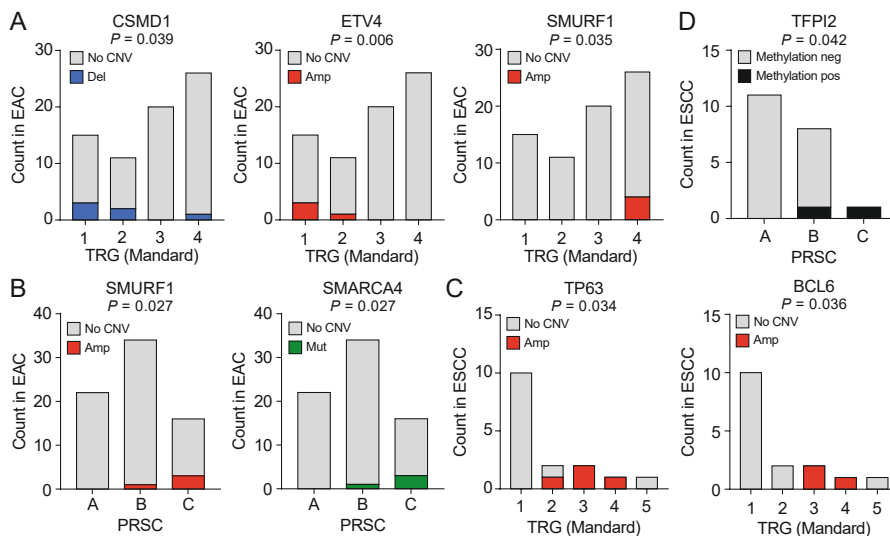
Figure 2. (Epi)genetic alterations in relation to histopathological response to neoadjuvant chemo-radiotherapy in patients with esophageal adenocarcinoma (EAC) (**A, B**) and esophageal squamous cell carcinoma (ESCC) (**C**). (**A**) *CSMD1* deletion and *ETV4* amplification were associated with a favorable tumor regression grade (TRG), whereas *SMURF1* amplification was associated with an unfavorable TRG in EAC. (**B**) *SMURF1* amplification and *SMARCA4* mutation were associated with an unfavorable prognostic score (PRSC) in EAC. (**C, D**) Associations between (epi)genetic alterations and histopathological response in esophageal squamous cell carcinoma (ESCC). (**C**) *TP63* and *BCL6* amplification (both on chromosomal region 3q27.3-28) were associated with an unfavorable TRG in ESCC. (**D**) *TFPI2* promoter methylation was associated with an unfavorable PRSC in ESCC. Linear-by-linear, exact test.

3.5 Prognostic value of molecular alterations

Next, we analyzed associations between genomic and epigenetic alterations and survival. Thereby, we identified that for EAC, amplification of *KRAS* (14.7%, 11/75) and the 8p23.1 chromosomal region, harboring *GATA4* (6.7%, 5/75), *NEIL2* (6.7%, 5/75) and *CTSB* (5.3%, 4/75), were associated with a shorter OS (median non-amplified vs amplified, 4.4 vs 1.4 years, $P = 0.0057$, HR 3.2 for *KRAS*; 4.3 vs 1.1 years, $P = 0.011$, HR 4.4, for *GATA4*; **Figure 3A**, **Table S3** and **Figure S6),** but not DFS. Despite their distant chromosomal location, *GATA4* amplification coincided in four out of five cases with *KRAS* amplification; hence they could not be identified as independent prognostic factors.

Additionally, associations between (epi)genetic events and an exceptionally early recurrence, i.e., recurrence within one year, were tested. In EAC, *CCND1* amplification (8%, 6/75) was associated with recurrence within one year ($P = 0.045$). There were no significant associations between CpG island promoter methylation of the selected genes and survival in EAC.
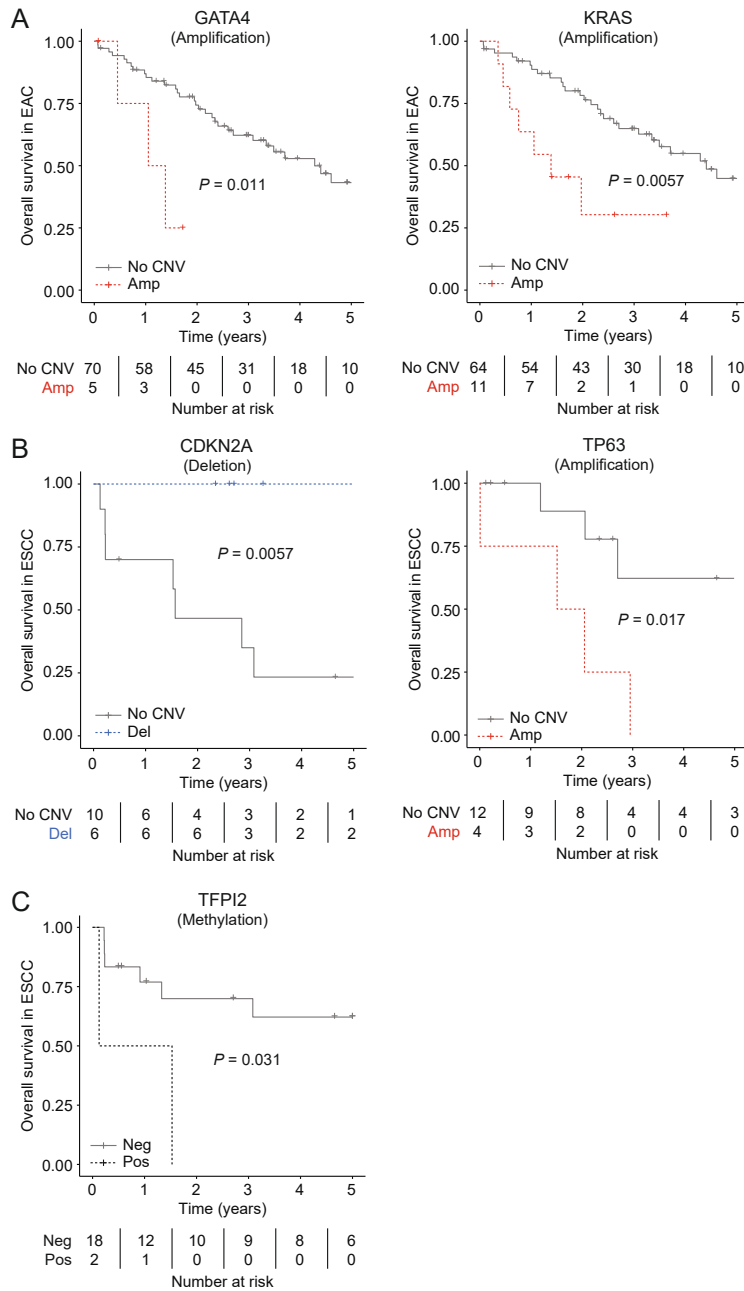
Figure 3. (Epi)genetic alterations in relation to survival in patients with (**A**) esophageal adeno-carcinoma (EAC) and (**B, C**) esophageal squamous cell carcinoma (ESCC). (**A**) *GATA4* and *KRAS* amplification were associated with a shorter overall survival (OS) in patients with EAC. (**B**) In patients with ESCC, *TP63* amplification was associated a shorter OS, whereas deletion of *CDKN2A* was associated with a longer OS. (**C**) Patients with ESCC and *TFPI2* promoter methylation had a shorter OS. Log-rank test.

In ESCC, amplification of *TP63* (25.0%, 4/16) was associated with a shorter DFS (median non-amplified vs amplified, not reached vs 1.5 years, *P* = 0.017, HR 2.6; **Figure 3B** and **Table S4**), which is in line with the significant association between *TP63* amplification and an unfavorable Mandard TRG. Furthermore, deletion of *CDKN2A* (37.5%, 6/16) was associated with a longer OS (median non-deleted vs deleted, 1.6 years vs not reached, *P* = 0.0057, q (*P*-value corrected for multiple comparisons) = 0.0419, HR 0.015).

For CpG island promoter methylation in ESCC, *TFPI2* promoter methylation was associated with worse OS (median unmethylated vs methylated, 5.8 vs 0.1 years, *P* = 0.031; **Figure 3C**). Since *CDKN2A* deletion was associated with a long OS, we tested the effect of *CDKN2A* deletion or promoter methylation on survival and found no significant associations. There were no significant associations between genomic and epigenetic alterations and recurrence within one year within the ESCC cohort.

Except for the association between *CDKN2A* deletion and a favorable OS in ESCC, none of the described associations with histopathological response or survival maintained significance after correction for multiple comparisons.

4. DISCUSSION

Esophageal cancer is a deadly disease and incidence rates, especially of adenocarcinoma, are on the rise[1]. Despite a survival increment due to the addition of neoadjuvant chemoradiotherapy (CRT) to surgical resection for stage II/III disease[3], success of neoadjuvant treatment varies greatly between patients. In order to improve our understanding of treatment response and in search for biomarkers for patient selection we performed molecular analyses on pre-treatment biopsies and identified several interesting associations.

We first showed feasibility of this approach by identifying previously described genomic and epigenetic alterations in comparable frequencies in both EAC and ESCC using (mostly formalin-fixed paraffin-embedded) biopsies. In EAC however, none of the highly recurrent alterations such as *TP53* mutation, *ERBB2* amplification, *CDKN2A* deletion or mutation, *KRAS* amplification, and *GATA6* amplification, were associated with histopathological response to neoadjuvant CRT. Instead, we found associations involving relatively rare genetic alterations: deletion of complement inhibitor *CSMD1* (8p23.2) and amplification of transcription factor *ETV4* (17q21.31) were associated with a favorable Mandard TRG, and amplification of E3 ubiquitin ligase *SMURF1* (7q22.1) was associated with an unfavorable Mandard TRG. *SMURF1* amplification was also associated with an unfavorable PRSC, as was mutation of SWI/SNF component *SMARCA4* (BRG1).

Beyond the need to validate these associations in additional larger cohorts to determine its reproducibility, it is not clear whether these genes are really associated with CRT

resistance or sensitivity or whether these genes are mere innocent bystanders. *SMARCA4* mutation and *SMURF1* amplification have been associated with a poor prognosis in gastro-esophageal adenocarcinoma before, potentially confirming a more aggressive phenotype, but the same accounts for *ETV4* amplification and *CSMD1* deletion[17–21]. Furthermore, inactivation of SMARCA4, the catalytic subunit of the SWI/SNF chromatin remodeling complex, has been linked to impaired nucleotide excision repair (NER)[22] and loss of Rb activity[23], and thereby increased platinum sensitivity in HNSCC and NSCLC cell lines[22] and NSCLC patients[24], which contrasts our findings of resistance to platinum-containing CRT.

For ubiquitin ligase SMURF1 no association with resistance to CRT has been described before. However, as SMURF1 induces degradation of several pro-apoptotic proteins[25], one could hypothesize that amplification of *SMURF1* disturbs the effect of CRT by preventing adequate execution of apoptosis[26]. Also for amplification of *ETV4* and deletion of *CSMD1*, no association with response to therapy has been described before, but as inducer of cyclin D3[27] and cyclin D1[28] upregulation, and p21 downregulation[29], *ETV4* amplification might contribute to CRT sensitivity by promoting cell cycle progression through potentially radiosensitive phases of the cell cycle. Lastly, CSMD1 is a membrane-bound complement inhibitor[30,31], whose tumor-suppressing properties have been linked to its short cytoplasmic tail that contains a tyrosine phosphorylation site[31]. In gastric cancer cells, *CSMD1* downregulation has been associated with increased NF-κB signaling, upregulation of c-Myc and CCND1, and downregulation of E-cadherin[21]. CSMD1 has been shown to inhibit the deposition of complement factors C3b and C9 on ovarian cancer cells and promote the degradation of C3b[31], thereby potentially inhibiting an anti-tumor immune response. Conversely, knockdown of *CSMD1* expression has been shown to increase the deposition of C3b on breast cancer cells[31]. The increased complement deposition on tumor cells due to CSMD1 deletion might be the link to a favorable Mandard TRG, but this needs further investigation.

In terms of survival, we did find some intriguing associations. Amplification of *KRAS* and *GATA4* were significantly associated with a shorter overall survival (OS) in our EAC cohort. Amplification of *GATA4* has already been identified as a poor prognosticator in EAC in at least two independent studies[9,32]. Also amplification of *KRAS* was previously found to be significantly associated with lymph node metastasis and poor OS in EAC patients treated with upfront resection[33]. Taken together, this data indicates *GATA4* and *KRAS* as promising biomarkers for early disease recurrence, which needs further investigation in prospective biomarkers studies.

In ESCC we also identified several associations between recurrent genomic alterations and response to CRT. Amplification of *TP63* was associated with an unfavorable Mandard TRG and a shorter disease-free survival (DFS). *TP63*, which encodes p53-related p63, is a transcription factor which overexpression has been associated with resistance

to radiotherapy in oral and cervical SCC[34,35], and conversely, p63 knockout has been shown to prevent apoptosis in non-cancerous cells[36]. Interestingly, deletion of *CDKN2A* (p16[INK4a]) was strongly associated with a favorable OS in our cohort, which contrasts other reports about *CDKN2A* loss and a poor prognosis[37], including other squamous cell carcinomas[38,39]. Although this controversy can potentially be explained by the effect of CRT in our study, this finding needs further investigation. Additionally, *TFPI2* promoter methylation was significantly associated with both an unfavorable PRSC and poor OS. *TFPI2* inhibits extracellular matrix (ECM) proteinases such as matrix metalloproteinases (MMPs), and thereby angiogenesis and invasive ability in ESCC cell lines, but its role in response to CRT has not been investigated before.

To our knowledge, this is the first publication on (epi)genetic profiling of pre-treatment biopsies in relation to response to neoadjuvant CRT and survival in esophageal cancer. With 75 and 85 EAC patients for genomic and methylation analyses, our EAC cohort was of reasonable size, and some potentially interesting associations with response to CRT were identified. The prevalence of these response-associated alterations, however, was low, which limits their suitability as biomarker for patient selection. None of the more prevalent genetic alterations such as amplification of *ERBB2*, *EGFR*, *KRAS* or *GATA4* were enriched in one of the response groups. Therefore, we are not convinced that targeted next generation sequencing of pre-treatment biopsies in EC will be practice changing. Although other factors such as immune cells or stromal components might have a bigger impact on success of CRT[40,41] than the tumor genome, our slightly disappointing results might be the result of intratumoral genomic heterogeneity; a hallmark of EACs[12,42,43]. Using multi-region sequencing of primary EACs we have previously identified significant differences within the primary tumor, including discrepancies in potentially clinically relevant alterations[12]. This intratumoral heterogeneity not only complicates representative tumor sampling, it also induces an heterogenic treatment response[42,44–47]. Therefore, approaches such as assessment of circulating cell-free DNA (cfDNA), which is shed by all tumor cells, may provide a more comprehensive view of the genomic landscape of EACs. However, sensitivity for cfDNA is still limited, especially in a setting without distant metastatic spread[12,48]. Improvements to cfDNA technology could provide opportunities to detect alterations more accurately and on a larger scale than in the current study, while circumventing possible sampling bias caused by tumor heterogeneity.

5. CONCLUSIONS

In conclusion, this study found low-prevalent candidate (epi)genetic biomarkers associated with response to neoadjuvant chemoradiotherapy in patients with localized esophageal cancer. These findings may assist approaches to further individualize treatment.

ACKNOWLEDGEMENTS

REFERENCES

1. Torre LA, Bray F, Siegel RL, Ferlay J, Lortet-Tieulent J & Jemal A (2015) Global cancer statistics, 2012. *CA Cancer J Clin* **65**, 87–108.

2. Cunningham D, Starling N, Rao S, Iveson T, Nicolson M, Coxon F, Middleton G, Daniel F, Oates J & Norman AR (2008) Capecitabine and Oxaliplatin for Advanced Esophagogastric Cancer. *N Engl J Med* **358**, 36–46.

3. van Hagen P, Hulshof MCCM, van Lanschot JJB, Steyerberg EW, Henegouwen MI van B, Wijnhoven BPL, Richel DJ, Nieuwenhuijzen GAP, Hospers GAP, Bonenkamp JJ *et al.* (2012) Preoperative Chemoradiotherapy for Esophageal or Junctional Cancer. *N Engl J Med* **366**, 2074–2084.

4. Mandard A-M, Dalibard F, Mandard J-C, Marnay J, Henry-Amar M, Petiot J-F, Roussel A, Jacob J-H, Segol P, Samama G *et al.* (1994) Pathologic assessment of tumor regression after preoperative chemoradiotherapy of esophageal carcinoma. Clinicopathologic correlations. *Cancer* **73**, 2680–2686.

5. Oppedijk V, Van Der Gaast A, Van Lanschot JJB, Van Hagen P, Van Os R, Van Rij CM, Van Der Sangen MJ, Beukema JC, Ruïten H, Spruit PH *et al.* (2014) Patterns of recurrence after surgery alone versus preoperative chemoradiotherapy and surgery in the CROSS trials. *J Clin Oncol* **32**, 385–391.

6. den Bakker CM, Smit JK, Bruynzeel AMEE, van Grieken NCTT, Daams F, Derks S, Cuesta MA, Plukker JTMM & van der Peet DL (2017) Non responders to neoadjuvant chemoradiation for esophageal cancer: why better prediction is necessary. *J Thorac Dis* **9**, S843–S850.

7. Tao C-J, Lin G, Xu Y-P & Mao W-M (2015) Predicting the Response of Neoadjuvant Therapy for Patients with Esophageal Carcinoma: an In-depth Literature Review. *J Cancer* **6**, 1179–1186.

8. The Cancer Genome Atlas Research Network (2017) Integrated genomic characterization of oesophageal carcinoma. *Nature* **541**, 169–175.

9. Frankell AM, Jammula S, Li X, Contino G, Killcoyne S, Abbas S, Perner J, Bower L, Devonshire G, Ococks E *et al.* (2019) The landscape of selection in 551 esophageal adenocarcinomas defines genomic biomarkers for the clinic. *Nat Genet* **51**, 506–516.

10. Jammula S, Katz-Summercorn AC, Li X, Linossi C, Smyth E, Killcoyne S, Biasci D, Subash V V., Abbas S, Blasko A *et al.* (2020) Identification of Subtypes of Barrett's Esophagus and Esophageal Adenocarcinoma Based on DNA Methylation Profiles and Integration of Transcriptome and Genome Data. *Gastroenterology* **158**, 1682-1697.e1.

11. Langer R, Becker K, Zlobec I, Gertler R, Sisic L, Büchler M, Lordick F, Slotta-Huspenina J, Weichert W, Höfler H *et al.* (2014) A multifactorial histopathologic score for the prediction of prognosis of resected esophageal adenocarcinomas after neoadjuvant chemotherapy. *Ann Surg Oncol* **21**, 915–921.

12. Pectasides E, Stachler MD, Derks S, Liu Y, Maron S, Islam M, Alpert L, Kwak H, Kindler H, Polite B *et al.* (2018) Genomic Heterogeneity as a Barrier to Precision Medicine in Gastroesophageal Adenocarcinoma. *Cancer Discov* **8**, 37–48.

13. Cibulskis K, Lawrence MS, Carter SL, Sivachenko A, Jaffe D, Sougnez C, Gabriel S, Meyerson M, Lander ES & Getz G (2013) Sensitive detection of somatic point mutations in impure and heterogeneous cancer samples. *Nat Biotechnol* **31**, 213–9.

14. Ramos AH, Lichtenstein L, Gupta M, Lawrence MS, Pugh TJ, Saksena G, Meyerson M & Getz G (2015) Oncotator: Cancer Variant Annotation Tool. *Hum Mutat* **36**, E2423–E2429.

2

15. Brandes JC, Van Engeland M, Wouters KAD, Weijenberg MP & Herman JG (2005) CHFR promoter hypermethylation in colon cancer correlates with the microsatellite instability phenotype. *Carcinogenesis* **26**, 1152–1156.

16. Schemper M & Smith TL (1996) A note on quantifying follow-up in studies of failure time. *Control Clin Trials* **17**, 343–346.

17. Huang SC, Ng KF, Yeh T Sen, Cheng CT, Chen MC, Chao YC, Chuang HC, Liu YJ & Chen TC (2020) The clinicopathological and molecular analysis of gastric cancer with altered SMARCA4 expression. *Histopathology* **77**, 250–261.

18. Keld R, Guo B, Downey P, Gulmann C, Ang YS & Sharrocks AD (2010) The ERK MAP kinase-PEA3/ETV4-MMP-1 axis is operative in oesophageal adenocarcinoma. *Mol Cancer* **9**, 313.

19. Keld R, Guo B, Downey P, Cummins R, Gulmann C, Ang YS & Sharrocks AD (2011) PEA3/ETV4-related transcription factors coupled with active ERK signalling are associated with poor prognosis in gastric adenocarcinoma. *Br J Cancer* **105**, 124–130.

20. Tao Y, Sun C, Zhang T & Song Y (2017) SMURF1 promotes the proliferation, migration and invasion of gastric cancer cells. *Oncol Rep* **38**, 1806–1814.

21. Chen XL, Hong LL, Wang KL, Liu X, Wang JL, Lei L, Xu ZY, Cheng XD & Ling ZQ (2019) Deregulation of CSMD1 targeted by microRNA-10b drives gastric cancer progression through the NF-κB pathway. *Int J Biol Sci* **15**, 2075–2086.

22. Kothandapani A, Gopalakrishnan K, Kahali B, Reisman D & Patrick SM (2012) Downregulation of SWI/SNF chromatin remodeling factor subunits modulates cisplatin cytotoxicity. *Exp Cell Res* **318**, 1973–1986.

23. Dunaief JL, Strober BE, Guha S, Khavari PA, Ålin K, Luban J, Begemann M, Crabtree GR & Goff SP (1994) The retinoblastoma protein and BRG1 form a complex and cooperate to induce cell cycle arrest. *Cell* **79**, 119–130.

24. Bell EH, Chakraborty AR, Mo X, Liu Z, Shilo K, Kirste S, Stegmaier P, McNulty M, Karachaliou N, Rosell R *et al.* (2016) SMARCA4/BRG1 is a novel prognostic biomarker predictive of cisplatin-based chemotherapy outcomes in resected non-small cell lung cancer. *Clin Cancer Res* **22**, 2396–2404.

25. Fu L, Cui C-P, Zhang X & Zhang L (2019) The functions and regulation of Smurfs in cancers. *Semin Cancer Biol* 0–1 doi:10.1016/j.semcancer.2019.12.023.

26. Pommier Y, Sordet O, Antony S, Hayward RL & Kohn KW (2004) Apoptosis defects and chemotherapy resistance: Molecular interaction maps and networks. *Oncogene* vol. 23 2934–2949.

27. Jiang J, Wei Y, Liu D, Zhou J, Shen J, Chen X, Zhang S, Kong X & Gu J (2007) E1AF promotes breast cancer cell cycle progression via upregulation of Cyclin D3 transcription. *Biochem Biophys Res Commun* **358**, 53–58.

28. Tyagi N, Deshmukh SK, Srivastava SK, Azim S, Ahmad A, AL-Ghadhban A, Singh AP, Carter JE, Wang B & Singh S (2018) ETV4 Facilitates Cell-Cycle Progression in Pancreatic Cells through Transcriptional Regulation of Cyclin D1. *Mol Cancer Res* **16**, 187–196.

29. Cosi I, Pellecchia A, De Lorenzo E, Torre E, Sica M, Nesi G, Notaro R & De Angioletti M (2020) ETV4 promotes late development of prostatic intraepithelial neoplasia and cell proliferation through direct and p53-mediated downregulation of p21. *J Hematol Oncol* **13**, 112.

30. Kraus DM, Elliott GS, Chute H, Horan T, Pfenninger KH, Sanford SD, Foster S, Scully S, Welcher AA & Holers VM (2006) CSMD1 Is a Novel Multiple Domain Complement-Regulatory Protein Highly Expressed in the Central Nervous System and Epithelial Tissues. *J Immunol* **176**, 4419–4430.

31. Escudero-Esparza A, Kalchishkova N, K urbasic E, Jiang WG & Blom AM (2013) The novel complement inhibitor human CUB and Sushi multiple domains 1 (CSMD1) protein promotes factor I-mediated degradation of C4b and C3b and inhibits the membrane attack complex assembly. *FASEB J* **27**, 5083–5093.

32. Frankel A, Armour N, Nancarrow D, Krause L, Hayward N, Lampe G, Smithers BM & Barbour A (2014) Genome-wide analysis of esophageal adenocarcinoma yields specific copy number aberrations that correlate with prognosis. *Genes, Chromosom Cancer* **53**, 324–338.

33. Essakly A, Loeser H, Kraemer M, Alakus H, Chon SH, Zander T, Buettner R, Hillmer AM, Bruns CJ, Schroeder W *et al.* (2020) PIK3CA and KRAS Amplification in Esophageal Adenocarcinoma and their Impact on the Inflammatory Tumor Microenvironment and Prognosis. *Transl Oncol* **13**, 157–164.

34. Moergel M, Abt E, Stockinger M & Kunkel M (2010) Overexpression of p63 is associated with radiation resistance and prognosis in oral squamous cell carcinoma. *Oral Oncol* **46**, 667–671.

35. Cho NH, Kim YB, Park TK, Kim GE, Park K & Song KJ (2003) P63 and EGFR as prognostic predictors in stage IIB radiation-treated cervical squamous cell carcinoma. *Gynecol Oncol* **91**, 346–353.

36. Livera G, Petre-Lazar B, Guerquin M-J, Trautmann E, Coffigny H & Habert R (2008) p63 null mutation protects mouse oocytes from radio-induced apoptosis. *Reproduction* **135**, 3–12.

37. Zhao R, Choi BY, Lee MH, Bode AM & Dong Z (2016) Implications of Genetic and Epigenetic Alterations of CDKN2A (p16INK4a) in Cancer. *EBioMedicine* **8**, 30–39.

38. Chen WS, Bindra RS, Mo A, Hayman T, Husain Z, Contessa JN, Gaffney SG, Townsend JP & Yu JB (2018) CDKN2A copy number loss is an independent prognostic factor in HPV-negative head and neck squamous cell carcinoma. *Front Oncol* **8**,.

39. Padhi SS, Roy S, Kar M, Saha A, Roy S, Adhya A, Baisakh M & Banerjee B (2017) Role of CDKN2A/p16 expression in the prognostication of oral squamous cell carcinoma. *Oral Oncol* **73**, 27–35.

40. Van Der Most RG, Currie A, Robinson BWS & Lake RA (2006) Cranking the immunologic engine with chemotherapy: Using context to drive tumor antigen cross-presentation towards useful antitumor immunity. *Cancer Res* **66**, 601–604.

41. Goedegebuure RSA, de Klerk LK, Bass AJ, Derks S & Thijssen VLJL (2019) Combining Radiotherapy With Anti-angiogenic Therapy and Immunotherapy; A Therapeutic Triad for Cancer? *Front Immunol* **9**, 1–15.

42. Murugaesu N, Wilson GA, Birkbak NJ, Watkins TBK, McGranahan N, Kumar S, Abbassi-Ghadi N, Salm M, Mitter R, Horswell S *et al.* (2015) Tracking the genomic evolution of esophageal adenocarcinoma through neoadjuvant chemotherapy. *Cancer Discov* **5**, 821–832.

43. Kato S, Okamura R, Baumgartner JM, Patel H, Leichman L, Kelly K, Sicklick JK, Fanta PT, Lippman SM & Kurzrock R (2018) Analysis of Circulating Tumor DNA and Clinical Correlates in Patients with Esophageal, Gastroesophageal Junction, and Gastric Adenocarcinoma. *Clin Cancer Res* **24**, 6248–6256.

44. Burrell RA, McGranahan N, Bartek J & Swanton C (2013) The causes and consequences of genetic heterogeneity in cancer evolution. *Nature* **501**, 338–345.

45. Dagogo-Jack I & Shaw AT (2018) Tumour heterogeneity and resistance to cancer therapies. *Nature Reviews Clinical Oncology* vol. 15 81–94.

46. Findlay JM, Castro-Giner F, Makino S, Rayner E, Kartsonaki C, Cross W, Kovac M, Ulahannan D, Palles C, Gillies RS *et al.* (2016) Differential clonal evolution in oesophageal cancers in response to neo-adjuvant chemotherapy. *Nat Commun* **7**,.

2

47. Kreso A, O'Brien CA, van Galen P, Gan OI, Notta F, Brown AMK, Ng K, Ma J, Wienholds E, Dunant C *et al.* (2013) Variable clonal repopulation dynamics influence chemotherapy response in colorectal cancer. *Science* **339**, 543–8.

48. Cristiano S, Leal A, Phallen J, Fiksel J, Adleff V, Bruhm DC, Jensen SØ, Medina JE, Hruban C, White JR *et al.* (2019) Genome-wide cell-free DNA fragmentation in patients with cancer. *Nature* **570**, 385–389.

SUPPLEMENTARY MATERIAL

Disease-free survival

EAC 75 | 55 | 38 | 27 | 14 | 8
ESCC 16 | 12 | 10 | 4 | 4 | 3
Number at risk

P = 0.86

Overall survival

EAC 75 | 61 | 45 | 31 | 18 | 10
ESCC 16 | 12 | 10 | 6 | 4 | 3
Number at risk

P = 0.91

Population (N)	Median DFS (years) (95% CI)	1-year DFS rate (%) (95% CI)	5-year DFS rate (%) (95% CI)
Overall (91)	3.21 (2.62-NA)	82.4 (74.6-90.9)	40.0 (29.2-54.8)
EAC (75)	3.53 (2.31-NA)	80.2 (71.5-90.1)	39.0 (27.1-56.1)
ESCC (16)	2.95 (2.05-NA)	93.8 (82.6-100)	41.7 (20.6-84.3)

Population (N)	Median OS (years) (95% CI)	1-year OS rate (%) (95% CI)	5-year OS rate (%) (95% CI)
Overall (91)	4.29 (2.85-NA)	85.3 (78.3-93.0)	43.1 (32.1-58.0)
EAC (75)	4.29 (2.70-NA)	86.3 (78.8-94.6)	41.5 (29.4-58.6)
ESCC (16)	3.08 (1.57-NA)	81.2 (64.2-100)	48.4 (27.0-86.6)

Figure S1. Overall survival and disease-free survival by histology in esophageal cancer patients treated with neoadjuvant chemoradiotherapy followed by surgery. Log-rank test.

2

C

ypN in EAC & ESCC (Disease-free survival, *P* = 0.00017)

ypN0	54	43	33	24	15	9
ypN1−3	35	24	15	7	3	2

Number at risk

ypN in EAC & ESCC (Overall survival, *P* < 0.0001)

ypN0	54	45	36	28	18	10
ypN1−3	35	28	19	9	4	3

Number at risk

ypT in EAC & ESCC (Disease-free survival, *P* = 0.014)

ypT0−2	42	32	26	19	12	7
ypT3−4	46	34	21	12	6	4

Number at risk

ypT in EAC & ESCC (Overall survival, *P* = 0.11)

ypT0−2	42	33	28	22	14	7
ypT3−4	46	39	26	15	8	6

Number at risk

TRG1/2/3 vs 4/5 in EAC & ESCC (Disease-free survival, *P* = 0.0017)

TRG1/2/3	60	47	36	22	13	8
TRG4/5	28	19	11	8	4	2

Number at risk

TRG1/2/3 vs 4/5 in EAC & ESCC (Overall survival, *P* = 0.031)

TRG1/2/3	60	49	38	27	15	8
TRG4/5	28	23	16	9	6	4

Number at risk

Figure S2. Associations between histopathological response grading systems and survival. Both Mandard's tumor regression grade (TRG) (**A**) and the prognostic score (PRSC) (**B**) are strongly associated with overall survival and disease-free survival in esophageal cancer patients. (**C**) Components of the PRSC and their association with survival are shown. Log-rank test.
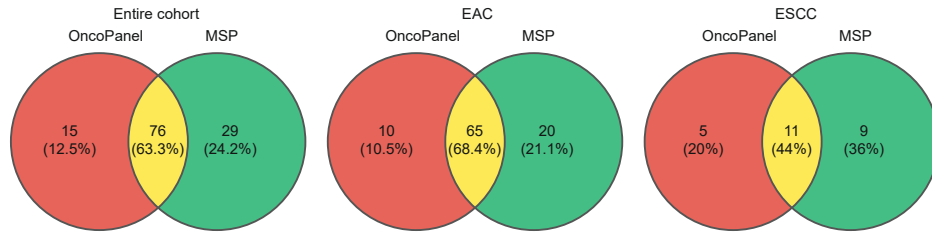
Figure S3. Venn diagram of samples used for the custom upper gastrointestinal cancer-specific targeted sequencing ("OncoPanel") vs. the promoter methylation analyses. MSP = methylation-specific polymerase chain reaction.
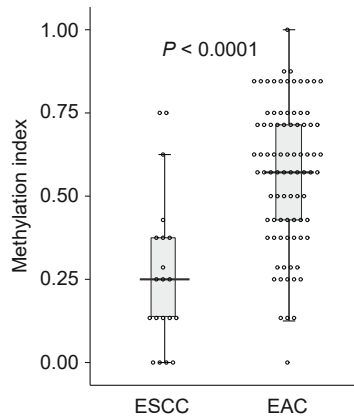
Figure S4. Methylation index by histological subtype. Esophageal adenocarcinomas (EAC) have a higher methylation index than esophageal squamous cell carcinomas (ESCC). The methylation index was calculated by dividing the number of methylated gene promoters (ranging from 0 to 8) by the number of successfully tested gene promoters (usually 8). Wilcoxon rank-sum test.
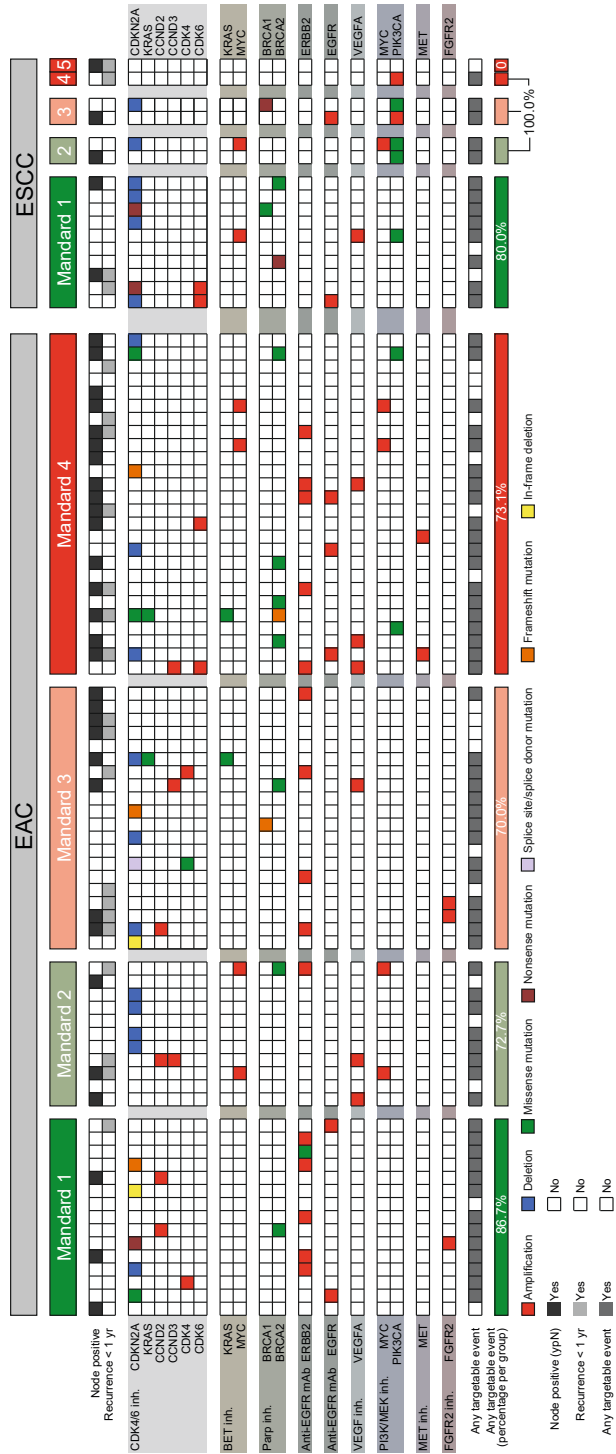
Figure S5. Targetable events in relation to histopathological response to neoadjuvant chemoradiotherapy
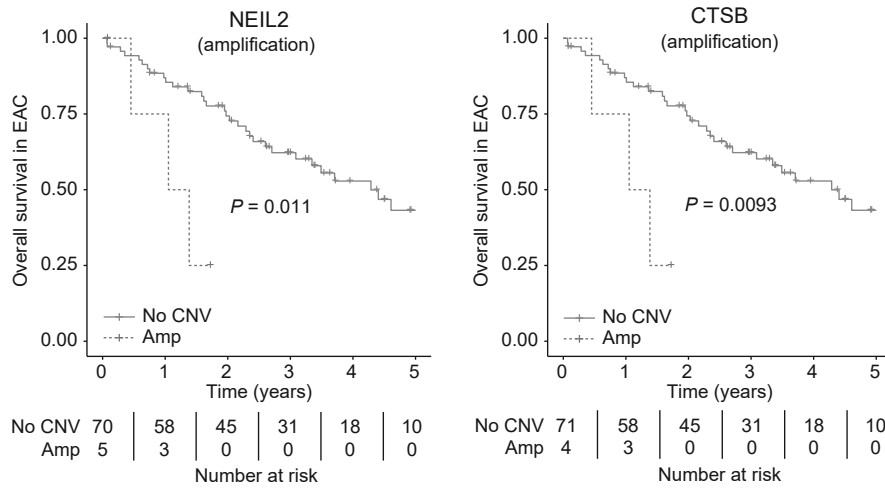
Figure S6. Additional Kaplan Meier curves: *NEIL2* and *CTSB* (colocalized with *GATA4* on 8p23.1) amplification are associated with shorter overall survival in patients with esophageal adeno-carcinoma (EAC). Log-rank test.

.

Table S1. Targeted next-generation DNA sequencing panel

|				Gene name					
AKT1	BCORL1	CDK9	EP300	GAB2	KLF12	MLL3	PCGF6	RICTOR	TERT
AKT2	BIRC5	CDKN1A	EPHB3	GATA4	KLF5	MSH2	PDCD1LG2	RNF43	TGFBR2
AKT3	BLM	CDKN1B	EPHB6	GATA6	KMT2D	MSH6	PDE4D	RPTOR	TLN1
ALK	BRAF	CDKN1C	ERBB2	GLI3	KRAS	MTOR	PDGFRA	RUNX1	TLR4
ALPK2	BRCA1	CDKN2A	ERBB2IP	GLIPR1	LARP4B	MUTYH	PDGFRB	RUNX1T1	TP53
APC	BRCA2	CDKN2B	ERBB3	GNAS	LRP1B	MYB	PGM5	RUNX3	TP63
AR	BRD4	CDKN2C	ERBB4	HES1	LRP6	MYC	PHLDA1	SFRP4	TP73
ARAF	CA9	CHL1	ETV4	HGF	MACF1	MYD88	PIK3CA	SMAD2	TRAF2
ARHGAP26	CACNA2D3	CHRD	EYA4	HLA-A	MACROD2	NEGR1	PIK3CG	SMAD3	TSC1
ARHGAP6	CASP3	CIC	FAM190A	HLA-B	MAGI3	NEIL2	PIK3R1	SMAD4	TSC2
ARID1A	CASZ1	CLDN18	FAT1	ID1	MAP2K1	NF1	PLK2	SMARCA4	USP9X
ARID1B	CCND1	CRIP1	FAT2	IDH1	MAP2K2	NFE2L2	POLB	SMARCA5	VEGFA
ARID2	CCND2	CRKL	FAT3	IDH2	MAP2K4	NKX2-1	POU5F1B	SMO	VPS13A
ATM	CCND3	CSMD1	FAT4	IGF1R	MAP3K1	NOTCH1	PREX2	SMURF1	WT1
AXL	CCNE1	CTNNA1	FBXW7	IGF2	MAP3K5	NOTCH2	PRKCi	SOHLH2	WWOX
B2M	CD274	CTNNA3	FGF19	IGF2BP3	MAP3K7	NOTCH3	PTCH1	SOX2	YAP1
BAK1	CD44	CTNNB1	FGF3	IGF2R	MAP3K8	NOTCH4	PTCH2	SOX9	ZNF217
BCL2	CDH1	CTSB	FGF4	IL8	MAP3K9	NR2F2	PTEN	SRC	ZNF750
BCL2A1	CDK1	CXCL10	FGFR1	ING5	MAPK1	NRAS	PTPN23	STAT3	
BCL2L1	CDK12	DOCK2	FGFR2	IRF2	MAPK3	PAK1	PTPRD	STAT6	
BCL2L12	CDK2	E2F1	FGFR3	JAK2	MCL1	PALB2	RASA1	STK11	
BCL2L2	CDK4	E2F3	FGFR4	KDM6A	MDM2	PARD3B	RASSF7	SYNE1	
BCL6	CDK5	EGFR	FHIT	KEAP1	MECOM	PARK2	RB1	TCF7L1	
BCL9	CDK6	ELF3	FRS2	KIF13A	MET	PAX9	RBPJ	TCF7L2	
BCOR	CDK8	ELMO1	GAB1	KIT		PBRM1	RhoA	TERC	

2

Table S2. Baseline characteristics of sequenced and unsequenced esophageal cancers

	complete series		sequenced cohort		failed sequencing cohort		P
	N = 131 (%)		*N* = 91 (%)		*N* = 39 (%)		
Age at diagnosis							
Median with range	64	(37-81)	64	(37-81)	65	(42-80)	ns
Gender							0.032*
Male	95	(72.5%)	71	(78.0%)	23	(59.0%)	
Female	36	(27.5%)	20	(22.0%)	16	(41.0%)	
Tumor type							ns
EAC	101	(77.1%)	75	(82.4%)	26	(66.7%)	
ESCC	28	(21.4%)	16	(17.6%)	12	(30.8%)	
Undifferentiated	2	(1.5%)	Excluded	(n = 1)	1	(2.6%)	
Clinical T stage							ns
T1	0	(0.0%)	0	(0.0%)	0	(0.0%)	
T2	12	(9.2%)	9	(9.9%)	3	(7.7%)	
T3	101	(77.1%)	67	(73.6%)	33	(84.6%)	
T4	10	(7.6%)	8	(8.8%)	2	(5.1%)	
Missing	8	(6.1%)	7	(7.7%)	1	(2.6%)	
Clinical N stage							ns
N0	45	(34.4%)	28	(30.8%)	17	(43.6%)	
N1	53	(40.5%)	37	(40.7%)	16	(41.0%)	
N2	24	(18.3%)	18	(19.8%)	5	(12.8%)	
N3	3	(1.5%)	2	(2.2%)	0	(0.0%)	
Missing	7	(5.3%)	6	(6.6%)	1	(2.6%)	
Resection							ns
Complete	121	(92.4%)	83	(91.2%)	37	(94.9%)	
Not complete	6	(4.6%)	4	(4.4%)	2	(5.1%)	
Missing	4	(3.1%)	4	(4.4%)	0	(0.0%)	
ypT stage							ns
ypT0	41	(31.3%)	25	(27.5%)	16	(41.0%)	
ypT1	13	(9.9%)	10	(11.0%)	3	(7.7%)	
ypT2	13	(9.9%)	7	(7.7%)	5	(12.8%)	
ypT3	61	(46.6%)	46	(50.5%)	15	(38.5%)	
Missing	3	(2.3%)	3	(3.3%)	0	(0.0%)	
ypN stage							ns
ypN0	80	(61.1%)	54	(59.3%)	26	(66.7%)	
ypN1	28	(21.4%)	20	(22.0%)	7	(17.9%)	
ypN2	16	(12.2%)	11	(12.1%)	5	(12.8%)	
ypN3	5	(3.8%)	4	(4.4%)	1	(2.6%)	
Missing	2	(1.5%)	2	(2.2%)	0	(0.0%)	

Table S2. Baseline characteristics of sequenced and unsequenced esophageal cancers (continued)

	complete series		sequenced cohort		failed sequencing cohort		
	N = 131 (%)		*N* = 91 (%)		*N* = 39 (%)		*P*
Mandard's TRG							ns
TRG 1	41	(31.3%)	25	(27.5%)	16	(41.0%)	
TRG 2	21	(16.0%)	13	(14.3%)	8	(20.5%)	
TRG 3	30	(22.9%)	22	(24.2%)	7	(17.9%)	
TRG 4	32	(24.4%)	27	(29.7%)	5	(12.8%)	
TRG 5	4	(3.1%)	1	(1.1%)	3	(7.7%)	
Missing	3	(2.3%)	3	(3.3%)	0	(0.0%)	
Prognostic Score							ns
PRSC A	48	(36.6%)	30	(33.0%)	18	(46.2%)	
PRSC B	58	(44.3%)	41	(45.1%)	16	(41.0%)	
PRSC C	22	(16.8%)	17	(18.7%)	5	(12.8%)	
Missing System	3	(2.3%)	3	(3.3%)	0	(0.0%)	
Recurrence < 1 year	34	(26.0%)	24	(26.4%)	10	(25.6%)	ns
Missing	2	(1.5%)	0	(0.0%)	2	(5.1%)	
Median OS (yrs (95% CI))	3.71	(2.3-5.1)	4.29	(2.9-5.7)	3.07	-	ns
Median DFS (yrs (95% CI))	3.53	(2.1-5.0)	3.21	(2.3-4.1)	-	-	ns
Year of surgery							0.026[†]
2005	1	(0.8%)	0	(0.0%)	1	(2.6%)	
2009	6	(4.6%)	4	(4.4%)	2	(5.1%)	
2010	17	(13.0%)	10	(11.0%)	7	(17.9%)	
2011	35	(26.7%)	24	(26.4%)	11	(28.2%)	
2012	44	(33.6%)	30	(33.0%)	14	(35.9%)	
2013	27	(20.6%)	22	(24.2%)	4	(10.3%)	
2014	1	(0.8%)	1	(1.1%)	0	(0.0%)	

2

Table S3. Genomic alterations and associations with response to neoadjuvant chemoradiotherapy in patients with esophageal adenocarcinoma.

Gene	Genetic alteration	Chromosomal location (NCBI)	N	(%)	Survival analyses			
					OS		DFS	
			N = 75					
					Mdn pos/neg (yrs)	P	Mdn pos/neg (yrs)	P
ATM	Mutation	11q22.3	5	6.67		ns		ns
BRCA2	Mutation	13q13.1	8	10.67		ns		ns
CASP3	Deletion	4q35.1	4	5.33		ns		ns
CCND1	Amplification	11q13.3	6	8.00		ns		ns
CCND2	Amplification	12p13.32	4	5.33		ns		ns
CCND3	Amplification	6p21.1	4	5.33		ns		ns
CCNE1	Amplification	19q12	4	5.33		ns		ns
CDK12	Amplification	17q12	6	8.00		ns		ns
CDKN2A	Mutation	9p21.3	10	13.33		ns		ns
CDKN2A	Deletion	9p21.3	12	16.00		ns		ns
CDKN2B	Deletion	9p21.3	10	13.30		ns		ns
CSMD1	Deletion	8p23.2	6	8.00		ns		ns
CTSB	Amplification	8p23.1	4	5.33	1.1/4.3	0.0093		ns
EGFR	Amplification	7p11.2	5	6.67		ns		ns
ERBB2	Amplification	17q12	15	20.00		ns		ns
ETV4	Amplification	17q21.31	4	5.33		ns		ns
GAB2	Amplification	11q14.1	4	5.33		ns		ns
GATA4	Deletion	8p23.1	4	5.33		0.077	NA/3.1	0.055
GATA4	Amplification	8p23.1	5	6.67	1.1/4.3	0.011		ns
GATA6	Amplification	18q11.2	11	14.67		ns		ns
IRF2	Deletion	4q35.1	5	6.67		ns		ns
KRAS	Amplification	12p12.1	11	14.67	1.4/4.4	0.0057		ns
MYC	Amplification	8q24.21	4	5.33	2.0/4.4	0.066	1.1/3.5	0.056
NEIL2	Amplification	8p23.1	5	6.67	1.1/4.3	0.011		ns
PDCD1LG2	Deletion	9p24.1	4	5.33		ns		ns
PTPRD	Deletion	9p24.1-p23	4	5.33		ns		ns
SMARCA4	Mutation	19p13.2	5	6.67		ns		ns
SMURF1	Amplification	7q22.1	4	5.33		ns		ns
TP53	Mutation	17p13.1	60	80.00	3.3/4.4	0.067	2.63/NA	0.061
VEGFA	Amplification	6p21.1	6	8.00		ns		ns

Events that occurred in ≥ 4/75 (5.3%) of patients are included. Legend on page 54

Association with histopathological response

PRSC		Mandard's TRG		Mandard's TRG		Clinical N stage		Clinical N stage		Methylation index	
A vs B vs C		1 vs 2 vs 3 vs 4		1/2/3 vs 4/5		0 vs 1 vs 2 vs 3		0 vs 1-3		*N = 65*	
St. stat	*P†*	St. stat	*P†*	OR	*P**	St. stat	*P†*	OR	*P**	Mdn pos/neg (%)	*P‡*
	ns		ns				ns		ns		ns
	ns		ns				ns	1.18	0.047	75/57	0.076
	ns		ns				ns		ns		ns
	ns		ns				ns		ns		ns
	ns	-1.86	0.072	ns			ns		ns		ns
	ns		ns				ns		ns		ns
	ns		ns				ns		ns		ns
	ns		ns				ns		ns		ns
	ns		ns				ns		ns	75/57	0.063
	ns		ns				ns		ns		ns
	ns		ns				ns		ns		ns
	ns	-2.13	0.039	ns			ns		ns		ns
	ns		ns	ns			ns		ns	86/57	0.011
	ns		ns				ns		ns		ns
	ns		ns			1.80	0.082		ns		ns
-1.89	0.078	-2.76	0.006	ns			ns		ns		ns
	ns		ns				ns		ns		ns
	ns		ns	ns			ns		ns		ns
	ns		ns	ns			ns		ns	86/57	0.002
	ns		ns	ns			ns		ns		ns
	ns		ns				ns		ns		ns
	ns		ns	ns			ns		ns		ns
	ns		ns				ns		ns		ns
	ns		ns	ns			ns		ns	86/57	0.002
	ns		ns	ns			ns		ns		ns
	ns		ns				ns		ns		ns
2.36	0.027		ns		ns		ns		ns	86/57	0.062
2.36	0.027	2.16	0.035	1.18	0.015		ns		ns		ns
	ns		ns				ns		ns		ns
	ns		ns				ns		ns		ns

Table S4. Genomic alterations and associations with response to neoadjuvant chemoradiotherapy in patients with esophageal squamous cell carcinoma.

Gene	Genetic alteration	Chromosomal location (NCBI)	N N = 16	(%)	Survival analyses			
					OS		DFS	
					Mdn pos/neg (yrs)	P	Mdn pos/neg (yrs)	P
BCL6	Amplification	3q27.3	3	18.8		ns	2.1/NA	0.074
CCND1	Amplification	11q13.3	9	56.3	NA/2.8	0.067		ns
CDKN2A	Deletion	9p21.3	6	37.5	NA/1.6	0.0057		ns
CDKN2B	Deletion	9p21.3	6	37.5		ns		ns
EGFR	Amplification	7p11.2	4	25.0		ns		ns
PIK3CA	Mutation	3q26.32	4	25.0		ns		ns
TP53	Mutation	17p13.1	12	75.0		ns		ns
TP63	Amplification	3q28	4	25.0		ns	1.5/NA	0.017

Events that occurred in ≥ 4/16 (25%) of patients are included. *BCL6* was included because of its colocalization with *TP63* and *PIK3CA* on chromosome 3p.
legend on page 54

Table S5. Gene promoter methylation status and association with response to neoadjuvant chemoradiotherapy in patients with esophageal adenocarcinoma.

Gene	Chromosomal location (NCBI)	Methylated in tumour		Methylated in normal		Survival analyses			
						OS		DFS	
		N/total	%	N/total	%	Mdn pos/neg (yrs)	P	Mdn pos/neg (yrs)	P
CDKN2A	9p21.3	21/66	31.8	0/26	0.00		ns		ns
CHFR	12q24.33	46/83	55.4	2/30	6.67		ns		ns
MGMT	10q26.3	62/85	72.9	2/30	6.67		ns		ns
MLH1	3p22.2	18/85	21.2	0/30	0.00		ns		ns
NDRG4	16q21	73/85	85.9	1/30	3.33		ns		ns
RASSF1	3p21.31	7/58	12.1	1/30	3.33		ns		ns
RUNX3	1p36.11	64/85	75.3	4/30	13.33		ns		ns
TFPI2	7q21.3	68/85	80.0	1/28	3.57		ns		ns

Results of all 8 genes in the methylation-specific PCR panel are shown.
legend on page 54

	Association with histopathological response								
PRSC		**Mandard's TRG**		**Mandard's TRG**		**Clinical N stage**		**Clinical N stage**	
A vs B vs C		1 vs 2 vs 3 vs 4 vs 5		1/2/3 vs 4/5		0 vs 1 vs 2 vs 3		0 vs 1-3	
St. stat	$P^†$	St. stat	$P^†$	OR	$P*$	St. stat	$P^†$	OR	$P*$
	ns	2.29	0.036				ns		ns
	ns		ns				ns		ns
	ns		ns				ns		ns
	ns		ns				ns		ns
	ns		ns				ns		ns
	ns		ns				ns		ns
	ns		ns				ns		ns
	ns	2.15	0.034				ns		ns

	Association with histopathological response										
PRSC		Mandard's TRG		Mandard's TRG		Clinical N stage		Clinical N stage		Clinical T stage	
A vs B vs C		1 vs 2 vs 3 vs 4 vs 5		1/2/3 vs 4/5		0 vs 1 vs 2 vs 3		0 vs 1-3		2 vs 3 vs 4	
St. stat	$P^†$	St. stat	$P^†$	OR	$P*$	St. stat	$P^†$	OR	$P^§$	St. stat	$P^†$
	ns		ns				ns		ns		ns
	ns		ns				ns		ns	-1.92	0.094
	ns		ns				ns		ns		ns
	ns		ns				ns	2.88	0.080		ns
	ns	1.97	0.050		ns		ns		ns		ns
	ns		ns				ns		ns		ns
	ns		ns				ns		ns		ns
	ns		ns				ns		ns		ns

Table S6. Gene promoter methylation status and association with response to neoadjuvant chemoradiotherapy in patients with esophageal squamous cell carcinoma.

Gene	Chromosomal location (NCBI)	Methylated in tumour		Methylated in normal		Survival analyses			
						OS		DFS	
		N/total	%	N/total	%	Mdn pos/neg (yrs)	P	Mdn pos/neg (yrs)	P
CDKN2A	9p21.3	5/12	41.7	0/26	0.00		ns		ns
CHFR	12q24.33	5/20	25.0	2/30	6.67	0.2/5.8	0.074		ns
MGMT	10q26.3	12/20	60.0	2/30	6.67		ns		ns
MLH1	3p22.2	6/20	30.0	0/30	0.00		ns		ns
NDRG4	16q21	1/20	5.0	1/30	3.33		ns		ns
RASSF1	3p21.31	3/20	15.0	1/30	3.33		ns		ns
RUNX3	1p36.11	8/20	40.0	4/30	13.33	1.5/NA	0.083	3.0/NA	0.099
TFPI2	7q21.3	2/20	10.0	1/28	3.57	0.1/5.8	0.031		ns

Results of all 8 genes in the methylation-specific PCR panel are shown.
legend on page 54

Tables S1-S6: *P*-values < 0.1 are written out, *P*-values < 0.05 in bold. *: Fisher's Exact test; †: Linear-by-linear, exact text; ‡: Wilcoxon rank-sum test; §: Chi-Squared test; OR = Odds ratio; St. stat = Standardized statistic. Mdn = Median; OS: overall survival; DFS: disease free survival; CI: confidence interval

Association with histopathological response									
PRSC		Mandard's TRG		Mandard's TRG		Clinical N stage		Clinical N stage	Clinical T stage
A vs B vs C		1 vs 2 vs 3 vs 4		1/2/3 vs 4/5		0 vs 1 vs 2 vs 3		0 vs 1-3	2 vs 3 vs 4
St. stat	$P^\dagger$	St. stat	$P^\dagger$	OR	$P*$	St. stat	$P^\dagger$	OR	$P*$	St. stat	$P^\dagger$
	ns		ns		ns		ns		ns		ns
	ns		ns		ns		ns		ns		ns
2.26	0.050	1.90	0.074		ns		ns		ns		ns
	ns		ns		ns		ns		ns		ns
	ns		ns		ns		ns		ns		ns
	ns		ns		ns		ns		ns		ns
2.26	0.050		ns		ns		ns		ns		ns
2.46	**0.042**		ns		ns		ns		ns		ns

2
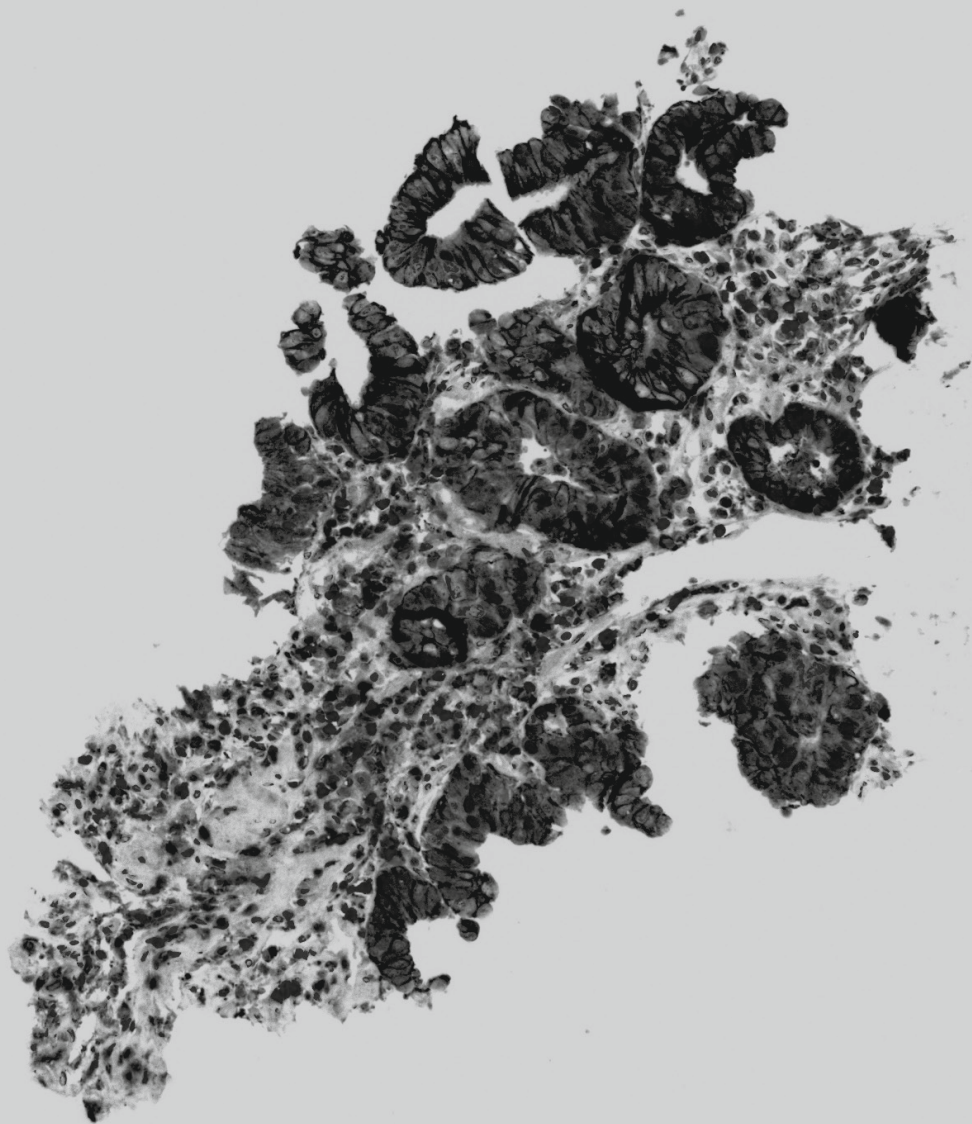
Chapter 3

Pre-treatment tumor-infiltrating T cells influence response to neoadjuvant chemoradiotherapy in esophageal adenocarcinoma

Ruben S.A. Goedegebuure*, Micalea Harrasser*, Leonie K. de Klerk, Tessa S. van Schooten, Nicole C.T. van Grieken, Merve Eken, Maeve S. Grifhorst, Noëlle Pocorni, Ekaterina S. Jordanova, Mark I. van Berge Henegouwen, Roos E. Pouw, Henk M.W. Verheul, Johannes J. van der Vliet, Hanneke W.M. van Laarhoven, Vicotr L.J.L Thijssen, Adam J. Bass, Tanja D. de Gruijl†, Sarah Derks†

* / † authors contributed equally to this article

ABSTRACT

Esophageal adenocarcinoma (EAC) is a disease with dismal treatment outcomes. Response to neoadjuvant chemoradiation (CRT) varies greatly. Although the underlying mechanisms of CRT resistance are not identified, accumulating evidence indicates an important role for local anti-tumor immunity. To explore the immune microenvironment in relation to response to CRT we performed an in-depth analysis using multiplex immunohistochemistry, flow cytometry and mRNA expression analysis (NanoString) to generate a detailed map of the immunological landscape of pre-treatment biopsies as well as peripheral blood mononuclear cells (PBMCs) of EAC patients. Response to CRT was assessed by Mandard's tumor regression grade (TRG), disease-free- and overall survival. Tumors with a complete pathological response (TRG 1) to neoadjuvant CRT had significantly higher tumor-infiltrating T cell levels compared to all other response groups (TRG 2–5). These T cells were also in closer proximity to tumor cells in complete responders compared to other response groups. Notably, immune profiles of near-complete responders (TRG 2) showed more resemblance to non-responders (TRG 3–5) than to complete responders. A high CD8:CD163 ratio in the tumor was associated with an improved disease-free survival. Gene expression analyses revealed that T cells in non-responders were Th2-skewed, while complete responders were enriched in cytotoxic immune cells. Finally, complete responders were enriched in circulating memory T cells. preexisting immune activation enhances the chance for a complete pathological response to neoadjuvant CRT. This information can potentially be used for future patient selection, but also fuels the development of immunomodulatory strategies to enhance CRT efficacy.

1. INTRODUCTION

In esophageal adenocarcinoma (EAC) and gastroesophageal junction adenocarcinomas, treatment with neoadjuvant chemoradiotherapy (CRT) with paclitaxel, carboplatin and concurrent radiotherapy followed by surgical resection has improved overall survival[1]. However, treatment responses are highly variable, with only 19% of EACs achieving a complete histopathological response after CRT[2]. Incomplete response is a strong predictor of disease recurrence and reduced survival following surgical resection[3,4]. It is still not apparent which biologic factors contribute to the variability in response, but accumulating evidence points towards a role for local anti-tumor immunity[5,6].

Over the last decades it has become recognized that radiotherapy influences the local anti-tumor immune response via several mechanisms[7], including enhanced T cell priming through immunogenic cell death and sensitization of cancer cells to T cell-mediated killing by upregulation of Fas and MHC-I[8,9]. The efficacy of radiotherapy, however, is also influenced by the composition of the preexisting tumor microenvironment (TME)[10,11]. In vivo mouse studies have identified that pre-treatment T cell features contribute to the efficacy of radiotherapy[12,13]. For example, in B16-F10 bearing mice irradiation increases antigen presenting capability along with more IFNγ-producing T cells within tumor-draining lymph nodes when compared to nonirradiated mice[14]. In another mouse model, preexisting intratumoral T cells survived irradiation up to 20 Gy and showed an improved effector function afterwards, being able to control tumor growth without new infiltrating T cells[15].

On the other hand, immunosuppressive cell types such as Th2-skewed CD4+ T cells, regulatory T cells, M2 macrophages and myeloid derived suppressor cells (MDSCs) can induce radiotherapy resistance by hampering CD8+ cytotoxic T cells, which are crucial for an effective radiotherapy-induced anti-tumor immune response[16].

How these findings translate to CRT efficacy in EAC is currently unknown. We have previously demonstrated that EACs are mostly immune cell excluded, although some degree of T cell infiltration was identified[17]. As EAC typically develops within a chronically inflamed and immunosuppressive environment characterized by PD-L2 expressing tumor cells, PD-L1 expressing immune cells, Th2-skewing and presence of tumor-promoting M2 macrophages and MDSCs[18,19], they might be resistant to CRT by nature.

In this study, we aimed to decipher the immunological characteristics of EAC in relation to response to CRT, and found that pre-treatment tumor infiltrating activated T cells were associated with a complete pathological response to neoadjuvant CRT. Given recent developments in immune modulating drugs[20], these data may not only be useful for selecting patients who may most benefit from neoadjuvant CRT, but may

also guide research and implementation of novel immunomodulatory strategies to improve outcome in localized EAC.

2. MATERIALS AND METHODS

2.1 Patient material

Patient material, as well as data on patient characteristics and disease outcome, were collected as part of an IRB-approved clinical trial (METC-VUmc identifier 2013.074). Patients with histologically confirmed, stages 2 and 3 esophagus- or gastroesophageal junction tumors were eligible for inclusion in this study. After obtaining informed consent, snap frozen, formalin-fixed paraffin embedded and fresh primary tumor biopsies were collected from the patients prior to neoadjuvant chemoradiation (paclitaxel, carboplatin and concurrent radiotherapy of 41.4 Gy in 23 fractions) during endoscopy. When possible, a heparin blood sample was obtained for isolation of plasmas and PBMCs. Only patients with adenocarcinoma who had completed the entire treatment regime (including surgery) and had sufficient quality tissue obtained were selected for further analysis. In addition, nine archival pre-treatment FFPE specimen from similar patients (previously collected for genetic profiling[21]), were included. Histology was assessed by an expert pathologist (NvG) on H&E stains from all biopsies and representative tumor areas were carefully annotated prior to processing for downstream applications.

2.2 Response evaluation

Response to neoadjuvant CRT was evaluated by Mandard's tumor regression grade (TRG) system using the post-treatment resection specimen. The Mandard's TRG score ranges from 1 (no residual cancer) to 5 (absence of regressive changes)[22]. A complete pathological response was defined as TRG 1.

2.3 Multiplex immunohistochemistry

Multiplex immunofluorescence staining was performed with the OPAL 7-color fluorescence immunohistochemistry (IHC) kit (Akoya Biosciences, USA) on 43 slides from formalin-fixed paraffin embedded tumor biopsies in 2 batches. After deparaffinization and rehydration, endogenous peroxidase was blocked with 0.3% H_2O_2 (VWR chemicals) in methanol for 20 minutes. Subsequently, an extra fixation step was included for 20 minutes with 10% neutral buffered formalin (Reagecon), followed by 2 minute rinses in Mili-Q water, then in 0.05% Tween 20 in Tris-buffered saline (TBST). The following primary antibodies were used: CK clone AE1/AE3 (Dako), CD8 clone C8/144B (Dako), CD3 polyclonal (Dako), FoxP3 clone 236A/E7 (Abcam), CD163 clone 10D6 (Novocastra) and Ki67 clone SP6 (Abcam). The following steps were repeated for each primary antibody; slides were heated in 0.05% ProClin300/Tris-EDTA buffer at pH 9.0 in an 800 W standard microwave at 100% power until boiling point (260 seconds), followed by 15 minutes at 30% power (240 W). Thereafter, slides were allowed to cool down, washed for 2 minutes

in Milli-Q at 30 rounds per minute (rpm) and 2 minutes 1× TBST at 30 rpm and then blocked with Antibody Diluent/Block (Perkin Elmer) for 10 minutes at room temperature (RT). After that, the slides were incubated with primary antibody diluted in Antibody Diluent/Block. Next, the slides were washed 3 × 2 minutes in TBST at RT and 30 rpm and were subsequently incubated with OPAL secondary antibody working solution for 15 minutes at RT. Afterward, slides were washed (same as above) and incubated with Opal fluorochromes (Opal520, Opal650, Opal570, Opal540 Opal620, and Opal690) diluted in amplification buffer for 10 minutes at RT. Slides were then washed as above. Finally, a microwave treatment with AR6 buffer was performed and the slides were rinsed for 2 minutes in Milli-Q, then in TSBT. Spectral DAPI working solution was applied for 5 minutes at RT and the slides were rinsed again in TSBT and Milli-Q, and then mounted under coverslips with ProLong Diamond anti-fade mounting medium (Life Technologies, USA). Slides were stored at 4°C until imaging.

Imaging was done on the Vectra® Polaris™ multispectral scanning microscope (Akoya Biosciences, USA). Whole slide scans were reviewed with Phenochart® (Akoya Biosciences, USA) for selection of multispectral regions. These regions were selected based on H&E stains from the same FFPE sections annotated for representative tumor areas by an expert pathologist (NvG). Three samples were excluded from further analysis because of substandard staining or tissue quality.

Multispectral images were analyzed per case in INFORM® (Akoya Biosciences, USA). First, trainable tissue segmentation based on expression of CK and DAPI was used to identify areas with tumor, stroma and no tissue. Second, adaptive cell segmentation was performed and single positive phenotypes (CD3+, CD8+, FoxP3+, CD163+, Ki67+, CK+ and Other) were identified by two researchers (ME and TvS) and reviewed by two other researchers (RG and MH); discrepancies were compared to a positive control tonsil slide and corrected upon mutual agreement between both reviewers. Third, data was exported for quantitative- and spatial analysis with the phenoptrReports package (Akoya Biosciences, USA) in RStudio version 1.2.5033 (RStudio, Inc., Boston, MA, USA). Cell densities were calculated and reported as cells per squared millimeter and cell to cell distances were compared in median micrometers. Of note, in the tumor area 55.7% (15.1 – 79.0%) of all cells were CK positive tumor cells, in contrast to 0.6% (0.0 – 2.5%) in the stromal region, confirming adequate tissue segmentation (data not sown). Heatmaps were generated by hierarchical agglomerative clustering using the Ward's minimum variance method by the Pheatmap package in RStudio version 1.2.5033 (RStudio, Inc., Boston, MA, USA).

2.4 Tumor dissociation and flow cytometry
Fresh primary tumor biopsies were collected in DMEM with 10% Fetal Calf Serum (FCS) on ice and immediately processed. After macro-dissociation with a scalpel, biopsy fragments were dissociated to a single-cell suspension on a magnet stirrer for 45

minutes at 37⁰C in the DMEM with 10% Fetal Calf Serum (FCS), DNAse type I (50 µg/ml final concentration, Roche) and Collagenase type IV (100 U/ml final concentration, Life Technologies). After 45 minutes this procedure was repeated with a fresh medium, after which cells were incubated with red blood cell lysis for 5 minutes at 4°C. After the washing step, cells were resuspended in PBS and dead? cells stained with trypan blue and counted on a hemocytometer before dividing the cells into FACS tubes for staining.

Peripheral blood mononuclear cells (PBMCs) from heparinized blood were isolated by standard Ficoll-Hypaque density centrifugation, counted and immediately frozen in FBS+10%DMSO. On the day of flow cytometry staining, PBMCs were thawed at 37°C, then incubated in RPMI+10% FCS and DNAse (final concentration 10 µg/ml) for 10 minutes at RT. After a washing step, viable cells were counted and 500,000 cells/FACS tube were used. For extracellular staining, cells were immediately incubated with antibodies for 30 minutes at 4°C. For intracellular staining (T cell panel), the cells were first permeabilized using the Foxp3/Transcription Factor Staining Buffer Set (eBioscience). The list of antibodies can be found in **Supplementary Table S10**. Data acquisition was performed on a LSRFortessa flow cytometer (BD Biosciences, CA, USA). Downstream analyses were performed using FlowJo™ Software for Windows Version 10.2.

For the PBMC analysis, 8,000 random events were collected from each sample from the manual live single cells gate (DownSampleV3 plugin) and combined together in one fcs file. Next, Phenograph was ran to determine the number of metaclusters to be created using FlowSOM plugin. Finally, tSNE algorithm was ran to visualize differences based on response and/or for each cell population. Graphs were made using GraphPad Prism version 8.2.1 (GraphPad Software, San Diego, CA, USA).

2.5 NanoString
RNA was isolated from tumor biopsies using the Qiagen RNeasy FFPE or AllPrep DNA/RNA FFPE kit (Qiagen, Germantown, MD). RNA was analyzed using the nCounter® PanCancer Immune Profiling panel (NanoString Technologies, Seattle, WA), which includes 770 genes that cover markers of different immune cell types and populations, recognized cancer antigens, and markers of key immune responses. The resulting data were analyzed with NanoString's nSolver software (version 4.0). All samples passed quality control (imaging QC, binding density QC, positive control linearity QC, and limit of detection QC). The nCounter Advanced Analysis 2.0 plugin was used for normalization, generation of gene set scores (cell types and pathways) and differential gene expression analysis. The normalization module utilizes the geNorm algorithm[23] for selection of the optimal amount of the most stable reference (housekeeping) genes. Gene sets defining cell types, signatures, and pathways can be found in **Supplementary Tables S8 and S9**. The total leukocytes (TLs) score is the average of the B, CD45+, cytotoxic, macrophage,

and T cell scores. Gene Set Enrichment Analysis was performed on the normalized count data, using the pathway gene sets as defined by NanoString[24].

2.6 Statistical analysis

Statistical analyses were performed using IBM SPSS Statistics for Windows (Version 25.0. Armonk, NY: IBM Corp.). Baseline characteristics were compared with either an independent samples t test, chi-square test or chi-square test for trend. Median cell densities and percentages were compared with a Mann-Whitney U test. Associations between cell type and pathway gene expression scores (NanoString) were tested with an independent samples t test or Mann-Whitney U test where appropriate. For Kaplan Meier survival analysis, multiplex IHC variables were dichotomized based on median and upper quartile range and subsequently compared with a logrank test. A two-sided p-value ≤ 0.05 was considered statistically significant.

3. RESULTS

3.1 Multiplex IHC identifies more abundant T cell infiltrates in complete responders.

To assess the relationship between local tumor immunity and sensitivity to neoadjuvant chemoradiotherapy (CRT), multicolor immunohistochemistry (mIHC) was performed on a series of pre-treatment biopsies of 40 EAC patients undergoing neoadjuvant CRT. Baseline characteristics are presented in **Supplementary Table S1**. Pathological response to neoadjuvant CRT was evaluated by the Mandard tumor regression grading (TRG) using the post-treatment resection specimen[22]; 30.8% of all patients had a complete histopathological response after neoadjuvant CRT (TRG 1), while 46.2% showed partial response (TRG 2-3) and 23.1% had limited to no response at all (TRG 4-5). Median disease-free survival (DFS) and overall survival (OS) were 38.5 and 67.2 months, respectively.

An average tissue area of 1.44 mm^2 from the pre-treatment biopsies, containing both tumor and stroma, was available for analysis (**Supplementary Figure S1a**). The cell densities (cells per mm^2) of T cell subtypes (CD3, CD8 and FoxP3), myeloid cells (CD163) and tumor cells (pancytokeratin (CK)), as well as their proliferation status (Ki67) and spatial distribution in tumor and stroma compartment (segmentation based on CK expression) were evaluated. Principal component analysis, performed to assess a potential batch effect between stained samples, identified one extremely inflamed outlier, which was excluded from further analyses (**Supplementary Figure S1b**). This outlier did not have microsatellite instability (MSI) or Epstein Barr virus positivity as potential explanation for its inflammatory state. Interestingly, the corresponding post-treatment resection specimen showed a large immunologically cold tumor with the absence of regressive changes (TRG 5). The discrepant results before and after CRT raise the potential for selective outgrowth of a region of tumor lacking immune infiltration.
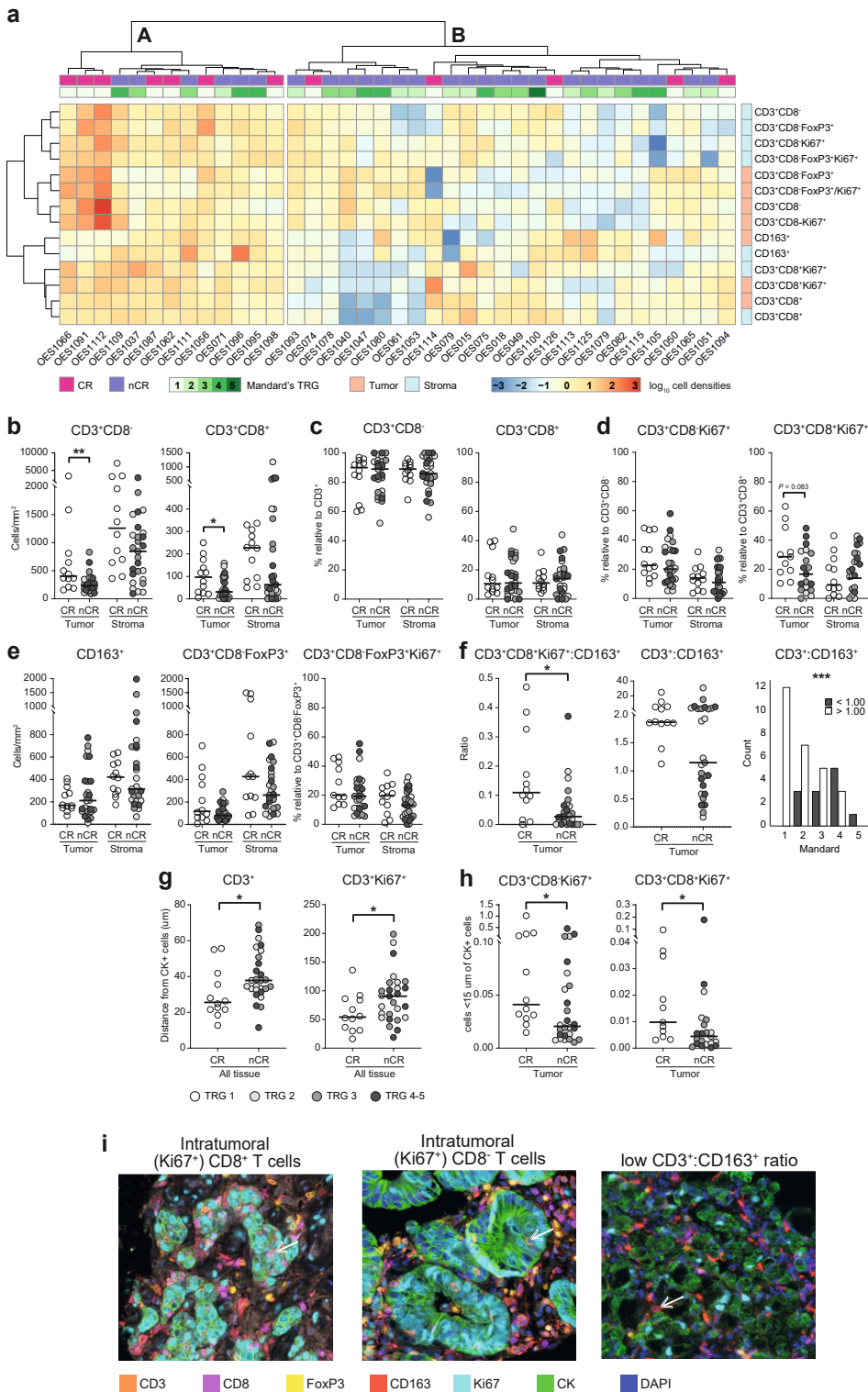
Figure 1. Multicolor IHC shows increased T cell infiltrate and importance of spatial distribution in the tumor of complete responders. Multicolor IHC panel with CD3, CD8, FoxP3, CD163, Ki67 and CK on 39 pre-treatment biopsies is shown. Unsupervised clustering analysis of cell densities for both tumor and stromal regions in **(a)** displays two distinct clusters (A and B), with TRG score (1 to 5) and response (CR, nCR) color coded. Median cell densities (cells/mm^2) were calculated and compared for CD3$^+$CD8$^-$ and CD3$^+$CD8$^+$ cells in **(b)**. Frequencies of CD8$^-$ and CD8$^+$ T cells relative to CD3 are shown in **(c)** and frequencies of proliferating (Ki67$^+$) CD8$^-$ and CD8$^+$ T cells are shown in **(d)**. Densities for CD163$^+$ myeloid cells and regulatory T cells (CD3$^+$CD8$^-$FoxP3$^+$), as well as the frequency of proliferating (Ki67$^+$) regulatory T cells is shown in **(e)**. In **(f)** the CD3$^+$CD8$^+$Ki67+:CD163$^+$ and CD3$^+$:CD163$^+$ ratios are shown. A CD3$^+$:CD163$^+$ ratio exceeding 1.0 is strongly associated with a favorable Mandard score. The distance (in µm) of T cells and proliferating T cells from CK$^+$ tumor cells is shown in **(g)**; cell numbers adjacent to CK+ tumor cells are shown in **(h)**. Panel **(i)** are representative pictures of multicolor IHC images, with from left to right tumor infiltrating CD8$^-$ T cells, CD8$^+$ T cells and a low CD3$^+$:CD163$^+$ ratio. * $P < 0.05$, ** $P < 0.005$, *** $P < 0.001$. All graphs show medians. Abbreviations: CR; complete responders, nCR; non-complete responders.

Quantitative analysis of immune cell phenotypes identified a large variation in distribution of both T cells and CD163$^+$ myeloid cells. The median density was 47 cells/mm^2 (range 0 – 831) for CD8$^+$ T cells (CD3$^+$CD8$^+$) and much higher, 509 cells/mm^2 (range 117 – 4573), for CD8$^-$ T cells (CD3$^+$CD8$^-$ cells which are mostly, but not necessarily limited to, CD4$^+$ T cells). In addition, median density for regulatory T cells (Tregs, CD3$^+$CD8$^-$FoxP3$^+$) was 182 cells/mm^2 (range 51 – 1009) and for CD163$^+$ myeloid cells 285 cells/mm^2 (range 34 – 851) (**Supplementary Figure S1c**). Of note, median T cell counts were on average 2-3 times higher in the stroma than in the tumor area, indicating an immune-excluded phenotype, as described before[17].

Since immune cells coordinately influence local immunity, unsupervised clustering analysis of cell densities was done for both tumor and stromal regions which identified two distinct clusters; cluster A, characterized by a T cell dominant immune infiltrate, and cluster B, characterized by a relative immune cell sparsity in general, except for a higher intratumoral CD163$^+$ density in 4 out of 24 cases (**Figure 1a**). Interestingly, the complete responders (CR; TRG 1) were overrepresented in cluster A (7/13 in cluster A vs. 5/26 in cluster B, $P = 0.027$, **Supplementary Table S2**), suggesting a role for T cells in response to CRT. None of the other baseline characteristics, including DFS or OS, differed significantly between patients in the two clusters.

The association between T cells and response to CRT was explored further, showing that patients with a complete histopathological response (TRG 1) had significantly higher intratumoral T cell densities in the pre-treatment biopsies compared to those with a non-complete response (nCR; TRG 2-5) ($P = 0.005$ for CD3$^+$, $P = 0.010$ for CD3$^+$CD8$^-$ and $P = 0.031$ for CD3$^+$CD8$^+$; **Figure 1b+i and Supplementary Table S3**). Of note, neither the stromal T cell densities (**Figure 1b**) nor the percentage of CD3$^+$CD8$^-$ and CD3$^+$CD8$^+$ relative to CD3 differed significantly between response groups (**Figure 1c**). We therefore questioned whether T cells were more active in complete responders but no differences in activation state was observed by assessing the proliferation marker Ki67, except for a trend toward higher intratumoral levels of proliferating CD8$^+$ T cells in CR compared to nCR ($P = 0.083$; **Figure 1d and Supplementary Table S3**).

Focusing on immune suppressive cells, which might hamper response to CRT, we found that the densities of Tregs, proliferating Tregs and CD163^{+} myeloid cells in the tumor and stromal compartments did not correlate with response (**Figure 1e and Supplementary Table S3**). However, when comparing myeloid cells relative to (proliferating) T cells, increased intratumoral CD3^{+}CD8[+](Ki67)[+]:CD163^{+} ratios in CR versus nCR were observed (P = 0.036 for Ki67^{-} and P = 0.011 for Ki67^{+} CD8^{+} T cells; **Figure 1f+i and Supplementary Table S3**). Moreover, the intratumoral ratio of CD3:CD163 exceeded 1.0 in all complete responders and was strongly associated with a favorable Mandard score (P = 0.001; **Figure 1f+i and Supplementary Table S3**), pinpointing that the balance between more pro-inflammatory and suppressive cells might be indicative for achieving a histopathological CR.

Next, the spatial relationship between tumor and immune cells was assessed by comparing the median distances from any CK[+] tumor cell to immune cells, as well as cell counts within a 15 µm radius of any CK[+] tumor cell, i.e. adjacent 'touching' cells; an indicator of increased anti-tumor immunity. In tumors of patients with CR, (proliferating) T cells were found to be in closer proximity of tumor cells compared to T cells of patients with nCR (P = 0.026 for CD3^{+} and P = 0.042 for CD3^{+}Ki67^{+}; **Figure 1g and Supplementary Table S3**). The same was observed for the number of proliferating T cells adjacent to CK^{+} tumor cells (P = 0.025 for CD8^{-} T cells, and P = 0.031 for CD8^{+} T cells; **Figure 1h, Supplementary Figure S2b and Supplementary Table S3**). For the Tregs and CD163^{+} myeloid cells no differences were seen (**Supplementary Figure S2a**).

As additional measurement of success of CRT[3,4,25], we compared immune scores to disease free survival (DFS) and overall survival (OS) and identified that a high (upper quartile) CD8^{+}:CD163^{+} ratio in the tumor was associated with an improved DFS (P = 0.050; **Supplementary Figure S3**). Also high T cell densities showed a trend toward improved DFS (P = 0.082 for CD8^{-} T cells and P = 0.054 for CD8^{+} T cells; **Supplementary Figure S3**). For Tregs and CD163^{+} myeloid cell densities no association was found. No correlations with OS were identified.

3.2 Phenotypic immune profiling with flow cytometry reveals high interpatient variability independent of response.

As multicolor IHC analyses allowed analyses of only a limited number of immune cell types we decided to perform a more detailed analyses of the tumor immune microenvironment using 13-color flow cytometry performed on fresh pre-treatment tumor biopsies of patients with CR (TRG 1, n = 9) and nCR (TRG 2-5, n = 21). Median cell viability was 69.8% (range 22.9-93.9%), resulting in a median of 12602 live single cells per patient (range 1099-133065). Based on the biopsy size, 20/30 samples were profiled by an extended T cell and myeloid panel.

Using this method, high heterogeneity in the composition of the tumor immune microenvironment between patients was observed. By looking at infiltrating immune cell subsets, we found two predominant cell populations in EAC tumors: CD11b$^+$CD14$^-$CD15$^+$ (granulocytic) gMDSCs with an overall median of 25% (range 1.9-70%, dark green bars, **Figure 2a**), and T cells with an overall median of 16.8% (range 5-40%, pink bars). In 11/20 patients gMDSCs were the most frequently occurring population, in 8/20 patients T cells were the most frequent population. gMDSC or T cell dominancy did not correlate with pathological response.

The third most frequent cell type was CD163$^+$ M2 macrophages, with a median of 5.7% (range 1.7-19.8%, dark blue bars). Other cell types identified were mMDSCs, M1 macrophages, Dendritic cells (DCs) and B cells, all with low frequencies. Nonannotated CD45$^+$ cells are likely granulocytes and neutrophils for which no antibodies were added to our panel. None of the immune cell subtypes was specifically enriched in CR or nCR.

Different from the mIHC findings, CR had a lower (but not significant) CD3:CD163 cell ratio compared to nCR (**Figure 2b**). Same results were found for CD8:CD163 ratios (**Supplementary Figure S4a**).
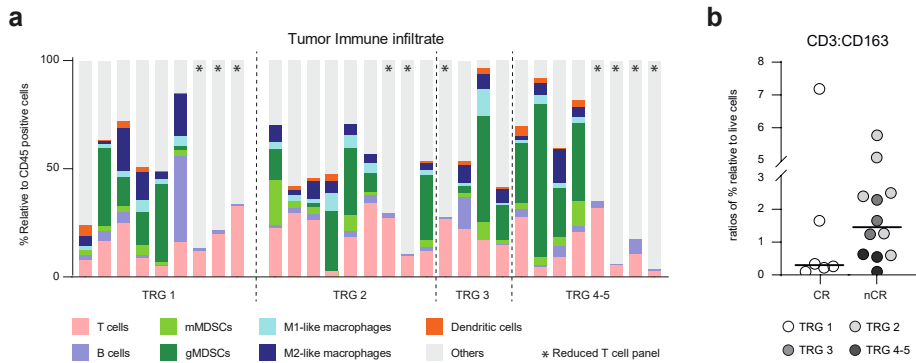

Figure 2. Flow cytometry on pre-treatment biopsies did not identify any response-specific immune signatures. Flow cytometry was performed on freshly processed pre-treatment biopsies. Patients were color coded based on TRG score (TRG 1 = CR, white circles; TRG2-5 = nCR; color-coded). Immune cell frequencies relative to CD45+ cells are shown for each patient in **(a)**. The following markers were used: CD3 for T cells, CD19 for B cells, CD11b$^+$ CD14$^+$ HLADR$^-$ for mMDSC, CD11b$^+$ CD14$^-$ CD15$^+$ for gMDSC, CD14$^{+/-}$ CD15$^-$ for macrophages, further subdivided into M1-like (CD80$^+$) and M2-like (CD163$^+$), CD11c$^-$ CD14^{high} CD19$^-$ CD1c$^+$ for DCs. Ratio of CD3+ to CD163+ cells (frequencies relative to live cells) with medians is shown in **(b)**. Mann-Whitney U was performed, all *P* values were > 0.1.

We next analyzed potential enrichment of T cell subtypes in CR or nCR and confirmed the general enrichment of CD4$^+$ T cells in 22 out of 30 patients (CD4:CD8 ratios >1, **Supplementary Figure S4b and Supplementary Table S4**). Furthermore, we identified central/effector memory dominance (high memory:naïve ratios, **Supplementary Figure S4b**) as well as proliferation (Ki67 expression) and activation in most CD4 and CD8 T cell subset (**Supplementary Figure S4c**). However, none of these T cell subtypes were enriched in one of the response groups. Additionally, (activated)Tregs were identified in 17/20 patients (>10% relative to CD4+ T cells, **Supplementary Figure S4c**), with a CD8:Treg ratio <1 in 13/30 patients (**Supplementary Figure S4b**) although once again, we found no associations with histopathological response (**Supplementary Table S4**).

3.3 mRNA expression analysis identified cytotoxic gene expression signatures in complete responders

To further investigate differences in local immunity between patients with a differential response to CRT, NanoString mRNA gene expression analysis was performed on 25 pre-treatment biopsies. Since partial responders (TRG 2 and 3) did not show a distinct immune profile in our multiplex IHC data, the opposite ends of the histopathological response spectrum were compared (TRG 1, complete responders (CR), n = 14 vs. TRG 4-5, non-responders (NR), n = 11, **Supplementary Figure S5a**). First, analysis of the cellular immune composition relative to total leukocytes (TLs; see **Supplementary Table S5** for definitions) confirmed a significant enrichment of cytotoxic cells (P = 0.026, t test) in CR compared to NR (**Figure 3a** and **Supplementary Figure S5b**). Moreover, there was a trend toward higher Th2-polarized CD4$^+$ T cell signature expression relative to total T cells in NR compared to CR (P = 0.059, t test) (**Figure 3b**).

Next, a differential gene expression analysis comparing CR and NR revealed a total of 40 significantly differentially expressed genes (**Figure 3c and Supplementary Table S6**). Although none of the associations remained significant after multiple comparison correction, it is striking that among genes upregulated in CR were several cytotoxicity-associated genes, such as granulysin, CD8A, perforin 1, granzyme H and granzyme B, as well as several interferon-induced cytokines associated with T cell chemotaxis such as CXCL9, CXCL10, and CXCL11, and their common receptor, CXCR3. Irrespective of response, CXCL9, CXCL10, and CXCL11 correlated positively with cytotoxic cells relative to TLs, and correlated negatively with Th2 cells relative to TLs, with Th2 cells relative to T cells and with Tregs relative to TLs (**Supplementary Table S7**). This suggests that CXCL9, CXCL10 and CXCL11 do indeed attract cytotoxically active T cells into the tumor. Among the genes upregulated in NR were several myeloid cell attractants such as CCL3L1 and CCL4 (both attract macrophages and DCs through interaction with CCR5) and neutrophil-attractant IL8. Moreover, NRs were enriched with antigens commonly found in myeloid cells, such as CD157 (bone marrow stromal antigen 1 (BST1); stimulator of pre-B-cell growth) and the innate pattern recognition receptor MARCO (macrophage receptor

with collagenous structure) found in macrophages. Interestingly, CLEC4A, a suppressive C-type lectin expressed in DCs upon TLR signaling, was also enriched in NRs.

Gene set pathway scoring showed a higher pathogen defense gene set score (P = 0.021, t test) in CRs, while NRs had a higher toll-like receptor signaling gene set score (P = 0.031, t test, **Figure 3d**), thereby confirming the association between activation of an innate immune response and resistance to CRT. Additional gene set enrichment analysis identified a significant enrichment of the interleukin gene set in NR (**Supplementary Figure S5c and Supplementary Table S8 and S9**).
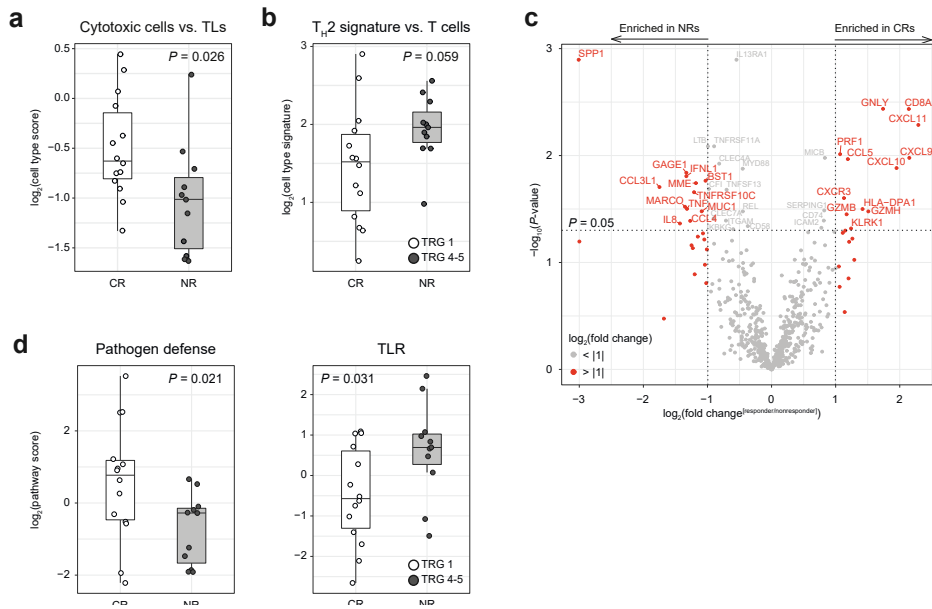
Figure 3. NanoString analysis shows an more cytotoxic cells complete responders than non-responders. NanoString gene expression analysis on mRNA from patients that were grouped based on TRG score: TRG1 = CR, TRG4-5 = NR. Cytotoxic cells relative to total leukocytes (TLs) plotted by response **(a)**. Th2 signature relative to T cells plotted by response (**b**) Volcano plot of the differential gene expression analysis, with genes with a log2 fold change between CRs and NRs greater than 1 or smaller than -1 highlighted in red **(c)**. Gene set pathway scoring analyses **(d)**.

3.4 Enrichment for circulating CD8 memory T cells in complete responders

Considering the challenges of studying the tumor immune microenvironment using fresh tumor tissue (e.g. limited material and an invasive procedure), we evaluated whether peripheral blood mononuclear cells (PBMCs) can be used as indicator of local response to CRT. Therefore, PBMCs, collected before the start of CRT, from eight complete responders (CR; TRG 1) and 18 non-complete responders (nCR; TRG 2-5) were assessed with an extensive phenotypical immune analysis using multicolor flow cytometry.

The collected data were combined and subjected to a t-distributed Stochastic Neighbor Embedding (tSNE) analysis to compare CRs versus nCRs. Next, FlowSOM was applied to identify myeloid subsets (**Figure 4a** and **Supplementary Figure S6c** for FlowSOM heatmaps and population frequencies). The most frequent myeloid subsets included monocytes (classical, intermediate-like) and neutrophils. While some populations were clearly differentially expressed between response groups (in black, purple and light green, **Figure 4a** and **Supplementary Figure S6b-c**), with manual gating we did not find correlations with histopathological response.

Next we focused on the T cell component and identified that CRs had visually enriched EM CD8+ T cells in CR, while nCR had enriched naïve CD8+ T cells. With manual gating, both populations resulted significantly enriched in CRs and nCRs, respectively ($P = 0{,}019$ for EM and $P = 0{,}016$ for naïve; **Figure 4b-c).**
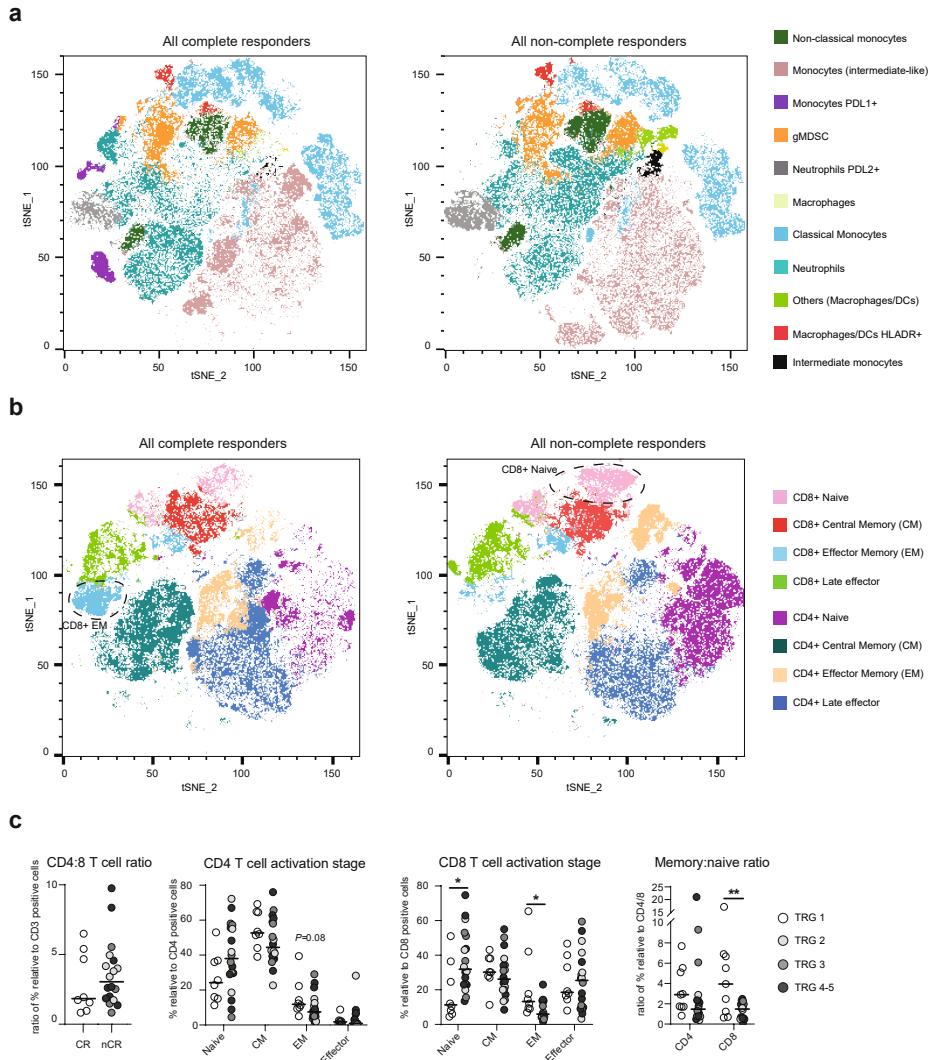
Figure 4. Flow analysis on circulating cells shows enriched CD8+ memory T cells in complete responders. Flow cytometry was performed on thawed PBMCs isolated from blood of pre-treated patients, which were grouped based on TRG score (TRG 1 = CR, white circles; TRG 2-5 = nCR, color coded in greyscale); median is shown. tSNE algorithm was performed on all samples for T cell panel and Myeloid panel following down-sampling (8,000 live cell events/sample) and concatenation. Next, FlowSOM was used to generate populations that were named based on MFI of fluorochromes used. tSNE plots of CR vs nCR showing the identified myeloid cell subsets **(a)**. Markers: CD14hiCD16- classical monocytes, CD14low CD6+ non-classical monocytes, CD14+CD16hi intermediate monocytes, CD16- CD14-/low/+ Macrophages and/or DCs, CD11b+ CD14- CD16- for gMDSC, CD16hi CD14- CD11b+ Neutrophils). tSNE plots of CR vs nCR are showing the memory status for both CD4+ and CD8+ T cells **(b)**. Ratio of CD4:CD8 frequencies relative to CD3+ T cells, CD8 and CD4 T cell activation stage, relative to CD4/8+ T cells (markers: CD27+CD45RA+ naïve, CD27+CD45RA- CM, CD27-CD45RA- EM, CD27-CD45RA+ Effector) and ratio of memory (sum of CM+EM) and naïve cell % relative to CD4/8+ T cells are all shown in **(c)**. *$P <0.05$, **$P <0.005$.

4. DISCUSSION

Accumulating evidence shows that the chance to respond to immunotherapy and conventional therapy, such as chemo- or radiotherapy, increases when there is preexisting immune cell activation in the tumor microenvironment[10–12,26]. T cells have been shown to be pivotal for effective radiotherapy and here we explore if this is also the case for EAC. Previous work in the context of esophageal cancer showed that high levels of tumor infiltrating T cells were associated with a favorable prognosis[27–30]. Using several complementary assays to characterize the pre-treatment tumor immune microenvironment of EACs, we found that localized immunity and T cell activation are associated significantly with the efficacy of therapy.

Specifically, the TME of complete responders (TRG 1) to CRT differed from non-complete responders (TRG 2-5) by having significantly higher numbers of tumor-infiltrating T cells (TILs). Recently, Göbel et al. identified low intratumoral FoxP3$^+$:CD8$^+$ ratio, high peritumoral CD163$^+$:CD68$^+$ ratio and high intratumoral TAM densities in EAC to be associated with poor tumor regression upon CRT[30]. In line with these findings we report an association between high intratumoral numbers of actively proliferating CD8$^+$ T cells and low numbers of CD163$^+$ M2 macrophages and CR and extended DFS. These results are in accordance with findings by DeNardo et al., who showed that a low CD68:CD8 ratio was associated with CR after neoadjuvant chemotherapy in breast cancer[26]. Although in this small series no associations with OS could be established, 'immunologically hot' EACs have been reported to have an increased OS compared to 'cold' tumors after neoadjuvant chemotherapy[31]. Interestingly, in our study activated/proliferating T cells were also in closer proximity to tumor cells in complete responders and higher frequencies of memory T cells were present in peripheral blood as compared to noncomplete responders. The location of TILs has been previously shown to positively affect prognosis in EAC[30] as well as in other tumor types such as colorectal cancer[32], suggesting that their location could be associated with their effector function and clinical impact.

Infiltrating regulatory T cells, higher numbers of which have been associated with advanced disease stage before treatment[33] and worse survival following CRT[34] by others, did not show correlation with pathological response in our cohort. These are all findings indicative of an enhanced preexisting activated immune response in complete responders.

The flow cytometry results on pre-treatment biopsies highlighted high variability in immune microenvironment between patients but in contrast to mIHC results no association with response to CRT. This discrepancy can potentially be explained by selective cell death of specific immune cell subsets during tumor dissociation and the lack of spatial context of immune cells, which is lost using flow cytometry.

Remarkably, near-complete pathological responders (TRG 2) displayed immune signatures resembling those of patients with a particularly unfavorable response (TRG 3-5) more than those of complete responders (TRG1), despite having a prognosis often comparable to TRG 1. Future studies should further elucidate how local immunity differs between near-complete- (TRG 2) and non-responders (TRG4-5).

For instance, the future possibility of early identification of patients likely to achieve a complete pathological response to CRT raises the question whether surgery could be omitted in selected patients. Additionally, immune signatures could be used to select patients for immune interventions to modulate the TME before CRT in order to improve response to therapy and therefore outcome. One potential immunomodulatory strategy would be to combine (chemo)radiotherapy with immune checkpoint blockade (ICB) to obtain a synergistic effect[35,36] and reinvigorate T cells. Indeed, the benefits of RT and ICB combinations have been reported in several cancer settings[37,38]; some with remarkable results. In the PACIFIC trial for example, non-small cell lung cancer patients receiving PD-L1 blockade after CRT had significantly prolonged survival compared to those receiving placebo[39]. In the context of EAC, the PERFECT study showed that compared to a propensity matched cohort of the Dutch Cancer Registry, good responders (CR) seemed to have an additional survival benefit from neoadjuvant checkpoint inhibition combined with CRT, while in NRs there was no difference in survival compared to patients receiving CRT only[40].

Recently, very promising results of the trial Checkmate-577 (adjuvant PD-1 blockade following resection of EC/Esophageal of the gastric junction cancer (EGJC) in patients with residual pathologic disease) were the first to show a statistically significant and clinically meaningful improvement in disease free survival compared to placebo (and a well-tolerated safety profile) in patients with resected EC/GEJC, who have received neoadjuvant CRT[41]. Additionally, the randomized, global phase III study CheckMate 649 showed that first line GC/GEJC/EAC patients that received PD-1 blocking NIVO + chemo had a statistically significant improvement in OS and PFS vs chemo only (when tumors expressed PD-L1)[42]. Unlike the squamous subtype[43], results from other clinical trials reported less exciting responses to PD-1 and other ICB therapies in the context of EAC (KEYNOTE-180 trial of PD-1 blockade for heavily pretreated patients with advanced, metastatic esophageal cancer[44], KEYNOTE-061 trial, with PD-1 blockade versus paclitaxel in patients with advanced gastric or GEJC that progressed on first-line chemotherapy with platinum and fluoropyrimidine[45] and anti-CTLA-4 versus best supportive care (BSC) among patients with advanced/metastatic gastric or GEJC who achieved at least stable disease with first-line chemotherapy[46]). These contrasting responses to ICB could be linked to the pre-treatment status of these patients and highlight that it is not readily apparent how to enhance anti-tumor immune responses in EAC.

3

73

In our analysis, we observed consistent expression of PD-1 and CTLA-4 by T cells in the TME; the latter was also reported by others[47,48]. The combination of PD-1 and CTLA-4 blockade before CRT could be beneficial for noncomplete responders. The same might be true for other immune checkpoint proteins of which the expression was not assessed in the current study; this could be mapped out in future research.

Gene expression analyses highlighted an enrichment of a Th2 signature in patients with a poor response (TRG 4-5), whereas a more cytotoxic environment correlated with complete response. Th2 skewed cells are generally associated with infiltration of myeloid-derived suppressor cells (MDSCs) and M2-polarized macrophages[19] that can suppress anti-tumor immunity. Moreover, tumors from non-responders were enriched in genes linked to immune suppression like CLEC4A (encoding for the suppressive receptor DCIR expressed on DCs upon TLR signaling)[49] and IL8 which promotes angiogenesis and inhibits CD8$^+$ T cell functions[50]. These findings provide a rational to test additional therapeutic strategies, such as shifting the balance from Th2 to Th1 (for example through inhibition of Notch signaling[51,52]), which can in turn affect MDSC and M2 macrophage development, or targeting M2 macrophages (for example through CXCR2 blockade[53]) that could ultimately improve response to CRT.

Together, these findings demonstrate that local immunity, and in particular T cell location, skewing and activation status, is associated with response to neoadjuvant CRT in EAC patients. Future research is needed to complement these findings and investigate prospectively whether the preexisting immune infiltrate can be used as a biomarker for selection of patients that might benefit from CRT, as well as whether neoadjuvant immunomodulatory strategies can be used to improve the outcome for patients with this deadly disease.

REFERENCES

1. Shapiro, J. *et al.* Neoadjuvant chemoradiotherapy plus surgery versus surgery alone for oesophageal or junctional cancer (CROSS): long-term results of a randomised controlled trial. *Lancet Oncol.* **16**, 1090–1098 (2015).

2. Al-Kaabi, A. *et al.* Impact of pathological tumor response after CROSS neoadjuvant chemoradiotherapy followed by surgery on long-term outcome of esophageal cancer: a population-based study. (2021) doi:10.1080/0284186X.2020.1870246.

3. van Hagen, P. *et al.* Preoperative chemoradiotherapy for esophageal or junctional cancer. *N Engl J Med* **366**, 2074–2084 (2012).

4. den Bakker, C. M. *et al.* Non responders to neoadjuvant chemoradiation for esophageal cancer: Why better prediction is necessary. *J. Thorac. Dis.* **9**, S843–S850 (2017).

5. Babar, L. *et al.* Prognostic immune markers for recurrence and survival in locally advanced esophageal adenocarcinoma. *Oncotarget* (2019) doi:10.1200/jco.2019.37.4_suppl.50.

6. Kamran, S. C. *et al.* Integrative molecular characterization of resistance to neoadjuvant chemoradiation in rectal cancer. *Clin. Cancer Res.* (2019) doi:10.1158/1078-0432.CCR-19-0908.

7. van den Ende, T. *et al.* Priming the tumor immune microenvironment with chemo(radio) therapy: A systematic review across tumor types. *Biochim. Biophys. Acta - Rev. Cancer* **1874**, 188386 (2020).

8. Garnett, C. T. *et al.* Sublethal irradiation of human tumor cells modulates phenotype resulting in enhanced killing by cytotoxic T lymphocytes. *Cancer Res.* (2004) doi:10.1158/0008-5472.CAN-04-1525.

9. Reits, E. A. *et al.* Radiation modulates the peptide repertoire, enhances MHC class I expression, and induces successful antitumor immunotherapy. *J. Exp. Med.* **203**, 1259–1271 (2006).

10. Formenti, S. C. & Demaria, S. Combining radiotherapy and cancer immunotherapy: A paradigm shift. *Journal of the National Cancer Institute* vol. 105 256–265 (2013).

11. Goedegebuure, R. S. A., De Klerk, L. K., Bass, A. J., Derks, S. & Thijssen, V. L. J. L. Combining radiotherapy with anti-angiogenic therapy and immunotherapy; A therapeutic triad for cancer? *Frontiers in Immunology* vol. 10 3107 (2019).

12. Spiotto, M., Fu, Y.-X. & Weichselbaum, R. R. The intersection of radiotherapy and immunotherapy: Mechanisms and clinical implications. *Sci. Immunol.* **1**, eaag1266 LP-eaag1266 (2016).

13. Demaria, S. & Formenti, S. C. Role of T lymphocytes in tumor response to radiotherapy. *Frontiers in Oncology* (2012) doi:10.3389/fonc.2012.00095.

14. Lugade, A. A. *et al.* Local Radiation Therapy of B16 Melanoma Tumors Increases the Generation of Tumor Antigen-Specific Effector Cells That Traffic to the Tumor. *J. Immunol.* (2005) doi:10.4049/jimmunol.174.12.7516.

15. Arina, A. *et al.* Tumor-reprogrammed resident T cells resist radiation to control tumors. *Nat. Commun.* **10**, (2019).

16. Shiao, S. L. *et al.* TH2-Polarized CD4+ T Cells and Macrophages Limit Efficacy of Radiotherapy. *Cancer Immunol. Res.* **3**, 518–525 (2015).

3

17. Derks, S. *et al.* Characterizing diversity in the tumor-immune microenvironment of distinct subclasses of gastroesophageal adenocarcinomas. *Ann. Oncol. Off. J. Eur. Soc. Med. Oncol.* **31**, 1011–1020 (2020).

18. Derks, S. *et al.* Epithelial PD-L2 expression marks Barrett's Esophagus and Esophageal Adenocarcinoma. *Cancer Immunol. Res.* 1123–1130 (2015) doi:10.1158/2326-6066.CIR-15-0046.

19. Gao, J. *et al.* Infiltration of alternatively activated macrophages in cancer tissue is associated with MDSC and Th2 polarization in patients with esophageal cancer. *PLoS One* **9**, (2014).

20. Yang, H. *et al.* The Combination Options and Predictive Biomarkers of PD-1/PD-L1 Inhibitors in Esophageal Cancer. *Front. Oncol.* **10**, 300 (2020).

21. de Klerk, L. K. *et al.* Molecular profiles of response to neoadjuvant chemoradiotherapy in oesophageal cancers to develop personalized treatment strategies. *Mol. Oncol.* (2021) doi:10.1002/1878-0261.12907.

22. Mandard, A.-M. *et al.* Pathologic assessment of tumor regression after preoperative chemoradiotherapy of esophageal carcinoma. Clinicopathologic correlations. *Cancer* **73**, 2680–2686 (1994).

23. Vandesompele, J. *et al.* Accurate normalization of real-time quantitative RT-PCR data by geometric averaging of multiple internal control genes. *Genome Biol.* **3**, (2002).

24. Subramanian, A. *et al.* Gene set enrichment analysis: A knowledge-based approach for interpreting genome-wide expression profiles. *Proc. Natl. Acad. Sci.* **102**, 15545–15550 (2005).

25. Oppedijk, V. *et al.* Patterns of recurrence after surgery alone versus preoperative chemoradiotherapy and surgery in the CROSS trials. *J. Clin. Oncol.* **32**, 385–391 (2014).

26. DeNardo, D. G. *et al.* Leukocyte complexity predicts breast cancer survival and functionally regulates response to chemotherapy. *Cancer Discov.* (2011) doi:10.1158/2159-8274.CD-10-0028.

27. Schumacher, K., Haensch, W., Röefzaad, C. & Schlag, P. M. Prognostic significance of activated CD8+ T cell infiltrations within esophageal carcinomas. *Cancer Res.* (2001).

28. Svensson, M. C. *et al.* The integrative clinical impact of tumor-infiltrating T lymphocytes and NK cells in relation to B lymphocyte and plasma cell density in esophageal and gastric adenocarcinoma. *Oncotarget* (2017) doi:10.18632/oncotarget.19437.

29. Stein, A. V *et al.* High intratumoural but not peritumoural inflammatory host response is associated with better prognosis in primary resected oesophageal adenocarcinomas. *Pathology* **49**, 30–37 (2017).

30. Göbel, H. H. *et al.* Cytotoxic and immunosuppressive inflammatory cells predict regression and prognosis following neoadjuvant radiochemotherapy of oesophageal adenocarcinoma. *Radiother. Oncol.* **146**, 151–160 (2020).

31. Humphries, M. P. *et al.* The adaptive immune and immune checkpoint landscape of neoadjuvant treated esophageal adenocarcinoma using digital pathology quantitation. *BMC Cancer* **20**, 1–11 (2020).

32. Naito, Y. *et al.* CD8+ T cells infiltrated within cancer cell nests as a prognostic factor in human colorectal cancer. *Cancer Res.* (1998).

33. Ichihara, F. *et al.* Increased populations of regulatory T cells in peripheral blood and tumor-infiltrating lymphocytes in patients with gastric and esophageal cancers. *Clin. Cancer Res.* (2003).

34. Vacchelli, E. *et al.* Immunosurveillance in esophageal carcinoma: The decisive impact of regulatory T cells. *Oncoimmunology* (2016) doi:10.1080/2162402X.2015.1064581.

35. Heinhuis, K. M. *et al.* Enhancing antitumor response by combining immune checkpoint inhibitors with chemotherapy in solid tumors. *Annals of Oncology* (2019) doi:10.1093/annonc/mdy551.

36. Kang, J., Demaria, S. & Formenti, S. Current clinical trials testing the combination of immunotherapy with radiotherapy. *J. Immunother. Cancer* **4**, 51 (2016).

37. Wang, Y. *et al.* Combining Immunotherapy and Radiotherapy for Cancer Treatment: Current Challenges and Future Directions. *Front. Pharmacol.* **9**, 1–11 (2018).

38. Dovedi, S. J. *et al.* Fractionated radiation therapy stimulates antitumor immunity mediated by both resident and infiltrating polyclonal T-cell populations when combined with PD-1 blockade. *Clin. Cancer Res.* (2017) doi:10.1158/1078-0432.CCR-16-1673.

39. Gray, J. E. *et al.* Three-Year Overall Survival with Durvalumab after Chemoradiotherapy in Stage III NSCLC—Update from PACIFIC. *J. Thorac. Oncol.* (2020) doi:10.1016/j.jtho.2019.10.002.

40. van den Ende, T. *et al.* Neoadjuvant Chemoradiotherapy Combined with Atezolizumab for Resectable Esophageal Adenocarcinoma: A Single Arm Phase II Feasibility Trial (PERFECT). *Clin. Cancer Res.* clincanres.4443.2020 (2021) doi:10.1158/1078-0432.ccr-20-4443.

41. Kelly, R. J. *et al.* Adjuvant Nivolumab in Resected Esophageal or Gastroesophageal Junction Cancer. *N. Engl. J. Med.* **384**, 1191–1203 (2021).

42. Moehler, M. *et al.* Nivolumab (nivo) plus chemotherapy (chemo) versus chemo as first-line (1L) treatment for advanced gastric cancer/gastroesophageal junction cancer (GC/GEJC)/esophageal adenocarcinoma (EAC): First results of the CheckMate 649 study. (2020) doi:10.1016/j.annonc.2020.08.2296.

43. Yamamoto, S. & Kato, K. Immuno-oncology for esophageal cancer. *Futur. Oncol.* fon-2020-0545 (2020) doi:10.2217/fon-2020-0545.

44. Shah, M. A. *et al.* Efficacy and Safety of Pembrolizumab for Heavily Pretreated Patients with Advanced, Metastatic Adenocarcinoma or Squamous Cell Carcinoma of the Esophagus: The Phase 2 KEYNOTE-180 Study. *JAMA Oncol.* (2019) doi:10.1001/jamaoncol.2018.5441.

45. Shitara, K. *et al.* Pembrolizumab versus paclitaxel for previously treated, advanced gastric or gastro-oesophageal junction cancer (KEYNOTE-061): a randomised, open-label, controlled, phase 3 trial. *Lancet* (2018) doi:10.1016/S0140-6736(18)31257-1.

46. Bang, Y. J. *et al.* Efficacy of sequential ipilimumab monotherapy versus best supportive care for unresectable locally advanced/metastatic gastric or gastroesophageal junction cancer. *Clin. Cancer Res.* (2017) doi:10.1158/1078-0432.CCR-17-0025.

47. Kelly, R. J. *et al.* The dynamic and transient immune microenvironment in locally advanced esophageal adenocarcinoma post chemoradiation. *Ann. Surg.* (2018) doi:10.1097/SLA.0000000000002410.

48. Jinhua, X. *et al.* Expression of immune checkpoints in T cells of esophageal cancer patients. *Oncotarget* (2016) doi:10.18632/oncotarget.11611.

49. Uto, T. *et al.* Clec4A4 is a regulatory receptor for dendritic cells that impairs inflammation and T-cell immunity. *Nat. Commun.* (2016) doi:10.1038/ncomms11273.

50. Lin, C. *et al.* Tumour-associated macrophages-derived CXCL8 determines immune evasion through autonomous PD-L1 expression in gastric cancer. *Gut* **68**, 1764–1773 (2019).

3

51. Li, Q. *et al.* Down-regulation of Notch signaling pathway reverses the Th1/Th2 imbalance in tuberculosis patients. *Int. Immunopharmacol.* **54**, 24–32 (2018).

52. Hu, C. *et al.* Glucocorticoids Modulate Th1 and Th2 Responses in Asthmatic Mouse Models by Inhibition of Notch1 Signaling. *Int. Arch. Allergy Immunol.* **175**, 44–52 (2018).

53. Di Mitri, D. *et al.* Re-education of Tumor-Associated Macrophages by CXCR2 Blockade Drives Senescence and Tumor Inhibition in Advanced Prostate Cancer. *Cell Rep.* (2019) doi:10.1016/j.celrep.2019.07.068.

SUPPLEMENTARY MATERIAL

A selection of supplementary figures S1 to S6 and tables S1 to S4 can be found in this thesis; a complete overview of supplementary material can be found in the online publication at https://www.tandfonline.com/doi/full/10.1080/2162402X.2021.1954807
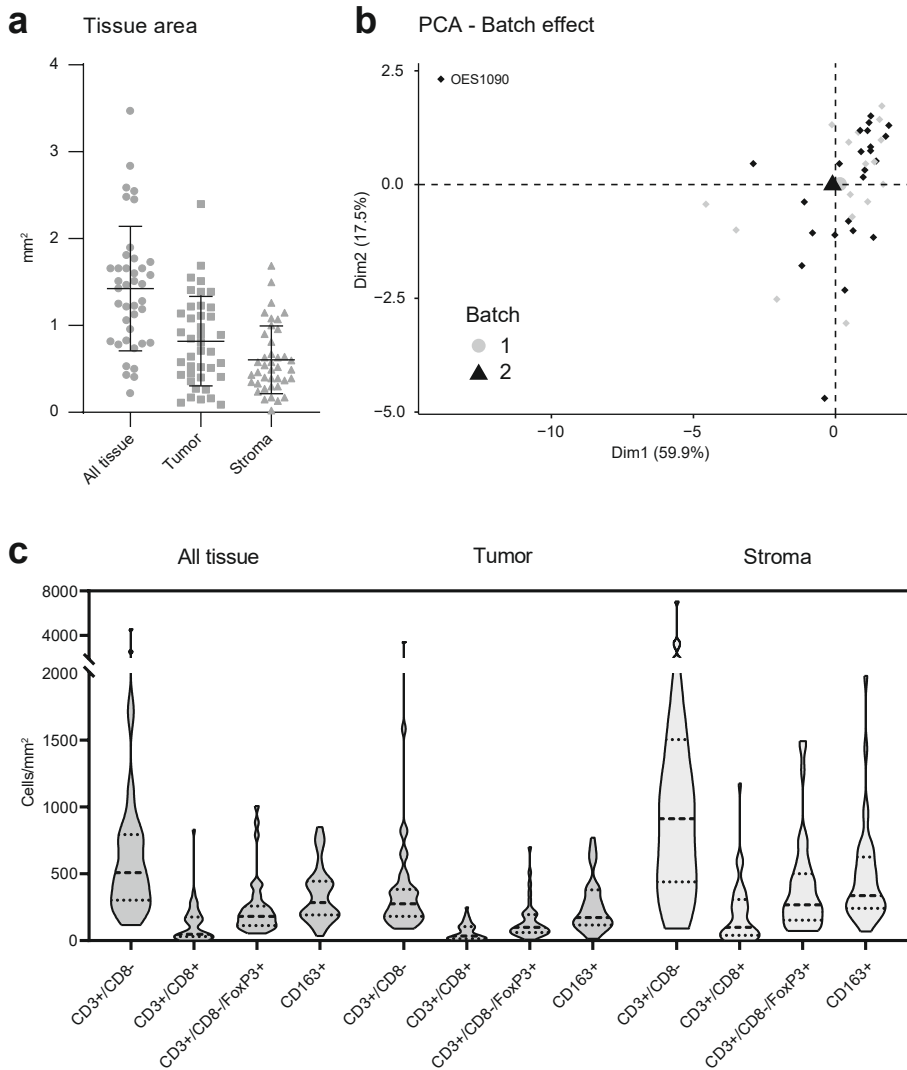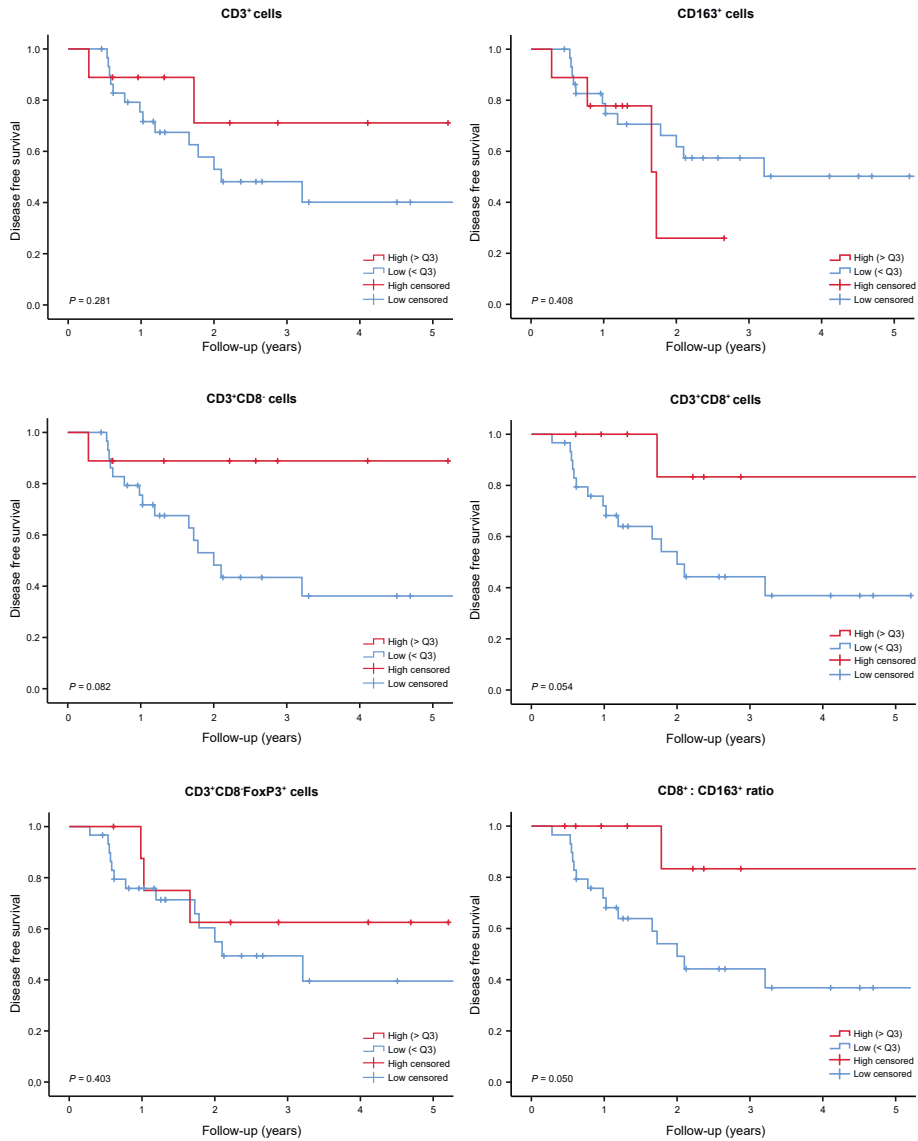

Supplementary Figure 1. PCA on multicolor IHC dataset identifies an outlier. Multicolor IHC panel with CD3, CD8, FoxP3, CD163, Ki67 and CK) on 39 pre-treatment biopsies is shown. The average tissue area was analyzed by a pathologist before staining with mm^2 values shown in **(a)**. PCA analysis between the two batches highlighted one outlier (OES1090) that was excluded from further analyses and is shown in **(b)**. Identified cells (x axis) and respective densities (mm^2) in all tissue, tumor and stroma are shown in **(c)**.

a

b
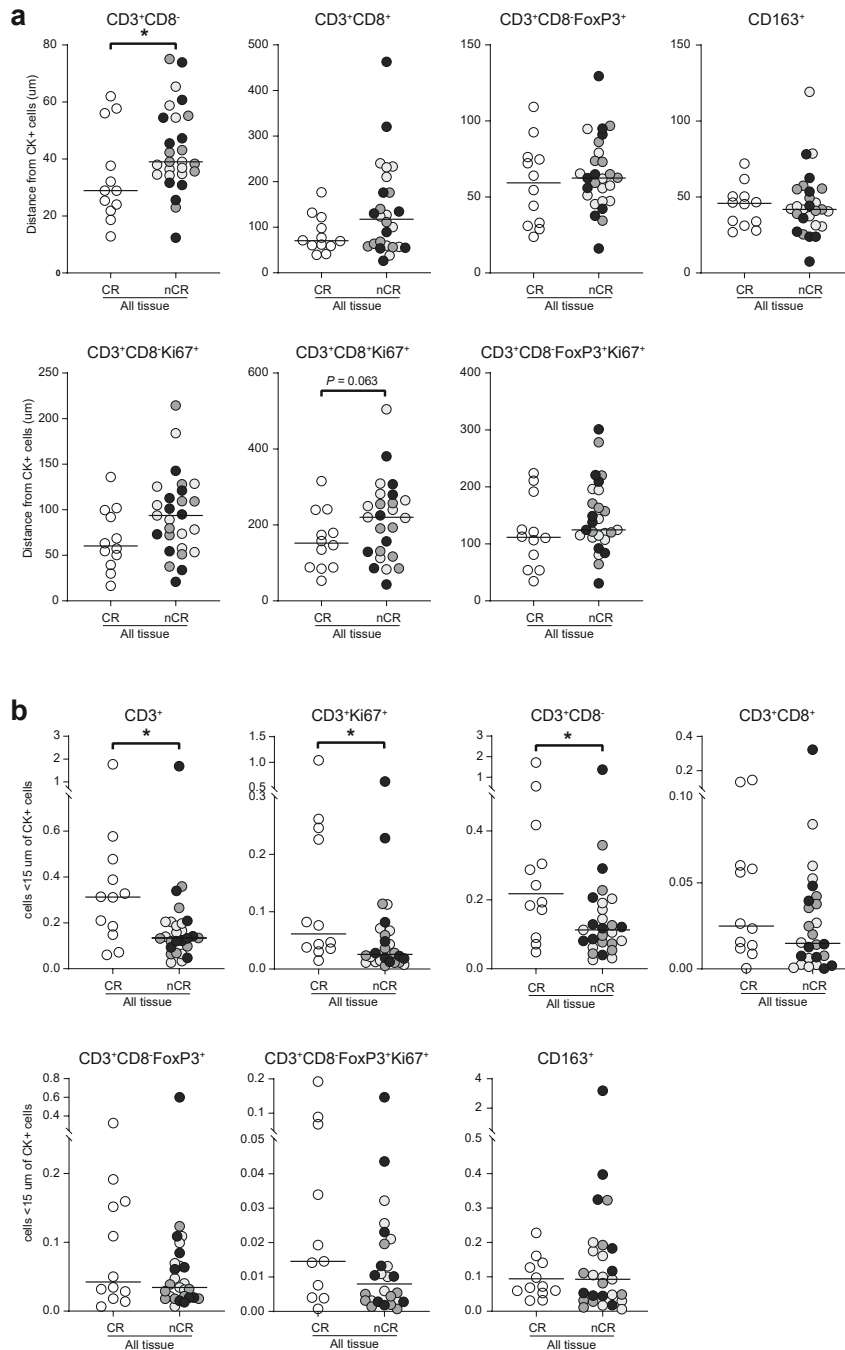
Supplementary Figure 2. multicolor IHC spatial distribution analysis highlights differences between response groups. Spatial analysis of the multicolor IHC panel with CD3, CD8, FoxP3, CD163, Ki67 and CK) on 39 pre-treatment biopsies is shown. Distance (micron) of cells from CK+ tumor cells is shown in **(a)**. Cell numbers adjacent to CK+ tumor cells are shown in **(b)**. *P <0.05

Supplementary Figure 3. Correlation between disease free survival and cell densities. Disease-free survival (DFS) of the multicolor IHC patient cohort was assessed. Cell frequencies/densities were divided into 4 and the upper quartile (high, >Q3) was compared to the rest (low, <Q3). Kaplan Meyer curves are shown for the following cell densities: CD3+ cells, CD163+ cells, CD3+CD8- cells, CD3+CD8+ cells, CD3+CD8-FoxP3+ and for CD8:CD163 ratio. *P = 0.05.

a

b

c


○ TRG 1   ○ TRG 2   ◑ TRG 3   ● TRG 4-5
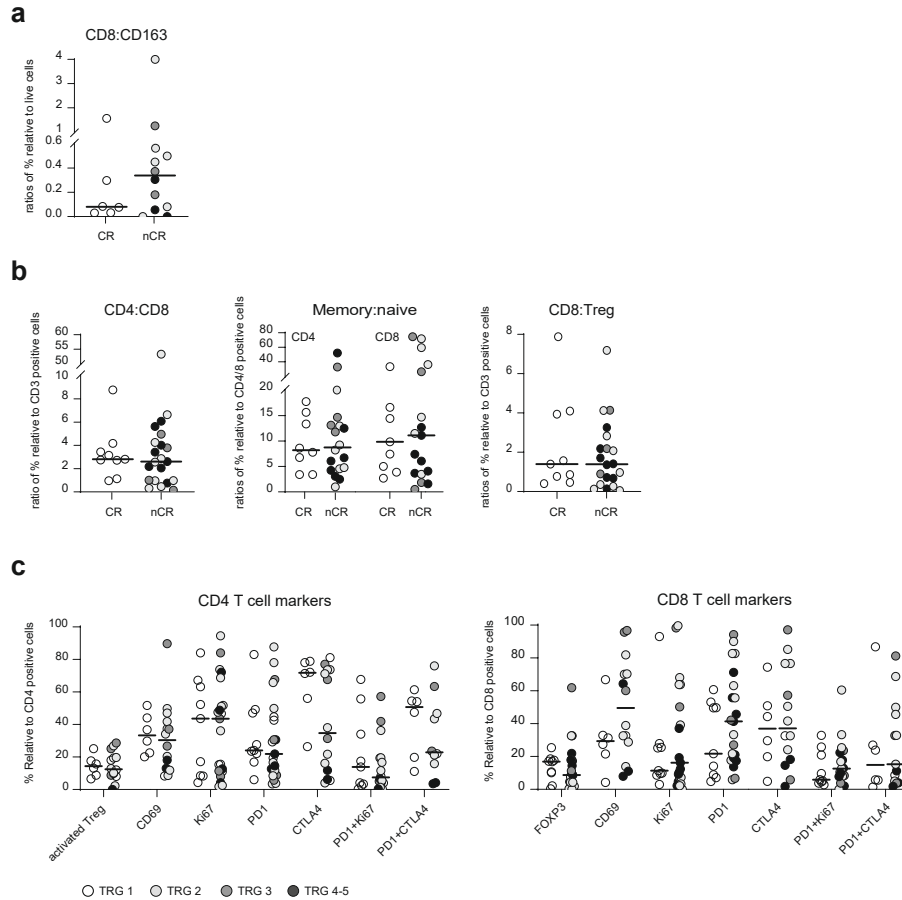
Supplementary Figure 4. Flow cytometry analysis of the tumor immune microenvironment. Flow cytometry was performed on freshly processed pre-treatment biopsies. Data was grouped and color-coded based on response: CR (TRG 1, white dots) and nCR (TRG 2-5, greyscale). Ratio of CD8$^+$:CD163$^+$ cell frequencies **(a)**. Ratios of CD4$^+$:CD8$^+$ cells, of memory (sum of CM+EM) versus naïve CD4/8$^+$ cells and ratio of CD8$^+$:Treg$^+$ frequencies are shown in **(b)**. Surface marker expression for CD4$^+$ T cells and CD8$^+$ T cells are shown in **(d)**. Activated T regs are defined as CD45RA$^-$ FoxP3^{hi}. Mann Whitney U was applied, all P values are >0.1.

a
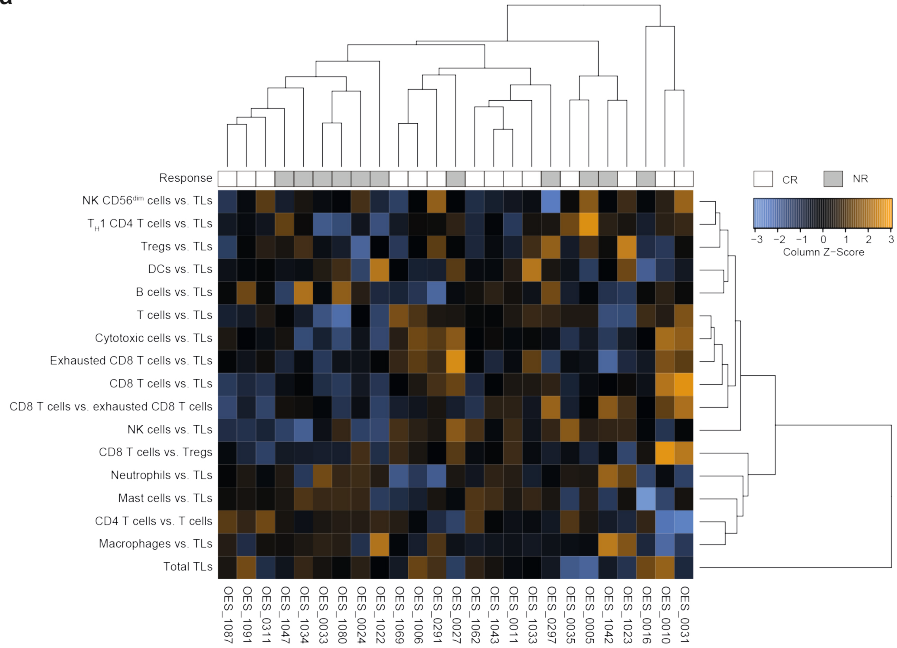
b

c
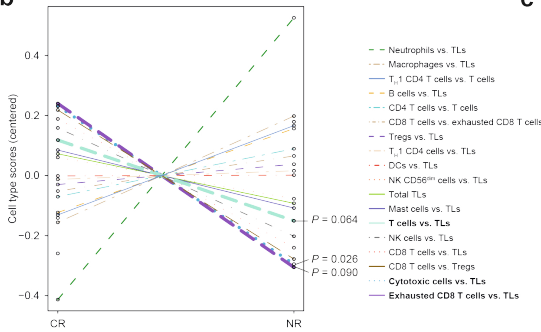
Supplementary Figure 5. NanoString gene expression analysis overview. NanoString gene expression analysis. Patients were grouped based on TRG score: TRG1 = CR, TRG4-5 = NR. Heatmap showing a summary of the immune cell composition relative to total leukocytes (TLs) **(a)**. Overview of the difference in cell types between the response groups **(b)**. Interleukin gene set enrichment analysis **(c)**.

Supplementary Figure 6. Flow cytometry analysis on PBMCs, heatmaps statistics in the tSNE maps and FlowSOM populations. Flow cytometry was performed on thawed PBMCs isolated from blo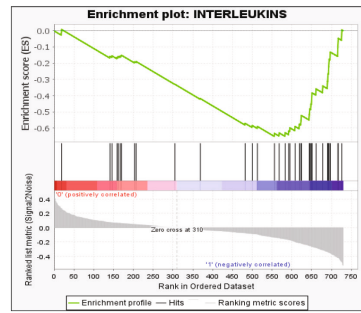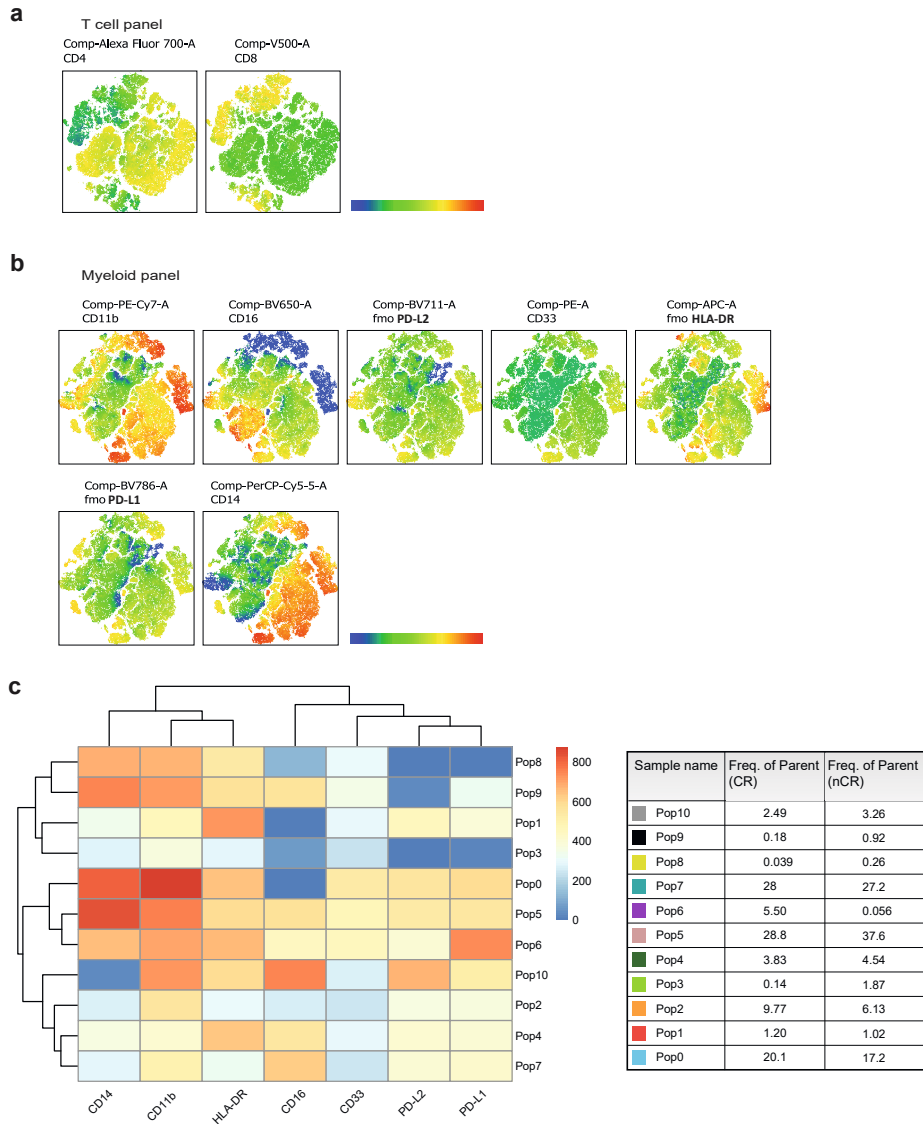od of pre-treated patients. tSNE algorithm was performed on all samples following down-sampling (8,000 live cell events/sample) and concatenation. Following tSNE analysis on all samples regardless of response, heatmap statistics were generated to show patterns of expression of each channel/maker (not specified: APC: HLADR, BV711: PDL2, BV786: PDL1) for two panels, one general **(a)**, and a T cell focused **(b)**. From FlowSOM plugin, the frequency for each patient was calculated and plotted using the same grouping and color coding for response, with the trends and significantly different populations showed in **(c)**, *P < 0.05.

Table S1 and S2. Baseline characteristics

	Total	Cluster A	Cluster B	*Cluster A vs B*	
	N=40	N=13	N=26	*P-value*	*Statistical test*
Age at diagnosis					
Median with range	65.0 (46-79)	61.0 (48-75)	66.5 (46-79)	*ns*	*student T-test*
Gender				*ns*	*chi-square test*
Male	34 (85.0%)	11 (84.6%)	22 (84.6%)		
Female	6 (15.0%)	2 (15.4%)	4 (15.4%)		
Clinical T stage				*ns*	*chi-square test for trend*
T1	0 (0.0%)	0 (0.0%)	0 (0.0%)		
T2	3 (7.5%)	2 (15.4%)	1 (3.8%)		
T3	35 (87.5%)	11 (84.6%)	23 (88.5%)		
T4	0 (0.0%)	0 (0.0%)	0 (0.0%)		
Missing	2 (5.0%)	0 (0.0%)	2 (7.7%)		
Clinical N stage				*ns*	*chi-square test for trend*
N0	13 (32.5%)	6 (46.2%)	7 (26.9%)		
N1	15 (37.5%)	2 (15.4.3%)	13 (50.0%)		
N2	7 (17.5%)	3 (23.1%)	4 (15.4%)		
N3	3 (7.5%)	2 (15.4.3%)	0 (0.0%)		
Missing	2 (5.0%)	0 (0.0%)	2 (7.7%)		
Location				*ns*	*chi-square test*
Mid esophagus	1 (2.5%)	0 (0.0%)	1 (3.8%)		
Distal esophagus	29 (72.5%)	12 (92.3%)	16 (61.5%)		
Gastro-esophageal junction	10 (25.0%)	1 (7.7%)	9 (34.6%)		
ypT stage				*ns*	*chi-square test for trend*
ypT0	12 (30.0%)	7 (53.8%)	5 (19.2%)		
ypT1	11 (27.5%)	2 (15.4.3%)	9 (34.6%)		
ypT2	4 (10.0%)	1 (7.7%)	3 (11.5%)		
ypT3	12 (30.0%)	3 (23.1%)	8 (30.8%)		
ypT4	1 (2.5%)	0 (0.0%)	1 (3.8%)		
Missing	0 (0.0%)	0 (0.0%)	0 (0.0%)		

3

Table S1 and S2. Baseline characteristics (continued)

	Total	Cluster A	Cluster B	Cluster A vs B	
	N=40	N=13	N=26	*P-value*	*Statistical test*
ypN stage				*ns*	*chi-square test for trend*
ypN0	27 (67.5%)	10 (76.9%)	16 (61.5%)		
ypN1	5 (12.5%)	1 (7.7%)	4 (15.4%)		
ypN2	6 (15.0%)	1 (7.7%)	5 (19.2%)		
ypN3	2 (5.0%)	1 (7.7%)	1 (3.8%)		
Missing	0 (0.0%)	0 (0.0%)	0 (0.0%)		
Mandard score				*ns*	*chi-square test for trend*
TRG 1	12 (30.0%)	7 (53.8%)	5 (19.2%)		
TRG 2	10 (25.0%)	1 (7.7%)	9 (34.6%)		
TRG 3	8 (20.0%)	2 (15.4.3%)	6 (23.1%)		
TRG 4	8 (20.0%)	3 (23.1%)	5 (19.2%)		
TRG 5	2 (5.0%)	0 (0.0%)	1 (2.6%)		
Missing	0 (0.0%)	0 (0.0%)	0 (0.0%)		
Complete response				*P = 0.027*	*chi-square test*
TRG1	12 (30.0%)	7 (53.8%)	5 (19.2%)		
TRG2-5	28 (70.0%)	6 (46.2%)	21 (80.8%)		
Survival					
Median DFS (months + 95% CI)	38.5 (NA)	20.7 (NA)	38.4 (NA)	*p = 0.377*	*log rank test*
Median OS (months + 95% CI)	67.2 (0.0-137.3)	Not reached	26.4 (0.0-70.3)	*p = 0.153*	*log rank test*

DFS: disease free survival, OS: overall survival, CI: confidence interval

Table S3. Multicolor IHC results

	Tumor (p-values)						Stroma (p-values)			Spatial (p-values)	
	TRG	TRG	TRG	TRG	DFS	OS	TRG	TRG	TRG	Distance	Radius
	1vs2345	*12vs345*	*123vs45*				*1vs2345*	*12vs345*	*123vs45*		
Cell type											
CD3+	0.005	0.092	ns	-	ns	ns	0.065	ns	ns	0.026	0.013
CD3+CD8-	0.010	ns	ns	-	0.082	ns	0.052	ns	ns	0.048	0.031
CD3+CD8+	0.031	ns	ns	-	0.054	ns	ns	ns	ns	ns	ns
CD3+CD8-FoxP3+	ns	ns	ns	-	ns	ns	ns	ns	ns	ns	ns
CD163+	ns	ns	ns	-	ns	ns	ns	ns	ns	ns	ns
Proliferation state											
CD3+Ki67+	ns	ns	ns	-	ns	ns	ns	ns	ns	0.042	0.018
CD3+CD8-Ki67+	ns	ns	ns	-	ns	ns	ns	ns	ns	0.065	0.025
CD3+CD8+Ki67+	0.083	ns	ns	-	ns	ns	ns	ns	ns	ns	0.031
CD3+CD8-FoxP3+Ki67+	ns	ns	ns	-	ns	ns	ns	ns	ns	ns	ns
T cell : myeloid ratio											
CD3+CD8+:CD163+	0.036	ns	ns	-	0.050	ns	0.074	ns	ns	-	-
CD3+CD8+Ki67+:CD163+	0.011	ns	ns	-	ns	ns	ns	0.048	ns	-	-
CD3+:CD163+ >1.0	-	-	-	0.001	ns	ns	-	-	-	-	-

TRG = Mandard's Tumor Regression Grade, DFS = Disease Free Survival, OS = Overall Survival. ns = not significant
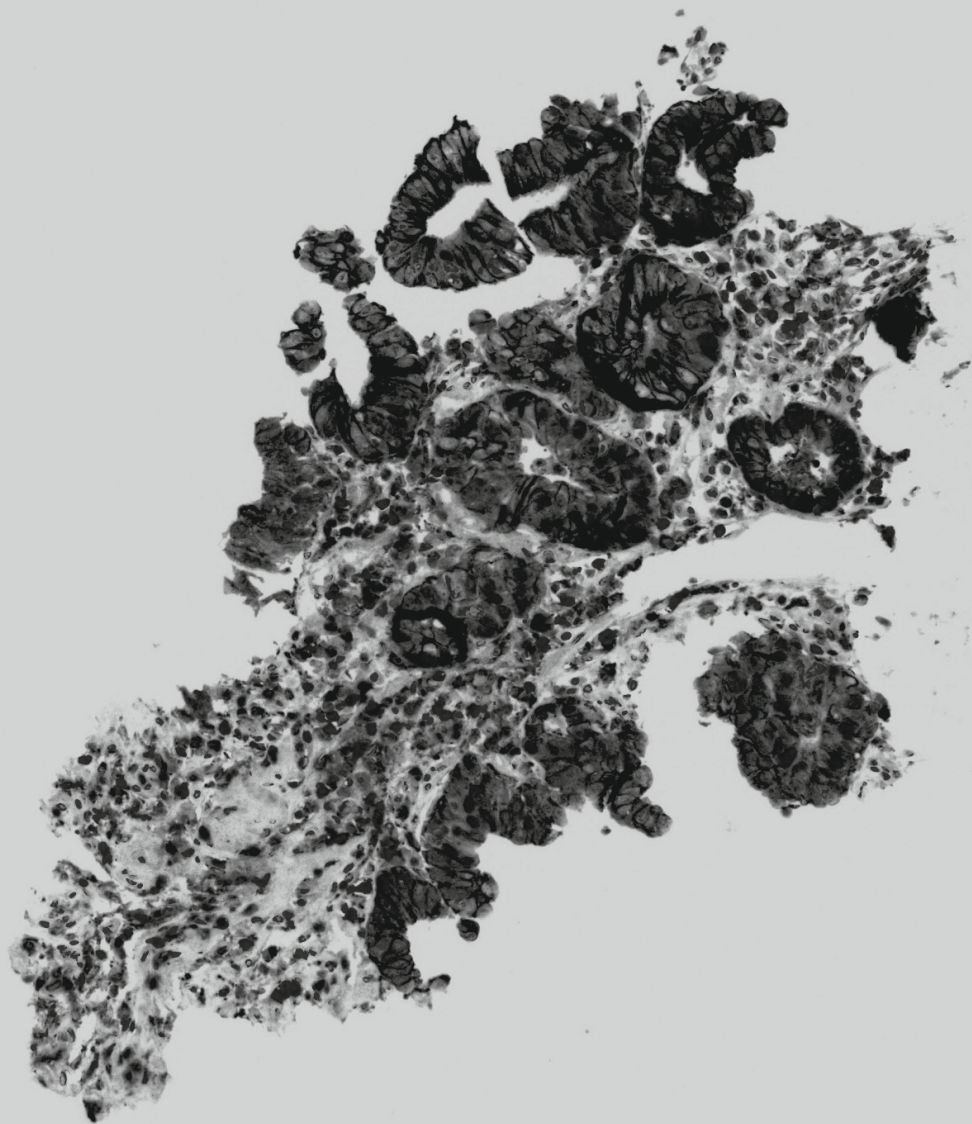
3

Table S4. Flow cytometry results

| | PBMCs | | Biopsies | |
Markers	*TRG 1vs2345*	Markers	*TRG 1vs2345*
CD3	0.003	CD4	0.773
CD4	0.070	CD8	0.364
CD8	0.083	CD4 Ki67	0.912
CD4 naïve	0.048	CD4 PD1	0.712
CD4 CM	0.021	CD4 PD1Ki67	0.815
CD4 EM	0.099	activeTregs	0.624
CD4 naïve/CM	0.011	CD4 PD1CTLA4	0.439
Treg	0.458	CD8 naïve	0.116
activeTreg	0.048	CD8 CM	0.165
CD4 HLADR	0.248	CD8 EM	0.026
CD4 CTLA	0.231	CD8 Effector	0.643
CD4 PD1	0.680	CD8 Ki67	0.658
CD8 naive	0.017	CD8 PD1	0.039
CD8 CM	0.284	CD8 PD1Ki67	0.105
CD8 EM	0.017	CD8 PD1CTLA4	0.071
CD8 Effector	0.869	CD8 CTLA4	0.540
CD8 memory:naïve ratio	0.005	CD8 CD69	0.153
CD4 memory:naïve ratio	0.032		
CD8 FoxP3	0.008		
CD8 Ki67	0.592		
CD8 CD28	0.187		
CD8 CTLA4	0.063		
CD8 LAG3	0.364		

Statistical test: Non Parametric Mann-Whitney
P value: Asymp. Sig. (2-tailed)
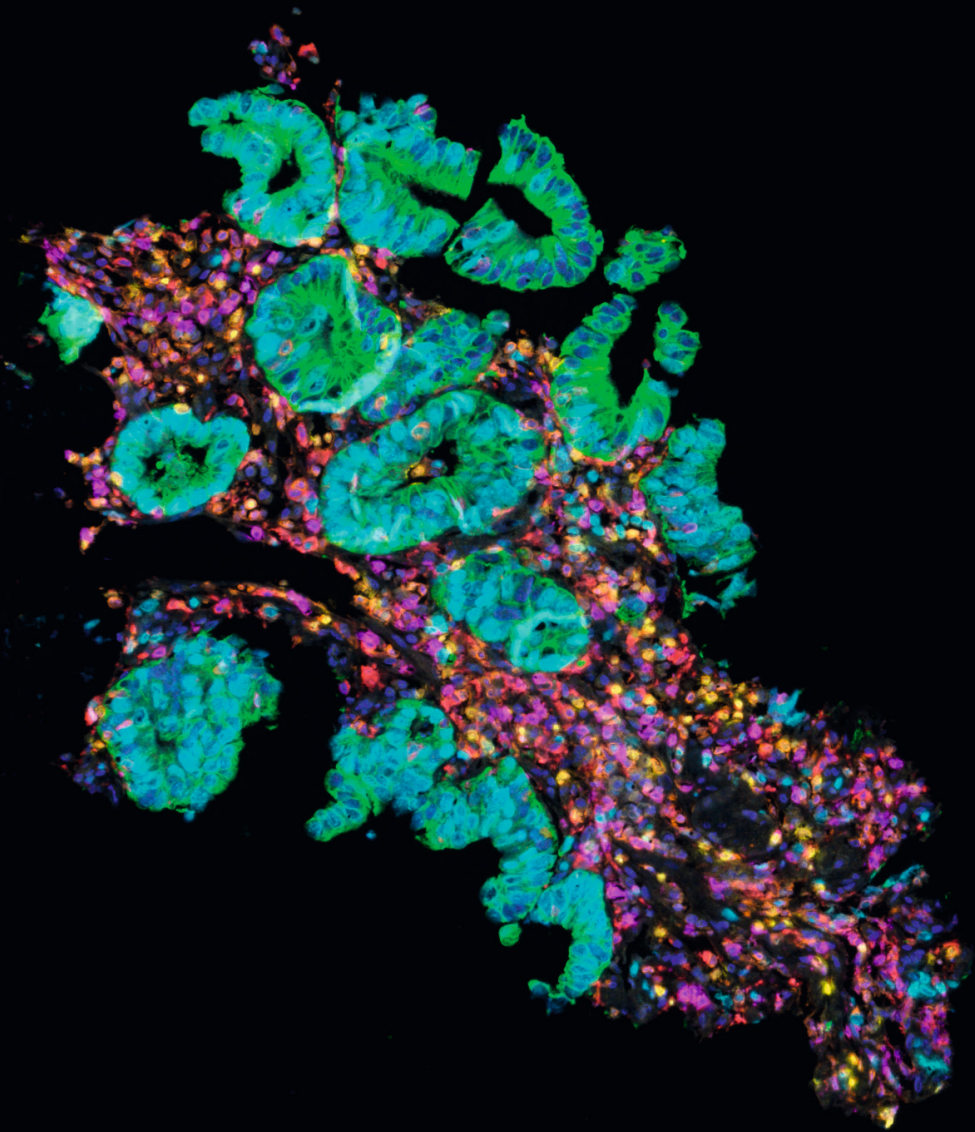
3

PART II

Elucidating molecular and immunological responses occurring upon fractionated radiotherapy; towards novel and improved combination treatments

Chapter 4

Combining radiotherapy with anti-angiogenic therapy and immunotherapy; a therapeutic triad for cancer?

Ruben S.A. Goedegebuure*, Leonie K. de Klerk*, Adam J. Bass, Sarah Derks†, Victor L.J.L. Thijssen†

* / † authors contributed equally to this article

ABSTRACT

Radiotherapy has been used for the treatment of cancer for over a century. Throughout this period, the therapeutic benefit of radiotherapy has continuously progressed due to technical developments and increased insight in the biological mechanisms underlying the cellular responses to irradiation. In order to further improve radiotherapy efficacy, there is a mounting interest in combining radiotherapy with other forms of therapy such as anti-angiogenic therapy or immunotherapy. These strategies provide different opportunities and challenges, especially with regard to dose scheduling and timing. Addressing these issues requires insight in the interaction between the different treatment modalities. In the current review, we describe the basic principles of the effects of radiotherapy on tumor vascularization and tumor immunity and vice versa. We discuss the main strategies to combine these treatment modalities and the hurdles that have to be overcome in order to maximize therapeutic effectivity. Finally, we evaluate the outstanding questions and present future prospects of a therapeutic triad for cancer.

INTRODUCTION

Radiotherapy has been an integral part of cancer treatment for over a century. More than half of all cancer patients undergo radiotherapy at some stage during treatment, either with curative intent, or in a palliative setting once the possibility for cure has been lost[1,2]. Radiotherapy was introduced shortly after the discovery of X-rays and gamma-rays in the late 19th century. Patients with different types of cancer were treated with radiotherapy, resulting in a paradigm shift in cancer therapy[3,4]. Since then, the clinical benefit of radiotherapy continuously improved, both by technical advancements and by increased insight in the biology behind the radiation response. For example, optimized treatment planning and more precise delivery techniques have made it possible to safely increase the tumor-targeted radiation dose while sparing the surrounding normal tissues. In addition, research into the cellular effects of ionizing radiation has provided detailed understanding of e.g. the cell cycle, apoptosis and DNA repair. This has offered insight in optimal dose-scheduling of radiotherapy[3]. For example, the advantages of delivering a high dose of irradiation in multiple smaller fractions was already recognized in the 1930's[5]. Further research has resulted in the definition of 'the five Rs of radiobiology' which represent five different cellular aspects that affect the efficacy of fractionated irradiation and that later have been exploited to develop combination therapies[6,7] (**Box 1**).

4

Box 1. The 5 Rs of radiotherapy

The 5 Rs of radiotherapy represent a conceptual framework that form the rationale behind fractionation of radiotherapy. The 5 Rs are: Repair, Redistribution, Reoxygenation, Repopulation, and Radiosensitivity. **Repair** is the one of the primary reasons to fractionate radiotherapy. By applying fractionated radiotherapy, normal cells have the opportunity to repair sublethal DNA damage between each fraction while cancer cells are unable to sufficiently repair DNA damage due to defective or suppressed repair pathways. **Redistribution** relates to the ability of cells to progress in the cell cycle. Cells in S-phase are typically radioresistant, while cells in late G_2 and M phase are relatively sensitive. Fractionated application of irradiation increases the chance that cells that were in a radioresistant phase at one fraction have ‹redistributed› to a radiosensitive phase at the following fraction. **Reoxygenation** is related to the dynamic and changing hypoxic status of tumor tissue. Fractionated radiotherapy increases the chance that all areas of the tumor tissue receive a dose of irradiation when oxygenation is improved. **Repopulation** refers to the increase in cell division that is seen in normal and cancer cells after radiation. Cells that proliferate between fractions increases the number of cells that have to be killed by radiotherapy. Consequently, repopulation is affected by the time between fractions. **Radiosensitivity** refers to the intrinsic radiosensitivity or radioresistance of different cell types. It influences the total dose that is required for a given level of damage.

Initially, radiobiology research was mainly focused on the cancer cells without appreciating the role of the tumor microenvironment. However, over the past decades it has become clear that components within the tumor microenvironment such as the

tumor vascular bed and tumor infiltrating immune cells have a pivotal impact on radiotherapy efficacy[5]. For instance, radiotherapy can exert opposing effects on tumor vascularization and perfusion depending on dose-scheduling[8,9]. In addition, the abscopal effect, i.e. the observation that local tumor irradiation can also lead to regression of distant tumor masses, has been linked to the immune system[10]. Consequently, both anti-angiogenic therapy and immunotherapy are evaluated in combination with radiotherapy. In the current review, we describe the basic concepts of the interactions between radiotherapy and the tumor vasculature as well as between radiotherapy and the tumor immune microenvironment. In addition, we discuss how both anti-angiogenic therapy and immunotherapy can influence the efficacy of radiotherapy and how a therapeutic triad might emerge as a powerful anti-cancer treatment modality.

Radiotherapy and the tumor vasculature
The relation between radiotherapy and tumor vascularization has become apparent when it became clear that the effects of ionizing radiation largely depend on the generation of reactive oxygen species (ROS)[11]. These highly reactive oxygen radicals can induce irreparable DNA damage that eventually leads to cancer cell death. As the generation of ROS depends on oxygen availability, well-vascularized and perfused tumor tissues are more susceptible to ionizing radiation. Thus, radiation damage is positively correlated with oxygen availability and lack of oxygen, e.g. in hypoxic tumors, hampers treatment efficiency[11,12]. Indeed, a clinical study in patients with head and neck squamous cell carcinoma (HNSCC) comparing tumors with a median oxygen tension below and above 10 mmHg, reported disease free survival rates after radiotherapy of 22% versus 78%, respectively[13]. Furthermore, the uptake of hypoxia PET tracers has been reported to be of prognostic value for response evaluation[14]. In line with this, it has been shown that tumor perfusion is a predictive factor for radiotherapy efficacy. Measuring blood flow and blood volume using either perfusion CT or the apparent diffusion coefficient with diffusion weighted MRI, has been found to predict the response to radiotherapy in patients with HNSCC[15,16]. Similar results were reported in patients with rectal cancer or cervical cancer[17,18]. These findings indicate that monitoring tumor perfusion and/or oxygenation prior to radiotherapy can be of value for setting up a proper treatment plan. This requires robust and reproducible imaging protocols as well as validated imaging biomarkers[14,19]. Modern PET/CT radiotherapy simulators already offer FDG-PET and dynamic contrast-enhanced CT imaging for a combined volumetric assessment of tumor metabolism and perfusion[14]. With the current advances of MRI-guided adaptive radiotherapy, real time evaluation of tumor perfusion for predicting and monitoring treatment response might also become available. To what extent the clinical implementation of such techniques is feasible awaits further studies.

Apart from predicting treatment outcome, measuring tumor perfusion and oxygenation might also be of value to monitor the response during radiotherapy. Especially since perfusion not only affects radiotherapy, but radiotherapy also affects perfusion. The

latter is related to the effects of radiotherapy on the vasculature, which are complex and appear to be dependent on the dose and scheduling of radiotherapy. Based on a literature review, Park *et al.* concluded that high dose irradiation, i.e. a dose above 10 Gy, induces acute vascular damage leading to deterioration of the tumor microenvironment and indirect cancer cell death[9]. This was recently confirmed in a study showing that irradiation with a dose of 15 to 30 Gy resulted in dose-dependent secondary cell death. This was not observed after low-dose radiotherapy and most likely caused by vascular damage[20]. Possibly, the vascular damage was caused by endothelial cell apoptosis, which can be induced by the upregulation of acid sphingomyelinase production in endothelial cells after high dose irradiation[21,22].

Interestingly, fractionated low dose radiotherapy, i.e. daily fractions of up to 2 Gy, appears to exert a positive effect on the tumor vasculature and tissue perfusion[9,23,24] in multiple tumor models[25–27] as well as in patients[28–33]. For example, an increased tumor blood volume during treatment with chemoradiation (27 x 1.8 Gy) was observed in cervical cancer patients[34]. Using dynamic contrast-enhanced MRI and contrast-enhanced ultrasonography, we recently also observed increased tumor perfusion following two weeks of fractionated irradiation in a xenograft mouse tumor model. This was accompanied by reduced intratumoral hypoxia and increased tumor viability[35]. Of note, increased tumor oxygenation during radiotherapy has been linked to different mechanisms, such as decreased oxygen consumption and vasorelaxation via increased inflammation[36]. In addition, fractionated low dose irradiation can promote the growth of new blood vessels which might also contribute to enhanced perfusion, as discussed in the next section[23,35,37].

Collectively, there is clear evidence of a reciprocal relation between radiotherapy and the tumor vasculature in which an adequate tumor vascularization enhances radiotherapy efficacy, while irradiation induces dose-dependent effects on the vasculature (Summarized in **Figure 1A**). Exploiting this relation for combination therapies with angioregulatory strategies appears both feasible and challenging, especially with regard to dose scheduling.

Combining radiotherapy and vascular targeted therapy
As described previously, proper tumor oxygenation is an important predictor of radiotherapy efficacy. Therefore, modification of tumor hypoxia and perfusion in order to enhance the clinical benefit of radiotherapy has been explored using different strategies. A straightforward approach to counteract a hypoxic tumor environment involves the use of hyperbaric oxygen or of hypoxic sensitizers like nitroimidazoles. Both strategies can result in a treatment benefit, as shown in a meta-analysis with HNSCC patients[38]. Unfortunately, data on other tumor types is scarce[11]. Today, neither hyperbaric oxygen nor nitroimidazoles have been implemented in routine clinical practice due to the small benefit in relation to either practical difficulties or toxicity.
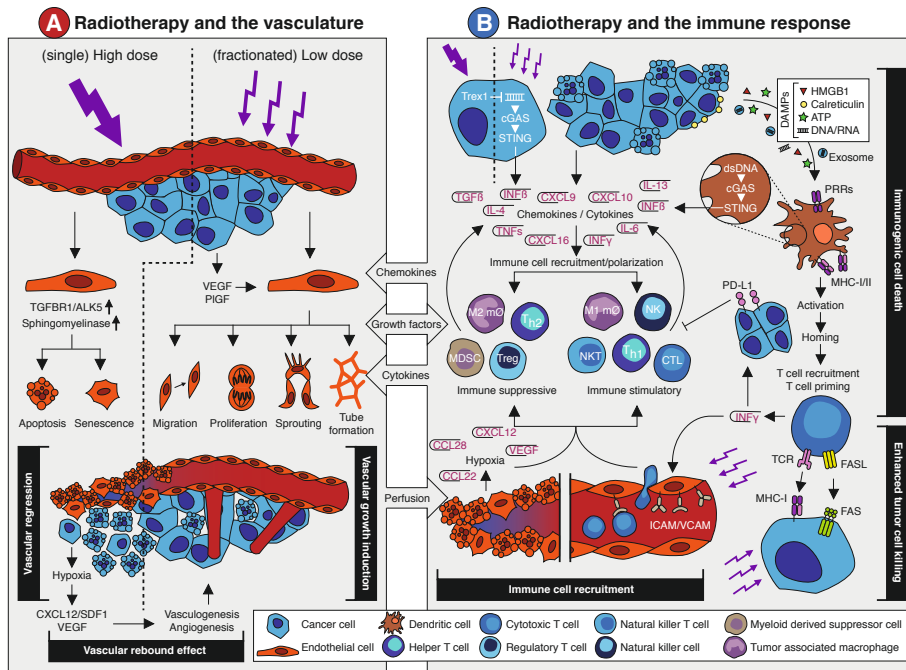
Figure 1. The effects of radiotherapy on the vasculature and the immune response. (**A**) Schematic overview of the main effects that occur in the vasculature in response to radiotherapy. A detailed description is provided in the main text. In brief, single high dose irradiation induces endothelial cell apoptosis and senescence via increased ALK5 and Sphingomyelinase expression. This causes vessel regression and vascular collapse which is accompanied by reduced perfusion. This eventually results in tissue hypoxia which leads to a vascular rebound effect by growth factor-induced vasculogenesis and angiogenesis. Fractionated low dose irradiation also induces an increased expression of angiostimulatory growth factors like VEGF and bFGF. This promotes different endothelial cell functions that results in vascular growth induction and enhanced tissue perfusion. Both the vascular rebound effect and vascular growth induction provide opportunities for therapeutic intervention in combination with radiotherapy. (**B**) Schematic overview of the main effects that occur in the vasculature in response to radiotherapy. A detailed description is provided in the main text. In brief, irradiation of tumor cells can induce expression of interferon beta (IFNb) through cytosolic dsDNA/cGAS/STING signaling. This is dependent on dosing, as high dose irradiation induces Trex1 which causes clearance of cytosolic dsDNA. Apart from IFNb, radiotherapy induces the expression and release of several chemokines, cytokines and growth factors that promote the recruitment of immune cells. This includes both suppressive and stimulatory immune cell subsets. At the same time, irradiation promotes an immune response via the induction of immunogenic cell death. The release of damage-associated molecular patterns (DAMPs) upon radiotherapy-induced cell death causes the activation of antigen presenting cells like dendritic cells through pattern recognition receptors (PPR). This eventually results in the recruitment and priming of cytotoxic T cells. This is accompanied by the release of cytokines like interferon gamma (IFNg) which exerts diverging effects on the immune response. At one hand, IFNg induces PD-L1 expression on tumor cells which is immunosuppressive. At the other hand, it stimulates the expression of leukocyte adhesion molecules in the vessel wall which contributes to increased immune cell recruitment. Vessel regression induces hypoxia which increases expression of growth factors and chemokines that affect immune cell recruitment and polarization. Finally, radiotherapy induces the expression of molecules on the tumor cell surface like MHC-I and Fas, which increases tumor cell killing by immune cells. Targeting the immune suppressive mechanisms provide opportunities for therapeutic intervention in combination with radiotherapy.

Accelerated radiotherapy with carbogen and nicotinamide (ARCON) is a more recent development, in which radiotherapy is combined with inhalation of a hyperoxic gas and a vasoactive agent, thereby decreasing both perfusion-limited hypoxia as well as diffusion-limited hypoxia in the lungs[39]. Although promising, results of clinical trials are not conclusive with respect to local tumor control[40,41]. Vasodilating agents, such as nitric oxide, calcium antagonists and hydralazine, have also been studied as an approach to improve tumor perfusion in order to enhance radiotherapy efficacy, as reviewed by Sonveaux[42]. However, both variable effects on radiosensitivity as well as the mutual systemic effects preclude their clinical use. To date, the most effective method to improve tumor perfusion in a clinical setting appears to be hyperthermia. While hyperthermia can promote cell death via induction of apoptosis or mitotic catastrophy, it has also been shown to improve the efficacy of radiotherapy by inhibition of DNA damage repair pathways and enhancement of tissue perfusion and oxygenation[43–45].

A somewhat unexpected method that was discovered to improve tumor perfusion and oxygenation is anti-angiogenic therapy. Anti-angiogenic therapy refers to treatment strategies that aim to block or hamper angiogenesis, i.e. the growth of new blood vessels of pre-existing capillaries (**Box 2**). It was proposed as an effective anti-cancer therapy in the early 1970's by prof. J. Folkman after his discovery that the growth of most solid tumors is dependent on angiogenesis[46]. Initially, it was anticipated that anti-angiogenic drugs would hamper the effect of radiotherapy due to decreased perfusion and oxygenation. However, multiple preclinical studies observed an enhanced effect of the combinatorial approach[47–49]. These findings have been confirmed in multiple conducted clinical trials investigating the combinatorial approach. For example, in a phase I study in patients with locally advanced pancreatic cancer the vascular endothelial growth factor (VEGF) blocker bevacizumab displayed acceptable toxicity in combination with radiotherapy and capecitabine. Interestingly, only one of the 46 patients had progressive disease and median survival from the start of the protocol was 11.6 months[50]. Promising results were also reported when bevacizumab was combined with capecitabine, oxaliplatin and radiotherapy in patients with rectal cancer[51]. Thus far, the results from larger and more recent clinical trials are less conclusive, reporting variable efficacy as well as increasing toxicity (extensively reviewed by us previously[52,53]).

While the clinical observations warrant further investigation regarding therapy optimization, the potential positive interaction between radiotherapy and anti-angiogenic therapy has been attributed to several distinct mechanisms, such as vessel normalization and the vascular rebound effect. The concept of vessel normalization was coined by prof. R. Jain to explain the paradoxical observation that drugs aimed at vessel pruning could in fact enhance the effect of therapies that rely on a functional vasculature, including radiotherapy[54].

4

Box 2. Angiogenesis

Angiogenesis is the growth of new blood vessels out of pre-existing capillaries. It is one of the hallmarks of cancer since most solid tumor cannot grow beyond a few cubic millimeters if they are unable to induce angiogenesis. The key players in the angiogenic process are endothelial cells. These cells form the inner lining of all blood vessels. Under hypoxic conditions, cancer cells undergo the so-called 'angiogenic switch' which results in an elevated expression and secretion of soluble factors like vascular endothelial growth factor (VEGF). Secreted VEGF binds to it receptors on surface of endothelial cells in a nearby capillary vessel. As a result, the endothelial cells become activated and secrete proteases that degrade the capillary basement membrane as well as the underlying extracellular matrix. Subsequently the activated endothelial cells to proliferate and migrate into the direction of the growth factor gradient, thereby forming novel vascular sprouts towards the tumor that will eventually reassemble into a capillary bed. Due to an imbalance between angiostimulatory and angioinhibitory factors, the newly formed vasculature is abnormally structured, dysfunctional and unable to adequately relief tumor hypoxia. As a consequence, the pro-angiogenic stimulus is maintained and endothelial cells lose some of their typical functional features, including the expression of adhesion molecules that regulate the extravasation of leukocyte into the tumor tissue (For an extensive review see Potente *et al.*[183]).

Based on the premise that the tumor vasculature is abnormally structured and dysfunctional due to a continuous imbalance between pro- and anti-angiogenic signaling, it was suggested that anti-angiogenic therapy restores the angiogenic balance thereby improving vessel function and tissue perfusion[54]. Normalization of the tumor vasculature would thus result in enhanced tumor oxygenation and thereby increase the efficacy of radiation therapy. Indeed, transient improvement of hypoxia and pericyte coverage was reported in different tumor models treated with either a VEGF-receptor 2 blocking antibody, or a VEGF-receptor tyrosine kinase inhibitor[55,56]. Dings *et al.* also studied tumor oxygenation in multiple tumor models during treatment with different anti-angiogenic drugs. Treatment with either bevacizumab or the anti-angiogenic peptide anginex induced elevated oxygenation levels and increased pericyte coverage in the first four days[57]. Moreover, the anti-tumor effect improved when radiotherapy was applied within the window of increased oxygenation[56,57].

While the previous findings indicate that vascular normalization could improve tumor perfusion, it has also become clear that vascular normalization occurs only transiently and that continuation of anti-angiogenic treatment eventually causes vessel regression and reduced tumor oxygenation[56–59]. This has important therapeutic consequences, especially since the data on the exact occurrence and timing of the vascular normalization window in patients is limited[60–62]. Characteristic features of vessel normalization like reduction of immature vessels and increased pericyte coverage have been observed in patient treated with bevacizumab[63]. Furthermore, improved perfusion has been reported in a subset of glioblastoma multiforme (GBM) patients treated with cediranib (a pan-VEGF TKI) or cediranib-containing regimens, and was

associated with survival benefit[60,64]. Notwithstanding these latter observations, the temporary character of vessel normalization in mice, i.e. a few days, seems to be in contrast with the beneficial effects for patients receiving anti-angiogenic drugs during several weeks of fractionated irradiation. Moreover, anti-angiogenic therapy is not only beneficial when applied prior to radiotherapy but also when given during or after radiotherapy[53]. Thus, although vessel normalization might partially explain the beneficial effects, other mechanisms might be equally relevant for the interaction between both radiotherapy and anti-angiogenic therapy.

Another possible mechanism that could explain the benefit of anti-angiogenic drugs involves the stimulation of angiogenesis by irradiation, referred to as the vascular rebound effect. As described previously, low dose irradiation has been found to increase tumor perfusion and oxygenation. While this was linked to mechanisms such as vasodilation by enhanced inflammation and reduced oxygen consumption[36], we and others have shown that low-dose irradiation can also influence angiogenesis by inducing the expression of pro-angiogenesis growth factors like VEGF by cancer cells or other cells that reside in the tumor microenvironment[35,65–67]. For example, Sofia-Vala *et al.* showed that low dose irradiation induces VEGF signaling in endothelial cells[23]. Likewise, macrophages in the stromal tissue have been shown to enhance their VEGF expression after irradiation[68]. We observed induction of VEGF and PlGF after two weeks of fractionated irradiation (daily fractions of 2 Gy) in cultured cancer cells as well as in xenograft tumor tissues[37]. The induction of VEGF coincided with increased tumor perfusion, increased tissue viability and reduced hypoxia. In addition, the levels of VEGF were sufficient to stimulate endothelial cell migration and sprouting. Importantly, the anti-angiogenic drug sunitinib, which blocks VEGF-dependent signaling, could hamper these effects[37]. These findings suggest that ionizing radiation can enhance tumor perfusion by induction of a pro-angiogenic response which can be counteracted by anti-angiogenesis treatment[35]. Interestingly, when exploring the optimal dose-scheduling of fractionated low-dose radiotherapy with sunitinib, a small molecule that inhibits multiple tyrosine kinase receptors including VEGFR, we observed that the beneficial effects of the combination treatment could be obtained with a lower dose of anti-angiogenic drugs than what is currently applied for cancer treatment[35,53]. A similar observation was made by Wachsberger *et al.* using VEGFtrap, a soluble receptor that 'traps' VEGF[69]. These findings are clinically relevant since the implementation of combination therapy is currently restricted due to increased toxicity in tumor types such as rectal cancer, nasopharyngeal cancer and glioblastoma[52]. Of note, high dose irradiation can also induce a vascular rebound effect due to the vascular collapse and subsequent tissue hypoxia. In addition, intermediate and high dose irradiation have been suggested to trigger vasculogenesis, i.e. the influx of endothelial progenitor cells from other parts of the body or bone marrow to build vessels[70]. This process is mediated via various chemokines including CXCL12/SDF1. Interfering in this process by blocking the CXCL12/SDF1 receptor (CXCR4) could be of interest in relation to radiotherapy[71].

4

Furthermore, recent research on the role of endothelial cell metabolism in cancer have led to new insights and potential targets for anti-angiogenesis therapy. For example, inhibition of PFKFB3, which is a regulator of glycolysis, can promote vessel normalization, albeit that this effect is dose-dependent [72]. Whether and to what extend such inhibitors synergize with radiotherapy awaits further investigation.

Collectively, the findings described above point towards the importance of proper dose-scheduling of both treatment modalities to achieve optimal beneficial effects. On one side, the dose-scheduling of anti-angiogenic drugs influences whether and when vessel normalization occurs and whether and when the angiogenic rebound effect is countered. On the other side, the dose-scheduling of radiotherapy influences whether and when tumor perfusion is affected and whether and when an angiogenic (rebound) effect occurs. This complex relation illustrates the challenges that accompany the combination of radiotherapy with anti-angiogenic therapy. It also explains that, while a plethora of pre-clinical evidence suggests a treatment benefit for the combination of radiotherapy with anti-angiogenic therapy, the clinical practice is less conclusive. The radiotherapy efficacy might be strengthened by a pro-angiogenic response, enhancing both tumor perfusion and oxygenation but this could at the same time induce unwanted tumor growth. Thus, optimal dose-scheduling of both treatment modalities is key to achieve beneficial effects and limit toxicity of the combination therapy.

Radiotherapy and the immune system
The link between radiotherapy and the immune system was recognized already several decades before the role of the tumor vasculature was uncovered. The first clear observation that the host immune system contributes to radiotherapy efficacy was presented in the late seventies of the previous century. In a preclinical study it was shown that the effect of radiotherapy is compromised in immunodeficient and CD8+ T cell depleted mice[73]. Prior to this, radiotherapy was more or less considered to be immunosuppressive[74,75]. Additional evidence for a role of the immune system during radiotherapy was obtained from preclinical research and multiple case studies that reported on regression of (metastatic) tumor masses that were distant from the irradiated site[76–78]. This so-called abscopal effect (**Box 3**) was already described in 1953, but it took about 50 years to link this to a systemic anti-tumor immune response initiated by radiotherapy[79,80]. Still, the exact mechanisms behind the abscopal effect are not entirely elucidated. Nevertheless, the clear link between radiotherapy and the immune response, together with the breakthrough of immunotherapy in recent years, has renewed the interest in combining radiotherapy and immunotherapy. Similar as for anti-angiogenic therapy, preclinical and clinical studies using this combination therapy have made it clear that successful implementation of radiotherapy combined with immunotherapy relies on a proper understanding of the interaction between both treatment modalities. In recent years, several mechanisms have been proposed that

explain how radiotherapy affects the tumor immune response[81,82] (Illustrated in **Figure 1B**).

Box 3: The abscopal effect

The concept and term 'abscopal' was proposed in 1953 by dr. R.H. Mole to describe effects of irradiation that occur distant from the site of irradiation, but within the same organism[77]. The term originates from the prefix *ab-* (away from) and Latin word *scopus* (mark or target). As such, it can be considered as a systemic response following a local trigger. Today, the abscopal effect has been reported in a wide variety of both solid and hematologic tumor types. While the mechanism is still not fully elucidated, it has been established the abscopal effect involves the immune system (For an extensive review see Rodríguez-Ruiz *et al.*[80]).

A well-recognized mechanism by which radiotherapy can enhance the anti-tumor immune response is the induction of immunogenic cell death. Unlike normal cell death, immunogenic cell death makes cancer cells visible to the immune system by the release of damage-associated molecular patterns (DAMPs), such as calreticulin, HMGB1 and ATP, along with the presentation of neoantigens and tumor associated antigens[83–90]. DAMPs bind to pattern recognition receptors (PRRs) such as Toll-like receptors (TLRs) on antigen presenting cells, including dendritic cells (DCs). This leads to DC activation which subsequently cross-present antigens and migrate to the tumor-draining lymph node[91,92], where they prime naive T cells and B cells to initiate a systemic immune response[91–98]. Recent studies have identified the STING pathway, activated upon recognition of double-stranded DNA (dsDNA) via cytosolic DNA sensors, as an important regulator of this immunogenic cell death response[99–104]. Double-stranded DNA can be transferred via exosomes from irradiated cancer cells to DCs. Subsequently, STING-dependent activation of type-I interferons and upregulation of co-stimulatory molecules is triggered[105]. Collectively, these findings show that radiotherapy can promote an anti-tumor immune response via immunogenic cell death-mediated activation of antigen presenting cells like DCs leading to increased priming of tumor antigen-specific T cells.

Apart from enhanced T cell priming through immunogenic cell death, radiotherapy can also promote the trafficking of immune cells into the tumor. In fact, multiple mechanisms contribute to this enhanced immune infiltration. Firstly, radiotherapy can improve tumor perfusion (as described above) which will increase the number of leukocytes passing through the tumor tissue. Secondly, irradiation induces the endothelial expression of leukocyte adhesion molecules like ICAM and VCAM[92,106–108]. Consequently, leukocyte extravasation from the circulation into the tumor tissue will be increased. Thirdly, radiotherapy has been shown to increase the expression of pro-inflammatory chemokines such as CXCL9, CXCL10, and CXCL16 by cancer cells. This will help to attract leukocyte populations like cytotoxic CD8+ T cells, Th1 cells, NK cells, and NKT cells[107,109,110]. Finally, radiation can induce MHC-I expression on cancer cells, either by an accumulation of damaged proteins and their break-down products[88,96,111],

or in response to a general increase of interferon gamma (IFNg) within the tumor microenvironment[107]. Preclinical studies have also shown that radiotherapy enhances the expression of the death receptor Fas (CD95) on cancer cells, making them more susceptible to Fas ligand mediated cell death[96,112–115]. Altogether, enhanced tumor perfusion, increased leukocyte chemoattraction and extravasation, as well as increased susceptibility to T cell-mediated cell death contribute to an improved immune response during radiotherapy.

Unfortunately, there are some ifs and buts to the immunostimulatory effect of radiotherapy. Similar as with the angioregulatory response, the immunoregulatory response to irradiation appears to be dose and schedule dependent. For example, the induction of MHC-I[96,111] and immunogenic cell death[88] depend on the dose, and in preclinical models moderate to high doses of radiotherapy seem to have most effect[91,116,117]. For instance, Filatenkov *et al*. showed in weakly immunogenic CT26 and MC38 colon tumors that only a single dose of 30 Gy increased intratumoral CD8+ T cells, whereas 10x 3 Gy did not[117]. On the other hand, radiotherapy doses of ≥ 12 Gy have been shown to attenuate radiotherapy-induced tumor immunogenicity through the induction of DNA exonuclease TREX1 (Three prime repair exonuclease 1), which degrades cytosolic dsDNA, thereby preventing cGAS/STING mediated induction of interferon beta (IFNb) [118]. With regard to the abscopal effect, only a few comparative studies are available, but a systematic review of 46 case reports revealed a broad range in cumulative dose at which the effect was observed (range 0.45 - 60.75 Gy; median 31 Gy)[76]. With regard to scheduling there is also no clear answer yet. It has been reported that a single fraction is better than multiple fractions[92], that there is no difference between single or multiple fractions[91], or that multiple fractions are better[119,120]. From a tumor perfusion perspective there is evidence that fractionated low dose is preferred over single high dose as described previously. At the same time, the induction of leukocyte adhesion molecule expression appears to be dose-dependent[108,121,122]. So, a major future challenge will be to unravel at what dose-scheduling regime an optimal immunostimulatory effect of radiotherapy will occur.

Most likely, the overall effect of radiotherapy on the immune response is not only dose-scheduling dependent but is also determined by tumor type and the tumor microenvironment. Regarding the latter, it has been shown that the efficacy of radiotherapy is influenced by the composition of the pretreatment tumor immune microenvironment[123]. Thus, it would be of interest to explore to what extent the pre-treatment immunogenic profile in the tumor tissue can predict the response to radiotherapy. This is also relevant given the observation that radiotherapy can induce an immunosuppressive microenvironment. After all, apart from the induction of pro-inflammatory chemokines, as described above, radiotherapy can also induce chemokines and cytokines that attract immunosuppressive cell populations such as Tregs[96], myeloid derived suppressor cells (MDSCs)[124], M2 macrophages, and Th2-skewed CD4+ T cells[125]

to the tumor immune microenvironment[126]. Multiple *in vitro* studies demonstrated that unpolarized macrophages tend to acquire a M1 phenotype after irradiation with 2 to 5 Gy. Interestingly, Klug et al. showed in an *in vivo* model reprogramming of TAMs to a M1 phenotype after irradiation with 2 Gy[127]. Different dose-effects of radiotherapy on TAMs, as well as mechanisms involved, has been described in detail by Genard *et al*[128]. Blockade of the macrophage chemoattractant CSF-1 and repolarization of macrophages into a M1 tumor suppressive phenotype by blocking interleukin-4 (IL-4) and IL-13 significantly improved responses to radiotherapy in a mouse breast cancer model[125,129]. In addition, IFNg expression within the tumor immune microenvironment is an important driver of PD-L1 expression on tumor and immune cell which leads to impairment of T cell function[130–132]. In fact, it were these kind of observations that led to the hypothesis that the combination of immunotherapy with radiotherapy might have clinical benefit.

Enhancement of immunotherapy efficacy by radiotherapy
One of the major breakthroughs in oncology in recent years has been the development of drugs that enhance the potency of the immune system. These drugs are predominantly inhibitors of so-called immune checkpoint proteins **(Box 4)** and they are able to re-activate T cells to attack cancer cells. Although we are only starting to understand the effect of such immune checkpoint inhibitors, it has become clear that these drugs are most effective when the T cells that they activate are already in the tumor microenvironment[133–135]. However, many tumors lack a proper lymphocyte infiltration. As described above, radiotherapy can elicit an anti-tumor T cell response, which has spurred the interest to apply radiotherapy in order to augment the local and systemic effect of immunotherapy. Evidence that radiotherapy can reliably and consistently achieve this effect in cancer patients is currently not available but multiple retrospective studies have shown that radiotherapy can increase the response to immunotherapy. Several studies (for overview see Kang *et al*.[136]) in predominantly melanoma and lung cancer patients have shown that radiotherapy given during the course of immunotherapy increases the median overall survival compared to no radiotherapy[137,138].

Box 4: Immune checkpoint proteins

Immune checkpoints programmed cell death protein 1 (PD-1) and cytotoxic T-lymphocyte associated protein 4 (CTLA-4) are negative regulators of T cell responses and act as a brake on the immune system. Although CTLA-4 and PD-1 have similar negative effects on T cells activity, the immune checkpoints operate on different stages of an immune response. CTLA-4 expression is confined to T cells and functions mostly during the priming phase of T cell activation in lymph nodes. The PD-1 checkpoint is predominantly at play during the effector phase within peripheral tissues, where it interacts with its ligand PD-L1 which is broadly expressed on both tumor and immune cells. Despite these differences, inhibitors of both PD-1/PD-L1 and CTLA-4 are able to (re-)activate T cells to attack cancer cells and have shown unprecedented durable responses in many cancer types.

Also in lung cancer it has been shown that radiotherapy somewhere in the course of the disease prior to the first cycle of PD-1 inhibitor pembrolizumab significantly increased overall and progression free survival[138]. In metastatic NSCLC preliminary results of an ongoing trial (NCT02492568) with pembrolizumab preceded by stereotactic body radiation therapy showed a doubling of the overall response rate[139]. However, other studies in melanoma and various solid tumors evaluating the combination of radiotherapy with ipilimumab[97] or pembrolizumab[140] showed disappointing results. The same holds true for a large phase III trial testing radiotherapy followed by ipilimumab or placebo in castration-resistant prostate cancer patients[141].

Interestingly, there is also a variety of case reports describing major systemic antitumor effects of palliative radiotherapy in patients that had progressed on immunotherapy. For instance, Postow *et al.* showed, in a case report of a metastatic melanoma patient that had progressed under ipilimumab, re-induction of an anti-tumor immune response after palliative radiotherapy. This response was accompanied by the expansion of existing, and appearance of new anti-tumor antibodies[93]. Another retrospective analysis of 21 patients with advanced melanoma who received radiotherapy after progression on ipilimumab showed partial systemic response and stable disease in 43% and 10% of cases, respectively[142]. A beneficial effect of radiotherapy following progression on checkpoint inhibition has also been reported for a patient with NSCLC[143] and HNSCC[144]. Another study of patients with stage IV melanoma treated with ipilimumab followed by palliative radiotherapy within the first five days of treatment showed that around 50% of patients experienced clinical benefit[145]. Nevertheless, most clinical success of combined radiotherapy with immunotherapy has been shown in the adjuvant use of PD-1 pathway inhibitors. The largest study among those is the PACIFIC study, a multicenter randomized controlled trial comparing the use of PD-L1 inhibitor durvalumab as consolidation therapy following definitive chemoradiation in stage III non-small cell lung cancer (NSCLC) which showed a median progression free survival of 16.8 months compared to 5.6 months with placebo and an acceptable toxicity profile, resulting in prompt FDA approval of the adjuvant use of durvalumab for stage III NSCLC patients[146]. Importantly, the combination of radiotherapy and immunotherapy appears to be safe and well tolerated without severe toxicities[137,145–149]. Altogether, these studies suggest a bright future for combined radiotherapy and immunotherapy for certain patients. Of note, the high expectations might be somewhat hampered by clinical studies that explored the concurrent use of immunotherapy and radiotherapy to stimulate an anti-tumor immune response by both modalities at the same time. Although the results of such studies are still in early phase, a recent phase I trial in patients with metastatic or locally advanced bladder cancer was paused early due to intolerable in-field toxicities[150]. Trials to test the safety and feasibility of neoadjuvant immunotherapy with radiotherapy in NSCLC, HNSCC and gastroesophageal cancer (NCT03245177, NCT03383094, and NCT03044613, respectively) amongst others are currently ongoing. Apparently, and in line with the

observations of anti-angiogenic therapy combined with radiotherapy, the timing, dosing and scheduling of both treatments is key in achieving optimal therapeutic effects.

Alternative combined radiotherapy-immunotherapy approaches

While currently most (pre)clinical research is mainly focused on the combination of radiotherapy with immune checkpoint inhibitors, several alternative immunomodulatory approaches are also being explored. For example, the combination of radiotherapy with immunostimulatory factors such as interleukin-2 (IL-2)[151,152], granulocyte-macrophage colony-stimulation-factor (GM-CSF)[153], and agonists of the T cell co-stimulatory receptor OX40[154,155] has yielded promising responses in early phase clinical trials. Also strategies to trigger an anti-tumor immune response by intratumoral injection of TLR9 agonists in combination with concurrent low-dose radiotherapy on the injection site has shown promising results and excellent safety and tolerability in different tumor types, including low-grade B cell lymphomas[156], cutaneous T cell lymphoma[157] and follicular lymphoma[158]. A TLR3 agonist in combination with concurrent fractionated radiotherapy was recently tested in a single arm phase II trial in 30 patients with newly diagnosed glioblastoma multiforme and was found to be well tolerated[159]. Others have performed studies in which radiotherapy was combined with intratumoral injections of autologous immature DCs after radiotherapy in hepatocellular carcinoma[160] and soft tissue sarcoma[161]. This treatment was also well tolerated and based on the observed responses, future phase II and III studies were recommended. Finally, efforts have been made to combine radiotherapy with vaccination against carcinoembryonic antigen (CEA) combined with GM-CSF in colorectal cancer[162], or against prostate specific antigen (PSA) combined with GM-CSF and IL-2 in patients with prostate cancer[163,164]. Despite the clear rationale behind these trials, both studies showed limited effectivity[162–164]. On the other hand, a phase I clinical trial in chemo-naïve esophageal squamous cell carcinoma did show vaccine-specific cellular and clinical responses (CT evaluation) after treatment with a peptide vaccine containing five tumor-associated peptides (TTK, URLC10, KOC1, VEGFR1, and VEGFR2) in combination with chemoradiation (60 Gy, cisplatin, 5-FU)[165]. All these studies exemplify the current interest and feasibility to combine radiotherapy with immunostimulatory treatments. Still, many questions have to be answered and challenges have to be met, especially with regard to dosing, scheduling and timing of both treatments. Nevertheless, the outlook for radiotherapy in combination with immunotherapy appears promising.

Future perspectives – a therapeutic triad

Based on aforementioned interactions and synergy, a trimodal approach combining radiotherapy with anti-angiogenic therapy and immunotherapy is a promising therapeutic strategy. To our best knowledge, no clinical trials have been published combining all three treatment modalities. Radiotherapy with either anti-angiogenic therapy or immunotherapy appears feasible, but presents both researchers and clinicians with many challenges.

While this review focused on the interaction of radiotherapy with either anti-angiogenic therapy or immunotherapy, there is growing awareness that the latter two treatments are also intrinsically interwoven. Indeed, the combination of immunotherapy and anti-angiogenic therapy has recently emerged as a novel therapeutic strategy[166]. This is based on the observation that anti-angiogenic therapy can enhance immune effector cell trafficking to the tumor site. This would strengthen the efficacy of immunotherapy since low immune cell infiltration still represents a major obstacle for cancer immunotherapy[167]. A recent review on this subject by Fukumura *et al*. provides an up-do-date table of pre-clinical and clinical trials[168]. The improved recruitment of immune cells during anti-angiogenic therapy is partly explained by vessel normalization. In the tumor endothelium, the expression of adhesion molecules that facilitate rolling, adhesion and extravasation of immune cells is reduced due to exposure of endothelial cells to tumor-derived angiogenic growth factors[169–171]. This phenomenon is referred to as endothelial cell anergy and it makes the underlying tumor tissue invisible or at least less reachable to the immune system[172]. In addition, hypoxia due to impaired perfusion results in the expression of several chemokines such as stromal cell–derived factor 1 (SDF1-α), CC-chemokine ligand 22 (CCL22) and CCL28. These chemokines initiate a state of tolerance by recruiting Tregs, MDSCs and M2-type TAMs to induce an immunosuppressive microenvironment[173,174]. Furthermore, hypoxia as well as VEGF can induce the expression of immune checkpoint molecules on cancer cells and immune cells[175,176]. Collectively, the hypoxic and pro-angiogenic tumor microenvironment are generally immunosuppressive. Thus, strategies that normalize the dysfunctional vasculature can not only restore immune cell functions and facilitate their antitumor activities, but also enhance immunotherapy effects[8]. As already described, anti-angiogenic therapy can induce vascular normalization and reduce hypoxia. In line with this, anti-angiogenic drugs have been shown to facilitate tumor infiltration of CD8+ T lymphocytes and potentiate cancer immunotherapy[177–180]. This effect could thus add up to the previously described induction of adhesion molecule expression in endothelial cells by radiotherapy itself. While anti-angiogenic therapy can influence the immune system, evidence is emerging that immunotherapy also affects the tumor vasculature. IFNg is suggested to play an important role in this process, as it is produced by activated T cells and, upregulates ICAM-1 and induces T cell migration. Interestingly, Th1 cell infiltration is reported to reciprocally promote blood vessel normalization which would further contribute to an immunostimulatory microenvironment, in a process that is also dependent on IFNg signaling. For example, in mice treated with anti PD-1 antibodies, Th1-mediated vessel normalization was improved[181]. Thus, a mutual regulatory feedback loop is identified in which vessel normalization and T lymphocyte infiltration can amplify the positive effects conferred by each individual effect. Possibly, this combinatorial approach could lead to a more pronounced vessel normalization window which could be exploited to enhance the effect of radiotherapy. In this context it is noteworthy to mention that is has been shown in melanoma models that the improved immune response following STING activation actually depends on the production of IFNb by

endothelial cells[182]. While this effect was observed after STING activation by intratumoral injection of cyclic dinucleotide GMP-AMP (cGAMP) and not by irradiation, it further indicates that targeting endothelial cells to improve immunotherapy could be of interest during radiotherapy. Thus, combining the three treatment modalities as a 'therapeutic triad' offers an innovative and interesting approach to cancer treatment (**Figure 2**), but will even present with additional challenges regarding optimal dose-scheduling, timing and overcoming potential toxicities as compared to the combination of two treatments.
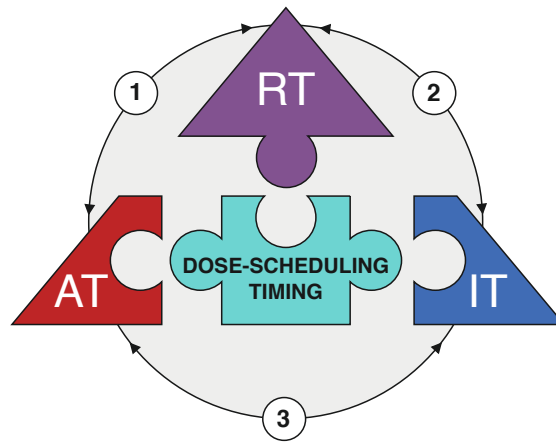

Figure 2. The therapeutic triad. Diagram depicting the main components of the 'therapeutic triad' as pieces of a jigsaw puzzle, i.e. radiotherapy (RT), anti-angiogenic therapy (AT) and immunotherapy (IT). Optimization of dose-scheduling and timing of the three treatment modalities is the center piece of the puzzle, for it is essential to achieve effective combination therapy with minimal toxicities. The arrows reflect the interactions between the different treatment modalities (see main text for more detailed information). In brief: 1) Radiotherapy has dose-dependent effects on tumor vessels resulting a vascular rebound effect due to either vascular collapse or direct induction of angiogenesis. This provides an opportunity for anti-angiogenic therapy. Anti-angiogenic therapy itself induces vessel normalization which improves tumor perfusion and oxygenation; this in turn enhances the efficacy of radiotherapy. 2) Radiotherapy induces immunogenic cell death which enhances specific T cell priming. In addition, radiotherapy can induce the expression of adhesion molecules on endothelial cell and chemokines by cancer cells which both improve the extravasation of immune cells into the tumor tissue. This enhances the efficacy of immunotherapy. In addition, the tumor immune microenvironment itself affects the response to radiotherapy. 3) Anti-angiogenic therapy induces vessel normalization which improves extravasation of immune cells into the tumor tissue. Likewise, immunotherapy might result in recruitment of immune subsets with angioregulatory activity which can be targeted by anti-angiogenic therapy.

Concluding remarks

Although combining radiotherapy with either anti-angiogenic therapy or immunotherapy has been extensively studied the last decade, phase III studies showing a clear benefit of combinatorial approaches are scarce. This not only illustrates the complex relationship between the cancer cells and the tumor microenvironment, but it also emphasizes that many challenges have to be overcome to make these combination therapies effective. In particular, future studies should shed light upon the optimal timing and dosing of

the different treatments. In addition, finding predictive and prognostic biomarkers could help determine which cancer types and disease stages are particularly suitable for combinatorial approaches. Interestingly, radiotherapy, anti-angiogenic therapy and immunotherapy all exert effects on both the tumor vasculature and the anti-tumor immune response. Better understanding of their reciprocal interactions in the tumor microenvironment is the main future challenge to allow the development of a therapeutic triad that combines the three treatment modalities for effective cancer therapy.

REFERENCES

1.   Geoff, D., Susannah, J., Carolyn, F. & Michael, B. The role of radiotherapy in cancer treatment. *Cancer* **104**, 1129–1137 (2005).

2.   Harrington, K. J. *et al.* Guidelines for preclinical and early phase clinical assessment of novel radiosensitisers. *Br. J. Cancer* **105**, 628–39 (2011).

3.   Bernier, J., Hall, E. J. & Giaccia, A. Radiation oncology: a century of achievements. *Nat. Rev. Cancer* **4**, 737–747 (2004).

4.   Grubbé, E. H. Priority in the Therapeutic Use of X-rays. *Radiology* **21**, 156–162 (1933).

5.   Barcellos-Hoff, M. H., Park, C. & Wright, E. G. Radiation and the microenvironment - tumorigenesis and therapy. *Nat. Rev. Cancer* **5**, 867–75 (2005).

6.   Withers, H. R. The four R's of radiotherapy. *Adv. Radiat. Biol.* 241–247 (1975).

7.   Steel, G. G., McMillan, T. J. & Peacock, J. H. The 5Rs of Radiobiology. *Int. J. Radiat. Biol.* **56**, 1045–1048 (1989).

8.   Jain, R. K. Normalization of Tumor Vasculature: An Emerging Concept in Antiangiogenic Therapy. *Science (80-.).* **307**, 58–62 (2005).

9.   Park, H. J., Griffin, R. J., Hui, S., Levitt, S. H. & Song, C. W. Radiation-Induced Vascular Damage in Tumors: Implications of Vascular Damage in Ablative Hypofractionated Radiotherapy (SBRT and SRS). *Radiat. Res.* **177**, 311–327 (2012).

10. Formenti, S. C. & Demaria, S. Systemic effects of local radiotherapy. *Lancet Oncol.* **10**, 718–726 (2009).

11. Overgaard, J. Hypoxic radiosensitization: Adored and ignored. *J. Clin. Oncol.* **25**, 4066–4074 (2007).

12. Gray, L. H., Conger, A. D., Ebert, M., Hornsey, S. & Scott, O. C. A. The Concentration of Oxygen Dissolved in Tissues at the Time of Irradiation as a Factor in Radiotherapy. *Br. J. Radiol.* **26**, 638–648 (1953).

13. Brizel, D. M., Sibley, G. S., Prosnitz, L. R., Scher, R. L. & Dewhirst, M. W. Tumor hypoxia adversely affects the prognosis of carcinoma of the head and neck. *Int. J. Radiat. Oncol.* **38**, 285–289 (1997).

14. Jentsch, C., Beuthien-Baumann, B., Troost, E. G. C. & Shakirin, G. Validation of functional imaging as a biomarker for radiation treatment response. *Br. J. Radiol.* **88**, 20150014 (2015).

15. Kim, S. *et al.* Diffusion-weighted magnetic resonance imaging for predicting and detecting early response to chemoradiation therapy of squamous cell carcinomas of the head and neck. *Clin. Cancer Res.* **15**, 986–994 (2009).

16. Preda, L., Calloni, S. F., Moscatelli, M. E. M., Cossu Rocca, M. & Bellomi, M. Role of CT Perfusion in Monitoring and Prediction of Response to Therapy of Head and Neck Squamous Cell Carcinoma. *Biomed Res. Int.* **2014**, 1–8 (2014).

17. Attenberger, U. I. *et al.* mMRI at 3.0 T as an Evaluation Tool of Therapeutic Response to Neoadjuvant CRT in Patients with Advanced-stage Rectal Cancer. *Anticancer Res.* **37**, 215–222 (2017).

18. Yang, W. *et al.* Multi-parametric MRI in cervical cancer: early prediction of response to concurrent chemoradiotherapy in combination with clinical prognostic factors. *Eur. Radiol.* 437–445 (2017) doi:10.1007/s00330-017-4989-3.

4

19. Colliez, F., Gallez, B. & Jordan, B. F. Assessing Tumor Oxygenation for Predicting Outcome in Radiation Oncology: A Review of Studies Correlating Tumor Hypoxic Status and Outcome in the Preclinical and Clinical Settings. *Front. Oncol.* **7**, (2017).

20. Song, C. W. *et al.* Indirect Tumor Cell Death After High-Dose Hypofractionated Irradiation: Implications for Stereotactic Body Radiation Therapy and Stereotactic Radiation Surgery. *Int. J. Radiat. Oncol. Biol. Phys.* **93**, 166–172 (2015).

21. Garcia-Barros, M. Tumor Response to Radiotherapy Regulated by Endothelial Cell Apoptosis. *Sci. (New York, NY)* **300**, 1155–1159 (2003).

22. Paris, F. Endothelial Apoptosis as the Primary Lesion Initiating Intestinal Radiation Damage in Mice. *Science (80-.).* **293**, 293–297 (2001).

23. Sofia Vala, I. *et al.* Low doses of ionizing radiation promote tumor growth and metastasis by enhancing angiogenesis. *PLoS One* **5**, (2010).

24. Yu, H., Mohan, S. & Natarajan, M. Radiation-triggered NF-κB activation is responsible for the angiogenic signaling pathway and neovascularization for breast cancer cell proliferation and growth. *Breast Cancer Basic Clin. Res.* **6**, 125–135 (2012).

25. Chen, F. H. *et al.* Combination of vessel-targeting agents and fractionated radiation therapy: The role of the SDF-1/CXCR4 pathway. *Int. J. Radiat. Oncol. Biol. Phys.* **86**, 777–784 (2013).

26. De Keyzer, F. *et al.* Dynamic contrast-enhanced and diffusion-weighted MRI for early detection of tumoral changes in single-dose and fractionated radiotherapy: evaluation in a rat rhabdomyosarcoma model. *Eur. Radiol.* **19**, 2663–2671 (2009).

27. Potiron, V. A. *et al.* Improved functionality of the vasculature during conventionally fractionated radiation therapy of prostate cancer. *PLoS One* **8**, (2013).

28. Cooper, R. A. *et al.* Changes in oxygenation during radiotherapy in carcinoma of the cervix. *Int. J. Radiat. Oncol. Biol. Phys.* **45**, 119–126 (1999).

29. Dunst, J., Hansgen, G., Lautenschlager, C., Fuchsel, G. & Becker, A. Oxygenation of cervical cancers during radiotherapy and radiotherapy + cis-retinoic acid/interferon. *Int. J. Radiat. Oncol. Biol. Phys.* **43**, 367–373 (1999).

30. Hohlweg-Majert, B. *et al.* Impact of radiotherapy on microsurgical reconstruction of the head and neck. *J. Cancer Res. Clin. Oncol.* **138**, 1799–1811 (2012).

31. Janssen, M. H. M. *et al.* Tumor perfusion increases during hypofractionated short-course radiotherapy in rectal cancer: Sequential perfusion-CT findings. *Radiother. Oncol.* **94**, 156–160 (2010).

32. Mayr, N. A. *et al.* Tumor perfusion studies using fast magnetic resonance imaging technique in advanced cervical cancer: A new noninvasive predictive assay. *Int. J. Radiat. Oncol. Biol. Phys.* **36**, 623–633 (1996).

33. Shibuya, K. *et al.* Blood flow change quantification in cervical cancer before and during radiation therapy using perfusion CT. *J. Radiat. Res.* **52**, 804–11 (2011).

34. Banks, T. I., von Eyben, R., Hristov, D. & Kidd, E. A. Pilot study of combined FDG-PET and dynamic contrast-enhanced CT of locally advanced cervical carcinoma before and during concurrent chemoradiotherapy suggests association between changes in tumor blood volume and treatment response. *Cancer Med.* **7**, 3642–3651 (2018).

35. Kleibeuker, E. A. *et al.* Low dose angiostatic treatment counteracts radiotherapy-induced tumor perfusion and enhances the anti-tumor effect. *Oncotarget* **7**, 76613–76627 (2016).

36. Crokart, N. *et al.* Early reoxygenation in tumors after irradiation: Determining factors and consequences for radiotherapy regimens using daily multiple fractions. *Int. J. Radiat. Oncol. Biol. Phys.* **63**, 901–910 (2005).

37. Sersa, G. *et al.* Vascular disrupting action of electroporation and electrochemotherapy with bleomycin in murine sarcoma. *Br. J. Cancer* **98**, 388–398 (2008).

38. Overgaard, J. Hypoxic modification of radiotherapy in squamous cell carcinoma of the head and neck - A systematic review and meta-analysis. *Radiother. Oncol.* **100**, 22–32 (2011).

39. Kaanders, J. H. A. M., Bussink, J. & Van der Kogel, A. J. ARCON: A novel biology-based approach in radiotherapy. *Lancet Oncol.* **3**, 728–737 (2002).

40. Hoskin, P. J., Rojas, A. M., Bentzen, S. M. & Saunders, M. I. Radiotherapy with concurrent carbogen and nicotinamide in bladder carcinoma. *J. Clin. Oncol.* **28**, 4912–4918 (2010).

41. Janssens, G. O. *et al.* Accelerated radiotherapy with carbogen and nicotinamide for laryngeal cancer: Results of a phase III randomized trial. *J. Clin. Oncol.* **30**, 1777–1783 (2012).

42. Sonveaux, P. Provascular strategy: Targeting functional adaptations of mature blood vessels in tumors to selectively influence the tumor vascular reactivity and improve cancer treatment. *Radiother. Oncol.* **86**, 300–313 (2008).

43. Griffin, R. J., Dings, R. P. M., Jamshidi-Parsian, A. & Song, C. W. Mild temperature hyperthermia and radiation therapy: Role of tumour vascular thermotolerance and relevant physiological factors. *Int. J. Hyperth.* **26**, 256–263 (2010).

44. Peeken, J. C., Vaupel, P. & Combs, S. E. Integrating Hyperthermia into Modern Radiation Oncology: What Evidence Is Necessary? *Front. Oncol.* **7**, 132 (2017).

45. Wust, P. *et al.* Hyperthermia in combined treatment of cancer. *Lancet Oncol.* **3**, 487–497 (2002).

46. Folkman, J. Tumor angiogenesis: therapeutic implications. *N. Engl. J. Med.* **285**, 1182–1186 (1971).

47. Mauceri, H. J. *et al.* Combined effects of angiostatin and ionizing radiation in antitumour therapy. *Nature* **394**, 287–291 (1998).

48. Teicher, B. A. *et al.* Antiangiogenic agents can increase tumor oxygenation and response to radiation therapy. *Radiat. Oncol. Investig.* **2**, 269–276 (1994).

49. Teicher, B. A. *et al.* Increased efficacy of chemo- and radio-therapy by a hemoglobin solution in the 9L gliosarcoma. *In Vivo* **9**, 11–18 (1995).

50. Crane, C. H. *et al.* Phase I trial evaluating the safety of bevacizumab with concurrent radiotherapy and capecitabine in locally advanced pancreatic cancer. *J. Clin. Oncol.* **24**, 1145–1151 (2006).

51. Czito, B. G. *et al.* Bevacizumab, Oxaliplatin, and Capecitabine With Radiation Therapy in Rectal Cancer: Phase I Trial Results. *Int. J. Radiat. Oncol. Biol. Phys.* **68**, 472–478 (2007).

52. Hamming, L. C., Slotman, B. J., Verheul, H. M. W. & Thijssen, V. L. The clinical application of angiostatic therapy in combination with radiotherapy: past, present, future. *Angiogenesis* **20**, 217–232 (2017).

53. Kleibeuker, E. A., Ten Hooven, M. A., Verheul, H. M., Slotman, B. J. & Thijssen, V. L. Combining radiotherapy with sunitinib: lessons (to be) learned. *Angiogenesis* **18**, 385–395 (2015).

54. Jain, R. K. Normalizing tumor vasculature with anti-angiogenic therapy: A new paradigm for combination therapy. *Nat. Med.* **7**, 987–989 (2001).

4

55. Kamoun, W. S. *et al.* Edema Control by Cediranib, a Vascular Endothelial Growth Factor Receptor–Targeted Kinase Inhibitor, Prolongs Survival Despite Persistent Brain Tumor Growth in Mice. *J. Clin. Oncol.* **27**, 2542–2552 (2009).

56. Winkler, F. *et al.* Kinetics of vascular normalization by VEGFR2 blockade governs brain tumor response to radiation: Role of oxygenation, angiopoietin-1, and matrix metalloproteinases. *Cancer Cell* **6**, 553–563 (2004).

57. Dings, R. P. M. *et al.* Scheduling of radiation with angiogenesis inhibitors anginex and Avastin improves therapeutic outcome via vessel normalization. *Clin. Cancer Res.* **13**, 3395–402 (2007).

58. Kleibeuker, E. A., Griffioen, A. W., Verheul, H. M., Slotman, B. J. & Thijssen, V. L. Combining angiogenesis inhibition and radiotherapy: A double-edged sword. *Drug Resist. Updat.* **15**, 173–182 (2012).

59. Matsumoto, S. *et al.* Antiangiogenic agent sunitinib transiently increases tumor oxygenation and suppresses cycling hypoxia. *Cancer Res.* **71**, 6350–6359 (2011).

60. Sorensen, A. G. *et al.* Increased survival of glioblastoma patients who respond to antiangiogenic therapy with elevated blood perfusion. *Cancer Res.* **72**, 402–407 (2012).

61. Tolaney, S. M. *et al.* Role of vascular density and normalization in response to neoadjuvant bevacizumab and chemotherapy in breast cancer patients. *Proc. Natl. Acad. Sci. U. S. A.* **112**, 14325–14330 (2015).

62. Willett, C. G. *et al.* Efficacy, safety, and biomarkers of neoadjuvant bevacizumab, radiation therapy, and fluorouracil in rectal cancer: A multidisciplinary phase II study. *J. Clin. Oncol.* **27**, 3020–3026 (2009).

63. Carmeliet, P. & Jain, R. K. Principles and mechanisms of vessel normalization for cancer and other angiogenic diseases. *Nat. Rev. Drug Discov.* **10**, 417–427 (2011).

64. Batchelor, T. T. *et al.* Phase III randomized trial comparing the efficacy of cediranib as monotherapy, and in combination with lomustine, versus lomustine alone in patients with recurrent glioblastoma. *J. Clin. Oncol.* **31**, 3212–3218 (2013).

65. Chuang, Y. Y. E. *et al.* Gene expression after treatment with hydrogen peroxide, menadione, or t-butyl hydroperoxide in breast cancer cells. *Cancer Res.* **62**, 6246–6254 (2002).

66. Feng, X. *et al.* Caspase 3 in dying tumor cells mediates post-irradiation angiogenesis. *Oncotarget* **6**, (2015).

67. Solberg, T. D., Nearman, J., Mullins, J., Li, S. & Baranowska-Kortylewicz, J. Correlation Between Tumor Growth Delay and Expression of Cancer and Host VEGF, VEGFR2, and Osteopontin in Response to Radiotherapy. *Int. J. Radiat. Oncol.* **72**, 918–926 (2008).

68. Meng, Y. *et al.* Blockade of tumor necrosis factor α signaling in tumor-associated macrophages as a radiosensitizing strategy. *Cancer Res.* **70**, 1534–1543 (2010).

69. Wachsberger, P. R. *et al.* VEGF Trap in Combination With Radiotherapy Improves Tumor Control in U87 Glioblastoma. *Int. J. Radiat. Oncol. Biol. Phys.* **67**, 1526–1537 (2007).

70. Thanik, V. D. *et al.* Cutaneous Low-Dose Radiation Increases Tissue Vascularity through Upregulation of Angiogenic and Vasculogenic Pathways. *J. Vasc. Res.* **47**, 472–480 (2010).

71. Martin, B. J. & J. Martin, B. Inhibiting Vasculogenesis After Radiation: A New Paradigm to Improve Local Control by Radiotherapy. *Semin. Radiat. Oncol.* **23**, 281–287 (2013).

72. Zecchin, A., Kalucka, J., Dubois, C. & Carmeliet, P. How Endothelial Cells Adapt Their Metabolism to Form Vessels in Tumors. *Front. Immunol.* **8**, 1750 (2017).

73. Stone, H. B., Peters, L. J. & Milas, L. Effect of host immune capability on radiocurability and subsequent transplantability of a murine fibrosarcoma. *J. Natl. Cancer Inst.* **63**, 1229–1235 (1979).

74. Order, S. E. The effects of therapeutic irradiation on lymphocytes and immunity. *Cancer* **39**, 737–743 (1977).

75. Wara, W. M. Immunosuppression Associated With Radiation Therapy. *Int. J. Radiat. Oncol. Biol. Phys.* **2**, 593–596 (1977).

76. Abuodeh, Y., Venkat, P. & Kim, S. Systematic review of case reports on the abscopal effect. *Curr. Probl. Cancer* **40**, 25–37 (2016).

77. Mole, R. H. Whole Body Irradiation—Radiobiology or Medicine? *Br. J. Radiol.* **26**, 234–241 (1953).

78. Ngwa, W. *et al.* Using immunotherapy to boost the abscopal effect. *Nat. Rev. Cancer* **18**, 313–322 (2018).

79. Demaria, S. *et al.* Ionizing radiation inhibition of distant untreated tumors (abscopal effect) is immune mediated. *Int. J. Radiat. Oncol. Biol. Phys.* **58**, 862–870 (2004).

80. Rodríguez-Ruiz, M. E., Vanpouille-Box, C., Melero, I., Formenti, S. C. & Demaria, S. Immunological Mechanisms Responsible for Radiation-Induced Abscopal Effect. *Trends Immunol.* **39**, 644–655 (2018).

81. Herrera, F. G., Bourhis, J. & Coukos, G. Radiotherapy combination opportunities leveraging immunity for the next oncology practice. *CA. Cancer J. Clin.* **67**, 65–85 (2017).

82. Walle, T. *et al.* Radiation effects on antitumor immune responses: current perspectives and challenges. *Ther. Adv. Med. Oncol.* **10**, 1–27 (2018).

83. Galluzzi, L., Buqué, A., Kepp, O., Zitvogel, L. & Kroemer, G. Immunogenic cell death in cancer and infectious disease. *Nat. Rev. Immunol.* **17**, 97–111 (2017).

84. Golden, E. B. & Apetoh, L. Radiotherapy and Immunogenic Cell Death. *Semin. Radiat. Oncol.* **25**, 11–17 (2015).

85. Krysko, D. V *et al.* Immunogenic cell death and DAMPs in cancer therapy. *Nat. Rev. Cancer* **12**, 860–75 (2012).

86. McBride, W. H. *et al.* A Sense of Danger from Radiation. *Radiat. Res.* **162**, 1–19 (2004).

87. Zitvogel, L., Kepp, O. & Kroemer, G. Decoding Cell Death Signals in Inflammation and Immunity. *Cell* **140**, 798–804 (2010).

88. Gameiro, S. R. *et al.* Radiation-induced immunogenic modulation of tumor enhances antigen processing and calreticulin exposure, resulting in enhanced T-cell killing. *Oncotarget* **5**, 403–416 (2014).

89. Golden, E. B. *et al.* Radiation fosters dose-dependent and chemotherapy-induced immunogenic cell death. *Oncoimmunology* **3**, (2014).

90. Obeid, M. *et al.* Calreticulin exposure dictates the immunogenicity of cancer cell death. *Nat. Med.* **13**, 54–61 (2007).

91. Lee, Y. *et al.* Therapeutic effects of ablative radiation on local tumor require CD8 + T cells : *Blood* **114**, 589–595 (2009).

92. Lugade, A. A. *et al.* Local Radiation Therapy of B16 Melanoma Tumors Increases the Generation of Tumor Antigen-Specific Effector Cells That Traffic to the Tumor. *J. Immunol.* **174**, 7516–7523 (2005).

4

93. Postow, M. *et al.* Abscopal Effect in a Patient with Melanoma. *N. Engl. J. Med.* **366**, 925–931 (2012).

94. Rudqvist, N.-P. *et al.* Radiotherapy and CTLA-4 blockade shape the TCR repertoire of tumor-infiltrating T cells. *Cancer Immunol. Res.* **6**, 139–150 (2018).

95. Schaue, D. *et al.* T-Cell Responses to Survivin in Cancer Patients Undergoing Radiation Therapy. *Clin. Cancer Res.* **14**, 4883–4890 (2008).

96. Sharabi, A. B. *et al.* Stereotactic Radiation Therapy Augments Antigen-Specific PD-1-Mediated Antitumor Immune Responses via Cross-Presentation of Tumor Antigen. *Cancer Immunol. Res.* **3**, 345–355 (2015).

97. Twyman-Saint Victor, C. *et al.* Radiation and dual checkpoint blockade activate non-redundant immune mechanisms in cancer. *Nature* **520**, 373–377 (2015).

98. Vanpouille-Box, C. *et al.* TGFβ is a master regulator of radiation therapy-induced antitumor immunity. *Cancer Res.* **75**, 2232–2242 (2015).

99. Burnette, B. C. *et al.* The efficacy of radiotherapy relies upon induction of type I interferon-dependent innate and adaptive immunity. *Cancer Res.* **71**, 2488–2496 (2011).

100. Deng, L. *et al.* STING-dependent cytosolic DNA sensing promotes radiation-induced type I interferon-dependent antitumor immunity in immunogenic tumors. *Immunity* **41**, 543–852 (2014).

101. Durante, M. & Formenti, S. C. Radiation-Induced Chromosomal Aberrations and Immunotherapy: Micronuclei, Cytosolic DNA, and Interferon-Production Pathway. *Front. Oncol.* **8**, (2018).

102. Minn, A. J. & Wherry, E. J. Combination Cancer Therapies with Immune Checkpoint Blockade: Convergence on Interferon Signaling. *Cell* **165**, 272–275 (2016).

103. Vanpouille-Box, C., Formenti, S. C. & Demaria, S. Toward precision radiotherapy for use with immune checkpoint blockers. *Clin. Cancer Res.* **24**, 259–265 (2018).

104. Woo, S. R. *et al.* STING-dependent cytosolic DNA sensing mediates innate immune recognition of immunogenic tumors. *Immunity* **41**, 830–842 (2014).

105. Diamond, J. M. *et al.* Exosomes Shuttle TREX1-Sensitive IFN-Stimulatory dsDNA from Irradiated Cancer Cells to DCs. *Cancer Immunol. Res.* **6**, 910–920 (2018).

106. Baluna, R. G., Eng, T. Y. & Thomas, C. R. Adhesion molecules in radiotherapy. *Radiat. Res.* **166**, 819–31 (2006).

107. Lugade, A. A. *et al.* Radiation-Induced IFN- Production within the Tumor Microenvironment Influences Antitumor Immunity. *J. Immunol.* **180**, 3132–3139 (2008).

108. Sievert, W. *et al.* Late proliferating and inflammatory effects on murine microvascular heart and lung endothelial cells after irradiation. *Radiother. Oncol.* **117**, 376–381 (2015).

109. Matsumura, S. *et al.* Radiation-Induced CXCL16 Release by Breast Cancer Cells Attracts Effector T Cells. *J. Immunol.* **181**, 3099–3107 (2008).

110. Matsumura, S. & Demaria, S. Up-regulation of the Pro-inflammatory Chemokine CXCL16 is a Common Response of Tumor Cells to Ionizing Radiation. *Radiat. Res.* **173**, 418–425 (2010).

111. Reits, E. A. *et al.* Radiation modulates the peptide repertoire, enhances MHC class I expression, and induces successful antitumor immunotherapy. *J. Exp. Med.* **203**, 1259–1271 (2006).

112. Chakraborty, M. *et al.* Irradiation of Tumor Cells Up-Regulates Fas and Enhances CTL Lytic Activity and CTL Adoptive Immunotherapy. *J. Immunol.* **170**, 6338–6347 (2003).

113. Chakraborty, M. *et al.* External beam radiation of tumors alters phenotype of tumor cells to render them susceptible to vaccine-mediated T-cell killing. *Cancer Res.* **64**, 4328–4337 (2004).

114. Garnett, C. T. *et al.* Sublethal Irradiation of Human Tumor Cells Modulates Phenotype Resulting in Enhanced Killing by Cytotoxic T Lymphocytes. *Cancer Res* **64**, 7985–7994 (2004).

115. Kuwabara, M., Takahashi, K. & Inanami, O. Induction of Apoptosis through the Activation of SAPK/JNK Followed by the Expression of Death Receptor Fas in X-irradiated Cells. *J. Radiat. Res.* **44**, 203–209 (2003).

116. Demaria, S. *et al.* Immune-mediated inhibition of metastases after treatment with local radiation and CTLA-4 blockade in a mouse model of breast cancer. *Clin. Cancer Res.* **11**, 728–34 (2005).

117. Filatenkov, A. *et al.* Ablative tumor radiation can change the tumor immune cell microenvironment to induce durable complete remissions. *Clin. Cancer Res.* **21**, 3727–3739 (2015).

118. Vanpouille-Box, C. *et al.* DNA exonuclease Trex1 regulates radiotherapy-induced tumour immunogenicity. *Nat. Commun.* **8**, 15618 (2017).

119. Dewan, M. Z. *et al.* Fractionated but not single-dose radiotherapy induces an immune-mediated abscopal effect when combined with anti-CTLA-4 antibody. *Clin. Cancer Res.* **15**, 5379–5388 (2009).

120. Schaue, D., Ratikan, J. A., Iwamoto, K. S. & McBride, W. H. Maximizing tumor immunity with fractionated radiation. *Int. J. Radiat. Oncol. Biol. Phys.* **83**, 1306–1310 (2012).

121. Rodriguez-Ruiz, M. E. *et al.* Intercellular Adhesion Molecule-1 and Vascular Cell Adhesion Molecule Are Induced by Ionizing Radiation on Lymphatic Endothelium. *Int. J. Radiat. Oncol. Biol. Phys.* **97**, 389–400 (2017).

122. Uehara, Y., Murata, Y., Shiga, S. & Hosoi, Y. NSAIDs diclofenac, indomethacin, and meloxicam highly upregulate expression of ICAM-1 and COX-2 induced by X-irradiation in human endothelial cells. *Biochem. Biophys. Res. Commun.* **479**, 847–852 (2016).

123. Formenti, S. C. & Demaria, S. Combining radiotherapy and cancer immunotherapy: A paradigm shift. *Journal of the National Cancer Institute* vol. 105 256–265 (2013).

124. Xu, J. *et al.* CSF1R signaling blockade stanches tumor-infiltrating myeloid cells and improves the efficacy of radiotherapy in prostate cancer. *Cancer Res.* **73**, 2782–2794 (2013).

125. Shiao, S. L. *et al.* Th2-Polarized CD4+ T Cells and Macrophages Limit Efficacy of Radiotherapy. *Cancer Immunol. Res.* **3**, 518–525 (2015).

126. Zitvogel, L. & Kroemer, G. Subversion of anticancer immunosurveillance by radiotherapy. *Nat. Immunol.* **16**, 1005–1007 (2015).

127. Klug, F. *et al.* Low-Dose Irradiation Programs Macrophage Differentiation to an iNOS+/M1 Phenotype that Orchestrates Effective T Cell Immunotherapy. *Cancer Cell* **24**, 589–602 (2013).

128. Genard, G., Lucas, S. & Michiels, C. Reprogramming of Tumor-Associated Macrophages with Anticancer Therapies: Radiotherapy versus Chemo- and Immunotherapies. *Front. Immunol.* **8**, (2017).

129. Ma, J. L. *et al.* The intensity of radiotherapy-elicited immune response is associated with esophageal cancer clearance. *J. Immunol. Res.* **2014**, 794249 (2014).

130. Deng, L. *et al.* Irradiation and anti – PD-L1 treatment synergistically promote antitumor immunity in mice. *J. Clin. Invest.* **124**, 687–695 (2014).
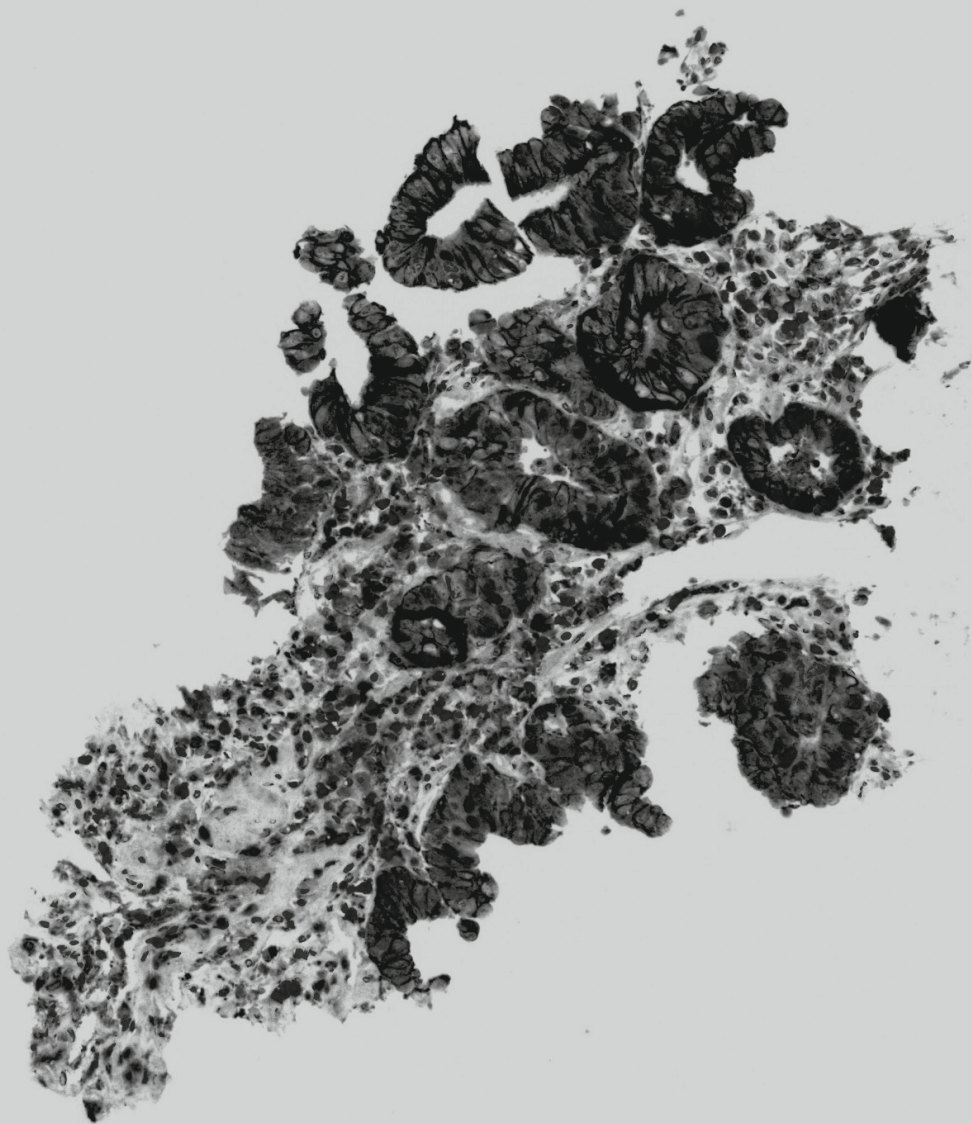
4

131. Dovedi, S. J. & Illidge, T. M. The antitumor immune response generated by fractionated radiation therapy may be limited by tumor cell adaptive resistance and can be circumvented by PD-L1 blockade. *Oncoimmunology* **4**, 1–4 (2015).

132. Derer, A. *et al.* Chemoradiation increases PD-L1 expression in certain melanoma and glioblastoma cells. *Front. Immunol.* **7**, 1–11 (2016).

133. Ribas, A. *et al.* Association of response to programmed death receptor 1 (PD-1) blockade with pembrolizumab (MK-3475) with an interferon-inflammatory immune gene signature. *J. Clin. Oncol.* **33**, 3001 (2015).

134. Seiwert, T. Y. *et al.* Inflamed-phenotype gene expression signatures to predict benefit from the anti-PD-1 antibody pembrolizumab in PD-L1+ head and neck cancer patients. *J. Clin. Oncol.* **33**, 6017 (2015).

135. Ayers, M. *et al.* Relationship between immune gene signatures and clinical response to PD-1 blockade with pembrolizumab (MK-3475) in patients with advanced solid tumors. *J. Immunother. Cancer* **3**, P80 (2015).

136. Kang, J., Demaria, S. & Formenti, S. Current clinical trials testing the combination of immunotherapy with radiotherapy. *J. Immunother. Cancer* **4**, 51 (2016).

137. Koller, K. M. *et al.* Improved survival and complete response rates in patients with advanced melanoma treated with concurrent ipilimumab and radiotherapy versus ipilimumab alone. *Cancer Biol. Ther.* **18**, 36–42 (2017).

138. Shaverdian, N. *et al.* Previous radiotherapy and the clinical activity and toxicity of pembrolizumab in the treatment of non-small-cell lung cancer: a secondary analysis of the KEYNOTE-001 phase 1 trial. *Lancet Oncol.* **18**, 895–903 (2017).

139. Theelen, W. *et al.* Randomized phase II study of pembrolizumab after stereotactic body radiotherapy (SBRT) versus pembrolizumab alone in patients with advanced non-small cell lung cancer: The PEMBRO-RT study. *J. Clin. Oncol.* **36**, 9023–9023 (2018).

140. Luke, J. J. *et al.* Safety and Clinical Activity of Pembrolizumab and Multisite Stereotactic Body Radiotherapy in Patients With Advanced Solid Tumors. *J. Clin. Oncol.* **36**, 1611–1618 (2018).

141. Kwon, E. D. *et al.* Ipilimumab versus placebo after radiotherapy in patients with metastatic castration-resistant prostate cancer that had progressed after docetaxel chemotherapy (CA184-043): A multicentre, randomised, double-blind, phase 3 trial. *Lancet Oncol.* **15**, 700–712 (2014).

142. Grimaldi, A. M. *et al.* Abscopal effects of radiotherapy on advanced melanoma patients who progressed after ipilimumab immunotherapy. *Oncoimmunology* **3**, e28780 (2014).

143. Yuan, Z. *et al.* Radiotherapy Rescue of a Nivolumab-Refractory Immune Response in a Patient with PD-L1–Negative Metastatic Squamous Cell Carcinoma of the Lung. *J. Thorac. Oncol.* **12**, e135–e136 (2017).

144. Nagasaka, M. *et al.* PD1/PD-L1 inhibition as a potential radiosensitizer in head and neck squamous cell carcinoma: A case report. *J. Immunother. Cancer* **4**, 1–4 (2016).

145. Hiniker, S. M. *et al.* A Prospective Clinical Trial Combining Radiation Therapy With Systemic Immunotherapy in Metastatic Melanoma. *Int. J. Radiat. Oncol. Biol. Phys.* **96**, 578–588 (2016).

146. Antonia, S. J. *et al.* Durvalumab after Chemoradiotherapy in Stage III Non–Small-Cell Lung Cancer. *N. Engl. J. Med.* **377**, 1919–1929 (2017).

147. Pike, L. R. G. *et al.* Radiation and PD-1 inhibition: Favorable outcomes after brain-directed radiation. *Radiother. Oncol.* **124**, 98–103 (2017).

148. Anderson, E. S. *et al.* Melanoma brain metastases treated with stereotactic radiosurgery and concurrent pembrolizumab display marked regression; efficacy and safety of combined treatment. *J. Immunother. Cancer* **5**, 1–8 (2017).

149. Kiess, A. P. *et al.* Stereotactic radiosurgery for melanoma brain metastases in patients receiving ipilimumab: Safety profile and efficacy of combined treatment. *Int. J. Radiat. Oncol. Biol. Phys.* **92**, 368–375 (2015).

150. Tree, A. C. *et al.* Dose-limiting Urinary Toxicity With Pembrolizumab Combined With Weekly Hypofractionated Radiation Therapy in Bladder Cancer. *Radiat. Oncol. Biol.* **101**, 1168–1171 (2018).

151. Ridolfi, L. *et al.* Radiotherapy as an immunological booster in patients with metastatic melanoma or renal cell carcinoma treated with high-dose Interleukin-2: Evaluation of biomarkers of immunologic and therapeutic response. *J. Transl. Med.* **12**, 1–11 (2014).

152. Seung, S. K. *et al.* Phase 1 Study of Stereotactic Body Radiotherapy and Interleukin-2: Tumor and Immunological Responses. *Sci. Transl. Med.* **4**, 137ra74 (2012).

153. Golden, E. B. *et al.* Local radiotherapy and granulocyte-macrophage colony-stimulating factor to generate abscopal responses in patients with metastatic solid tumours: A proof-of-principle trial. *Lancet Oncol.* **16**, 795–803 (2015).

154. Curti, B. D. *et al.* OX40 is a potent immune-stimulating target in late-stage cancer patients. *Cancer Res.* **73**, 7189–7198 (2013).

155. Kovacsovics-Bankowski, M. *et al.* Phase I/II clinical trial of anti-OX40, radiation and cyclophosphamide in patients with prostate cancer: immunological analysis. *J. Immunother. Cancer* **1**, P255 (2013).

156. Brody, J. D. *et al.* In situ vaccination with a TLR9 agonist induces systemic lymphoma regression: A phase I/II study. *J. Clin. Oncol.* **28**, 4324–4332 (2010).

157. Kim, Y. H. *et al.* In situ vaccination against mycosis fungoides by intratumoral injection of a TLR9 agonist combined with radiation: a phase 1/2 study. *Blood* **119**, 355–363 (2012).

158. Kohrt, H. E. *et al.* Dose-Escalated, Intratumoral TLR9 Agonist and Low-Dose Radiation Induce Abscopal Effects in Follicular Lymphoma. *Blood* **124**, 3092 (2014).

159. Butowski, N. *et al.* A phase II clinical trial of poly-ICLC with radiation for adult patients with newly diagnosed supratentorial glioblastoma: A North American Brain Tumor Consortium (NABTC01-05). *J. Neurooncol.* **91**, 175–182 (2009).

160. Chi, K. *et al.* Combination of Conformal Radiotherapy and Intratumoral Injection of Adoptive Dendritic Cell Immunotherapy in Refractory Hepatoma. *J. Immunother.* **28**, 129–135 (2005).

161. Raj, S. *et al.* Long-term clinical responses of neoadjuvant dendritic cell infusions and radiation in soft tissue sarcoma. *Sarcoma* **2015**, (2015).

162. Gulley, J. L. *et al.* A pilot safety trial investigating a vector-based vaccine targeting carcinoembryonic antigen in combination with radiotherapy in patients with gastrointestinal malignancies metastatic to the liver. *Expert Opin. Biol. Ther.* **11**, 1409–1418 (2011).

163. Lechleider, R. J. *et al.* Safety and immunologic response of a viral vaccine to prostate-specific antigen in combination with radiation therapy when metronomic-dose interleukin 2 is used as an adjuvant. *Clin. Cancer Res.* **14**, 5284–5291 (2008).

164. Gulley, J. L. *et al.* Combining a Recombinant Cancer Vaccine with Standard Definitive Radiotherapy in Patients with Localized Prostate Cancer. *Clin. Cancer Res.* **11**, 3353–3362 (2005).

4

165. Iinuma, H. *et al.* Phase I clinical study of multiple epitope peptide vaccine combined with chemoradiation therapy in esophageal cancer patients. *J. Transl. Med.* **12**, 1–12 (2014).

166. Ramjiawan, R. R., Griffioen, A. W. & Duda, D. G. Anti-angiogenesis for cancer revisited: Is there a role for combinations with immunotherapy? *Angiogenesis* **20**, 185–204 (2017).

167. Tang, H. *et al.* Facilitating T Cell Infiltration in Tumor Microenvironment Overcomes Resistance to PD-L1 Blockade. *Cancer Cell* **29**, 285–296 (2016).

168. Fukumura, D., Kloepper, J., Amoozgar, Z., Duda, D. G. & Jain, R. K. Enhancing cancer immunotherapy using antiangiogenics: opportunities and challenges. *Nat. Rev. Clin. Oncol.* **15**, 325–340 (2018).

169. Wu, N. Z., Klitzman, B., Dodge, R. & Dewhirst, M. W. Diminished leukocyte-endothelium interaction in tumor microvessels. *Cancer Res.* **52**, 4265–4268 (1992).

170. Griffioen, A. W., Damen, C. A., Martinotti, S., Blijham, G. H. & Groenewegen, G. Endothelial Intercellular Adhesion Molecule-1 Expression Is Suppressed in Human Malignancies: The Role of Angiogenic Factors. *Cancer Res.* **56**, 1111 LP – 1117 (1996).

171. Griffioen, A. W. & Molema, G. Angiogenesis: potentials for pharmacologic intervention in the treatment of cancer, cardiovascular diseases, and chronic inflammation. *Pharmacol. Rev.* **52**, 237–68 (2000).

172. Griffioen, A. W. & Vyth-Dreese, F. A. Angiostasis as a way to improve immunotherapy. *Thromb. Haemost.* **101**, 1025–1031 (2009).

173. Facciabene, A. *et al.* Tumour hypoxia promotes tolerance and angiogenesis via CCL28 and Treg cells. *Nature* **475**, 226 (2011).

174. Curiel, T. J. *et al.* Specific recruitment of regulatory T cells in ovarian carcinoma fosters immune privilege and predicts reduced survival. *Nat. Med.* **10**, 942 (2004).

175. Barsoum, I. B., Smallwood, C. A., Siemens, D. R. & Graham, C. H. A Mechanism of Hypoxia-Mediated Escape from Adaptive Immunity in Cancer Cells. *Cancer Res.* **74**, 665–674 (2014).

176. Voron, T. *et al.* VEGF-A modulates expression of inhibitory checkpoints on CD8 + T cells in tumors. *J. Exp. Med.* **212**, 139–148 (2015).

177. Griffioen, A. W. Anti-angiogenesis: Making the tumor vulnerable to the immune system. *Cancer Immunol. Immunother.* **57**, 1553–1558 (2008).

178. Shrimali, R. K. *et al.* Antiangiogenic Agents Can Increase Lymphocyte Infiltration into Tumor and Enhance the Effectiveness of Adoptive Immunotherapy of Cancer. *Cancer Res.* **70**, 6171–6180 (2010).

179. Huang, Y. *et al.* Vascular normalizing doses of antiangiogenic treatment reprogram the immunosuppressive tumor microenvironment and enhance immunotherapy. *Proc. Natl. Acad. Sci.* **109**, 17561–17566 (2012).

180. Rahbari, N. N. *et al.* Anti-VEGF therapy induces ECM remodeling and mechanical barriers to therapy in colorectal cancer liver metastases. *Sci. Transl. Med.* **8**, 360ra135 (2016).

181. Tian, L. *et al.* Mutual regulation of tumour vessel normalization and immunostimulatory reprogramming. *Nature* **544**, 250–254 (2017).

182. Demaria, O. *et al.* STING activation of tumor endothelial cells initiates spontaneous and therapeutic antitumor immunity. *Proc. Natl. Acad. Sci.* **112**, 15408–15413 (2015).

183. Potente, M., Gerhardt, H. & Carmeliet, P. Basic and therapeutic aspects of angiogenesis. *Cell* **146**, 873–887 (2011).

Radiotherapy, anti-angiogenic therapy and immunotherapy; a therapeutic triad?

4

Chapter 5

Interferon- and STING-independent induction of type I interferon stimulated genes during fractionated irradiation

Ruben S.A. Goedegebuure*, Esther A. Kleibeuker*, Francesca M. Buffa, Kitty C.M. Castricum, Syed Haider, Iris A. Schulkens, Luuk ten Kroode, Jaap van den Berg, Maarten A.J.M. Jacobs, Anne-Marie van Berkel, Nicole C.T. van Grieken, Sarah Derks, Ben J. Slotman, Henk M.W. Verheul, Adrian L. Harris, Victor L.J.L. Thijssen

* authors contributed equally.

ABSTRACT

Background
Improvement of radiotherapy efficacy requires better insight in the dynamic responses that occur during irradiation. Here, we aimed to identify the molecular responses that are triggered during clinically applied fractionated irradiation.

Methods
Gene expression analysis was performed by RNAseq or microarray analysis of cancer cells or xenograft tumors, respectively, subjected to 3-5 weeks of 5x 2 Gy/week. Validation of altered gene expression was performed by qPCR and/or ELISA in multiple cancer cell lines as well as in pre- and on-treatment biopsies from esophageal cancer patients (NCT02072720). Targeted protein inhibition and CRISPR/Cas-induced gene knockout was used to analyze the role of type I interferons and cGAS/STING signaling pathway in the molecular and cellular response to fractionated irradiation.

Results
Gene expression analysis identified type I interferon signaling as the most significantly enriched biological process induced during fractionated irradiation. The commonality of this response was confirmed in all irradiated cell lines, the xenograft tumors and in biopsies from esophageal cancer patients. Time-course analyses demonstrated a peak in interferon-stimulated gene (ISG) expression within 2-3 weeks of treatment. The response was accompanied by a variable induction of predominantly interferon-beta and/or -lambda, but blocking these interferons did not affect ISG expression induction. The same was true for targeted inhibition of the upstream regulatory STING protein while knockout of STING expression only delayed the ISG expression induction.

Conclusions
Collectively, the presented data show that clinically applied fractionated low-dose irradiation can induce a delayed type I interferon response that occurs independently of interferon expression or STING signaling. These findings have implications for current efforts that aim to target the type I interferon response for cancer treatment.

1. BACKGROUND

Radiotherapy (RTx) remains a key modality of cancer treatment. For over a century, the clinical benefit of RTx has increased due to technical innovations that allow a more precise and targeted delivery of ionizing radiation to malignant tissues[1]. In addition, better insight in the biological and cellular response mechanisms to RTx has instigated the development of combination treatments that further improved the therapeutic outcome[2–4]. Many of the combination therapies comprise drugs that target tumor cell response mechanisms involved in radiotolerance or radioresistance[5, 6]. The efficacy of such combination therapies depends on adequate dose-scheduling and timing of the different treatment modalities[6]. To further improve combination radiotherapy, it is vital to better understand cellular and molecular responses and their time course during treatment. Gaining insight in the dynamic responses to radiotherapy is especially relevant for patients that are treated with a daily dose of irradiation for several weeks (conventional fractionated radiotherapy). Indeed, exploring molecular responses to irradiation has been recognized as an unmet need to develop rational approaches of combination radiotherapies[6].

While radiation-induced changes of gene expression have been explored previously[7–10], most studies have been aimed at identifying mechanisms that are involved in the development of acquired radioresistance. The induction of such a radioresistant phenotype usually requires irradiation schedules that are not commonly used in a clinical setting. Consequently, there is still only limited insight in the dynamics of cellular and molecular responses that actually occur during the time course of clinically applied low-dose fractionated irradiation. This lack of knowledge hampers the development and optimization of effective combination treatments with radiotherapy. Recently, we have shown that conventional fractionated RTx (daily 2 Gy irradiation, 5 days per week, up to 6 weeks) can induce a reversible radiotolerant phenotype in cancer cells *in vitro*; a response we coined as adaptive radioresistance. This response occurs in cancer cells of different origin and is characterized by convergence of clonogenic survival to a steady state level during treatment[11]. The observation that the surviving cells display the same radiosensitivity as non-irradiated cells following treatment suggests that cancer cells do not acquire radioresistance as a genetic trait. Possibly, a balance between cell death and repopulation occurs with cells adopting a phenotype that allows them to tolerate repetitive cycles of irradiation. This might represent a radioresistance mechanism with potentially clinical implications which urged us to further study the molecular pathways that are triggered during conventional low-dose fractionated irradiation.

Here, we report that clinically applied fractionated irradiation is accompanied by the induction of a type I interferon response which is characterized by the increased expression of interferon stimulated genes *in vitro*, *in vivo* and in esophageal cancer patients. Importantly, the observed response occurs independently of induction of

5

125

specific type I/III interferon expression or upstream activation of the STING signaling pathway. Our findings have implications for current efforts to develop drugs that target the type I interferon response and warrant further investigation into the role of the type I interferons and interferon stimulated genes during fractionated radiotherapy.

2. METHODS

2.1 Cell culture
The high-grade astrocytoma cell line D384 (grade III), colorectal cancer cell lines HT29, RKO, SW480, COLO320 and HCT116 and esophageal cancer cell line OE19 were cultured in Dulbecco's Modified Eagle Medium (DMEM), supplemented with 10% fetal calf serum, 100 IU/mL penicillin and 100 μg/mL streptomycin. Cells were maintained at 37°C and 5%CO2 under humidified conditions. Cell lines were authenticated by STR profiling (BaseClear, Leiden, The Netherlands) and were repeatedly found negative for mycoplasm infection as checked by PCR.

2.2 In vitro and in vivo irradiation
Irradiation of cultured cells in vitro was performed with γ-radiation using a ^{60}Co source (2.80 Gy/min; Gammacell 200; Atomic Energy of Canada, Mississauga, Ontario, Canada) or a ^{137}Cs laboratory irradiator (0.81 Gy/min; IBL 637, CIS Bio International). Cells were irradiated with a daily dose of 2 Gy from Monday till Friday for up to 6 weeks, i.e., a maximum of 30x 2 Gy). Culture medium was refreshed every Monday. At the end of each treatment week, culture medium was collected and cells were harvested and stored at -80ºC until further analysis. All experiments were performed in triplicate unless indicated otherwise.

Irradiation of xenograft HT29 tumor in nude mice were carried out as published previously[12]. In brief, $5x10^6$ HT29 cells in 100 μL Matrigel/DMEM suspension were injected subcutaneously in the lower right flank of 6- to 7-week-old female BALB/c nude mice. Tumor growth was monitored 3-4 times per week measuring the tumor length (L), width (W), and height (H) with calipers. Tumor volume was calculated as 1/6*π*L*W*H. When the average tumor size reached a volume of approximately 100 mm^3, the mice were randomized into experimental groups. Irradiated mice received daily 2 Gy fractions from Monday to Friday using an Xstrahl RS320 X-Ray irradiator (Xstrahl Ltd. UK). For this, mice were anesthesized by i.p. injection of 100 μL 1:1:8 hypnorm: hypnovel: sterile water after which they were placed in ±12 mm thick lead tubes with only the tumor exposed for irradiation. Following treatment, tumor tissues were collected, snap frozen and stored at -80ºC until further analysis.

2.3 Patient material
Snap frozen and formalin-fixed paraffin embedded primary tumor biopsies from esophageal cancer patients receiving neoadjuvant chemoradiation (paclitaxel,

carboplatin and concurrent radiotherapy of 41.4 Gy in 23 fractions) were collected via endoscopy as part of an IRB-approved clinical trial (NCT02072720, METC-VUmc identifier 2013.340). Tumor biopsies were collected at baseline and during treatment, either after 1, 2, 3 or 4 weeks depending on the study cohort. Histology from all obtained biopsies was assessed by an expert pathologist (NvG). Pre-treatment biopsies were included when tumor cell percentage was >20%. As during treatment samples could be extensively affected by radiotherapy induced tumor necrosis, accurate assessment of tumor cell was not feasible. Instead, these biopsies were obtained with extra care from a representative area on the tumor border by an expert gastroenterologist.

2.4 RNA extraction and qPCR

RNA isolation from mouse xenografts tumors and cultured cells for RNA sequencing analysis was performed using the mirVANA kit (Life technologies), excluding the purifying miRNA step. For all other RNA isolations, TRIzol (Invitrogen) was used according to the supplier's protocol, using chloroform for phase separation and isopropanol to precipitate the RNA. The final RNA concentration was determined using the Nanodrop ND-1000. Subsequent reverse transcription was performed on 1 μg RNA using the iScript kit (Biorad) following the suppliers' protocol. cDNA was stored at -20ºC until further use. qPCR was performed using 1x SYBR green supermix (Biorad), 1.5 μL cDNA and 400 nM primers in a total sample volume of 25 μL. For normalization, the primers targeting reference genes β-actin (F: TTCCTATGTGGGCGACGAG R: TCCTCGGGAGCCACACG), HPRT (F: TGCTGAGGATTTGGAAAGG R: TCACATCTCGAGCAAGACGT) and cyclo-A (F: AGCATGTGGTGTTTGGCAAA R: TCGAGTTGTCCACAGTCAGC) were used unless stated otherwise. All other primer sequences are listed in **Supplementary Table 1**. qPCR was performed in a CFX96 cycler (Biorad) and the following cycling conditions were used: 95ºC for 5 minutes, followed by 40 cycles of 95ºC for 10 seconds and 60ºC for 30 seconds, after which standard meltcurve analysis was performed.

2.5 mRNA Sequencing and data analysis

Approximately 1 μg total RNA was normalized and enriched using the NEBNext PolyA mRNA Magnetic Isolation Module (New England Biolabs) with a final elution in 18 μL, to feed into the NEBNext mRNA Library Prep Master Mix Set for Illumina (New England Biolabs) with the following modifications: post fragmentation purification was a RNA Clean Ampure XP (Agencourt) magnetic bead clean-up (2.8x volume) with 3x 80% ethanol washes and a final elution in 15 μL buffer EB (QIAGEN). The first strand reverse transcription was conducted following protocol, but with the addition of Actinomycin D (0.05 μg/μl final concentration). The second strand reverse transcription followed the E7490 protocol, but the reaction buffer was replaced with NEBNext® Second Strand Synthesis (dNTP-free) Reaction Buffer (New England Biolabs) and a dNTP mix containing A,C,G,U at 0.3 mM for each final concentration. Double strand cDNA purification was done using Ampure XP magnetic bead clean-up (1.2x volume). End repair, A-tailing and adapter ligation were conducted following protocol with 1.8x volume Ampure XP clean-

5

ups between steps. The PCR amplification was performed following protocol with 2 μL H2O being replaced with 2 μL USER enzyme and the Phusion polymerase being added after a 37 ºC incubation for 30 minutes. A subsequent 12 cycles of PCR were performed using custom PCR primers[13]. Post-PCR libraries were quantified with Picogreen (Invitrogen) and size range determined using the Tapestation D1K (Agilent). Libraries were pooled equimolarly with a final quantification by qPCR before sequencing. Then, quality control was performed using FASTQC version 0.11.2. Subsequently, data filtering such as removal of technical sequences (e.g. adaptors), duplicate reads, and secondary reads were performed using Prof. Buffa's laboratory pipelines. Quality control task was performed again after the data filtering procedures to double confirm the quality. The clean short reads were aligned to human reference genome GRCH37 using tophat2 version 2.0.13. The library type in tophat2 was set to fr-firststrand, which specified the right-most end of fragment is the first sequenced. The expected inner distance between mate pairs is set to --mate-inner-dist=90. After that, the differential expression of each gene was estimated by cuffdiff version 2.2.1. The setting of library type is fr-firststrand, which is the same with the setting in tophat2. In the end, the consistently up-regulated genes and down-regulated genes, based on statistics of rank product, among samples are generated. The R library of Rank Product is version 2.40.0. The p-value and the probability of false positive of gene rank were estimated by a resampling technique with 100 random permutations.

2.6 Microarray gene expression and data analysis
High-density oligonucleotide Expression BeadChips (Human HT12_V4, Illumina) were used for whole Genome-Wide gene expression profiling, for 3 to 4 biological replicates. In brief, 500 ng of total RNAs were reverse transcribed to synthesize first- and second-strand cDNA, purified and in vitro transcribed to synthesize biotin-labeled cRNA using the Illumina TotalPrep-96 RNA Amplification Kit (Ambion). A total of 1500 ng of biotin-labeled cRNA was then hybridized to the BeadChips at 55 ºC for 18 hours. The hybridized BeadChip was washed and stained with streptavidin-Cy3 according to the manufacture protocols using Illumina whole-genome gene expression direct hybridization assay (Illumina). GenomeStudio Data Analysis Software was used to visualize and analyze images generated. The Illumina microarrays were pre-processed using R package LIMMA (v3.16.8). Briefly, background correction was performed using negative controls, followed by quantile normalization and log2 transformation. Any probes whereby all samples had detection p-value ≥ 0.05 were regarded as not-expressed and subsequently removed from the dataset. Paired analysis was performed, as at least 3 matched samples were available in each group. Gene ontology enrichment analyses of differentially expressed genes were conducted using R package GOstats (v2.26.0). All visualizations and statistical analyses were performed in R statistical environment (v4.0.2).

2.7 ELISA

Enzyme-linked immunosorbent assays were performed according to the manufacturer's instructions (R&D systems, Abingdon, UK). Expression levels were normalized to the number of cells for the *in vitro* experiments and to the total protein level for the tumor xenografts.

2.8 Clonogenic survival assay

Clonogenic survival assays were determined as described before[11]. In brief, cells were collected at different time points during the treatment period and 10.000 to 100.000 cells were plated in duplicate in T25 culture flasks and cells were grown for 14 days under normal culture conditions. At the end of each experiment, cells were fixed with 100% ethanol for 30 minutes, and stained with Giemsa solution (Merck, Darmstadt, Germany). Colonies (>50 cells) were counted visually and plating efficiency (PE) was calculated by dividing the number of colonies counted by the number of cells plated. Surviving fractions (SF) were calculated by dividing the PE of irradiated cells by the PE of the non-irradiated controls.

2.9 Statistical analysis

For the statistical analyses of mRNA sequencing and micro-array studies, please refer to the specific method description. Differences in mRNA and protein expression were tested for statistical significance with either the non-parametrical Wilcoxon signed rank test or Mann-Whitney U test for comparison of paired or independent observations in 2 groups, respectively. For multiple groups or time-course comparisons a Kruskal-Wallis test with Bonferroni post-hoc test was performed. For the comparison of HT29 xenograft tumor volumes a 2-way ANOVA with Bonferroni post-hoc test was performed. A p-value ≤ 0.05 was considered as statistically significant. Statistical analyses were performed using GraphPad Prism 8.0.0, GraphPad Software, San Diego, California US.

3. RESULTS

To identify the molecular mechanism(s) involved in the response to conventional fractionated irradiation, we set out to compare gene expression profiles in irradiated vs. non-irradiated cells. For this, HT29 colorectal carcinoma cells were subjected to a common clinically applied treatment schedule of daily 2 Gy irradiation, 5 days per week for up to 5 weeks (**Figure 1a**). Since our previous work showed that clonogenic survival converges to a steady state after two weeks of treatment, i.e. 10 fractions (**Figure 1b**), we first compared the expression at that timepoint with the expression in non-irradiated cells, cultured identically for 2 weeks. Gene expression analysis by RNA sequencing identified over a thousand differentially expressed genes (adjusted p-value ≤ 0.05) in irradiated vs. non-irradiated cells (**Figure 1c and Supplementary tables 2+3**).
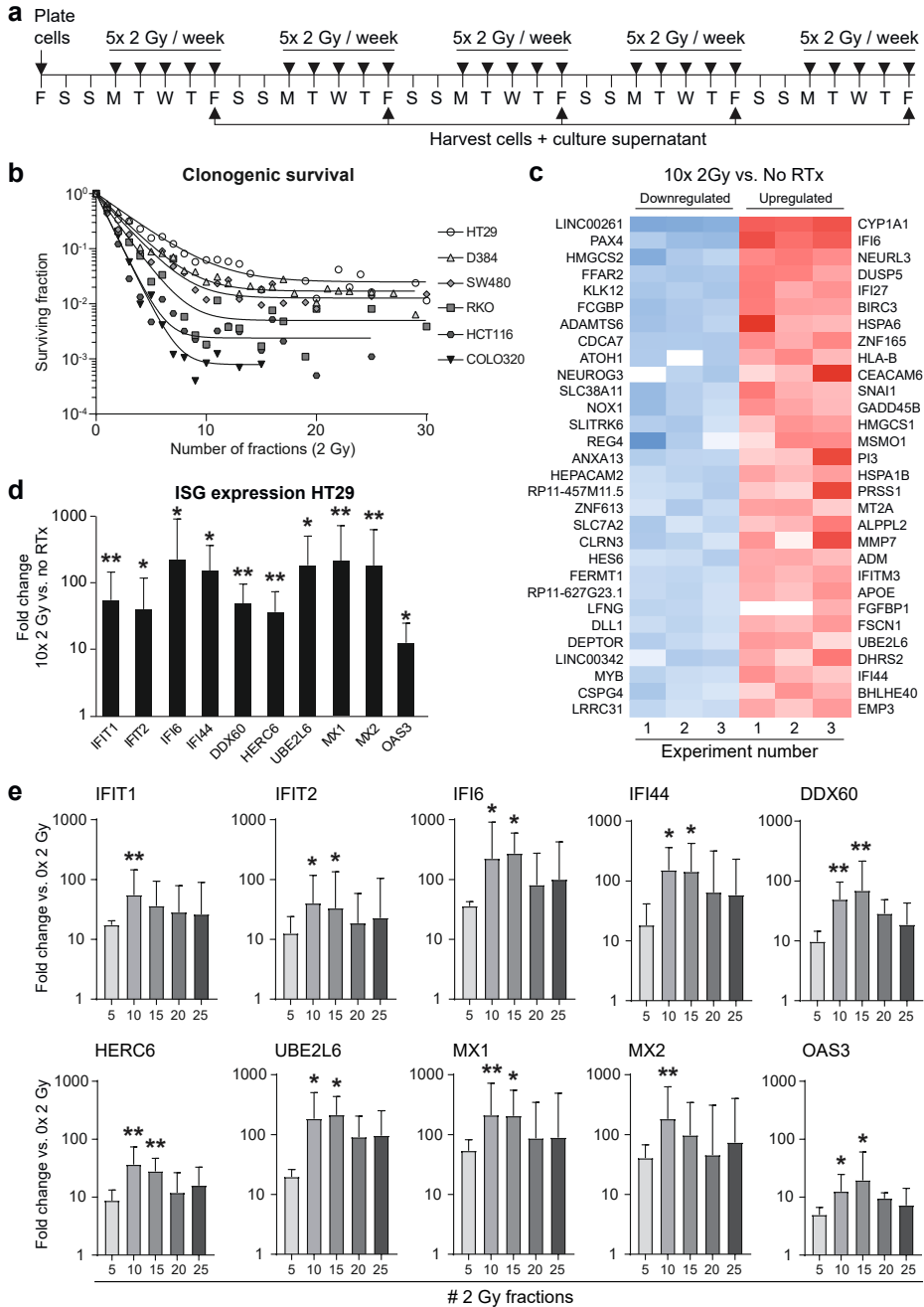
Figure 1. Induction of a type I IFN response in cancer cells peaks after 2 weeks of fractionated irradiation *in vitro*. Fractionated irradiation induces a type I IFN response in cancer cells, which peaks after 2 weeks and coincides with a convergence in clonogenic survival to a steady state. (**a**) Scheme of fractionated irradiation applied to human cancer cells *in vitro*. (**b**) Clonogenic survival analyses show a log-linear decline in survival during the first 2 weeks of treatment

after which a steady-state survival is reached up to 6 weeks of treatment. Adapted from Van den Berg et al. (11). (**c**) Heat map showing the 30 most downregulated and upregulated genes after 2 weeks of treatment vs. untreated as determined by RNA deep-sequencing of HT29 cells (n=3). (**d**) The mRNA expression induction of a panel of 10 IFN-stimulated genes (ISGs) after 2 weeks of treatment was confirmed by qPCR (n=3). Geometric mean + SD is shown. * p-value ≤ 0.05 vs. no radiotherapy (RTx). (**e**) Time course analysis of ISG mRNA expression induction shows a peak starting around 2 weeks of treatment (n=3). Geometric mean + SD is shown. * p-value ≤ 0.05 vs 0x 2 Gy.

Gene ontology (GO) analysis revealed over 250 significantly enriched upregulated biological processes, amongst which the 'type I IFN-mediated signaling pathway' was identified as the most significantly enriched biological process (adjusted p-value ≤ 0.0001) (**Supplementary figure S1a** and **Supplementary table 4**). Other identified GO terms were closely related to biological processes such as positive regulation of cell migration, angiogenesis, negative regulation of cell proliferation, amine metabolism, response to virus and nucleosome assembly. Additionally, over a hundred significantly enriched downregulated biological processes were identified, mainly related to translational processes and cell cycle (**Supplementary figure S1b**). Given the current insights in radiotherapy-induced type I interferon signaling[14, 15], as well as previous (pre) clinical trials on the combination of radiotherapy with type I interferons in cancer[16], we further focused our research on this particular response.

The induction of the type I IFN response in HT29 cells could be confirmed by qPCR with a panel of 10 interferon stimulated genes (ISGs) that are linked to this response (**Figure 1d**). Moreover, the increased expression of ISGs by 10x 2 Gy irradiation could be confirmed in multiple cancer cell lines, including high-grade astrocytoma cells (D384) and different colorectal cancer cell lines (SW480, HCT116, COLO320, RKO; **Supplementary figure S2**). To determine the dynamics of the response, the ISG expression was analyzed weekly for up to 5 weeks. This showed a slight induction in expression for most ISGs after 5 fractions, and a peak induction after 2 to 3 weeks of treatment (**Figure 1e and Supplementary figure S3a**). Continuation of RTx eventually resulted in a decreased expression, although it generally remained above the level of non-irradiated cells. Of note, while single dose irradiation also induced dose-dependent ISG expression, this typically leveled off after 6 Gy (**Supplementary figure S3b**). Collectively, these data show that fractionated RTx induces an intrinsic type I interferon response *in vitro* which peaks within 2 to 3 weeks of treatment and coincides with the development of a steady state in clonogenic survival.

To extend these findings, HT29 xenograft tumors were locally irradiated using the same clinical schedule as the cultured cells, i.e., 2 Gy per day, 5 days per week for up to 3 weeks (**Figure 2a**). Tumor growth showed a delay after 2 weeks of treatment but appeared to recover in week 3 (**Figure 2b and Supplementary figure S4a**). Next, gene expression profiles of non-irradiated tumors vs. tumors that received 1, 2 and 3 weeks of radiotherapy were obtained using human microarray analysis.

5

a IFN expression HT29

b HT29 cell culture supernatant

c IFN expression *in vitro*

d IFN expression *in vivo*

e IFN-β *in vivo*

f ISGs in EC patients

g IFNs in EC patients

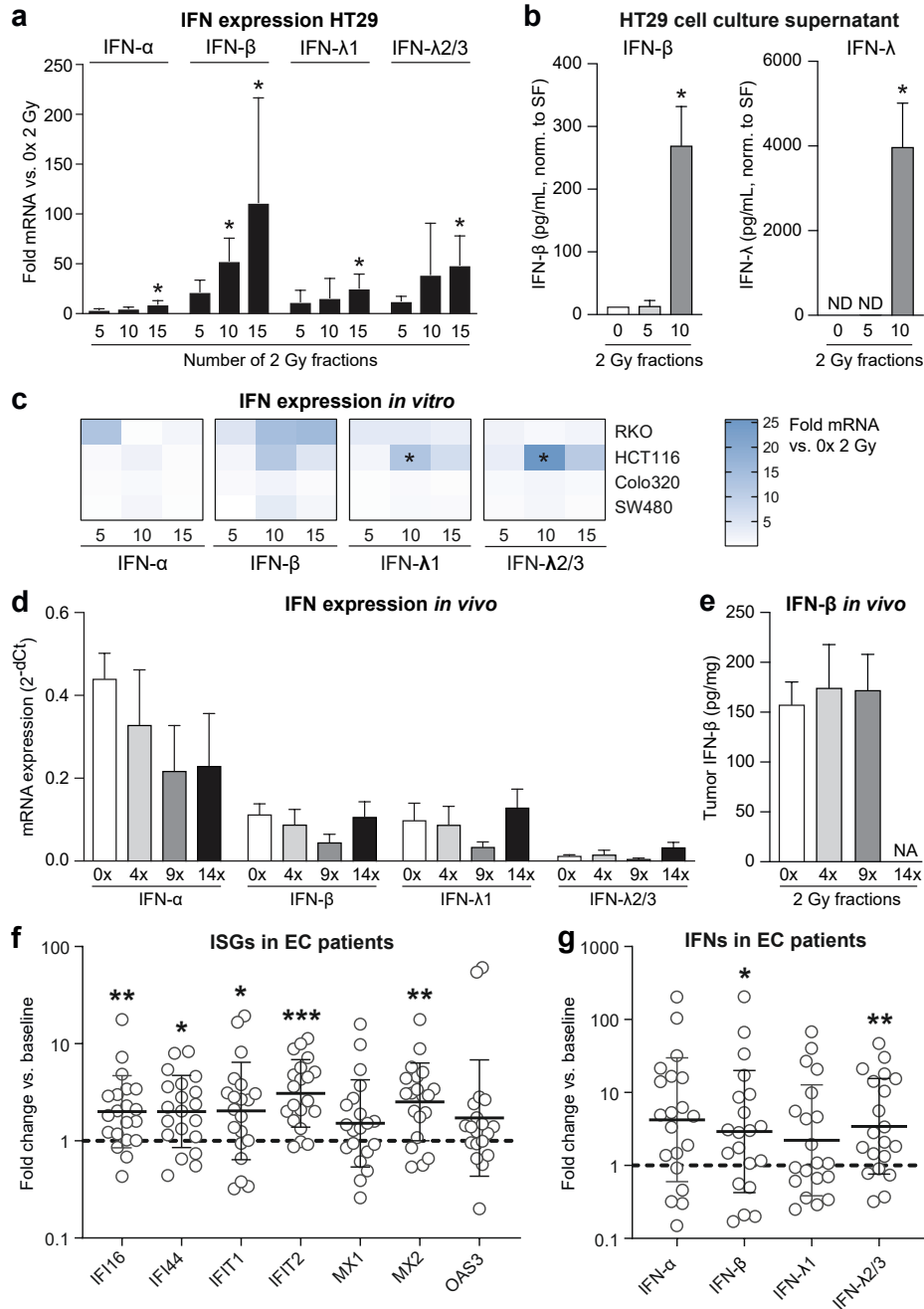**Figure 2.** Induction of a type I IFN response in tumor tissue peaks after 2 weeks of fractionated irradiation *in vivo.* The induction of a type I IFN response upon fractionated radiotherapy is confirmed in a HT29 xenograft model. (**a**) Scheme of fractionated irradiation applied to HT29 xenograft tumor in mice. (**b**) Tumor growth curves of HT29 xenograft tumors with (black squares)

or without (white squares) irradiation. Note the growth delay starts around day 10 and recovers around day 17 (n=5 mice/group). (**c**) Volcano plot of microarray data comparing gene expression in HT29 xenograft tumors after 2 weeks of RTx vs. no radiotherapy (RTx). NS = not significant. FC = fold change. (**d**) Time course analysis of ISG mRNA expression induction shows a gradual increase that peaks around 2 weeks of treatment. * p-value ≤ 0.05 vs. 0x 2 Gy.

After 2 weeks of treatment, 34 differentially expressed genes in irradiated vs. non-irradiated tumor tissues were identified, of which 5 showed decreased expression and 29 showed increased expression (**Figure 2c**, **Supplementary table 5**). Gene ontology analysis revealed 52 significantly enriched biological processes, amongst which the 'type I IFN-mediated signaling pathway' was again identified as the most significantly enriched pathway (p-value ≤ 0.0001, count 18/61) (**Supplementary figure S4b and Supplementary table 6**). Interestingly, a less pronounced but similar gene expression profile was observed after 1 and 3 weeks of irradiation, whereas a single dose of 5 Gy resulted in more differentially expressed genes (**Supplementary figure S4c)**. Expression analysis of the same ISG signature panel as used before, again confirmed the induction of a type I IFN response (**Supplementary figure S4d**). Moreover, in line with our observations in the cell lines, time course analysis revealed that the expression of the ISGs peaked after 2 to 3 weeks of treatment (**Figure 2d**). Altogether, these results show that fractionated RTx induces a potent type I interferon response in tumor cells after 2 to 3 weeks of treatment.

To determine which type I IFN could have triggered the response, we analyzed the mRNA expression of two key family members *in vitro*, i.e., IFN alpha (*IFN-α*) and IFN beta (*IFN-β*). Since type III interferons (IFN lambda; IFN-λ) were recently shown to be induced by RTx in HT29[17], these cells were included as a positive control. Analysis of fractionally irradiated HT29 tumor cells revealed that the treatment predominantly induced the mRNA expression and protein secretion of IFN-β and IFN-λ (**Figure 3a+b**). Other cell lines subjected to fractionated irradiation displayed either a modest increase in mRNA expression of either *IFN-α*, *IFN-β*, *IFN-λ* or a combination (HCT116 and RKO), or no interferon induction at all (SW480 and Colo320) (**Figure 3c**).

Interestingly, all of these cell lines showed clear induction of ISG expression in response to irradiation, albeit less profound in the cell lines lacking interferon expression (**Supplementary figure S2**). In the xenograft tumors, no changes in the expression of any of the different interferons could be detected (**Figure 3d+e**). These findings suggest an uncoupling between the induction of ISGs and the expression of interferons, the latter usually mediating ISG expression. Of note, all the cell lines expressed the appropriate IFN receptors required to be responsive to the different IFNs (**Supplementary figure S5**).

5

133

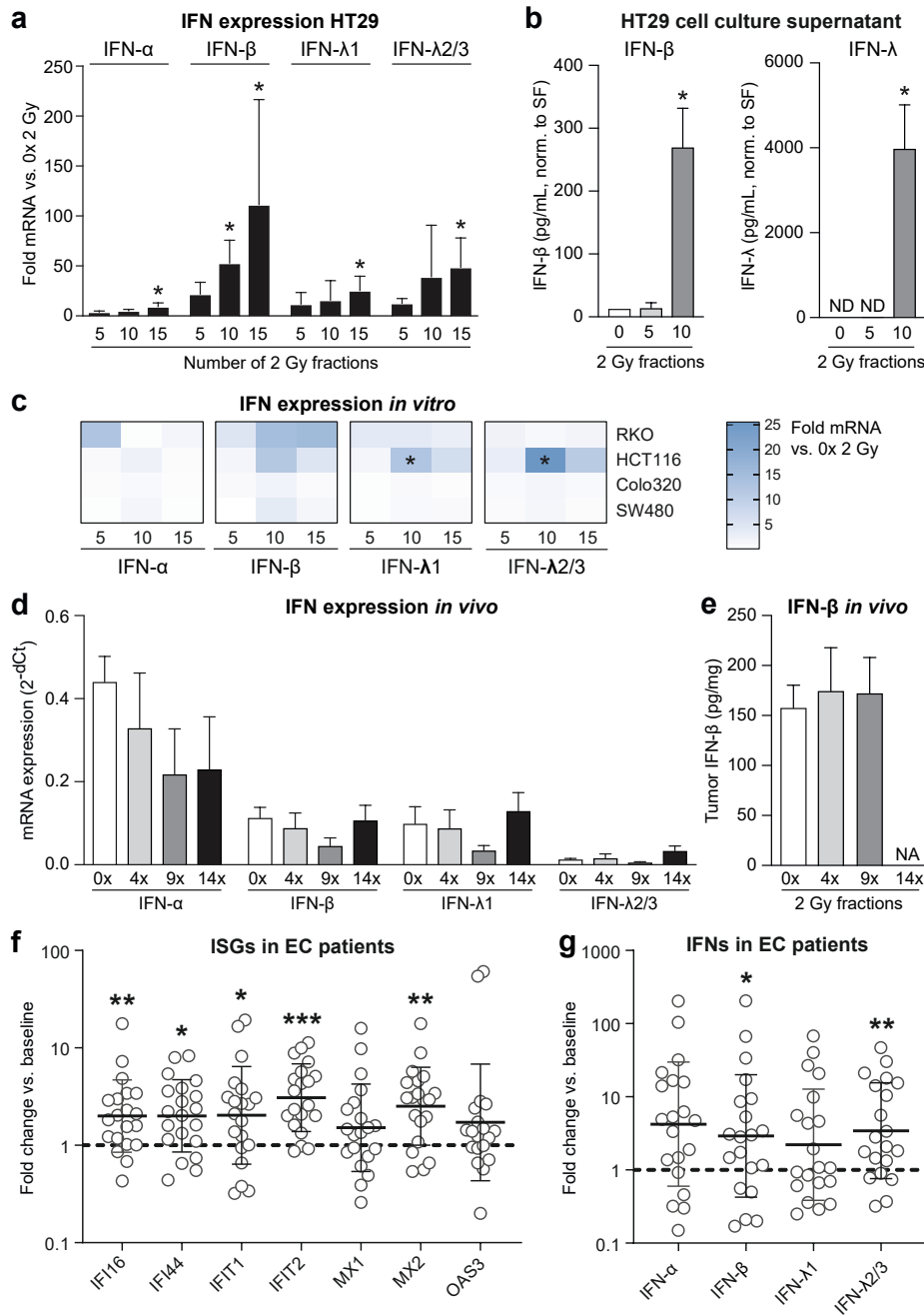**Figure 3.** Patterns of type I and III interferon induction upon fractionated irradiation. Different patterns of either type I and/or type III interferon induction occur *in vitro, in vivo* and patients with esophageal cancer during the course of fractionated radiotherapy, independent of ISG induction. (**a**) mRNA expression analyses of interferon expression in HT29 cells during fraction-

134

ated irradiation (n=3). * p-value ≤ 0.05 vs. 0x 2 Gy. (**b**) Levels of IFN-β and IFN-λ protein in cell culture supernatants of HT29 cells during fractionated irradiation (n=3). * p-value ≤ 0.05 vs. 0x 2 Gy. CM = culture medium. SF = surviving fraction. (**c**) mRNA expression analyses of interferon expression in RKO, HCT116, COLO320 and SW480 cells during fractionated irradiation vs. 0x 2 Gy. * p-value ≤ 0.05 vs. 0x 2 Gy. (**d**) mRNA expression analyses of interferon expression in HT29 xenograft tumors during fractionated irradiation (n=5 mice/group). (**e**) Levels of IFN-β and IFN-λ protein in mouse serum during fractionated irradiation (n=5 mice/group). (**f**) mRNA expression levels of ISG expression in patient-matched tumor samples from esophageal cancer patients (n=20) prior to or during chemoradiotherapy. Fold expression in on-treatment samples vs. pre-treatment is shown. * p-value ≤ 0.05 vs. matched pre-treatment samples. (**g**) Similar as in (**f**) for fold change in mRNA expression levels of different IFNs. * p-value ≤ 0.05 vs. matched pre-treatment samples.

To assess the clinical relevance of these findings, we analyzed whether a type I IFN response occurs in cancer patients, in the context of a clinical pilot study (NCT02072720) in esophageal cancer patients receiving neoadjuvant chemoradiotherapy (CRT) with paclitaxel, carboplatin and concurrent radiotherapy (41.4 Gy in 23 fractions of 1.8 Gy). Tumor biopsies of 20 patients (see **Supplementary table S7** for patient characteristics) were collected at baseline and after 1, 2, 3 or 4 weeks of treatment, in successive cohorts. Subsequent expression analysis revealed that expression levels of 5 out of 7 investigated ISGs were significantly elevated during treatment as compared to baseline (**Figure 3f**). Of note, while the number of patients in this small pilot study did not allow us to confirm an association between pre-treatment ISG expression levels and response to treatment[18, 19], we did observe ISG expression levels were highest in patients that had received two weeks of treatment (**Supplementary figure S6a**). The latter is in line with our findings in tumor cells and xenograft tumors. Furthermore, a modest induction of all interferons was seen (significant for IFN-β and IFNλ2/3; **Figure 3g**), but again ISG expression appeared to occur independent of type I interferons, as only a weak correlation was observed between induction of IFN-β and 3 out of 7 ISGs (**Supplementary figure S6b**). Thus, both in a preclinical immunocompromised xenograft model as well as in a clinical setting, commonly applied fractionated irradiation triggers a type I interferon response independent of actual type I interferon expression induction.

Since the induction of a type I interferon response during radiotherapy has been linked to cGAS/STING signaling[14, 20, 21], we further evaluated the role of STING as well as of interferon expression on the induction of ISGs during fractionated irradiation. Analysis of both mRNA and protein expression showed low or even absent basal expression of cGAS, STING or both in the majority of cell lines, except for HT29 (**Figure 4a+b**). Since all cell lines did show elevated ISG expression during fractionated irradiation, these findings suggest that the radiation-induced type I interferon response does not depend on cGAS/STING signaling. Of note, when cells that were deficient in either cGAS or STING were irradiated, the expression of the absent proteins was not induced (**Supplementary figure S7a**).
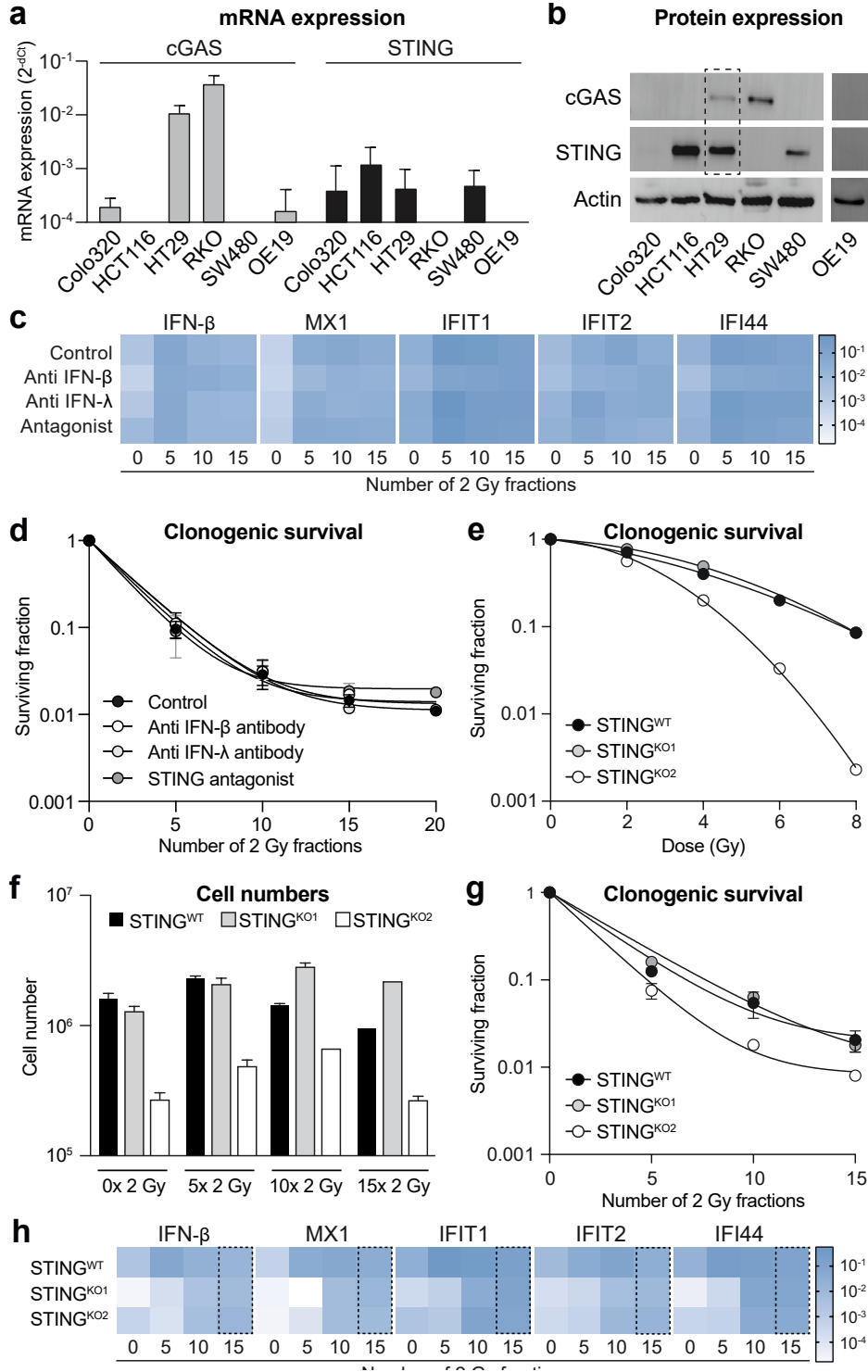
5

135

a mRNA expression

b Protein expression

c

d Clonogenic survival

e Clonogenic survival

f Cell numbers

g Clonogenic survival

h

Figure 4. ISG induction upon fractionated irradiation occurs independent of STING, IFN-β or IFN-λ. Interferon stimulated genes (ISGs) can be induced independent of the interferons known to mediate this response, or the upstream regulator protein STING. (**a**) mRNA expression levels of cGAS (grey bars) and STING (black bars) in different cancer cell lines. (**b**) Western blots showing protein expression of cGAS and STING in different cancer cell lines. Actin staining was used as loading control. The dotted box shows the only cell line, i.e. HT29, in which both cGAS and STING protein expression could be detected. (**c**) Heat map of mRNA expression of different ISGs and IFN-β in HT29 cells treated with fractionated irradiation in the presence or absence of either anti IFN-β antibody, anti IFN-λ antibody or a STING antagonist. No significant changes were observed in the presence of any of the treatments as compared to irradiation alone (n=3). (**d**) Clonogenic survival of HT29 during fractionated irradiation in the presence or absence of either anti IFN-β antibody, anti IFN-λ antibody or a STING antagonist. No significant changes in surviving fractions were observed in the presence of any of the latter treatments as compared to irradiation alone (n=3). (**e**) Clonogenic survival of HT29 wild-type cells and two HT29 STING knockout cells in response to single dose irradiation. STING^{KO2} shows higher radiosensitivity as compared to wild type cells. (**f**) Cell numbers of HT29 wild-type cells and two HT29 STING knockout cells during fractionated irradiation. While STING^{KO2} displayed slower growth already at base-line, fractionated irradiation did not affect growth of knockout cells compared to wild type cells. (**g**) Clonogenic survival of HT29 wild-type cells and two HT29 STING knockout cells during fractionated irradiation. STING^{KO2} shows higher radiosensitivity as compared to wild type cells. (**h**) Heat map of mRNA expression of different ISGs and IFN-β in HT29 wild-type cells and two HT29 STING knockout cells during fractionated irradiation (n=2). At baseline (0x 2 Gy) both knockout cell lines show lower expression of all genes analyzed as compared to wild-type cells. At the end of the treatment period (15x 2 Gy, dotted box) no more difference in expression levels is observed in wild-type vs. knockout cells for any of the genes analyzed.

To further study the disconnection between the radiation-induced type I interferon response and cGAS/STING activation or type I interferon expression, we irradiated HT29 cells (which express all components of the pathway) in the presence of either anti-IFN-β antibody, anti-IFN-λ antibody or a STING antagonist. Optimal antibody treatment conditions were based on literature[16] and the levels of IFN-β and IFN-λ in cell culture supernatants. In addition, direct effects of treatment on cell viability were excluded (**Supplementary figure S7b**). Also, the inhibitory function of the STING antagonist was confirmed by Western blot showing reduced phosphorylation of the downstream target protein Tank Binding Kinase (pTBK) after 4 Gy irradiation as compared to no irradiation (**Supplementary figure S7c**). In line with our previous observations, neither treatment with anti-IFN antibodies nor treatment with the STING antagonist had any effect on the induction of ISG or IFN expression during fractionated irradiation (**Figure 4c**). Moreover, neither treatment affected the clonogenic survival of HT29 cells prior to irradiation (**Supplementary figure S7d**) or during fractionated irradiation (**Figure 5d**). This was not due to lack of treatment efficacy, since anti-IFNβ antibody treatment did neutralize the known inhibitory effect of IFN-β on cell growth (**Supplementary figure S7e**). Again, these data suggest that the type I IFN response that is triggered by fractionated irradiation occurs independent of cGAS/STING signaling or induction of IFN expression.

Since our findings are different from the previously published role of STING in the response to radiotherapy and could be due to minimal undetected levels of STING, we also generated HT29 STING knockout cells using CRISPR/Cas gene editing. In 8 out of 10 single cell clones, knockdown could be confirmed by Western Blot (**Supplementary**

5

figure S8a). Two clones were selected for further analysis and DNA sequencing confirmed gene editing at the expected location in exon 6, causing a frameshift with two adjacent premature stop codons (**Supplementary figure S8b**). Interestingly, one of the STING knockout clones showed a phenotype similar to the wild type cells while the other knockout clone showed reduced cell growth (data not shown) and increased radiosensitivity (**Figure 4e**). This clonal difference in growth and radiosensitivity was further illustrated when both clones were subjected to fractionated irradiation for 3 weeks (**Figure 4f+g**). Despite these differences in phenotype, both knockout cell lines showed a similar, albeit delayed, induction of ISG expression as compared to the wild type cells (**Figure 4h**). The latter suggests that STING, while it contributes to the induction of a type I IFN response during fractionated irradiation, is not essential for this response to occur. Altogether, STING, IFN-β as well as IFN-λ appear to be dispensable for activation of a type I IFN response during fractionated irradiation.

4. DISCUSSIONS

In this study we demonstrate that a commonly applied clinical schedule of conventional low-dose fractionated irradiation (daily fractions of 2 Gy for 5 days per week, up to 6 weeks) induces an intrinsic type I interferon (IFN) response in tumor cells that is characterized by an increased expression of interferon stimulated genes (ISGs). The response peaks within 3 weeks of treatment and coincides with a convergence to a plateau in clonogenic survival *in vitro* and treatment resistance *in vivo*. It also occurs in tumor tissues from esophageal cancer patients during chemoradiotherapy. Importantly, the type I IFN response can be induced independently of a specific type I IFN or of STING-mediated signaling. Collectively, these findings suggest a potential clinical benefit of targeting specific type I interferon response genes (ISGs), irrespective of targeting STING or type I interferons during fractionated low-dose radiotherapy.

The induction of a type I IFN response by fractionated irradiation has been described previously in cancer cells of different origin. For example, using either breast cancer cells, prostate cancer cells or gliosarcoma cells Tsai et al. found significant induction of several ISGs after 5x 2 Gy while 1x 10 Gy did not trigger expression[9]. This was repeatedly confirmed by another group that described a more prominent induction of ISGs in prostate cancer cells after fractionated irradiation (10x 1 Gy) as compared to single dose (1x 10 Gy) irradiation[22–24]. More recently, Vanpouille-Box et al. reported increased expression of ISGs in different mouse and human breast cancer cells after fractionated irradiation (3x 8 Gy), but not after single dose irradiation (1x 20 Gy)[10]. Our current data are in line with all these *in vitro* findings and confirm that the response is triggered in *in vivo* as well, albeit to a somewhat lesser extent[9, 10]. Importantly, we show that the response becomes particularly activated after 2 weeks of radiotherapy and remains highly activated throughout the course of treatment. Together with the observation that the response is activated during fractionated radiotherapy in esophageal cancer

patients, these findings suggest a potential clinical relevance of type I IFN signaling in the response to treatment. In line with this, the induction of type I interferons as well as other molecules by radiotherapy has been shown to elicit an anti-tumor immune response[4, 25]. At the same time, radiotherapy can hamper an adequate immune response which, together with the potential immune induction, has spurred interest to combine radiotherapy with immunotherapy, particular with checkpoint inhibitors[4, 25, 26]. Regarding the direct combination of radiotherapy with type I IFNs, the outcomes of clinical trials have been ambiguous and increased toxicity frequently led to negative recommendations on this treatment approach[16]. Possibly, this is related to inadequate dose-scheduling of both treatment modalities as radiation dose and scheduling have been shown to affect the immunostimulatory activity[26]. Our current findings indeed suggest that there is no rational for prolonged administration of IFNs or STING agonists during radiotherapy, particularly if this results in increased toxicity. At the same time, to boost anti-tumor immune responses, IFNs or STING-agonists might be beneficial but only when administered briefly, i.e., in the first weeks of fractionated radiotherapy. Future studies should thus focus on optimal dose-scheduling of radiotherapy in combination with type I IFN-targeted treatment.

Apart from therapeutic options, the observed type I IFN expression signature could also have diagnostic/prognostic value. Previously, an IFN-related DNA damage resistance signature (IRDS) has been found to be predictive for poor survival outcome in GBM patients[18] as well as for the efficacy of adjuvant chemotherapy and local-regional control after radiation in breast cancer patients[19]. Although we could not confirm the latter in our patient series due to the small sample size, it can be speculated that the observed induction of a type I IFN response in our patient group during (chemo)radiotherapy serves as a radioprotective mechanism. This is supported by our finding that the peak in ISG expression after two weeks of irradiation coincides with the convergence to a plateau in clonogenic survival[11]. On the other hand, Guggenberger et al. described that 4 weeks of fractionated low-dose irradiation (daily dose of 0.5 or 1.0 Gy) of primary cultures of benign prostate epithelial cells resulted in downregulation of a type I interferon expression signature[27]. Interestingly, the expression analyses in that study were performed 1 week after completion of the fractionated irradiation schedule. Apart from differences in fraction dose and cell type, this difference in timing of expression analysis most likely accounts for the discrepancy between both observations. In fact, a normalization or downregulation of the IFN response in the days or weeks after therapy supports our previous observation that fractionated irradiation induces transient and reversible radioresistance rather than acquired radioresistance[11]. This reversal or 'normalization' of the response should be further investigated, especially in the context of clinical samples, as it could provide therapeutic opportunities.

Although we observed that fractionated irradiation consistently induced expression signatures that are characteristic of a type I IFN response, there was no clear association

with the expression of a specific type I IFN. Generally, antigen-presenting cells are considered as the main source of type I IFNs although intrinsic cancer cell production has been demonstrated after anthracycline-based chemotherapy[28] and radiotherapy[10]. In line with this, we did observe that irradiation can induce IFN-β or IFN-λ expression in cancer cells[17, 20, 29]. However, the induction did not occur in all cell lines even though downstream ISG expression was always triggered. Furthermore, blocking either IFN-β or IFN-λ did not affect the induction of ISGs during fractionated irradiation. This contradicts studies that have shown that the induction of a type I IFN response does not occur in cells that lack IFNAR1 (Interferon Alpha and Beta Receptor Subunit 1) expression. Since we did not block IFNAR1 or any of the other IFN receptors, we cannot rule out that other IFN family members might be responsible for the induction of ISG expression. While this could be further explored, our data still indicate that neither IFN-β nor IFN-λ are required for the induction of a type I IFN response during fractionated irradiation.

Of note, a mechanism that has been proposed to prevent the induction of the type I IFN response involves induction of the DNA exonuclease Three Prime Repair Exonuclease 1 (TREX1)[10]. This protein was found to degrade cytosolic DNA that accumulates in irradiated cancer cells, thereby impeding a type I IFN response[10]. It has been shown that this mechanism is triggered after single high dose (>12-18 Gy) irradiation and not after fractionated irradiation (3x 8 Gy)[10]. Interestingly, Erdal et al. linked accumulation of cytosolic DNA in TREX1-deficient human breast cancer cells and mouse embryonic fibroblast cells to increased radioresistance and ISG signaling after a single dose of 6 to 10 Gy. Disrupting the downstream transcription factor interferon regulatory factor 3 (IRF-3) in these cells completely abolished ISG induction and the observed radioresistance. Although we cannot rule out involvement of TREX1 in cancer cells that do not show increased IFN expression after fractionated irradiation with 2 Gy (Colo320 and SW480), these cells still showed induction of ISG expression and a steady state in clonogenic survival[11].

The disconnection between specific type I or type III IFN expression and the induction of ISG expression is further supported by our finding that the response also occurs in cancer cells that lack either cGAS (cyclic GMP-AMP Synthase) or STING (Stimulator of interferon genes) expression. It has been shown that the cGAS/STING signaling axis is a key regulator of the innate immune response[21, 30, 31]. This pathway also triggers type I IFN expression in response to DNA damage[10, 14, 17, 29]. Indeed, several studies have described that inhibition or complete knockout of either cGAS or STING hampers an adequate type I IFN response *in vitro* and *in vivo*[10, 14, 17, 29, 32]. In contrast, we observed comparable induction of ISGs during fractionated irradiation of cancer cell lines, irrespective of cGAS or STING expression. Also, treatment with a STING antagonist or knockout of STING could not prevent ISG expression induction. However, we did observe a delay in expression induction in the absence of STING in HT29 STING-knockout cells. Apparently, STING facilitates or contributes to the activation of ISG expression during the early phase

of fractionated irradiation, but it is not indispensable. Our observation also implies that other pathways contribute to the activation of ISG expression. In that regard, pattern-recognition receptors, such as Toll-like receptors, (TLRs) are known to activate innate type I IFN signaling[33] and agonists of TLRs can improve the response to radiotherapy[34, 35]. On the other hand, it has previously been demonstrated that key downstream adapter molecules of TLR signaling, like Myeloid Differentiation primary-response protein 88 (MyD88) and TIR-domain-containing adaptor protein inducing IFN-b (TRIF), are not essential to induce a type I IFN response during radiotherapy[14]. Interestingly, RNA activated innate immune pathways controlled by RIG-I (retinoic acid-inducible gene I) and MDA5 (melanoma differentiation-associated protein 5) are significantly less affected by loss-of-function mutations or epigenetic silencing as compared to STING[36] and can be linked type I IFN signaling in a STING-independent manner. RIG-I and MDA-5, triggered by either RNA from dying neighboring cells or production of small cytosolic RNA fragments via RNA Polymerase III[37, 38], could elicit a similar set of transcription factors involved in expression of type I IFNs via Mitochondrial Antiviral-Signaling protein (MAVS). Also, other cytosolic DNA sensors, e.g. IFI16 and DDX41, might play a role as extensively reviewed recently[39]. The interplay between such cytosolic DNA/RNA sensing mechanisms in controlling type I IFN signaling during (fractionated) irradiation should be further studied.

Finally, the exact role of type I IFN signaling in the response to radiotherapy should be further explored. As recently reviewed by us and others, type I IFNs can exert both intrinsic and extrinsic anti-tumor effects. This includes inhibition of cell growth and migration, induction of apoptosis and senescence, and activation of T-cell mediated immunity[16, 40]. As such, the induction of a type I IFN response during fractionated irradiation could be considered as beneficial. At the same time, as described above, combining type I IFN treatment with radiation therapy in the clinic has been met with increased toxicity and limited or no clinical benefit[16]. In addition, high tumoral expression of ISGs or upstream transcription factors like STAT1 (Signal Transducer and Activator of Transcription 1) are indicators of radioresistance and a predictor of poor patient survival[18, 19, 41, 42]. We also observed an elevated type I IFN response in cancer cells at the time they adopt a radiotolerant phenotype. Thus, activation of type I IFN signaling by DNA damaging agents like radiotherapy might not be beneficial at all[43].

5. CONCLUSIONS

In conclusion, our current findings indicate that clinically applied fractionated low-dose irradiation triggers expression of type I IFN stimulated genes independent of interferons or STING-mediated signaling. While the exact underlying mechanism needs to be resolved, our data provide novel insights in the relevance of the type I interferon response and STING signaling during low-dose fractionated irradiation which are relevant for current efforts that aim to target this response in the context

of combination radiotherapy. In particular, the timing of type I IFN-targeted treatment during radiotherapy should be carefully explored as it might induce beneficial and detrimental effects depending upon a delicate balance between responses within the tumor microenvironment, including but not restricted to STING signaling pathway capacity.

REFERENCES

1. Bernier J, Hall EJ, Giaccia A. Radiation oncology: a century of achievements. Nat Rev Cancer. 2004;4:737-747.

2. Baumann M, Krause M, Hill R. Exploring the role of cancer stem cells in radioresistance. Nat Rev Cancer. 2008;8:545-554.

3. Begg AC, Stewart FA, Vens C. Strategies to improve radiotherapy with targeted drugs. Nat Rev Cancer. 2011;11:239-253.

4. Goedegebuure RSA, de Klerk LK, Bass AJ, Derks S, Thijssen VLJL. Combining Radiotherapy With Anti-angiogenic Therapy and Immunotherapy; A Therapeutic Triad for Cancer. Front Immunol. 2019;9:3107.

5. Morgan MA, Lawrence TS. Molecular Pathways: Overcoming Radiation Resistance by Targeting DNA Damage Response Pathways. Clin Cancer Res. 2015;21:2898-2904.

6. Sharma RA, Plummer R, Stock JK et al. Clinical development of new drug-radiotherapy combinations. Nat Rev Clin Oncol. 2016;13:627-642.

7. Ahn SJ, Choi C, Choi YD et al. Microarray analysis of gene expression in lung cancer cell lines treated by fractionated irradiation. Anticancer Res. 2014;34:4939-4948.

8. Hennel R, Brix N, Seidl K et al. Release of monocyte migration signals by breast cancer cell lines after ablative and fractionated γ-irradiation. Radiat Oncol. 2014;9:85.

9. Tsai M-H, Cook JA, Chandramouli GVR et al. Gene Expression Profiling of Breast, Prostate, and Glioma Cells following Single versus Fractionated Doses of Radiation. Cancer Research. 2007;67:3845-3852.

10. Vanpouille-Box C, Alard A, Aryankalayil MJ et al. DNA exonuclease Trex1 regulates radiotherapy-induced tumour immunogenicity. Nat Commun. 2017;8:15618.

11. van den Berg J, Castricum KCM, Meel MH et al. Development of transient radioresistance during fractionated irradiation in vitro. Radiother Oncol. 2020;148:107-114.

12. Kleibeuker EA, Fokas E, Allen PD et al. Low dose angiostatic treatment counteracts radiotherapy-induced tumor perfusion and enhances the anti-tumor effect. Oncotarget. 2016;7:76613-76627.

13. Lamble S, Batty E, Attar M et al. Improved workflows for high throughput library preparation using the transposome-based Nextera system. BMC Biotechnol. 2013;13:104.

14. Deng L, Liang H, Xu M et al. STING-Dependent Cytosolic DNA Sensing Promotes Radiation-Induced Type I Interferon-Dependent Antitumor Immunity in Immunogenic Tumors. Immunity. 2014;41:843-852.

15. Wilkins AC, Patin EC, Harrington KJ, Melcher AA. The immunological consequences of radiation-induced DNA damage. J Pathol. 2019;247:606-614.

16. Goedegebuure RSA, Vonk C, Kooij LP, Derks S, Thijssen VLJL. Combining Radiation Therapy With Interferons: Back to the Future. Int J Radiat Oncol Biol Phys. 2020

17. Chen J, Markelc B, Kaeppler J et al. STING-Dependent Interferon-λ1 Induction in HT29 Cells, a Human Colorectal Cancer Cell Line, After Gamma-Radiation. Int J Radiat Oncol Biol Phys. 2018;101:97-106.

18. Duarte CW, Willey CD, Zhi D et al. Expression signature of IFN/STAT1 signaling genes predicts poor survival outcome in glioblastoma multiforme in a subtype-specific manner. PLoS One. 2012;7:e29653.

5

19. Weichselbaum RR, Ishwaran H, Yoon T et al. An interferon-related gene signature for DNA damage resistance is a predictive marker for chemotherapy and radiation for breast cancer. Proc Natl Acad Sci U S A. 2008;105:18490-18495.

20. Burnette BC, Liang H, Lee Y et al. The efficacy of radiotherapy relies upon induction of type i interferon-dependent innate and adaptive immunity. Cancer Res. 2011;71:2488-2496.

21. Ishikawa H, Ma Z, Barber GN. STING regulates intracellular DNA-mediated, type I interferon-dependent innate immunity. Nature. 2009;461:788-792.

22. Simone CB, John-Aryankalayil M, Palayoor ST et al. mRNA Expression Profiles for Prostate Cancer following Fractionated Irradiation Are Influenced by p53 Status. Transl Oncol. 2013;6:573-585.

23. John-Aryankalayil M, Palayoor ST, Cerna D et al. Fractionated radiation therapy can induce a molecular profile for therapeutic targeting. Radiat Res. 2010;174:446-458.

24. Aryankalayil MJ, Makinde AY, Gameiro SR et al. Defining molecular signature of pro-immunogenic radiotherapy targets in human prostate cancer cells. Radiat Res. 2014;182:139-148.

25. Weichselbaum RR, Liang H, Deng L, Fu YX. Radiotherapy and immunotherapy: a beneficial liaison. Nat Rev Clin Oncol. 2017;14:365-379.

26. Gandhi SJ, Minn AJ, Vonderheide RH, Wherry EJ, Hahn SM, Maity A. Awakening the immune system with radiation: Optimal dose and fractionation. Cancer Lett. 2015;368:185-190.

27. Guggenberger F, van de Werken HJG, Erb HHH et al. Fractionated Radiation of Primary Prostate Basal Cells Results in Downplay of Interferon Stem Cell and Cell Cycle Checkpoint Signatures.[letter]. Eur Urol 2018;74(6):847-849.

28. Sistigu A, Yamazaki T, Vacchelli E et al. Cancer cell-autonomous contribution of type I interferon signaling to the efficacy of chemotherapy. Nat Med. 2014;20:1301-1309.

29. Härtlova A, Erttmann SF, Raffi FA et al. DNA damage primes the type I interferon system via the cytosolic DNA sensor STING to promote anti-microbial innate immunity. Immunity. 2015;42:332-343.

30. Ishikawa H, Barber GN. STING is an endoplasmic reticulum adaptor that facilitates innate immune signalling. Nature. 2008;455:674-678.

31. Sun L, Wu J, Du F, Chen X, Chen ZJ. Cyclic GMP-AMP synthase is a cytosolic DNA sensor that activates the type I interferon pathway. Science. 2013;339:786-791.

32. Erdal E, Haider S, Rehwinkel J, Harris AL, McHugh PJ. A prosurvival DNA damage-induced cytoplasmic interferon response is mediated by end resection factors and is limited by Trex1. Genes Dev. 2017;31:353-369.

33. Akira S, Takeda K. Toll-like receptor signalling. Nat Rev Immunol. 2004;4:499-511.

34. Apetoh L, Ghiringhelli F, Tesniere A et al. Toll-like receptor 4-dependent contribution of the immune system to anticancer chemotherapy and radiotherapy. Nat Med. 2007;13:1050-1059.

35. Dovedi SJ, Melis MHM, Wilkinson RW et al. Systemic delivery of a TLR7 agonist in combination with radiation primes durable antitumor immune responses in mouse models of lymphoma. Blood. 2013;121:251-259.

36. Konno H, Yamauchi S, Berglund A, Putney RM, Mulé JJ, Barber GN. Suppression of STING signaling through epigenetic silencing and missense mutation impedes DNA damage mediated cytokine production. Oncogene. 2018;37:2037-2051.

37. Chiu YH, Macmillan JB, Chen ZJ. RNA polymerase III detects cytosolic DNA and induces type I interferons through the RIG-I pathway. Cell. 2009;138:576-591.

38. Ablasser A, Bauernfeind F, Hartmann G, Latz E, Fitzgerald KA, Hornung V. RIG-I-dependent sensing of poly(dA:dT) through the induction of an RNA polymerase III-transcribed RNA intermediate. Nat Immunol. 2009;10:1065-1072.

39. Vanpouille-Box C, Demaria S, Formenti SC, Galluzzi L. Cytosolic DNA Sensing in Organismal Tumor Control. Cancer Cell. 2018;34:361-378.

40. Parker BS, Rautela J, Hertzog PJ. Antitumour actions of interferons: implications for cancer therapy. Nat Rev Cancer. 2016;16:131-144.

41. Khodarev NN, Beckett M, Labay E, Darga T, Roizman B, Weichselbaum RR. STAT1 is overexpressed in tumors selected for radioresistance and confers protection from radiation in transduced sensitive cells. Proc Natl Acad Sci U S A. 2004;101:1714-1719.

42. Pitroda SP, Wakim BT, Sood RF et al. STAT1-dependent expression of energy metabolic pathways links tumour growth and radioresistance to the Warburg effect. BMC Med. 2009;7:68.

43. Cheon H, Borden EC, Stark GR. Interferons and their stimulated genes in the tumor microenvironment. Semin Oncol. 2014;41:156-173.

5

SUPPLEMENTARY MATERIAL
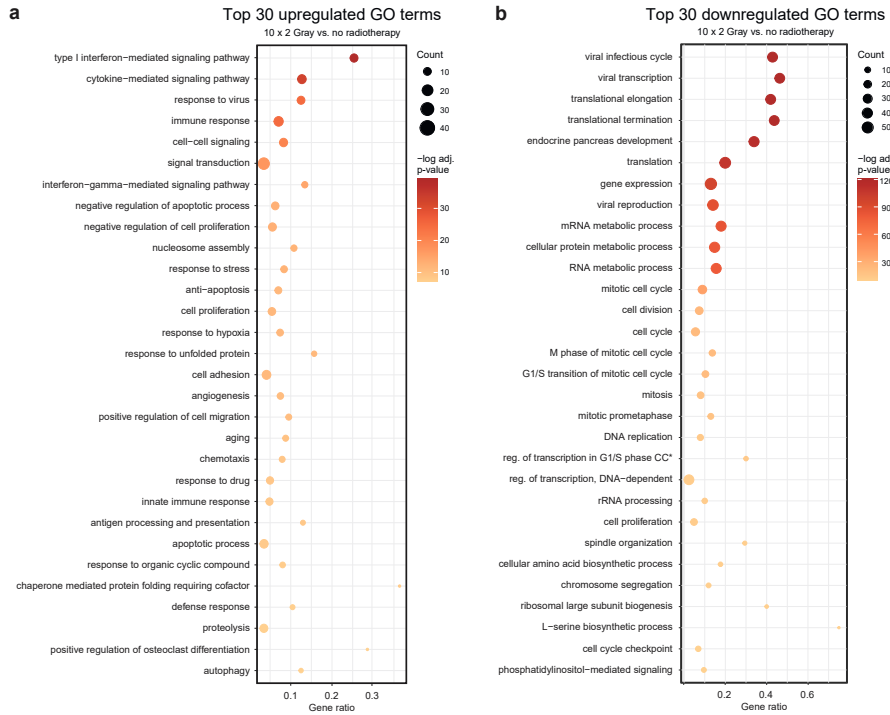
Supplementary figure S1. (a) Dotplot showing the top 30 most significantly upregulated Gene Ontology (GO) terms (biological processes) after 2 weeks of treatment vs. untreated based on RNA deep-sequencing of HT29 cells. **(b)** Top 30 downregulated GO terms. * regulation of transcription in G1/S phase of mitotic cell cycle. **(c)** REVIGO treemap summarizing upregulated and related non-redundant GO terms (biological processes) after 2 weeks of treatment vs. untreated based on RNA deep-sequencing of HT29 cells.

146
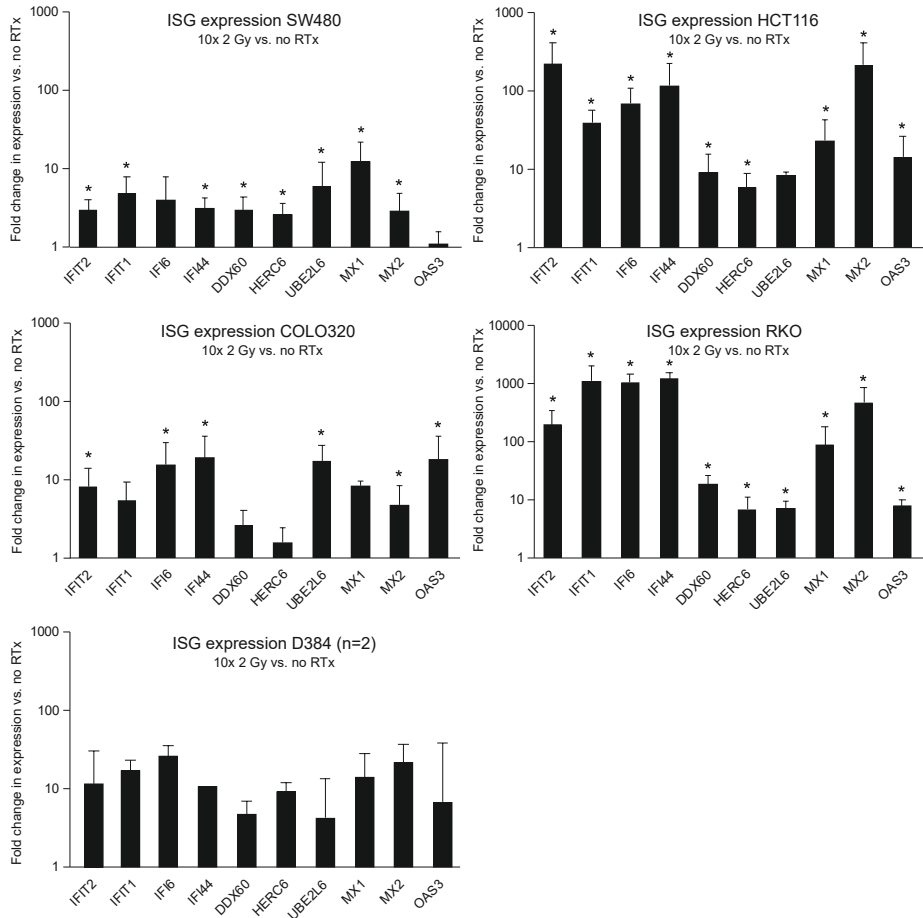
Supplementary figure S2. Bar graphs showing fold change in mRNA expression levels of a panel of ISGs in different cancer cell lines subjected to 10x 2 Gy as compared to no irradiation. SW480, HCT116, COLO320 and RKO are colon adenocarcinoma cell lines, D384 is a glioma cell line. * p-value ≤ 0.05 vs. no irradiation.

5
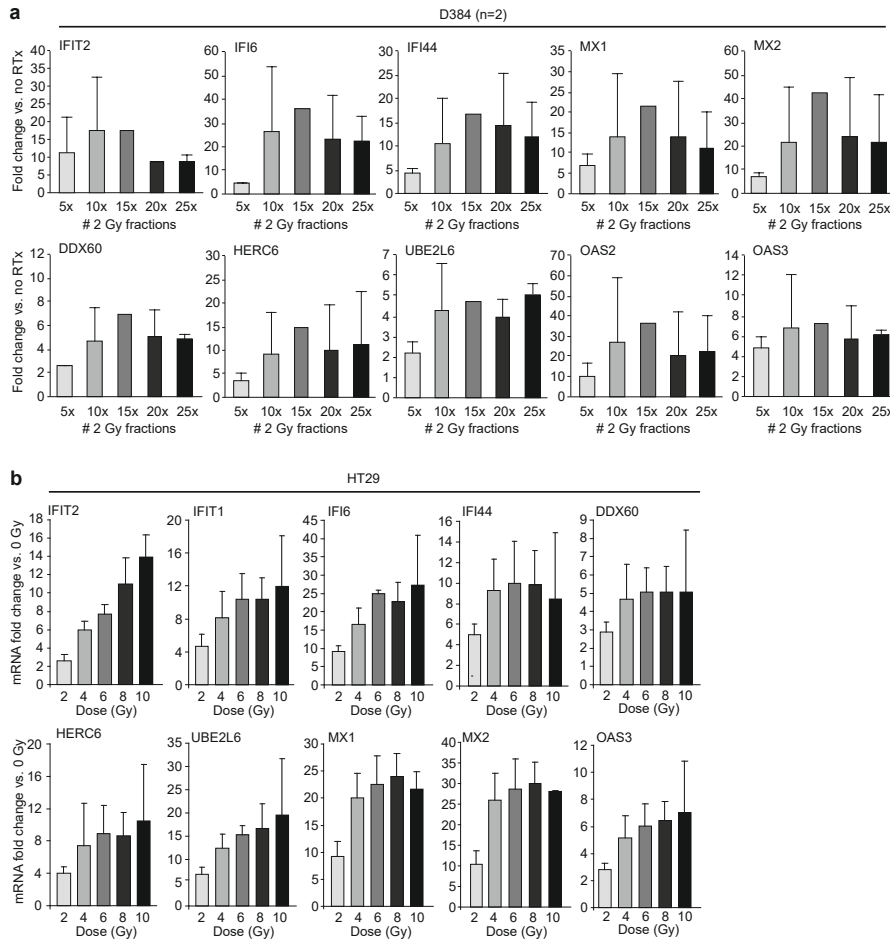
Supplementary figure S3. (a) Time course analysis of ISG mRNA expression in D384 glioma cells. Data are expressed as fold-change vs. 0x 2 Gy irradiation (n=2). **(b)** Bar graphs showing fold change in mRNA expression levels of a panel of ISGs in HT29 cells subjected to single dose irradiation with increasing dose fraction.
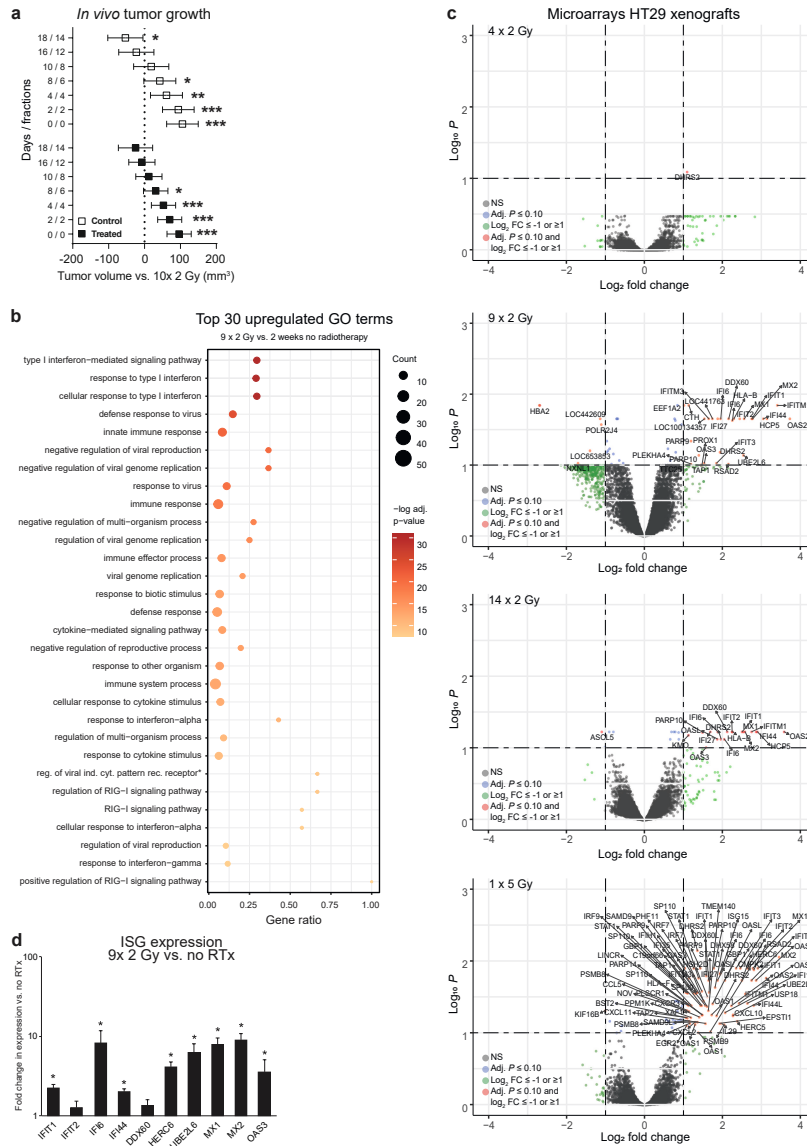
Supplementary figure S4. (**a**) Tumor volume (mm³) of HT29 xenograft tumors with (black squares) or without (white squares) irradiation after 0, 2, 4, 6, 8, 12 and 14 fractions of 2 Gy, compared to 10 fractions (day 14, dashed line). Note that the volumes of irradiated tumors are not significantly different after 8-14 fractions, whereas the volume of non-irradiated tumors has significantly increased after 18 days compared to day 14. * p-value ≤ 0.05 vs. day 14/10x 2Gy. (**b**) Dotplot showing the top 30 most significantly upregulated Gene Ontology (GO) terms (biological processes) in HT29 xenograft tumors after 2 weeks of RTx vs. no irradiation based on human microarray analysis. (**c**) Volcano plots of microarray data comparing gene expression in HT29 xenograft tumors after 1, 2, 3 weeks and a single dose (SD) of 5 Gy of irradiation vs. no irradiation. NS = not significant. FC = fold change. (**d**) Bar graphs showing fold change in mRNA expression levels of a panel of ISGs in HT29 xenograft tumor subjected to 9x 2 Gy irradiation vs. non-irradiated tumors. n=5 mice/group. * p-value ≤ 0.05 vs. non-irradiated tumors.
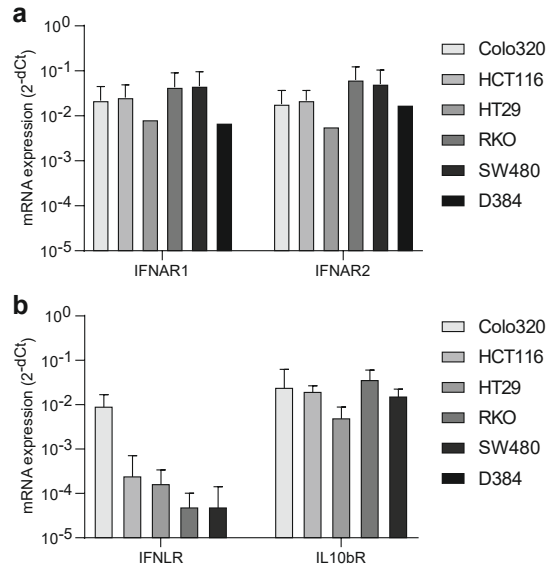
Supplementary figure S5. (a) Bar graphs showing fold change in mRNA expression levels of different IFNs in multiple colon adenocarcinoma cancer cell lines during fractionated irradiation. Fold difference vs. non-irradiated cells is shown. For comparison, the scaling of the y-axis is set to a similar range for each specific IFN (columns). **(b)** Bar graphs showing detectable expression of IFNAR1/2 (type I IFN receptors) as well as of IFNLR and IL10bR (type III IFN receptors) in all cell lines.
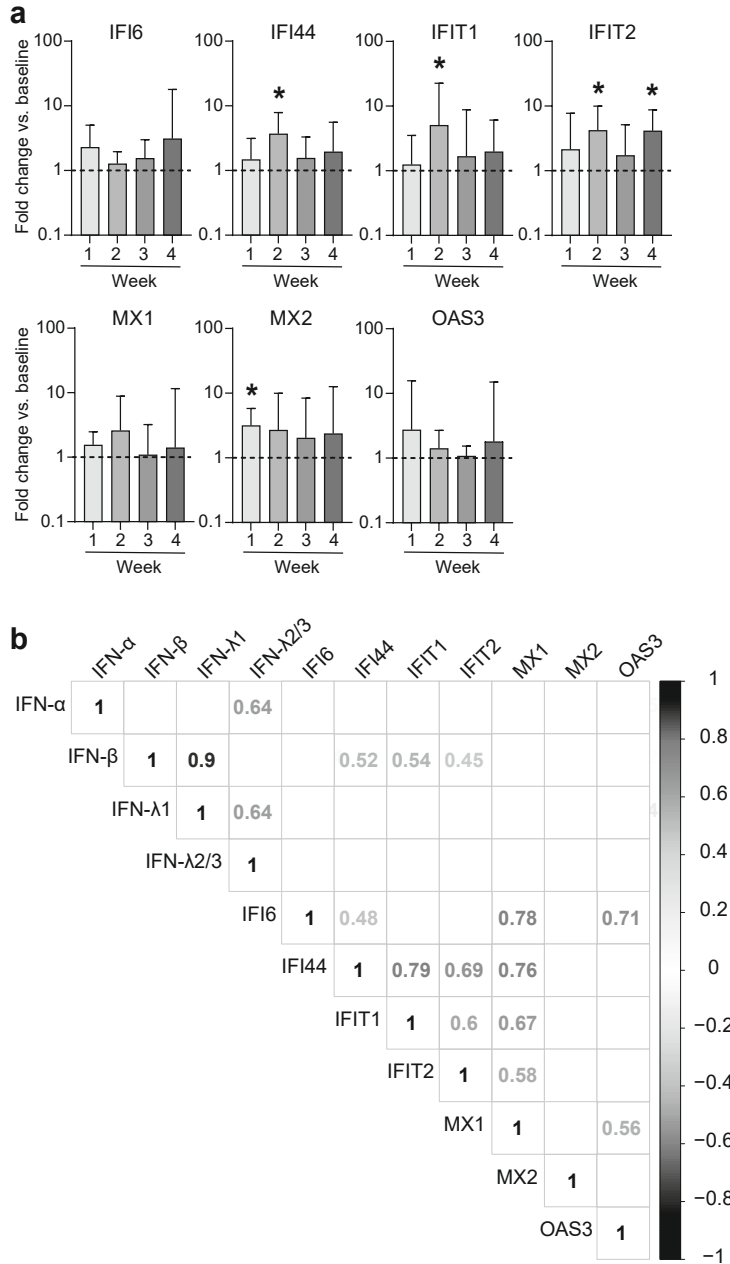
Supplementary figure S6. (**a**) mRNA expression levels of ISGs in patient-matched tumor samples from esophageal cancer patients (n=20) prior to or during chemoradiotherapy. The levels in the different cohorts are shown, i.e. 1 week (n= 6), 2 weeks (n= 5), 3 weeks (n= 4), 4 weeks (n= 5). * p-value ≤ 0.05 vs. matched pre-treatment samples. Fold expression in on-treatment samples vs. pre-treatment is shown. (**b**) Correlation plot showing the significant correlations between IFN and ISG induction levels from esophageal cancer patients during chemoradiotherapy (Pearson correlation coefficient only shown if p-value ≤ 0.05).
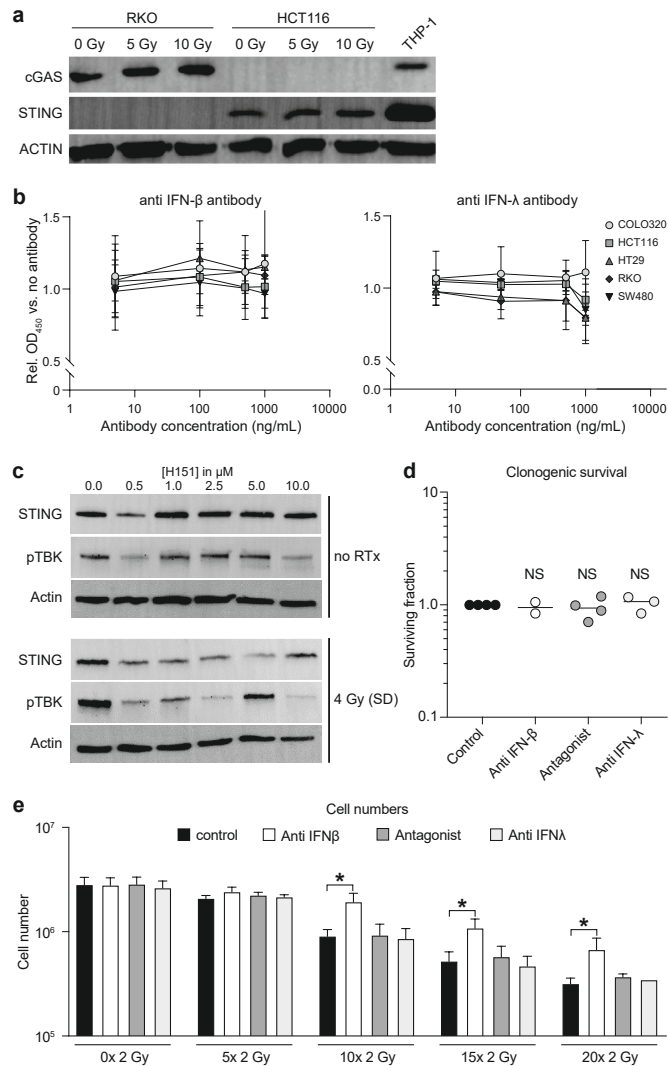
Supplementary figure S7. (a) Western blot of cGAS and STING in RKO cells (which lack STING) and HCT116 cells (which lack cGAS) subject to single dose irradiation. Irradiation did not induce expression of the absent proteins. THP-1 represents the positive control for cGAS and STING, Actin staining was used as loading control. (**b**) Dose response analyses of effect of anti IFN-β (left panel) and anti IFN-λ (right panel) on growth (MTT assay) of different colon cell lines. (**c**) Western blot of STING and phosphorylated TBK1 in cells subject to 0 Gy or 4 Gy irradiation in the absence or presence of increasing concentrations of the STING antagonist H151. When no irradiation is applied (upper panel) TBK1 phosphorylation is low and is not affected by H151. When cells are irradiated (lower panel) TBK1 phosphorylation is increased in the absence of H151 but inhibited in the presence of H151. This indicates effective STING inhibition by H151. (**d**) Effect of either anti IFN-β (white dots), anti IFN-λ (light grey dots) or H151 (dark grey dots) on basal clonogenic survival of HT29 cells. Neither treatment significantly affects clonogenic survival in non-irradiated cells. (**e**) Effect of either anti IFN-β, anti IFN-λ or H151 on HT29 cell numbers during fractionated irradiation. Starting from 10x 2 Gy, anti IFN-β antibody prevented inhibition of cell growth, in line with the known growth inhibitory role of IFN-β and the observed induction of IFN-β from 10x 2 Gy onwards. No effect of anti IFN-λ treatment or STING antagonist H151 could be observed.

152

a

b STING/TMEM173 (ENST00000330794.9)
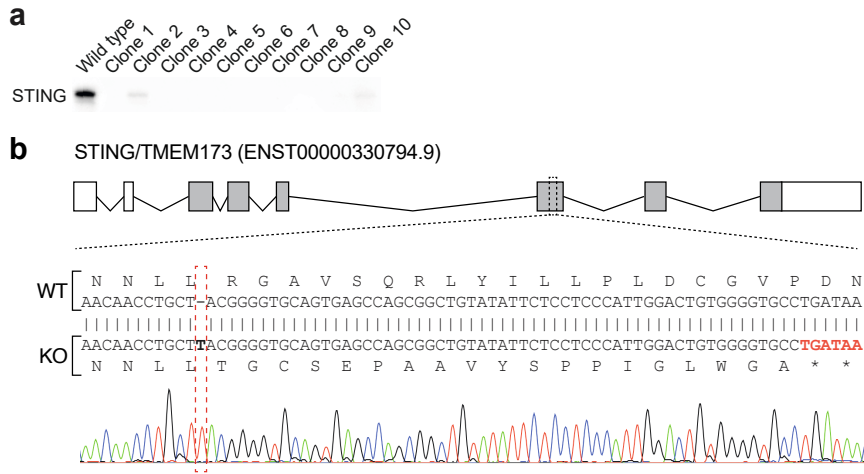
Supplementary figure S8. (**a**) Western blot of STING on HT29 wild type cells and 10 different knockout clones. (**b**) Schematic representation of the STING gene. Exons are shown as boxes and introns as lines. Grey areas represent protein coding regions and white areas represent un-translated regions. The dotted line indicates the target region of the CRISPR/CAS guide. Below, the sequence of the wild-type HT29 cells and one of the HT29 STING knockout cells is shown. CRISPR/CAS gene editing resulted in insertion of a thymidine causing a frame shift resulting in two premature and adjacent STOP codons (shown as asterisks).

5

Supplementary Table 1. Primer sequences

Gene (human)	Forward primer (5'-3')	Reverse primer (5'-3')
DDX60	GTTTCTTGGAAGAGAGTTACCC	GACCTTCCTTGCCCAAGAATG
IFI6v2	CAGGTGAGAATGCGGGTAAG	ATCGCAGACCAGCTCATCAG
IFI44	ACAGATGTTGTAATCAAGGGCC	GGTGTACATAGTCCTAGTTTCC
UBE2L6v2	CGTCTCCGCACAAAGACC	GCAGGTTGAAGGCTTTCAGG
HERC6	ACAAAGCTAACTGTCGACTACC	ACTGAAAATAACAGGACTGGG
INF alpha pan	CCATCYCTGYCYTCCATGAG	GATTTCTGCTCTGACAACCTCC
IFN beta	AAACTCATGAGCAGTCTGCA	AGGAGATCTTCAGTTTCGGAGG
IFN lambda 1	CGCCTTGGAAGAGTCACTCA	GAAGCCTCAGGTCCCAATTC
IFN lambda 2/3	GCCACATAGCCCAGTTCAAG	TCCTTCAGCAGAAGCGACTC
IFIT1	ATGGTGATGTCATCAGGTCAAG	CACACTGTATTTGGTGTCTAGG
IFIT2	CAATAGCAAGCTACCGTC	GAACATCTGTTACACCTGG
MX1	CCATATTTCAGGGATCTGC	GCTCCTCTGTTATTCTCTG
MX2	AGTATCGAGGCAAGGAGC	ACGTTAATGAAAGCTTGCTG
OAS2	GACAACTTTGACATTGCTG	AACTGGATCCAAGATTACTG
OAS3	GGTCAACTATAGCACTGAG	GATGTCCCGTCTCTACTC

Supplementary Table 2. RNA-sequencing of non-irradiated versus 10x 2 Gy HT29 cells *in vitro*. List of top 50 up-regulated genes in HT29 cells *in vitro* after 10x 2 Gy, compared to non-irradiated cells (n=3). Change in expression displayed as log(2) fold change.

Gene ID	Name	Symbol	Log(2) fold change		
			exp 1	exp 2	exp 3
ENSG00000140465	cytochrome P450, family 1, subfamily A, polypeptide 1	CYP1A1	5.9	5.7	6.4
ENSG00000126709	interferon, alpha-inducible protein 6	IFI6	6.5	5.2	5.9
ENSG00000163121	neuralized E3 ubiquitin protein ligase 3	NEURL3	4.4	4.9	4.2
ENSG00000138166	dual specificity phosphatase 5	DUSP5	4.8	4.6	3.4
ENSG00000165949	interferon, alpha-inducible protein 27	IFI27	4.9	3.2	4.1
ENSG00000023445	baculoviral IAP repeat containing 3	BIRC3	4.8	3.6	3.5
ENSG00000173110	heat shock 70kDa protein 6 (HSP70B')	HSPA6	7.9	2.9	2.6
ENSG00000197279	zinc finger protein 165	ZNF165	4.3	3.1	4.4
ENSG00000234745	major histocompatibility complex, class I, B	HLA-B	3.2	4.4	2.6
ENSG00000086548	carcinoembryonic antigen-related cell adhesion molecule 6	CEACAM6	1.5	2.5	8.5
ENSG00000124216	snail family zinc finger 1	SNAI1	4.9	3.0	2.5
ENSG00000099860	growth arrest and DNA-damage-inducible, beta	GADD45B	4.2	3.4	2.6
ENSG00000112972	3-hydroxy-3-methylglutaryl-CoA synthase 1 (soluble)	HMGCS1	2.2	4.0	3.6
ENSG00000052802	methylsterol monooxygenase 1	MSMO1	1.4	4.4	4.3
ENSG00000124102	peptidase inhibitor 3, skin-derived	PI3	1.9	2.2	6.9

Supplementary Table 2. RNA-sequencing of non-irradiated versus 10x 2 Gy HT29 cells *in vitro*. List of top 50 up-regulated genes in HT29 cells *in vitro* after 10x 2 Gy, compared to non-irradiated cells (n=3). Change in expression displayed as log(2) fold change. (continued)

Gene ID	Name	Symbol	Log(2) fold change		
			exp 1	exp 2	exp 3
ENSG00000204388	heat shock 70kDa protein 1B	HSPA1B	3.4	2.6	3.6
ENSG00000204983	protease, serine, 1 (trypsin 1)	PRSS1	2.2	1.7	6.9
ENSG00000125148	metallothionein 2A	MT2A	3.5	3.6	1.9
ENSG00000163286	alkaline phosphatase, placental-like 2	ALPPL2	2.2	2.7	4.8
ENSG00000137673	matrix metallopeptidase 7	MMP7	3.9	0.6	6.5
ENSG00000148926	adrenomedullin	ADM	3.2	3.3	2.5
ENSG00000142089	interferon induced transmembrane protein 3	IFITM3	3.2	2.6	3.5
ENSG00000130203	apolipoprotein E	APOE	3.0	2.3	4.0
ENSG00000137440	fibroblast growth factor binding protein 1	FGFBP1	NA	NA	3.0
ENSG00000075618	fascin homolog 1, actin-bundling protein	FSCN1	2.9	2.5	3.8
ENSG00000156587	ubiquitin-conjugating enzyme E2L 6	UBE2L6	3.7	3.6	1.5
ENSG00000100867	dehydrogenase/reductase (SDR family) member 2	DHRS2	3.1	1.7	5.0
ENSG00000137965	interferon-induced protein 44	IFI44	4.1	2.8	2.1
ENSG00000134107	basic helix-loop-helix family, member e40	BHLHE40	1.7	4.0	2.9
ENSG00000142227	epithelial membrane protein 3	EMP3	3.3	2.1	3.7
ENSG00000177469	polymerase I and transcript release factor	PTRF	4.3	1.7	3.4
ENSG00000163659	TCDD-inducible poly(ADP-ribose) polymerase	TIPARP	2.7	3.4	2.5
ENSG00000166831	RNA binding protein with multiple splicing 2	RBPMS2	2.6	3.4	2.5
ENSG00000196352	CD55 molecule, decay accelerating factor for complement	CD55	1.3	3.7	3.6
ENSG00000204389	heat shock 70kDa protein 1A	HSPA1A	3.1	2.2	3.7
ENSG00000181126	major histocompatibility complex, class I, V (pseudogene)	HLA-P	3.3	2.9	2.5
ENSG00000171401	keratin 13	KRT13	2.7	1.6	5.3
ENSG00000204103	v-maf avian musculoaponeurotic fibrosarcoma oncogene homolog B	MAFB	4.7	1.8	2.7
ENSG00000185022	v-maf avian musculoaponeurotic fibrosarcoma oncogene homolog F	MAFF	3.6	3.4	1.4
ENSG00000125657	tumor necrosis factor (ligand) superfamily, member 9	TNFSF9	3.6	3.4	1.4
ENSG00000105388	carcinoembryonic antigen-related cell adhesion molecule 5	CEACAM5	1.4	2.2	6.3
ENSG00000186480	insulin induced gene 1	INSIG1	1.1	4.2	3.1
ENSG00000189325	chromosome 6 open reading frame 222	C6orf222	3.1	2.5	3.0
ENSG00000164949	GTP binding protein overexpressed in skeletal muscle	GEM	3.3	3.0	1.9
ENSG00000232810	tumor necrosis factor	TNF	3.6	2.6	2.2
ENSG00000250606	protease, serine, 3 pseudogene 2	PRSS3P2	2.4	1.8	4.5
ENSG00000156966	UDP-GlcNAc:betaGal beta-1,3-N-acetylglucosaminyltransferase 7	B3GNT7	2.1	2.1	4.3
ENSG00000035862	TIMP Metallopeptidase Inhibitor 2	TIMP2	1.6	3.1	3.6
ENSG00000172602	Rho Family GTPase 1	RND1	4.3	2.1	2.0
ENSG00000112299	vanin 1	VNN1	3.6	1.8	3.2

5

Supplementary Table 3. RNA-sequencing of non-irradiated versus 10x 2 Gy HT29 cells *in vitro*. List of top 50 down-regulated genes in HT29 cells *in vitro* after 10x 2 Gy, compared to non-irradiated cells (n=3). Change in expression displayed as log(2) fold change.

Gene ID	Name	Symbol	Log(2) fold change		
			exp 1	exp 2	exp 3
ENSG00000259974	long intergenic non-protein coding RNA 261	LINC00261	-5.1	-5.0	-4.7
ENSG00000106331	paired box 4	PAX4	-3.1	-4.0	-4.2
ENSG00000134240	3-hydroxy-3-methylglutaryl-CoA synthase 2 (mitochondrial)	HMGCS2	-5.0	-3.3	-2.6
ENSG00000126262	free fatty acid receptor 2	FFAR2	-3.1	-3.5	-3.3
ENSG00000186474	kallikrein-related peptidase 12	KLK12	-3.5	-3.0	-3.5
ENSG00000090920	Fc fragment of IgG binding protein	FCGBP	-3.9	-3.3	-2.9
ENSG00000049192	ADAM metallopeptidase with thrombospondin type 1 motif, 6	ADAMTS6	-3.8	-3.3	-2.7
ENSG00000144354	cell division cycle associated 7	CDCA7	-3.2	-3.2	-3.3
ENSG00000172238	atonal homolog 1 (Drosophila)	ATOH1	-3.1	NA	-3.2
ENSG00000122859	neurogenin 3	NEUROG3	NA	-2.8	-3.5
ENSG00000169507	solute carrier family 38, member 11	SLC38A11	-4.2	-2.9	-2.4
ENSG00000007952	NADPH oxidase 1	NOX1	-4.2	-2.9	-2.1
ENSG00000184564	SLIT and NTRK-like family, member 6	SLITRK6	-3.0	-3.4	-1.8
ENSG00000134193	regenerating islet-derived family, member 4	REG4	-6.3	-3.1	-0.7
ENSG00000104537	annexin A13	ANXA13	-3.1	-2.6	-2.6
ENSG00000188175	HEPACAM family member 2	HEPACAM2	-2.2	-2.7	-3.0
ENSG00000176024	zinc finger protein 613	ZNF613	-1.7	-3.3	-2.3
ENSG00000003989	solute carrier family 7, member 2	SLC7A2	-3.4	-1.7	-2.6
ENSG00000180745	clarin 3	CLRN3	-3.3	-2.8	-1.7
ENSG00000144485	hes family bHLH transcription factor 6	HES6	-2.0	-2.2	-3.0
ENSG00000101311	fermitin family member 1	FERMT1	-2.4	-2.6	-2.1
ENSG00000106003	LFNG O-fucosylpeptide 3-beta-N-acetylglucosaminyltransferase	LFNG	-2.7	-2.5	-1.9
ENSG00000198719	delta-like 1 (Drosophila)	DLL1	-2.2	-2.7	-2.0
ENSG00000155792	DEP domain containing MTOR-interacting protein	DEPTOR	-3.0	-2.4	-1.8
ENSG00000232931	long intergenic non-protein coding RNA 342	LINC00342	-0.9	-3.1	-2.9
ENSG00000118513	v-myb avian myeloblastosis viral oncogene homolog	MYB	-2.8	-2.2	-2.0
ENSG00000173546	chondroitin sulfate proteoglycan 4	CSPG4	-3.4	-2.1	-1.6
ENSG00000114248	leucine rich repeat containing 31	LRRC31	-2.6	-1.9	-2.2
ENSG00000168874	atonal homolog 8 (Drosophila)	ATOH8	-2.0	-2.7	-2.0
ENSG00000249267	long intergenic non-protein coding RNA 939	RP5-916L7.1	-1.6	-2.9	-2.1
ENSG00000121966	chemokine (C-X-C motif) receptor 4	CXCR4	-2.9	-1.9	-2.0
ENSG00000169218	R-spondin 1	RSPO1	-2.3	-4.0	-0.4
ENSG00000144579	CTD (carboxy-terminal domain, RNA polymerase II, polypeptide A) small phosphatase 1	CTDSP1	-1.6	-3.1	-1.9
ENSG00000215478	carboxylesterase 5A pseudogene 1	CES5AP1	-4.0	-1.9	-1.2
ENSG00000163501	indian hedgehog	IHH	-3.4	-3.2	-0.5
ENSG00000197408	cytochrome P450, family 2, subfamily B, polypeptide 6	CYP2B6	-3.6	-1.5	-1.7
ENSG00000265150	RNA, 7SL, cytoplasmic 2	RN7SL2	-4.0	-0.1	-2.5

Continued on next page

Supplementary Table 3. RNA-sequencing of non-irradiated versus 10x 2 Gy HT29 cells *in vitro*. List of top 50 down-regulated genes in HT29 cells *in vitro* after 10x 2 Gy, compared to non-irradiated cells (n=3). Change in expression displayed as log(2) fold change. (continued)

Gene ID	Name	Symbol	Log(2) fold change		
			exp 1	exp 2	exp 3
ENSG00000157399	arylsulfatase E (chondrodysplasia punctata 1)	ARSE	-2.9	-2.2	-1.6
ENSG00000243766	HOXA distal transcript antisense RNA	HOTTIP	-2.5	-2.0	-1.9
ENSG00000157388	calcium channel, voltage-dependent, L type, alpha 1D subunit	CACNA1D	-2.2	-1.6	-2.4
ENSG00000214290	colorectal cancer associated 2	C11orf93	-4.5	-1.6	-1.0
ENSG00000196659	tetratricopeptide repeat domain 30B	TTC30B	-1.2	-2.9	-2.1
ENSG00000172086	lysine-rich coiled-coil 1	KRCC1	-1.4	-2.9	-1.9
ENSG00000124766	SRY (sex determining region Y)-box 4	SOX4	-1.6	-1.9	-2.6
ENSG00000165092	aldehyde dehydrogenase 1 family, member A1	ALDH1A1	-4.2	-1.6	-0.9
ENSG00000128000	zinc finger protein 780B	ZNF780B	-1.3	-2.4	-2.4
ENSG00000198835	gap junction protein, gamma 2, 47kDa	GJC2	-2.4	-2.5	-1.4
ENSG00000174586	zinc finger protein 497	ZNF497	-0.6	-3.2	-2.2
ENSG00000198890	protein arginine methyltransferase 6	PRMT6	-0.4	-3.6	-1.7
ENSG00000186376	zinc finger protein 75D	ZNF75D	-1.6	-2.4	-2.1

Supplementary Table 4. Top 50 most enriched gene ontology biological processes in non-irradiated versus 10x 2 Gy HT29 cells *in vitro*

GO	Term	Count	Size
0060337	type I interferon-mediated signaling pathway	19	75
0019221	cytokine-mediated signaling pathway	23	181
0009615	response to virus	18	144
0006955	immune response	27	382
0007267	cell-cell signaling	20	242
0007165	signal transduction	41	1176
0060333	interferon-gamma-mediated signaling pathway	11	82
0043066	negative regulation of apoptotic process	17	272
0008285	negative regulation of cell proliferation	19	341
0006334	nucleosome assembly	11	102
0006950	response to stress	13	155
0006916	anti-apoptosis	14	200
0008283	cell proliferation	17	312
0001666	response to hypoxia	13	175
0006986	response to unfolded protein	8	51
0007155	cell adhesion	23	556
0001525	angiogenesis	12	160
0030335	positive regulation of cell migration	10	105
0007568	aging	10	114
0006935	chemotaxis	10	126
0042493	response to drug	15	301
0045087	innate immune response	15	309
0019882	antigen processing and presentation	7	54
0006915	apoptotic process	21	594

5

Supplementary Table 4. Top 50 most enriched gene ontology biological processes in non-irradiated versus 10x 2 Gy HT29 cells *in vitro (continued)*

GO	Term	Count	Size
0014070	response to organic cyclic compound	9	112
0051085	chaperone mediated protein folding requiring cofactor	4	11
0006952	defense response	7	67
0006508	proteolysis	19	543
0045672	positive regulation of osteoclast differentiation	4	14
0006914	autophagy	6	48
0007596	blood coagulation	17	457
0015992	proton transport	6	50
0032480	negative regulation of type I interferon production	5	30
0033572	transferrin transport	5	30
0044419	interspecies interaction between organisms	14	328
0032020	ISG15-protein conjugation	3	6
0042117	monocyte activation	3	6
0009308	amine metabolic process	3	6
0030199	collagen fibril organization	5	32
0015991	ATP hydrolysis coupled proton transport	5	32
0008633	activation of pro-apoptotic gene products	5	32
0045071	negative regulation of viral genome replication	4	16
0000079	regulation of cyclin-dependent protein kinase activity	6	55
0030308	negative regulation of cell growth	8	113
0010718	positive regulation of epithelial to mesenchymal transition	4	18
0060317	cardiac epithelial to mesenchymal transition	3	7
0032727	positive regulation of interferon-alpha production	3	7
0050714	positive regulation of protein secretion	4	19
0008219	cell death	9	156

GO = gene ontology
Count = number of induced genes in the sample
Size = total number of genes in the GO term

Supplementary Table 5. Genes with an average log(2) fold change ≤ -1 or ≥ 1 (adjusted p-value < 0.10) as identified by human micro-array analysis of 9x 2 Gy vs. non-irradiated HT29 xenografts (n=4)

Gene ID	Name	Symbol	Log(2) fold change
ILMN_1674063	2-5-oligoadenylate synthetase 2	OAS2	3.73
ILMN_1801246	interferon induced transmembrane protein 1	IFITM1	3.41
ILMN_1803945	HLA complex P5	HCP5	3.15
ILMN_1760062	interferon-induced protein 44	IFI44	3.05
ILMN_2231928	myxovirus (influenza virus) resistance 2	MX2	2.78
ILMN_1707695	interferon-induced protein with tetratricopeptide repeats 1	IFIT1	2.76
ILMN_1662358	myxovirus resistance 1, interferon-inducible protein p78	MX1	2.56

158

Supplementary Table 5. Genes with an average log(2) fold change ≤ -1 or ≥ 1 (adjusted p-value < 0.10) as identified by human micro-array analysis of 9x 2 Gy vs. non-irradiated HT29 xenografts (n=4) (continued)

Gene ID	Name	Symbol	Log(2) fold change
ILMN_1769520	ubiquitin-conjugating enzyme E2L 6	UBE2L6	2.54
ILMN_1739428	interferon-induced protein with tetratricopeptide repeats 2	IFIT2	2.45
ILMN_1778401	major histocompatibility complex, class I, B	HLA-B	2.30
ILMN_2347798	interferon, alpha-inducible protein 6	IFI6	2.26
ILMN_1795181	DEAD (Asp-Glu-Ala-Asp) box polypeptide 60	DDX60	2.16
ILMN_1657871	radical S-adenosyl methionine domain containing 2	RSAD2	2.16
ILMN_1687384	interferon, alpha-inducible protein 6	IFI6	1.96
ILMN_2384857	dehydrogenase/reductase (SDR family) member 2	DHRS2	1.94
ILMN_2058782	interferon, alpha-inducible protein 27	IFI27	1.89
ILMN_2239754	interferon-induced protein with tetratricopeptide repeats 3	IFIT3	1.85
ILMN_1703337	hypothetical LOC441763	LOC441763	1.75
ILMN_1805750	interferon induced transmembrane protein 3 (1-8U)	IFITM3	1.65
ILMN_3239606	hypothetical LOC100134357	LOC100134357	1.54
ILMN_1745397	2-5-oligoadenylate synthetase 3	OAS3	1.54
ILMN_1752622	prospero homeobox 1	PROX1	1.48
ILMN_1751079	transporter 1, ATP-binding cassette, sub-family B	TAP1	1.46
ILMN_2262044	poly (ADP-ribose) polymerase family, member 10	PARP10	1.40
ILMN_2053527	poly (ADP-ribose) polymerase family, member 9	PARP9	1.20
ILMN_1755173	pleckstrin homology domain containing, family A, member 4	PLEKHA4	1.20
ILMN_2305112	cystathionase (cystathionine gamma-lyase)	CTH	1.14
ILMN_1710303	tetratricopeptide repeat domain 25	TTC25	1.03
ILMN_2108735	eukaryotic translation elongation factor 1 alpha 2	EEF1A2	1.02
ILMN_1762769	polymerase (RNA) II (DNA directed) polypeptide J	POLR2J4	-1.09
ILMN_3200018	similar to hCG1815881	LOC442609	-1.12
ILMN_1655864	similar to hypothetical protein FLJ40722, transcript variant 2	LOC653853	-1.38
ILMN_1742917	nucleoredoxin-like 1	NXNL1	-1.69
ILMN_1667796	hemoglobin, alpha 2	HBA2	-2.68

5

159

Supplementary Table 6. Top 50 most enriched gene ontology biological processes in non-irradiated versus 9x 2 Gy HT29 xenografts

GO	Term	Count	Size
0060337	type I interferon-mediated signaling pathway	18	61
0071357	cellular response to type I interferon	18	61
0034340	response to type I interferon	18	62
0051607	defense response to virus	22	149
0045087	innate immune response	32	383
0045071	negative regulation of viral genome replication	11	30
0048525	negative regulation of viral reproduction	11	30
0009615	response to virus	23	209
0006955	immune response	42	722
0043901	negative regulation of multi-organism process	11	40
0045069	regulation of viral genome replication	11	44
0002252	immune effector process	25	318
0019079	viral genome replication	11	53
0009607	response to biotic stimulus	28	419
0019221	cytokine-mediated signaling pathway	22	265
0006952	defense response	39	752
2000242	negative regulation of reproductive process	11	56
0051707	response to other organism	27	402
0002376	immune system process	54	1321
0071345	cellular response to cytokine stimulus	23	323
0035455	response to interferon-alpha	6	14
0043900	regulation of multi-organism process	16	176
0034097	response to cytokine stimulus	24	391
0039531	regulation of viral-induced cytoplasmic pattern recognition receptor signaling pathway	4	6
0039535	regulation of RIG-I signaling pathway	4	6
0035457	cellular response to interferon-alpha	4	7
0039529	RIG-I signaling pathway	4	7
0050792	regulation of viral reproduction	11	105
0034341	response to interferon-gamma	10	86
1900246	positive regulation of RIG-I signaling pathway	3	3
0006950	response to stress	69	2249
0039528	cytoplasmic pattern recognition receptor signaling pathway in response to virus	4	10
0035456	response to interferon-beta	4	13
0050688	regulation of defense response to virus	7	56
0070887	cellular response to chemical stimulus	44	1310
0032020	ISG15-protein conjugation	3	6
2000241	regulation of reproductive process	11	157
0071310	cellular response to organic substance	36	1031
0001817	regulation of cytokine production	15	277
0002831	regulation of response to biotic stimulus	7	69
0010212	response to ionizing radiation	8	91
0002682	regulation of immune system process	25	629

Continued on next page

Supplementary Table 6. Top 50 most enriched gene ontology biological processes in non-irradiated versus 9x 2 Gy HT29 xenografts (continued)

GO	Term	Count	Size
0060700	regulation of ribonuclease activity	2	2
1900245	positive regulation of MDA-5 signaling pathway	2	2
0031347	regulation of defense response	16	322
0043331	response to dsRNA	5	34
0071346	cellular response to interferon-gamma	7	73
0045088	regulation of innate immune response	11	178
2000116	regulation of cysteine-type endopeptidase activity	10	153

GO = gene ontology identifier
Count = number of induced genes in the sample
Size = total number of genes in the GO term

Supplementary Table 7. Baseline characteristics esophageal cancer patients

	Cohort 1	Cohort 2	Cohort 3	Cohort 4	Total	
Age*	64 (57-75)	68 (54-71)	69 (46-71)	70 (65-75)	68.5 (46-75)	
Gender						
male	5	5	3	5	18	75.0%
female	0	1	2	0	3	12.5%
Missing	2	0	1	0	3	12.5%
Histology						
EAC#	7	5	5	4	21	87.5%
ESCC##	0	1	0	1	2	8.3%
Missing	0	0	1	0	1	4.2%
Fractions of RTx	5 (3-7)	11.5 (10-12)	15.5 (14-17)	22 (20-22)	12 (3-22)	
T stage						
T1	0	0	0	0	0	0.0%
T2	1	1	0	0	2	8.3%
T3	6	5	5	5	21	87.5%
Missing	0	0	1	0	1	4.2%
N stage						
N0	2	3	1	3	9	37.5%
N1	4	1	2	1	8	33.3%
N2	1	1	2	0	4	16.7%
N3	0	0	0	1	1	4.2%
Missing	0	0	1	0	2	8.3%
Total	7	6	6	5	24	100.0%
Excluded**	1	1	2	0	4	17.7%

* Median + range is shown for age and fractions of radiotherapy (RTx)
# Esophageal adenocarcinoma
Esophageal squamous cell carcinoma
** Excluded after assessment of representative tumor biopsy area on H&E stain (NvG).

Chapter 6

Combining radiotherapy with interferons; back to the future

Ruben S.A. Goedegebuure, Christian Vonk, Laura P. Kooij, Sarah Derks, Victor L.J.L. Thijssen

ABSTRACT

Radiotherapy has been linked to the induction of an intratumoral type I interferon (IFN) response which positively impacts response to treatment. This has linked the immunomodulatory effects of interferons to an increased radiotherapy efficacy which has spiked the interest to combine radiotherapy with IFN-based treatment. Interestingly, this combination treatment has been considered previously, based on preclinical studies demonstrating a radiosensitizing effects of interferons. As a result, multiple clinical trials have been performed combining radiotherapy with interferons in different tumor types. While potential benefit has been suggested, the outcomes of the trials are diverse and challenging to interpret. In addition, increased grade ≥3 toxicity frequently resulted in a negative recommendation regarding the combination therapy. This conclusion appears premature since many studies were small and several aspects of the combination treatment have not yet been sufficiently explored to justify such a definite conclusion. This review summarizes the available literature on this combination therapy, with a focus on IFN-α and IFN-β. Based on preclinical studies and clinical trials, we evaluate the potential opportunities and describe the current challenges, In addition we identify several issues that should be addressed in order to fully exploit the potential benefit of this combinatorial treatment approach.

1. INTRODUCTION

Radiotherapy is still one of the most effective non-surgical curative treatment options for cancer patients. Over 50% of cancer patients receive radiotherapy of which 60% are treated with curative intent[1]. Ever since the introduction of radiation as a therapeutic modality more than a century ago, the efficacy of radiotherapy has continuously been improved. This can be partly attributed to technological innovations which have perfected the delivery of irradiation to the tumor tissue[2]. In addition, increasing insight in the physical, chemical, and biological principles underlying radiation-induced damage has allowed the development of more efficient treatment schedules[3, 4]. At the same time, unraveling the cellular responses to radiation has paved and continues to pave the way for the development of combination therapies[5, 6]. While all these advancements have made radiotherapy an indispensable treatment modality, there is still room for improvement as clinical benefit of radiotherapy differs greatly between patients.

Currently, there is increasing interest to combine radiotherapy with therapies that target the tumor microenvironment, including anti-angiogenesis therapy[7, 8] and immunotherapy[9]. Regarding the latter, the link between radiotherapy and the immune response is well established. Although initially presumed to be mainly immunosuppressive, both stimulatory and immunoinhibitory effects of radiotherapy have now been described[9–12]. In fact, several mechanisms have been identified that underlie the immunostimulatory effects of radiotherapy, including improved immune cell recruitment, enhanced susceptibility to T cell-mediated cell death and increased tumor immunogenicity[9, 13, 14].

The immunostimulatory effect of radiotherapy has also been linked to the induction of interferon (IFN) responses[15, 16]. Consequently, at the end of the previous century, several clinical trials were performed to evaluate the combination of IFN therapy with radiotherapy, predominantly because of the radiosensitzing effects. Due to limited efficacy and increased toxicity the interest in combining radiotherapy with IFN therapy gradually diminished. However, in light of the current efforts to combine radiotherapy with immunotherapies like checkpoint inhibitors or cell based approaches[17, 18], a review on the insights obtained from these previous studies is timely. Here, we summarize and evaluate the results of previous research that explored the combination of radiotherapy and interferon treatment in preclinical studies and clinical trials.

6

2. INTERFERONS AND CANCER

Interferons constitute a pleiotropic cytokine subfamily that is involved in regulation of innate and adaptive immune responses. The IFN family consists of three types of small molecules that induce signaling via different receptor complexes (**Figure 1A**). Human type I IFNs comprise multiple subtypes (IFN-α/-β/-ω/-κ/-ε) that signal via a heterodimeric receptor complex composed of the IFN-α/β/ω receptor (IFNAR) 1 and IFNAR2. Type II IFNs are represented by IFN-γ, which signals by forming antiparallel homodimers of which each monomer binds a receptor complexes that consists of IFN-γ receptor (IFNGR) 1 and IFNGR2. Type III IFNs comprise four members (IFN-λ 1-4) and are a more recent addition to the IFN family. They signal via the IFN-λ receptor complex which is formed by heterodimerization of a specific IFN-λ receptor 1 (IFNLR1) and the IL-10 receptor 2 (IL-10R2)[19, 20].

Signaling via IFNs is complex and tightly regulated and will not be discussed here in detail (for extensive reviews on interferon signaling see references[19, 21, 22]). In brief, the main signaling response to IFNs involves the JAK/STAT pathway (Janus Kinases / Signal Transducer and Activator of Transcription proteins). The type I and III IFN receptors are associated with JAK1 and TYK2 (Tyrosine Kinase 2) while the type II receptors associate with JAK1 and JAK2. Upon ligand binding, these kinases are phosphorylated and induce receptor phosphorylation. This allows the recruitment of specific STATs that are also phosphorylated which promotes the formation of STAT homo- or heterodimers. These dimers can interact with additional factors that facilitate translocation to the nucleus (**Figure 1B**). Ultimately, this results in the transcriptional activation of so-called interferon-stimulated genes (ISGs, also referred to as interferon-regulated genes (IRGs)). Hundreds of ISGs have been identified and they are involved in the regulation of different cellular processes, such as proliferation, differentiation, migration and apoptosis[19, 22]. Obviously, the JAK/STAT signaling pathway is controlled by many different regulatory mechanisms which account for the complex responses which are cell type and context dependent[20, 21, 23, 24].

While initially identified as mediators of antiviral responses, IFNs are nowadays well recognized for their regulatory functions in both the innate and adaptive immune response during e.g. pathogen infections, inflammatory diseases, and cancer. Regarding the latter, aberrations in interferons and interferon-related signaling pathways are known to affect the formation of tumors and to exert pleiotropic effects during tumor progression[25]. As recently reviewed by Parker et al. [22], the - predominantly anti-tumor - effects of IFNs occur on an intrinsic and extrinsic level (**Figure 2**) The intrinsic, or direct, effects include inhibition of tumor cell growth, induction of apoptosis/necroptosis and inhibition of metastasis[22, 26, 27]. The extrinsic, or more indirect, effects involve the ability of IFNs to modulate the tumor microenvironment e.g. by activating an antitumor immune response or by inhibiting tumor angiogenesis[22, 24, 28–31].
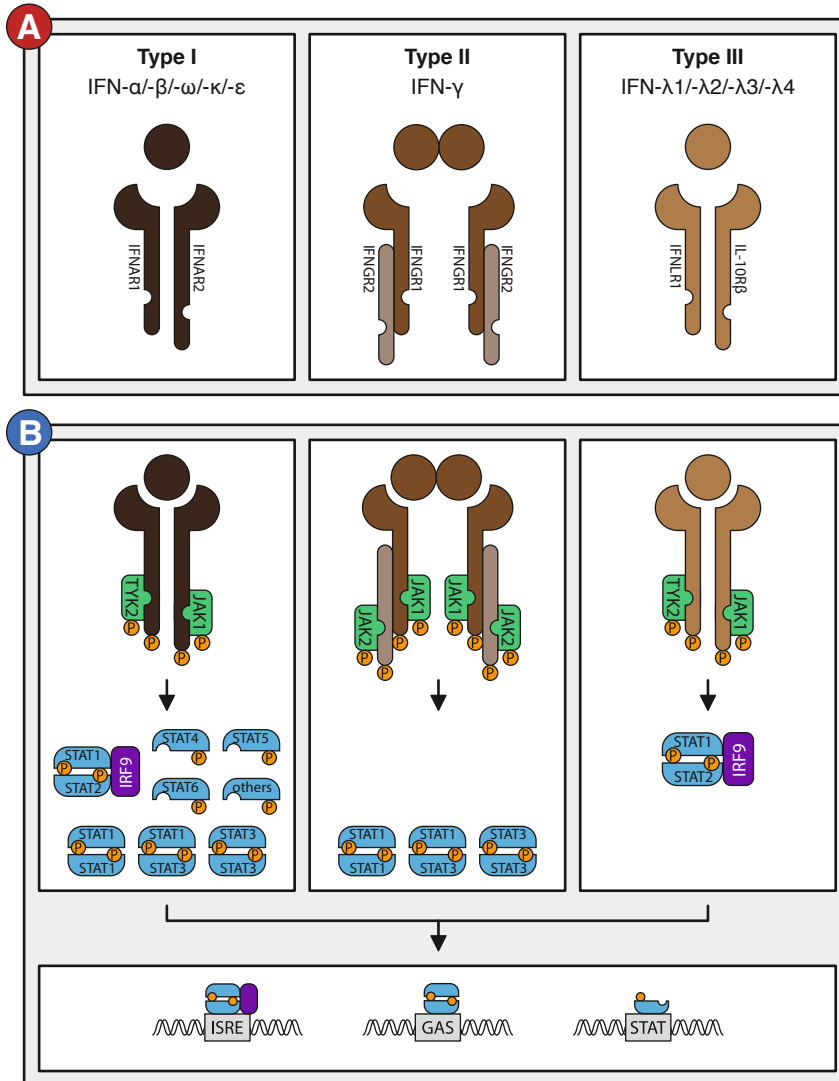
Figure 1. The interferon receptor family and signaling pathways. (**A**) Interferon (IFN) signaling is induced via different receptor complexes. Human type I IFNs (IFN-α/-β/-ω/-κ/-ε) signal via a heterodimeric receptor complex composed of the IFN-α/β/ω receptor (IFNAR) 1 and IFNAR2. Type II IFNs (IFN-γ) signal by forming antiparallel homodimers; each monomer binds a receptor complex that consists of IFN-γ receptor 1 (IFNGR) 1 and IFNGR2. Type III IFNs (IFN-λ 1-4) signal via the IFN-λ receptor complex, formed by heterodimerization of the IFN-λ receptor 1 (IFNLR1) and the IL-10 receptor 2 (IL-10R2). (**B**) The main signaling response to IFNs involves the JAK/STAT pathway (Janus Kinases / Signal Transducer and Activator of Transcription proteins). JAK1 and TYK2 (Tyrosine Kinase 2) associate with type I and III IFN receptors; JAK1 and JAK2 associate with the type II receptor. Upon ligand binding, these kinases are phosphorylated and induce receptor phosphorylation. This allows for the recruitment of specific STATs which are also phosphorylated and promote the formation of STAT homo- or heterodimers. These dimers can interact with additional factors that facilitate translocation to the nucleus. Ultimately, this results in the transcriptional activation of so-called Interferon-Stimulated Genes (ISGs), also referred to as interferon-regulated genes (IRGs).

167

Given these tumor-inhibitory activities, several clinical trials have been performed to evaluate the therapeutic application of IFNs in cancer patients. Most of this work was performed in the last two decades of the previous century and, as summarized by Borden recently, the overall results of these trials confirmed the potential anti-tumor effect and clinical benefit of mainly type I IFNs[24]. However, due to the systemic adverse effects associated with IFN treatment as well as the occurrence of resistance and the development of more potent novel drugs, IFN therapy somewhat disappeared into the background[24, 32, 33]. The observation that radiotherapy can trigger a type I IFN response has renewed the interest in these proteins.
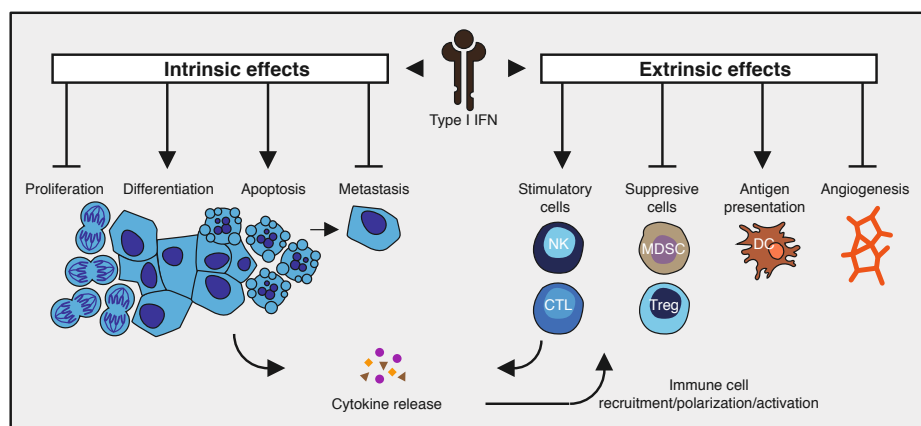

Figure 2. The intrinsic and extrinsic effects of type I interferons. A schematic overview of most important antitumor effects of type I IFNs is presented. The intrinsic, or more direct, effects include inhibition of tumor cell growth, induction of apoptosis/necroptosis and inhibition of metastasis. Extrinsic, or more indirect, effects involve the ability of type I IFNs to modulate the tumor microenvironment, e.g. by inhibiting tumor angiogenesis or activating an antitumor immune response via stimulation of cytotoxic T cells, natural killer (NK) cells and dendritic cells (DCs) as well as by negative regulation of suppressive cell types, i.e. myeloid-derived suppressor cells (MDSCs) and regulatory T cells (Tregs). Since type I IFNs can be produced by both tumor- and immune cells and the intrinsic and extrinsic effects complement each other, the mutual crosstalk between immune cells and tumor cells in the tumor microenvironment is crucial for the antitumor potential of IFNs.

3. RADIATION AND INTERFERONS

Since IFNs were not the anticipated 'magic bullets' for cancer treatment, the incentive to further develop IFN therapy has faded over the years. However, different recent scientific advancements have rekindled the interest in IFN-based therapy. These developments include the current achievements in immunotherapy, e.g. check point inhibitors and cell based therapies, as well as the novel insights in the mechanisms that guide IFN responses. For example, it has been found that type I IFNs play a critical role in generating an effective anti-tumor immune response and priming tumor reactive CD8+ T cells by stimulating the cross-presentation of tumor antigens by CD8α+ dendritic cells[28, 34]. In addition, the efficacy of radiotherapy has been associated with the induction of a

type I IFN response[16]. Interestingly, while induction of IFN expression was considered to be linked to Toll-like receptors (TLRs) signaling[19, 22], the type I IFN response during irradiation was found to occur TLR-independent. Deng et al. found that type I IFN induction was triggered via a cytosolic DNA sensing mechanism involving cGAS (Cyclic GMP-AMP synthase) and STING (STimulator of INterferon Genes)[35–37]. Moreover, it was shown that this response is dose dependent as high dose irradiation (above a threshold of 12-18 Gy) can induce a mechanism leading to degradation of cytosolic DNA, thereby preventing the activation of cGAS/STING signaling[38].

Collectively, these findings link radiotherapy directly to type I IFN induction and show that this response is required to achieve radiotherapy efficacy. This has renewed the interest to combine IFN therapy with radiotherapy as it might be beneficial for patients with diminished STING pathway functionality or with low intra-tumoral type I IFN levels. In addition, in patients that are treated with high dose irradiation, additional IFN administration might be of value in case of limited IFN induction due to inadequate cGAS/STING signaling. In that regard, it is vital to determine optimal treatment dose scheduling strategies. Interestingly, the combination of IFN treatment with radiotherapy has already been extensively explored in preclinical and clinical studies. The outcome of this prior work provides important leads for future research regarding this combination treatment.

4. COMBINING RADIOTHERAPY WITH INTERFERON TREATMENT

4.1 Lessons from preclinical studies
Compelling evidence of a potential therapeutic link between radiation and interferons arose around the same time that the first clinical trials with IFNs were performed. Within a couple of years, numerous *in vitro* studies were performed to determine the radiosensitizing effect of IFNs in different cancer cell lines (**Table 1**). With regard to IFN-α, one of the first *in vitro* studies on the combination with radiotherapy described an additive inhibitory effect on the cell growth of human glioma cells[39]. Chang & Keng reported in 1983 that IFN-α1 increases the radiation-induced cell death of human renal adenocarcinoma cells[40]. This confirmed a previous observation in murine cells[41] and was followed up by similar observations in other cancer cells. However, the effects were dependent on many variables, including the cancer cell type, the IFN type, and duration of treatment. For example, in a study using pancreatic cancer cell lines, enhanced radiosensitivity by IFN-α (3000 units/mL) was observed after preincubation of 72 hours prior to irradiation (2-6 Gy)[42]. On the other hand, in the study by Chang & Keng, the renal cancer cells were preincubated with IFN-α (1000 units/mL) for just two hours before receiving 1x 6 Gy[40]. In a follow-up study, the same authors substantiated that preincubation with IFN-α potentiates tumor cell killing by radiation. However, this was only observed after 24 hours of incubation and not after two or six hours[43].

Table 1. Preclinical studies

Author	IFN type	Cancer type (cell line)	IFN dose (IU/mL)	Pre-treatment time	RTx dose (Gray)	Effect
Dritschilo et al. [41]	-	Mouse fibroblasts (NIH-3T3)	10	2 hours	6.25	Yes
Kardamakis et al. [125]	IFN-α	Lung cancer (Unk)	-	-	-	Yes
Gould et al. [49]	IFN-α	Lung cancer (A549)	300	48 hours	1.8	No
DeLaney et al. [47]	IFN-α	Head/neck cancer (FaDu)	1000	8-10 hours	1-10	No
Hoffmann et al. [45]	IFN-α	Head/neck cancer (HTB43, SCC4, SCC9)	25-50	24 hours	1-8 or 5x 2	Yes
Angioli et al. [44]	IFN-α	Cervical Cancer (ME-180/SiHa)	100-5000	24 hours	2-15	Yes
Hoffmann et al. [45]	IFN-α	Cervical cancer (HTB35, Caski)	25-50	24 hours	1-8 or 5x 2	Yes
Ryu et al. [46]	IFN-α	Cervical cancer (HeLa-S3/ME-180)	500-5000	24 hours	2-8	Yes
Chang and Keng[43]	IFN-α	Kidney cancer (ACHN)	1000	2, 6, 24 hours	1-12	Yes
Chang and Keng[40]	IFN-α	Kidney cancer (ACHN)	1000	2 hours	6	Yes
Morak et al. [42]	IFN-α	Pancreatic cancer (MiaPaca-2/ Panc-1)	3000	72 hours	2-6	Yes
Malone et al. [48]	IFN-α	Glioblastoma (U-373 MG)	25	24 hours	2, 4, 8, 16	Yes
Schmidberger et al. [50]	IFN-ß	Lung cancer (A549)	30-8000	24 hours	1-6	Yes
Schmidberger et al. [51]	IFN-ß	Lung cancer (A549)	30-3000	24 hours	1-6	Yes
Gould et al. [49]	IFN-ß	Lung cancer (A549)	300	48 hours	1.8	Yes
Schmidberger et al. [51]	IFN-ß	Head/neck cancer (ZMK-1)	30-3000	24 hours	1-6	Yes
Schmidberger et al. [51]	IFN-ß	Cervical cancer (CaSki)	30-3000	24 hours	1-6	Yes
Angioli et al. [44]	IFN-ß	Cervical Cancer (ME-180/SiHa)	100-5000	24 hours	2-15	Yes
Schmidberger et al. [51]	IFN-ß	Breast cancer (MCF-7)	30-3000	24 hours	1-6	Yes
Chang and Keng[43]	IFN-ß	Kidney cancer (ACHN)	1000	2, 6, 24 hours	1-12	Yes
Schmidberger et al. [51]	IFN-ß	Colon cancer (WiDr)	30-3000	24 hours	1-6	Yes
Morak et al. [42]	IFN-ß	Pancreatic cancer (MiaPaca-2/Panc-1)	100	72 hours	2-6	Yes
Nederman et al. [39]	IFN-ß	Glioblastoma (U-118MG/U-251MG)	100	14 days	3	No

Preincubation of 24 hours was also used during a study with human cervical cancer cell lines. Here, incubation with IFN-α ranging from 100 to 5000 units/mL also exerted a positive effect on radiation cytotoxicity[44]. In the presence of retinoic acid, the radiosensitizing effect of IFN-α on cervical cancer cells already occurred at IFN-α doses of 25-50 units/mL[45] up to 5000 units/mL[46]. Of note, the in vitro sensitizing effect of combining IFN-α, RA and radiotherapy was described in other studies as well, including head and neck squamous cell carcinoma cells (HNSCC)[47], and glioblastoma[48].

All these results indicate that IFN-α treatment induces cell type specific effects that are influenced by a broad range of conditions, including the duration and dose of the treatment as well as the presence of additional compounds. However, it should be noted that not all studies confirmed the radiosensitizing effect of IFN-α. For example, Delaney et al. analyzed the effect of IFN-α as a radiosensitizer in HNSCC. Incubation of a FaDu cell line for 8 to 10 hours with IFN-α (1000 units/mL) yielded no significant increase in radiation cytotoxicity compared to controls[47]. Gould et al., using a longer incubation period (48 hours) but lower IFN-α concentration (300 units/mL), did also not observe a radiosensitizing effect in bronchogenic carcinoma cells[49]. While these results could be related to a too low IFN concentration, Gould et al. did observe significantly decreased cell survival rates when using IFN-β[49]. Consequently, additional studies were conducted to determine the radiosensitizing effect of IFN-β.

The majority of studies that combined IFN-β with radiotherapy confirmed the initial findings of Gould et al.[42–44, 50, 51]. For example, using bronchogenic carcinoma cells as well as four other cell lines, Schmidberger et al. observed radiosensitization using an incubation period of 24 hours and both lower and higher concentrations of IFN-β[51]. As no shorter incubation than 24 hours was used, it is impossible to conclude whether IFN-ß requires shorter incubation than IFN-α. However, these results did indicate that IFN-ß treatment might require lower concentrations than IFN-α. Of note, a relatively old study contradicts this assumption, as incubation of glioma cell lines with IFN-β at low concentrations (100 units/mL) did not yield any significant results[39]. Nevertheless, both IFN-α and IFN-β appear to exert a radiosensitizing effect on tumor cells that occurs within 24 hours and requires a minimal concentration of approximately 500 units/mL. The latter will most likely depend on the expression level of the interferon receptors.

Taking into account the -mainly promising- results from the *in vitro* studies, a surprisingly low number of preclinical *in vivo* studies have been conducted to explore the combination of radiotherapy with IFN treatment. McDonald et al. investigated the effect of IFN-ß in combination with radiotherapy on pulmonary toxicity in mice[52]. Based on pharmacokinetic analyses, IFN-ß ($1x10^4$, $3x10^4$, or $1x10^5$ units) were administered intravenously two hours before irradiation (7.5 to 15 Gy). The results suggested that IFN-ß potentiated the acute effects of radiotherapy in the healthy mouse lung but also provided some protection against long term fibrosis[52]. Of note, earlier studies already

showed that treatment with IFN could provide a radioprotective effect in irradiated mice[53].

With regard to cancer treatment, Zhu et al. performed a study in an orthotopic immune competent mouse model of pancreatic cancer. The authors did not observe an increased antitumor effect when IFN-α (3x 1x10^4 units) was combined with radiotherapy (5x 5 Gy) compared to radiotherapy alone[54]. In contrast, Nakamura et al. explored the combination of IFN-β and radiation in nude mice with subcutaneously injected human glioblastoma cells. They observed that IFN-β treatment (5x10^6 units/kg/day for 21 days) following radiotherapy (3.9 or 6.5 Gy) increased the anti-tumor effect compared to either treatment alone[55]. Similar as for the *in vitro* studies, these differences between IFN-α and IFN-β are most likely related to differences in the dose scheduling of the combination treatments. To our knowledge, no preclinical studies have been performed that compared different dose scheduling regimes. Of note, Burnette et al. provided more indirect evidence that IFN treatment could increase the tumor growth control by radiotherapy. The authors showed that high dose (ablative) irradiation induced intratumoral IFN-β expression and that this was required for effective cross-priming by tumor-infiltrating dendritic cells[16]. Adenoviral-mediated expression of IFN-β could even mimic the radiotherapy-induced effects, leading to selective expansion of antigen-specific T cells and subsequent tumor regression[16].

Collectively, based on the preclinical *in vitro* studies, the combination of radiation with IFN treatment appears to be beneficial, although the effects depend on the tumor type, the experimental setup and the dose scheduling. The number of preclinical *in vivo* studies is insufficient to draw definite conclusions and additional work should be performed especially with regard to the dose-scheduling of IFNs and radiotherapy.

4.2 Lessons from clinical trials
Soon after the first positive *in vitro* results, the combination of radiotherapy with IFN treatment was evaluated in clinical trials. In the last 3 decades, multiple clinical phase I, II and III trials were conducted combining radiotherapy with different IFNs in a variety of dose-scheduling regimes in several tumor types including head and neck cancer, melanoma, pancreatic cancer, glioma, cervical cancer and lung cancer (**Table S1**). Regarding the latter, Mattson et al. conducted a small clinical trial in 15 patients with previously untreated small cell lung cancer (SCLC) patients[56]. Both a high-dose (5 days 800x10^6 IU IFN-α i.v., followed by three weekly 6x10^6 IU IFN-α i.m.) and low-dose IFN-α treatment (three weekly 6x10^6 IU IFN-α i.m.) was evaluated. Radiotherapy was started (while continuing the interferon treatment) in case of locoregional progression (30 Gy in 10 fractions, 3 weeks rest, 25 Gy in 10 fractions) or isolated CNS relapse (whole brain 30 Gy in 10 fractions). Although the authors suggested that IFN-α might potentially delay metastatic dissemination and potentiate the radiation effect, considerable toxicity (not objectively graded,) was observed. Fever, tremors, malaise

and muscle pain occurred throughout all patients and anorexia, weight loss, complains of memory- and psychomotor dysfunction were dose limiting factors in both treatment groups. Furthermore, severe radiation pneumonitis was found in three out of the five patients who received radiotherapy[56]. In a follow-up study in 12 SCLC patients, tumor growth regression was confirmed for both scheduling regimens[57]. However, due to radiation-induced early and severe lung reactions (not objectively graded), the radiation dose had to be reduced in two patients. Two months after the treatment, five patients showed radiological grade III fibrosis, especially in the high-dose treatment group. The authors called for more clinical studies to evaluate the effects of dose-scheduling when combining IFN-α with radiotherapy in SCLC patients[57]. To our knowledge, such studies have not been performed. Rather, additional studies were conducted in non-small cell lung cancer (NSCLC) patients. In a pilot study by Niiranen et al., 14 NSCLC patients were treated with a lower dose of IFN-α (5 weekly 6x10^6 IU i.m. for 12 weeks)[58]. Fever and flu-like symptoms (grade 1-4) occurred in all patients and neurologic side effects (grade 1-2) in 75% of patients. Three out of four patients that completed the 12-week monotherapy received subsequent radiotherapy (55 Gy in twice daily fractions of 1.25 Gy for 5 days per week) while continuing IFN-α treatment. In two patients, a partial response was observed while one patient had stable disease. The toxicity did not increase during the sequential therapy, apart from early moderately severe radiation pneumonitis,[58]. Radiation pneumonitis was also reported in three patients enrolled in a phase I study that evaluated the combination of radiotherapy (1.25 Gy twice daily for 5 days per week) with IFN-α (multiple dose-levels, 0 to 5x10^6 IU/m^2 s.c.given 2 hours before irradiation) and cisplatin (multiple dose-levels, mostly 8mg/m^2/day continues i.v.) in 48 patients, half of them with NSCLC[59]. Finally, increased toxicity was observed in a study that evaluated inhalation of IFN-α, as an alternative administration route, in combination with a hyperfractionated radiation schedule (60 Gy in twice daily fractions of 1.25 Gy for 5 days per week). Thirty minutes prior to each radiation, half of the patients received a single administration of IFN-α (3x10^6 IU i.m.) followed by IFN-α inhalation (1.5x10^6 IU). The combination treatment was poorly tolerated and was accompanied with flu-like symptoms, anorexia and moderate to severe esophagitis, pneumonitis and bronchial obstruction. Only two patients could receive radiotherapy without dose-schedule modifications. In addition, IFN-α treatment did not result in a clinical benefit and the authors reported possible treatment related deaths[60]. Of note, a trial that evaluated the use of adjuvant IFN-α treatment in SCLC patients responsive to chemoradiation did also not show any clinical benefit[61]. These negative findings might explain why later studies in lung cancer patients mainly focused on combining radiotherapy with IFN-ß and IFN-γ rather than with IFN-α. The use of IFN-γ was quickly dismissed due to a lack of efficacy and unfavorable toxicities in both SCLC and NSCLC patients[62–64].

The results with IFN-ß appeared more promising. In a phase I/II study in 39 NSCLC patients IFN-ß (10x10^6 to 90x10^6 IU i.v.) was administered concurrently with conventional radiation treatment (1.8 Gy for 5 days per week)[65]. This combination strategy yielded

positive results, showing enhanced survival compared to radiotherapy alone without severe or long-term toxicity; 67% of patients experienced grade 1 or 2 IFN-ß related side effects and one patient was reported to experience grade 4 fever after IFN- ß administration[65]. In addition, a phase I study in 12 inoperable NSCLC patients that combined radiotherapy (60 Gy in 5 weekly fractions of 2 Gy for 6 weeks) with IFN-ß in a dose-escalating design (1.5 to 24×10^6 IU/m^2 s.c.) established 12×10^6 IU/m^2 IFN-ß as maximal tolerable dose (MTD). One complete response and six partial responses were observed, as well as a trend towards an improved survival[66]. Nevertheless, a phase III trial in locally advanced, non-metastatic NSCLC patients using a similar setup as the promising phase II trial failed to substantiate the beneficial effect of IFN-ß treatment while the number of grade 3 and 4 acute toxicities, primarily related to lung and esophagus, was significantly higher on the IFN- ß arm, as compared to the radiotherapy only arm[67].

Comparable observations were made in glioma patients despite the encouraging initial studies. For example, in 1984, an exploratory study was published by Mahaley et al. that evaluated the combination of radiotherapy and interferon treatment in nine patients with anaplastic glioma[68]. Following surgery, the patients were treated with a weekly escalating doses of IFN-α for three weeks (three weekly 10, 20 and 30×10^6 IU/m^2 i.v.) after which radiotherapy was started (43 Gy to whole brain and 17 Gy to the tumor area over a 7-week period). No dose-limiting toxicities were encountered and it was proposed to further evaluate this combination in a concurrent treatment setting[68]. Using such a treatment schedule, Dillman et al. concluded in that IFN-α (three weekly $3\text{-}5\times10^6$ IU s.c.) in combination with radiotherapy (1.8 Gy per day) was a safe regimen, although higher doses of IFN-α led to grade 4 toxicity and possible treatment related deaths.[69] When IFN-α (3×10^6 IU/day s.c. for 28 days, followed by three weekly 3×10^6 IU s.c. for 6 weeks) was given after completion of radiotherapy it was generally well tolerated, although no clinical benefit could be demonstrated[70]. This was different in two other studies in which patients who progressed after radiotherapy were treated with a combination of IFN-α and carmustine[71, 72]. Both studies reported positively with regard to tumor response rates, albeit concerns were raised regarding exacerbation of neurological symptoms. Unfortunately, a phase III trial that evaluated the added value of IFN-α (12×10^6 IU/m2 on days 1–3 in weeks 1, 3 and 5, every 7 weeks) to carmustine treatment after radiotherapy in 214 evaluable high-grade glioma patients, did not show an improved progression free- or overall survival. Unfortunately, patients receiving IFN-α experienced more grade ≥3 toxicity including fever, chills, myalgia and neurological symptoms such as somnolence, confusion and exacerbation of neurologic deficits[73]. The combination of radiotherapy with IFN-ß (in combination with alkylating agents like temozolomide or nitrosourea) has also been explored in primary- as well as in recurrent glioma[74–81]. While the majority of these studies suggested that this combination could be effective with limited adverse effects, a recent randomized phase II trial recommended that IFN-ß should not be further considered for phase III clinical

trials[82]. This was based on the observation that the addition of IFN-ß did not improve progression free- and overall survival, while increased grade ≥3 hematological and gastrointestinal toxicity was observed[82]. Thus, both in lung cancer and brain cancer, the combination of radiotherapy with IFN treatment appeared to be associated with limited, if any, clinical benefit and increased grade ≥3 toxicity.

Actually, in other cancer types the occurrence of increased toxicity is a recurring theme as well when radiotherapy is combined with either IFN-α or IFN-ß. For example, in a small case series of ten rectal cancer patients, it was advised not to exceed a dosage of three weekly $3x10^6$ IU IFN-α s.c. concurrent with radiotherapy due to acute grade ≥3 leukopenia, diarrhea and concerns regarding possible late complications[83]. Moreover, a pilot study in 22 head and neck cancer patients that compared the effects of radiotherapy alone to radiotherapy with IFN-α ($6x10^6$ IU/day for 4 weeks) was halted due to severe grade ≥3 mucosal reactions in the latter treatment group[84]. Likewise, a phase I dose-escalation study in patients with different cancer types, mostly lung cancer, that aimed to explore the combination of radiotherapy with IFN-α (up to $30x10^6$ IU/m^2 s.c. 3 or 5 times per week), found three weekly $5x10^6$ IU/m^2 IFN-α to be the MTD. Grade 1-2 flu-like symptoms occurred in 14/16 of patients, grade ≥3 dehydration was observed in 6 cases and one possible treatment related death due to gastrointestinal hemorrhage was reported. Furthermore, common side-effects associated with radiotherapy, such as radiation dermatitis and esophagitis seemed to appear earlier and more pronounced than expected, although no objective grading was reported[85]. Finally, a trial by Picozzi et al. in 43 resected pancreatic cancer patients evaluated adjuvant IFN-α (three weekly $3x10^6$ IU s.c.) together with chemoradiation (28 fractions of 1.8 Gy in 6 weeks with continuous 5-FU 175mg/m^2 and weekly cisplatin 30mg/m^2, followed by 2 additional cycles of 6 weeks of 5-FU). Although an 18 month OS of 69,1% compared to a historical OS of 50% was found, patient accrual was stopped due to an all-cause grade ≥3 toxicity rate of 95% (80 patients). Grade 3 and 4 hematologic toxic effects included neutropenia (35% of patients) and thrombocytopenia (11% of patients). The most common grade 3 or 4 non-hematologic toxic effects were gastrointestinal and electrolyte disturbances[86]. A randomized multicenter phase III trial was performed by Schmidt et al. In this trial the IFN-α plus chemoradiation protocol as described above was compared to 5-FU and folinic acid in patients with resected pancreatic adenocarcinoma. Unfortunately, this trial failed to demonstrate any clinical benefit and reported 85% grade ≥ 3 toxicity (mostly neutropenia) in the IFN-α group, versus 16% in the 5-FU and folinic acid group, respectively[87]. Interestingly, a recent update of the survival of the patients enrolled in the 2003 trial of Picozzi et al. reported a clear benefit of IFN-α based adjuvant chemoradiation as compared to standard adjuvant chemoradiation[88]. After a follow up at least 10 years since surgery for pancreatic cancer, the 5-year survival was 42% and the 10-year survival was 28%. Nine patients survived beyond 10 years and the median overall survival was 42 months (95% CI: 22–110 months)[88]. Still, grade ≥ 3 toxicity required interruption of the combination treatment in 70% of the patients and 42%

6

of patients had to be hospitalized[88]. Thus, the addition of IFN-α could be worthwhile provided that the extensive toxicities can be addressed. Thus far, small adjustments in the type or dose of chemotherapy did not reduce the high percentages of grade ≥ 3 adverse events[89, 90] and further research should be performed.

The occurrence of substantial late toxicities was also the reason that Stock et al. advised against the use of IFN-α and cisplatin combined with radiotherapy in cervical cancer patients. The authors evaluated the combination of IFN-α (three weekly 5×10^6 IU/day) with radiotherapy (45 Gy in five weekly fractions of 1.8 Gy, followed by 2 brachytherapy procedures) and weekly cisplatin (25 mg/m²) in twenty-one cervical cancer patients. While the treatment showed promising clinical benefit with 100% local tumor control after two years, it was accompanied by significant grade 4 complications in the rectosigmoid, bladder and small bowel. Moreover, these complications occurred earlier than expected[91]. This might have been cisplatin-related since subsequent trials that did not include cisplatin were more positive[92–94]. More recently, a phase II trial was performed in cervical cancer patients receiving IFN-α in combination with retinoic acid (RA)[95]. The study was based on preclinical studies and clinical trials which indicated that this combination was active and tolerable[46, 92, 93, 96]. It was suggested that IFN/RA treatment could improve tumor oxygenation which might underlie the better local tumor control by radiotherapy[97, 98]. In total 209 patients were randomized to receive either IFN-α (three weekly 3×10^6 IU s.c.) with a daily dose of 13-cis-retinoic acid, or weekly cisplatin treatment. Both groups also received concurrent radiotherapy (25 fractions of 2 Gy for 5 weeks). While the results showed that the IFN/RA treatment induced less grade ≥3 toxicity, the survival rates appeared somewhat poorer as compared to the cisplatin treatment. Consequently, the combination was not recommended for further analysis in a phase III setting[95].

Collectively, despite the overall promising results that were observed in preclinical studies, the clinical trials that evaluated the combination of radiotherapy with interferon treatment have shown diverse outcomes. Six out of seven randomized clinical trials that have been conducted report increased grade ≥3 toxicity of interferon treatment regimes. Unfortunately, none of them demonstrated a survival benefit **(Table 2)**. Thus, based on current insights, it remains unclear whether and how the combination of IFN treatment with radiotherapy might benefit cancer patients. Nevertheless, it should be noted that there is considerable variation between the different trials with regard to e.g. cancer types, tumor stage/grade, treatment dose and therapy scheduling. All this makes it difficult to draw any definite conclusions. The observation that some studies also report a potential benefit with acceptable toxicities indicates that there might be a therapeutic window that can be exploited. However, as described in the following paragraphs, many hurdles have to be taken and several outstanding questions have to be answered for this combination treatment to become successful.

Table 2. Randomized controlled trials

Author	N	Tumor type	Treatment	Survival (IFN group vs. Control group)	Toxicity
Buckner et al. [73]	275	Brain	Radiotherapy/BCNU followed by BCNU +/- IFN-α	OS: (n.s)	Increased grade ≥3 toxicity IFN-α arm
Valavaara et al.* [84]	22	HNSCC	Radiotherapy +/- IFN-α	OS: med 27.7 vs. 26.5 months (n.s.)	Increased grade ≥3 toxicity IFN-α arm
Basu et al. [95]	209	Cervix	Radiotherapy/IFN-α/RA vs. radiotherapy/cisplatin	OS: HR: 0.67 (95%CI: 0.44-1.01)	Increased grade ≥3 toxicity control arm
Yazigi et al. [94]	74	Cervix	Radiotherapy +/- IFN-α2b	OS: (n.s.)	Increased fever (grade unknown) IFN-arm
Schmidt et al. [87]	132	Pancreas	Radiotherapy/cisplatin/5FU + IFN-α2b vs. 5FU	OS: HR 1.04 (95%CI 0.66-1.53)	Grade ≥3 toxicity 85% (IFN-α), 16% (control)
Wakabayashi et al. [82]	112	Brain	Radiotherapy/TMZ +/- IFN-β	OS: HR 1.00 (95%CI 0.65-1.55)	Grade ≥3 neutropenia 20.7% (IFN-β), 12.7% (control)
Bradley et al. [67]	123	Lung	Radiotherapy +/- IFN-β	OS: med 10.3 vs. 9.5 months (n.s.)	Grade ≥3 toxicity 31% (IFN-β), 19% (control)

*Accrual stopped due to toxicity. OS: overall survival, HR: hazard ratio, med: median, n.s.: not significant

6

5. FUTURE PERSPECTIVES AND OUTSTANDING QUESTIONS

The recent insights that link the efficacy of radiotherapy with the ability to induce an intratumoral type I IFN response has renewed the interest to combine radiotherapy with IFN treatment. In order to determine the potential opportunities and current challenges of this approach, we re-evaluated the available scientific literature on this combination therapy. Based on the majority of pre-clinical studies it can be concluded that IFN treatment can have a radiosensitizing effect on a broad panel of cancer cells. At the same time, the results of the clinical trials are more diverse and less promising. Actually, the observation that combining IFN treatment with radiotherapy is often accompanied by increased toxicity has frequently resulted in a negative recommendation regarding this combination therapy. While understandable, this conclusion appears premature since data has mostly been derived from small observational studies. In addition, objective grading of adverse events has not always been completely documented. Rather than a justification to dismiss this combination treatment, the results of the preclinical studies and clinical trials have identified several important questions that should be addressed in order to further explore the potential benefit of this combinatorial approach.

For example, it might be relevant to determine which interferon is most effective in combination with radiotherapy. In light of the observed link between irradiation and type I IFN signaling, this review mainly focused on IFN-α and IFN-ß. The available *in vitro* studies provide some indication that IFN-ß may be slightly more potent as compared to IFN-α, since lower doses are required in combination with radiation. Gould et al. even found that human bronchogenic carcinoma cells were only radiosensitized by IFN-ß and not by IFN-α[49]. While the clinical trials appear to suggest that IFN-ß induces less side effects as compared to IFN-α, this is less apparent when only similar tumor types are compared. To our knowledge no clinical trials have been performed in which the efficacy and toxicity of different IFN types were compared. At the same time, considering that IFN-α and IFN-ß act through the same receptors, it can be argued that small differences in their activity are not relevant in light of the variability in responses that are clinically observed. In that regard, it might be more worthwhile to explore to what extent the overall IFN status prior to treatment can predict the efficacy and toxicity of the combinatorial approach. This should also include analysis of IFN receptor expression in the tumor cells as this is likely linked to radiosensitization during IFN treatment. Such information might give insight in the value of adding IFNs to radiotherapy. Of note, it has been suggested that radiotherapy can also induce the expression of IFN-λ[99], a type III IFN which drives similar pathways as type I IFNs[22]. Given the limited expression of the IFN-λ receptor, type III IFNs have more restricted effects and might be a more safe and effective anti-cancer treatment[100, 101]. In line with the above, it is well recognized that radiotherapy can exert different effects on the specific cell populations that reside in the tumor microenvironment[9, 102]. Apart from interferons, radiotherapy triggers the release of a plethora of (immunomodulatory) cytokines and other factors that can

influence the response to irradiation[103]. To optimize combination therapies with IFNs, it will be vital to obtain more insight in the interactions between different responses in the tumor microenvironment and to understand the paracrine and autocrine effects as well as the interplay of IFNs and other cytokines in this multicellular tumor compartment.

The most effective route of administration is also something that could be further explored. For example, inhalation of IFN-α was accompanied by severe toxicity[60]. The main routes of administration used in clinical trials are intravenous, subcutaneous and intramuscular injection. Since systemic IFN therapy is accompanied by dose-limiting toxicity, targeted delivery of IFN might provide a better alternative. This could be achieved by e.g. intratumoral injection, chaperone adenoviruses[104, 105], or IFN conjugated antibodies[106, 107]. It is certainly valuable to further explore such alternative application strategies in combination with radiotherapy in clinical trials. In addition, alternative strategies could be considered to enhance type I IFN levels, e.g. by using IFN agonists. Although there is no conclusive evidence yet, such agonists might be preferred over the use of IFNs themselves due to superior pharmacokinetics and the ability to induce other immunoregulatory cytokines in addition to IFNs[22]. For example, agonists of the STING pathway are currently in the pipeline of multiple pharmaceutical and biotech companies, even though the systemic toxicity appear to be considerable[108].

An important issue that needs to be resolved involves the optimal dose scheduling of interferon treatment. For example, a wide variety of IFN doses has been used in the clinical trials, ranging from 0.5×10^6 to 800×10^6 IU. These different doses were also administered using different schedules, ranging from only once every week up to 7 days per week. Moreover, the total treatment periods stretched from 1 week up to years if IFN was also part of maintenance therapy. All these variables resulted in a broad range of total IFN doses which are likely to affect the serum levels that are reached during treatment. Since it is poorly understood what levels are required to achieve optimal interaction with radiotherapy this should be further explored. Especially given the known side effects of IFN mono-therapy[22], the dose of IFNs in combination with radiotherapy could be further optimized and IFN levels should be monitored during treatment. On the other hand, it should be realized that interferon treatment can trigger biological effects without detectable serum levels of interferons[109, 110]. This most likely is a reflection of the intrinsic and extrinsic effects of interferons, of which the former is specifically observed in vitro while the latter also contribute to the in vivo effects.

Apart from the dose, the scheduling of IFN treatment could also be optimized, especially with regard to the timing and duration. The prolonged and concurrent treatment schedules used in most trials appeared to be based on the concept that the radiosensitizing effects were caused by the ability of IFNs to inhibit cell cycle progression at the G2-M phase[40, 43]. In addition, impaired radiation damage repair and accumulation of sublethal damage were proposed mechanisms of IFN-related radiosensitization[43, 51].

6

In light of these mechanisms, a continuous IFN treatment should enhance the effects of irradiation. While this might be true in an *in vitro* setting where cultured cancer cells are treated with both IFN and irradiation, our current knowledge suggests that the beneficial effects of IFNs *in vivo* are more related to their role in generating an effective anti-tumor immune response[16, 28, 34]. In that regard, it can be questioned whether prolonged and concurrent IFN treatment during radiotherapy has added value over brief IFN administration in e.g. a neoadjuvant setting or in the first 1 or 2 weeks of radiotherapy. Especially since it has been shown that the increased expression of IFN response genes is also associated with radioresistance[111–113]. In addition, prolonged type I and type II IFN signaling can trigger mechanisms that confer resistance to e.g. anti-PD1 treatment[114]. Thus, continuous IFN treatment during radiotherapy might interfere with efforts to develop effective immuno-radiotherapy. Moreover, based on the insight that irradiation itself activates IFN production via the cGAS/STING pathway, it could be argued that the addition of exogenous IFN administration during radiation should only be considered in patients that have defects in this pathway or in patients that receive radiotherapy which does not adequately induce a type I IFN response. The latter also highlights the import role of dose scheduling radiotherapy in the efficacy of IFN treatment. In fact, based on our limited understanding of the relationship between e.g. dose-fractionation of radiotherapy and local molecular responses, most clinical trials on radiation combination therapies are guided by standard of care practices that might be suboptimal[115]. For example, it has been shown that radiotherapy can induce dose dependent effects on the tumor vasculature[7, 116]. While high dose irradiation induces vascular collapse, fractionated low dose radiotherapy can promote tumor vascularization which can be counteracted by angiostatic treatment[7, 116]. However, similar to combination treatments with IFNs, trials that combined radiotherapy with angiostatic drugs show limited efficacy and increased toxicity[7].

Interestingly, we found that optimized dose scheduling of radiotherapy and angiostatic drug treatment allowed dose reductions of either the drug or the radiation dose, without affecting treatment efficacy[116, 117]. This could be clinically relevant. With regard to IFN combination treatment there is also evidence that the radiation dose and scheduling are important. Using a murine B16 melanoma model, Lugade et al. showed that a single dose of 15 Gy generated a better anti-tumor (IFN-γ) immune response compared to 5x3 Gy[118]. On the other hand, it has been shown that high dose irradiation (above a threshold of 12-18 Gy) can induce Trex1, an exonuclease that can degrade cytosolic DNA. This abolishes the activation of the STING pathway and type I IFN production and thus results in limited anti-tumor immunity[38]. All this is relevant in the context of clinical studies since most of the trials that combined e.g. IFN treatment with radiotherapy used a conventional fractionated radiation schedule of 1.8–2.0 Gy per day, 5 days per week for several weeks. How such schedules affect type IFN signaling is still poorly understood. Currently, an emerging research field aims to further unravel the complex interplay between radiation-induced DNA damage, the occurrence of

cytosolic DNA and activation of IFN-signaling via e.g. the cGAS/STING pathway. This has shown that IFN signaling can occur as an intrinsic response in different cell types in the tumor microenvironment[119–121]. Moreover, the response can also be triggered by other cytokines exemplifying that more research is required to better understand the interplay between radiation and immunological responses and the consequences for immunoradiotherapy (For recent reviews on these subjects see Wilkins et al.[122] and Shevtsov et al.[123]). Better insight in the underlying mechanisms will allow for better hypothesis-driven design of clinical trials, which is needed to optimally exploit the involvement of type I IFN responses in establishing anti-tumor immunity.

In summary, while the combination of radiotherapy with IFN holds potential as anti-cancer therapy, many questions remain to be answered in order to safely and effectively implement this treatment in daily clinical practice. As already stated in 1995 by Mattson: *"Interferons are potent biological modifiers and there are indications that they could be used to potentiate the responses of lung tumors to other therapies, particularly radiotherapy. However, the balance between positive interactions and toxicity is fine, so that care must be taken when developing suitable regimens to ensure that the potentiation of effect achieved is for the benefit of the patients."*[124]. Clearly, this statement is not only true for lung cancer, and 25 years of research have shown that combining IFN therapy with (chemo)radiation is challenging in most, if not all tumor types. Nevertheless, further research into the interactions between both treatments, and unraveling the mechanisms that drive IFN responses during radiotherapy will help to decipher the optimal setting for further clinical evaluation of this potentially valuable combination therapy.

6

181

REFERENCES

1. Barnett, G. C.; West, C. M.; Dunning, A. M.; Elliott, R. M.; Coles, C. E.; Pharoah, P. D. et al. Normal tissue reactions to radiotherapy: towards tailoring treatment dose by genotype. *Nat Rev Cancer* 9:134-142; 2009.

2. Baumann, M.; Krause, M.; Overgaard, J.; Debus, J.; Bentzen, S. M.; Daartz, J. et al. Radiation oncology in the era of precision medicine. *Nat Rev Cancer* 16:234-249; 2016.

3. Bernier, J.; Hall, E. J.; Giaccia, A. Radiation oncology: a century of achievements. *Nat Rev Cancer* 4:737-747; 2004.

4. Pouget, J. P.; Lozza, C.; Deshayes, E.; Boudousq, V.; Navarro-Teulon, I. Introduction to radiobiology of targeted radionuclide therapy. *Front Med (Lausanne)* 2:12; 2015.

5. Begg, A. C.; Stewart, F. A.; Vens, C. Strategies to improve radiotherapy with targeted drugs. *Nat Rev Cancer* 11:239-253; 2011.

6. Sharma, R. A.; Plummer, R.; Stock, J. K.; Greenhalgh, T. A.; Ataman, O.; Kelly, S. et al. Clinical development of new drug-radiotherapy combinations. *Nat Rev Clin Oncol* 13:627-642; 2016.

7. Hamming, L. C.; Slotman, B. J.; Verheul, H. M. W.; Thijssen, V. L. The clinical application of angiostatic therapy in combination with radiotherapy: past, present, future. *Angiogenesis* 20:217-232; 2017.

8. Kleibeuker, E. A.; Griffioen, A. W.; Verheul, H. M.; Slotman, B. J.; Thijssen, V. L. Combining angiogenesis inhibition and radiotherapy: a double-edged sword. *Drug Resist Updat* 15:173-182; 2012.

9. Goedegebuure, R. S. A.; de Klerk, L. K.; Bass, A. J.; Derks, S.; Thijssen, V. L. J. L. Combining Radiotherapy With Anti-angiogenic Therapy and Immunotherapy; A Therapeutic Triad for Cancer. *Front Immunol* 9:3107; 2018.

10. Baird, J. R.; Monjazeb, A. M.; Shah, O.; McGee, H.; Murphy, W. J.; Crittenden, M. R. et al. Stimulating Innate Immunity to Enhance Radiation Therapy-Induced Tumor Control. *Int J Radiat Oncol Biol Phys* 99:362-373; 2017.

11. Deloch, L.; Derer, A.; Hartmann, J.; Frey, B.; Fietkau, R.; Gaipl, U. S. Modern Radiotherapy Concepts and the Impact of Radiation on Immune Activation. *Front Oncol* 6:141; 2016.

12. Galluzzi, L.; Buqué, A.; Kepp, O.; Zitvogel, L.; Kroemer, G. Immunogenic cell death in cancer and infectious disease. *Nat Rev Immunol* 17:97-111; 2017.

13. Galluzzi, L.; Zitvogel, L.; Kroemer, G. Immunological Mechanisms Underneath the Efficacy of Cancer Therapy. *Cancer Immunol Res* 4:895-902; 2016.

14. Walle, T.; Martinez Monge, R.; Cerwenka, A.; Ajona, D.; Melero, I.; Lecanda, F. Radiation effects on antitumor immune responses: current perspectives and challenges. *Ther Adv Med Oncol* 10:1-27; 2018.

15. Apetoh, L.; Ghiringhelli, F.; Tesniere, A.; Obeid, M.; Ortiz, C.; Criollo, A. et al. Toll-like receptor 4-dependent contribution of the immune system to anticancer chemotherapy and radiotherapy. *Nat Med* 13:1050-1059; 2007.

16. Burnette, B. C.; Liang, H.; Lee, Y.; Chlewicki, L.; Khodarev, N. N.; Weichselbaum, R. R. et al. The efficacy of radiotherapy relies upon induction of type i interferon-dependent innate and adaptive immunity. *Cancer Res* 71:2488-2496; 2011.

17. Kang, J.; Demaria, S.; Formenti, S. Current clinical trials testing the combination of immunotherapy with radiotherapy. *J Immunother Cancer* 4:51; 2016.

18. Ko, E. C.; Formenti, S. C. Radiotherapy and checkpoint inhibitors: a winning new combination. *Ther Adv Med Oncol* 10:1758835918768240; 2018.

19. Borden, E. C.; Sen, G. C.; Uze, G.; Silverman, R. H.; Ransohoff, R. M.; Foster, G. R. et al. Interferons at age 50: past, current and future impact on biomedicine. *Nat Rev Drug Discov* 6:975-990; 2007.

20. Wack, A.; Terczyńska-Dyla, E.; Hartmann, R. Guarding the frontiers: the biology of type III interferons. *Nat Immunol* 16:802-809; 2015.

21. Ivashkiv, L. B.; Donlin, L. T. Regulation of type I interferon responses. *Nat Rev Immunol* 14:36-49; 2014.

22. Parker, B. S.; Rautela, J.; Hertzog, P. J. Antitumour actions of interferons: implications for cancer therapy. *Nat Rev Cancer* 16:131-144; 2016.

23. Stark, G. R.; Darnell, J. E. The JAK-STAT pathway at twenty. *Immunity* 36:503-514; 2012.

24. Borden, E. C. Interferons α and β in cancer: therapeutic opportunities from new insights. *Nat Rev Drug Discov* 18:219-234; 2019.

25. Cheon, H.; Borden, E. C.; Stark, G. R. Interferons and their stimulated genes in the tumor microenvironment. *Semin Oncol* 41:156-173; 2014.

26. Ortiz, A.; Fuchs, S. Y. Anti-metastatic functions of type 1 interferons: Foundation for the adjuvant therapy of cancer. *Cytokine* 89:4-11; 2017.

27. Knuth, A. K.; Rösler, S.; Schenk, B.; Kowald, L.; van Wijk, S. J. L.; Fulda, S. Interferons Transcriptionally Up-Regulate MLKL Expression in Cancer Cells. *Neoplasia* 21:74-81; 2019.

28. Diamond, M. S.; Kinder, M.; Matsushita, H.; Mashayekhi, M.; Dunn, G. P.; Archambault, J. M. et al. Type I interferon is selectively required by dendritic cells for immune rejection of tumors. *J Exp Med* 208:1989-2003; 2011.

29. Fuertes, M. B.; Woo, S. R.; Burnett, B.; Fu, Y. X.; Gajewski, T. F. Type I interferon response and innate immune sensing of cancer. *Trends Immunol* 34:67-73; 2013.

30. González-Navajas, J. M.; Lee, J.; David, M.; Raz, E. Immunomodulatory functions of type I interferons. *Nat Rev Immunol* 12:125-135; 2012.

31. Woo, S.-R.; Corrales, L.; Gajewski, T. F. Innate immune recognition of cancer. *Annu Rev Immunol* 33:445-474; 2015.

32. Di Franco, S.; Turdo, A.; Todaro, M.; Stassi, G. Role of Type I and II Interferons in Colorectal Cancer and Melanoma. *Front Immunol* 8:878; 2017.

33. Minn, A. J.; Wherry, E. J. Combination Cancer Therapies with Immune Checkpoint Blockade: Convergence on Interferon Signaling. *Cell* 165:272-275; 2016.

34. Fuertes, M. B.; Kacha, A. K.; Kline, J.; Woo, S. R.; Kranz, D. M.; Murphy, K. M. et al. Host type I IFN signals are required for antitumor CD8+ T cell responses through CD8{alpha}+ dendritic cells. *J Exp Med* 208:2005-2016; 2011.

35. Burdette, D. L.; Vance, R. E. STING and the innate immune response to nucleic acids in the cytosol. *Nat Immunol* 14:19-26; 2013.

36. Ishikawa, H.; Ma, Z.; Barber, G. N. STING regulates intracellular DNA-mediated, type I interferon-dependent innate immunity. *Nature* 461:788-792; 2009.

37. Deng, L.; Liang, H.; Xu, M.; Yang, X.; Burnette, B.; Arina, A. et al. STING-Dependent Cytosolic DNA Sensing Promotes Radiation-Induced Type I Interferon-Dependent Antitumor Immunity in Immunogenic Tumors. *Immunity* 41:843-852; 2014.

6

38. Vanpouille-Box, C.; Alard, A.; Aryankalayil, M. J.; Sarfraz, Y.; Diamond, J. M.; Schneider, R. J. et al. DNA exonuclease Trex1 regulates radiotherapy-induced tumour immunogenicity. *Nat Commun* 8:15618; 2017.

39. Nederman, T.; Benediktsson, G. Effects of interferon on growth rate and radiation sensitivity of cultured, human glioma cells. *Acta Radiol Oncol* 21:231-234; 1982.

40. Chang, A. Y.; Keng, P. C. Inhibition of cell growth in synchronous human hypernephroma cells by recombinant interferon alpha-D and irradiation. *J Interferon Res* 3:379-385; 1983.

41. Dritschilo, A.; Mossman, K.; Gray, M.; Sreevalsan, T. Potentiation of radiation injury by interferon. *Am J Clin Oncol* 5:79-82; 1982.

42. Morak, M. J.; van Koetsveld, P. M.; Kanaar, R.; Hofland, L. J.; van Eijck, C. H. Type I interferons as radiosensitisers for pancreatic cancer. *Eur J Cancer* 47:1938-1945; 2011.

43. Chang, A. Y.; Keng, P. C. Potentiation of radiation cytotoxicity by recombinant interferons, a phenomenon associated with increased blockage at the G2-M phase of the cell cycle. *Cancer Res* 47:4338-4341; 1987.

44. Angioli, R.; Sevin, B. U.; Perras, J. P.; Untch, M.; Koechli, O. R.; Nguyen, H. N. et al. In vitro potentiation of radiation cytotoxicity by recombinant interferons in cervical cancer cell lines. *Cancer* 71:3717-3725; 1993.

45. Hoffmann, W.; Bläse, M. A.; Santo-Hoeltje, L.; Herskind, C.; Bamberg, M.; Rodemann, H. P. Radiation sensitivity of human squamous cell carcinoma cells in vitro is modulated by all-trans and 13-cis-retinoic acid in combination with interferon-alpha. *Int J Radiat Oncol Biol Phys* 45:991-998; 1999.

46. Ryu, S.; Kim, O. B.; Kim, S. H.; He, S. Q.; Kim, J. H. In vitro radiosensitization of human cervical carcinoma cells by combined use of 13-cis-retinoic acid and interferon-alpha2a. *Int J Radiat Oncol Biol Phys* 41:869-873; 1998.

47. DeLaney, T. F.; Afridi, N.; Taghian, A. G.; Sanders, D. A.; Fuleihan, N. S.; Faller, D. V. et al. 13-cis-retinoic acid with alpha-2a-interferon enhances radiation cytotoxicity in head and neck squamous cell carcinoma in vitro. *Cancer Res* 56:2277-2280; 1996.

48. Malone, C.; Schiltz, P. M.; Nayak, S. K.; Shea, M. W.; Dillman, R. O. Combination interferon-alpha2a and 13-cis-retinoic acid enhances radiosensitization of human malignant glioma cells in vitro. *Clin Cancer Res* 5:417-423; 1999.

49. Gould, M. N.; Kakria, R. C.; Olson, S.; Borden, E. C. Radiosensitization of human bronchogenic carcinoma cells by interferon beta. *J Interferon Res* 4:123-128; 1984.

50. Schmidberger, H.; Rave-Fränk, M.; Lehmann, J.; Schweinfurth, S.; Pradier, O.; Hess, C. F. Radiosensitizing effect of natural and recombinant beta-interferons in a human lung carcinoma in vitro. *J Cancer Res Clin Oncol* 125:350-356; 1999.

51. Schmidberger, H.; Rave-Fränk, M.; Lehmann, J.; Schweinfurth, S.; Rehring, E.; Henckel, K. et al. The combined effect of interferon beta and radiation on five human tumor cell lines and embryonal lung fibroblasts. *Int J Radiat Oncol Biol Phys* 43:405-412; 1999.

52. McDonald, S.; Rubin, P.; Chang, A. Y.; Penney, D. P.; Finkelstein, J. N.; Grossberg, S. et al. Pulmonary changes induced by combined mouse beta-interferon (rMuIFN-beta) and irradiation in normal mice--toxic versus protective effects. *Radiother Oncol* 26:212-218; 1993.

53. Mossman, K. L.; Hill, L. T.; Dritschilo, A. Utility of interferons in clinical radiotherapy. *J Natl Med Assoc* 74:1083-1087; 1982.

54. Zhu, Y.; Tibensky, I.; Schmidt, J.; Ryschich, E.; Märten, A. Interferon-alpha enhances antitumor effect of chemotherapy in an orthotopic mouse model for pancreatic adenocarcinoma. *J Immunother* 31:599-606; 2008.

55. Nakamura, O.; Maruo, K.; Ueyama, Y.; Nomura, K.; Takakura, K. Interactions of human fibroblast interferon with chemotherapeutic agents and radiation against human gliomas in nude mice. *Neurol Res* 8:152-156; 1986.

56. Mattson, K.; Holsti, L. R.; Niiranen, A.; Kivisaari, L.; Iivanainen, M.; Sovijärvi, A. et al. Human leukocyte interferon as part of a combined treatment for previously untreated small cell lung cancer. *J Biol Response Mod* 4:8-17; 1985.

57. Holsti, L. R.; Mattson, K.; Niiranen, A.; Standertskiöld-Nordenstam, C. G.; Stenman, S.; Sovijärvi, A. et al. Enhancement of radiation effects by alpha interferon in the treatment of small cell carcinoma of the lung. *Int J Radiat Oncol Biol Phys* 13:1161-1166; 1987.

58. Niiranen, A.; Holsti, L. R.; Cantell, K.; Mattson, K. Natural interferon-alpha alone and in combination with conventional therapies in non-small cell lung cancer. A pilot study. *Acta Oncol* 29:927-930; 1990.

59. Vokes, E. E.; Haraf, D. J.; Hoffman, P. C. Escalating doses of interferon alpha-2A with cisplatin and concomitant radiotherapy: a phase I study. *Cancer Chemother Pharmacol* 33:203-209; 1993.

60. Maasilta, P.; Holsti, L. R.; Halme, M.; Kivisaari, L.; Cantell, K.; Mattson, K. Natural alpha-interferon in combination with hyperfractionated radiotherapy in the treatment of non-small cell lung cancer. *Int J Radiat Oncol Biol Phys* 23:863-868; 1992.

61. Kelly, K.; Crowley, J. J.; Bunn, P. A.; Hazuka, M. B.; Beasley, K.; Upchurch, C. et al. Role of recombinant interferon alfa-2a maintenance in patients with limited-stage small-cell lung cancer responding to concurrent chemoradiation: a Southwest Oncology Group study. *J Clin Oncol* 13:2924-2930; 1995.

62. Shaw, E. G.; Deming, R. L.; Creagan, E. T.; Nair, S.; Su, J. Q.; Levitt, R. et al. Pilot study of human recombinant interferon gamma and accelerated hyperfractionated thoracic radiation therapy in patients with unresectable stage IIIA/B nonsmall cell lung cancer. *Int J Radiat Oncol Biol Phys* 31:827-831; 1995.

63. Jett, J. R.; Maksymiuk, A. W.; Su, J. Q.; Mailliard, J. A.; Krook, J. E.; Tschetter, L. K. et al. Phase III trial of recombinant interferon gamma in complete responders with small-cell lung cancer. *J Clin Oncol* 12:2321-2326; 1994.

64. van Zandwijk, N.; Groen, H. J.; Postmus, P. E.; Burghouts, J. T.; ten Velde, G. P.; Ardizzoni, A. et al. Role of recombinant interferon-gamma maintenance in responding patients with small cell lung cancer. A randomised phase III study of the EORTC Lung Cancer Cooperative Group. *Eur J Cancer* 33:1759-1766; 1997.

65. McDonald, S.; Chang, A. Y.; Rubin, P.; Wallenberg, J.; Kim, I. S.; Sobel, S. et al. Combined Betaseron R (recombinant human interferon beta) and radiation for inoperable non-small cell lung cancer. *Int J Radiat Oncol Biol Phys* 27:613-619; 1993.

66. Byhardt, R. W.; Vaickus, L.; Witt, P. L.; Chang, A. Y.; McAuliffe, T.; Wilson, J. F. et al. Recombinant human interferon-beta (rHuIFN-beta) and radiation therapy for inoperable non-small cell lung cancer. *J Interferon Cytokine Res* 16:891-902; 1996.

67. Bradley, J. D.; Scott, C. B.; Paris, K. J.; Demas, W. F.; Machtay, M.; Komaki, R. et al. A phase III comparison of radiation therapy with or without recombinant beta-interferon for poor-risk patients with locally advanced non-small-cell lung cancer (RTOG 93-04). *Int J Radiat Oncol Biol Phys* 52:1173-1179; 2002.

6

185

68. Mahaley, M. S.; Urso, M. B.; Whaley, R. A.; Williams, T. E.; Guaspari, A. Interferon as adjuvant therapy with initial radiotherapy of patients with anaplastic gliomas. *J Neurosurg* 61:1069-1071; 1984.

69. Dillman, R. O.; Wiemann, M.; Oldham, R. K.; Soori, G.; Bury, M.; Hafer, R. et al. Interferon alpha-2a and external beam radiotherapy in the initial management of patients with glioma: a pilot study of the National Biotherapy Study Group. *Cancer Biother* 10:265-271; 1995.

70. Priestman, T. J.; Bleehen, N. M.; Rampling, R.; Stenning, S.; Nethersell, A. J.; Scott, J. A phase II evaluation of human lymphoblastoid interferon (Wellferon) in relapsed high grade malignant glioma. Medical Research Council Brain Tumour Working Party. *Clin Oncol (R Coll Radiol)* 5:165-168; 1993.

71. Buckner, J. C.; Brown, L. D.; Kugler, J. W.; Cascino, T. L.; Krook, J. E.; Mailliard, J. A. et al. Phase II evaluation of recombinant interferon alpha and BCNU in recurrent glioma. *J Neurosurg* 82:430-435; 1995.

72. Rajkumar, S. V.; Buckner, J. C.; Schomberg, P. J.; Cascino, T. L.; Burch, P. A.; Dinapoli, R. P. Phase I evaluation of radiation combined with recombinant interferon alpha-2a and BCNU for patients with high-grade glioma. *Int J Radiat Oncol Biol Phys* 40:297-302; 1998.

73. Buckner, J. C.; Schomberg, P. J.; McGinnis, W. L.; Cascino, T. L.; Scheithauer, B. W.; O'Fallon, J. R. et al. A phase III study of radiation therapy plus carmustine with or without recombinant interferon-alpha in the treatment of patients with newly diagnosed high-grade glioma. *Cancer* 92:420-433; 2001.

74. Wakabayashi, T.; Yoshida, J.; Mizuno, M.; Kito, A.; Sugita, K. Effectiveness of interferon-beta, ACNU, and radiation therapy in pediatric patients with brainstem glioma. *Neurol Med Chir (Tokyo)* 32:942-946; 1992.

75. Yoshida, J.; Kajita, Y.; Wakabayashi, T.; Sugita, K. Long-term follow-up results of 175 patients with malignant glioma: importance of radical tumour resection and postoperative adjuvant therapy with interferon, ACNU and radiation. *Acta Neurochir (Wien)* 127:55-59; 1994.

76. Packer, R. J.; Prados, M.; Phillips, P.; Nicholson, H. S.; Boyett, J. M.; Goldwein, J. et al. Treatment of children with newly diagnosed brain stem gliomas with intravenous recombinant beta-interferon and hyperfractionated radiation therapy: a childrens cancer group phase I/II study. *Cancer* 77:2150-2156; 1996.

77. Hatano, N.; Wakabayashi, T.; Kajita, Y.; Mizuno, M.; Ohno, T.; Nakayashiki, N. et al. Efficacy of post operative adjuvant therapy with human interferon beta, MCNU and radiation (IMR) for malignant glioma: comparison among three protocols. *Acta Neurochir (Wien)* 142:633-8; discussion 639; 2000.

78. Wakabayashi, T.; Hatano, N.; Kajita, Y.; Yoshida, T.; Mizuno, M.; Taniguchi, K. et al. Initial and maintenance combination treatment with interferon-beta, MCNU (Ranimustine), and radiotherapy for patients with previously untreated malignant glioma. *J Neurooncol* 49:57-62; 2000.

79. Watanabe, T.; Katayama, Y.; Yoshino, A.; Fukaya, C.; Yamamoto, T. Human interferon beta, nimustine hydrochloride, and radiation therapy in the treatment of newly diagnosed malignant astrocytomas. *J Neurooncol* 72:57-62; 2005.

80. Colman, H.; Berkey, B. A.; Maor, M. H.; Groves, M. D.; Schultz, C. J.; Vermeulen, S. et al. Phase II Radiation Therapy Oncology Group trial of conventional radiation therapy followed by treatment with recombinant interferon-beta for supratentorial glioblastoma: results of RTOG 9710. *Int J Radiat Oncol Biol Phys* 66:818-824; 2006.

81. Wakabayashi, T.; Kayama, T.; Nishikawa, R.; Takahashi, H.; Hashimoto, N.; Takahashi, J. et al. A multicenter phase I trial of combination therapy with interferon-β and temozolomide for high-grade gliomas (INTEGRA study): the final report. *J Neurooncol* 104:573-577; 2011.

82. Wakabayashi, T.; Natsume, A.; Mizusawa, J.; Katayama, H.; Fukuda, H.; Sumi, M. et al. JCOG0911 INTEGRA study: a randomized screening phase II trial of interferonβ plus temozolomide in comparison with temozolomide alone for newly diagnosed glioblastoma. *J Neurooncol* 138:627-636; 2018.

83. Perera, F.; Fisher, B.; Kocha, W.; Plewes, E.; Taylor, M.; Vincent, M. A phase I pilot study of pelvic radiation and alpha-2A interferon in patients with locally advanced or recurrent rectal cancer. *Int J Radiat Oncol Biol Phys* 37:297-303; 1997.

84. Valavaara, R.; Kortekangas, A. E.; Nordman, E.; Cantell, K. Interferon combined with irradiation in the treatment of operable head and neck carcinoma. A pilot study. *Acta Oncol* 31:429-431; 1992.

85. Torrisi, J.; Berg, C.; Harter, K.; Lvovsky, E.; Yeung, K.; Woolley, P. et al. Phase I combined modality clinical trial of alpha-2-interferon and radiotherapy. *Int J Radiat Oncol Biol Phys* 12:1453-1456; 1986.

86. Picozzi, V. J.; Abrams, R. A.; Traverso, L. W.; O'Reilly, E. M.; Greeno, E.; Martin, R. C. et al. ACOSOG Z05031: Report on a multicenter, phase II trial for adjuvant therapy of resected pancreatic cancer using cisplatin, 5- FU, and alpha-interferon. *Journal of Clinical Oncology* 26:4505-4505; 2008.

87. Schmidt, J.; Abel, U.; Debus, J.; Harig, S.; Hoffmann, K.; Herrmann, T. et al. Open-label, multicenter, randomized phase III trial of adjuvant chemoradiation plus interferon Alfa-2b versus fluorouracil and folinic acid for patients with resected pancreatic adenocarcinoma. *J Clin Oncol* 30:4077-4083; 2012.

88. Rocha, F. G.; Hashimoto, Y.; Traverso, L. W.; Dorer, R.; Kozarek, R.; Helton, W. S. et al. Interferon-based Adjuvant Chemoradiation for Resected Pancreatic Head Cancer: Long-term Follow-up of the Virginia Mason Protocol. *Ann Surg* 263:376-384; 2016.

89. Linehan, D. C.; Tan, M. C.; Strasberg, S. M.; Drebin, J. A.; Hawkins, W. G.; Picus, J. et al. Adjuvant interferon-based chemoradiation followed by gemcitabine for resected pancreatic adenocarcinoma: a single-institution phase II study. *Ann Surg* 248:145-151; 2008.

90. Katz, M. H.; Wolff, R.; Crane, C. H.; Varadhachary, G.; Javle, M.; Lin, E. et al. Survival and quality of life of patients with resected pancreatic adenocarcinoma treated with adjuvant interferon-based chemoradiation: a phase II trial. *Ann Surg Oncol* 18:3615-3622; 2011.

91. Stock, R. G.; Dottino, P.; Jennings, T. S.; Terk, M.; DeWyngaert, J. K.; Beddoe, A. M. et al. Enhanced radiosensitization with interferon-alpha-2b and cisplatin in the treatment of locally advanced cervical carcinoma. *Gynecol Oncol* 67:309-315; 1997.

92. Verastegui-Aviles, E.; Mohar, A.; Mota, A.; Guadarrama, A.; De La Garza-Salazar, J. Combination of radiation therapy and interferon alpha-2b in patients with advanced cervical carcinoma: a pilot study. *Int J Gynecol Cancer* 9:401-405; 1999.

93. Park, T. K.; Lee, J. P.; Kim, S. N.; Choi, S. M.; Kudelka, A. P.; Kavanagh, J. J. Interferon-alpha 2a, 13-cis-retinoic acid and radiotherapy for locally advanced carcinoma of the cervix: a pilot study. *Eur J Gynaecol Oncol* 19:35-38; 1998.

94. Yazigi, R.; Aliste, G.; Torres, R.; Ciudad, A. M.; Cuevas, M.; Garrido, J. et al. Phase III randomized pilot study comparing interferon alpha-2b in combination with radiation therapy versus radiation therapy alone in patients with stage III-B carcinoma of the cervix. *Int J Gynecol Cancer* 13:164-169; 2003.

95. Basu, P.; Jenson, A. B.; Majhi, T.; Choudhury, P.; Mandal, R.; Banerjee, D. et al. Phase 2 Randomized Controlled Trial of Radiation Therapy Plus Concurrent Interferon-Alpha and Retinoic Acid Versus Cisplatin for Stage III Cervical Carcinoma. *Int J Radiat Oncol Biol Phys* 94:102-110; 2016.

6

96. Hoffmann, W.; Schiebe, M.; Hirnle, P.; Souchon, R.; Clemens, M.; Adamietz, I. et al. 13-cis retinoic acid and interferon-alpha +/- irradiation in the treatment of squamous-cell carcinomas. *Int J Cancer* 70:475-477; 1997.

97. Dunst, J.; Hänsgen, G.; Krause, U.; Füchsel, G.; Köhler, U.; Becker, A. A 2-week pretreatment with 13-cis-retinoic acid + interferon-alpha-2a prior to definitive radiation improves tumor tissue oxygenation in cervical cancers. *Strahlenther Onkol* 174:571-574; 1998.

98. Dunst, J.; Hänsgen, G.; Lautenschläger, C.; Füchsel, G.; Becker, A. Oxygenation of cervical cancers during radiotherapy and radiotherapy + cis-retinoic acid/interferon. *Int J Radiat Oncol Biol Phys* 43:367-373; 1999.

99. Chen, J.; Markelc, B.; Kaeppler, J.; Ogundipe, V. M. L.; Cao, Y.; McKenna, W. G. et al. STING-Dependent Interferon-λ1 Induction in HT29 Cells, a Human Colorectal Cancer Cell Line, After Gamma-Radiation. *Int J Radiat Oncol Biol Phys* 101:97-106; 2018.

100. Lasfar, A.; Abushahba, W.; Balan, M.; Cohen-Solal, K. A. Interferon lambda: a new sword in cancer immunotherapy. *Clin Dev Immunol* 2011:349575; 2011.

101. Stiff, A.; Carson, W. Investigations of interferon-lambda for the treatment of cancer. *J Innate Immun* 7:243-250; 2015.

102. Rodriguez-Ruiz, M. E.; Vitale, I.; Harrington, K. J.; Melero, I.; Galluzzi, L. Immunological impact of cell death signaling driven by radiation on the tumor microenvironment. *Nat Immunol* 2019.

103. Palata, O.; Hradilova Podzimkova, N.; Nedvedova, E.; Umprecht, A.; Sadilkova, L.; Palova Jelinkova, L. et al. Radiotherapy in Combination With Cytokine Treatment. *Front Oncol* 9:367; 2019.

104. Huang, J. L.; LaRocca, C. J.; Yamamoto, M. Showing the Way: Oncolytic Adenoviruses as Chaperones of Immunostimulatory Adjuncts. *Biomedicines* 42016.

105. Salzwedel, A. O.; Han, J.; LaRocca, C. J.; Shanley, R.; Yamamoto, M.; Davydova, J. Combination of interferon-expressing oncolytic adenovirus with chemotherapy and radiation is highly synergistic in hamster model of pancreatic cancer. *Oncotarget* 9:18041-18052; 2018.

106. Neri, D.; Sondel, P. M. Immunocytokines for cancer treatment: past, present and future. *Curr Opin Immunol* 40:96-102; 2016.

107. Hemmerle, T.; Neri, D. The dose-dependent tumor targeting of antibody-IFNγ fusion proteins reveals an unexpected receptor-trapping mechanism in vivo. *Cancer Immunol Res* 2:559-567; 2014.

108. Vermaelen, K. Vaccine Strategies to Improve Anti-cancer Cellular Immune Responses. *Front Immunol* 10:8; 2019.

109. Hawkins, M. J.; Krown, S. E.; Borden, E. C.; Krim, M.; Real, F. X.; Edwards, B. S. et al. American cancer society Phase I trial of naturally produced beta-interferon. *Cancer Res* 44:5934-5938; 1984.

110. Goldstein, D.; Sielaff, K. M.; Storer, B. E.; Brown, R. R.; Datta, S. P.; Witt, P. L. et al. Human biologic response modification by interferon in the absence of measurable serum concentrations: a comparative trial of subcutaneous and intravenous interferon-beta serine. *J Natl Cancer Inst* 81:1061-1068; 1989.

111. Khodarev, N. N.; Beckett, M.; Labay, E.; Darga, T.; Roizman, B.; Weichselbaum, R. R. STAT1 is overexpressed in tumors selected for radioresistance and confers protection from radiation in transduced sensitive cells. *Proc Natl Acad Sci U S A* 101:1714-1719; 2004.

112. Kita, K.; Sugaya, S.; Zhai, L.; Wu, Y. P.; Wano, C.; Chigira, S. et al. Involvement of LEU13 in interferon-induced refractoriness of human RSa cells to cell killing by X rays. *Radiat Res* 160:302-308; 2003.

113. Sirota, N. P.; Bezlepkin, V. G.; Kuznetsova, E. A.; Lomayeva, M. G.; Milonova, I. N.; Ravin, V. K. et al. Modifying effect in vivo of interferon alpha on induction and repair of lesions of DNA of lymphoid cells of gamma-irradiated mice. *Radiat Res* 146:100-105; 1996.

114. Benci, J. L.; Xu, B.; Qiu, Y.; Wu, T. J.; Dada, H.; Twyman-Saint Victor, C. et al. Tumor Interferon Signaling Regulates a Multigenic Resistance Program to Immune Checkpoint Blockade. *Cell* 167:1540-1554.e12; 2016.

115. Demaria, S.; Coleman, C. N.; Formenti, S. C. Radiotherapy: Changing the Game in Immunotherapy. *Trends Cancer* 2:286-294; 2016.

116. Kleibeuker, E. A.; Fokas, E.; Allen, P. D.; Kersemans, V.; Griffioen, A. W.; Beech, J. et al. Low dose angiostatic treatment counteracts radiotherapy-induced tumor perfusion and enhances the anti-tumor effect. *Oncotarget* 7:76613-76627; 2016.

117. Kleibeuker, E. A.; Ten Hooven, M. A.; Castricum, K. C.; Honeywell, R.; Griffioen, A. W.; Verheul, H. M. et al. Optimal treatment scheduling of ionizing radiation and sunitinib improves the antitumor activity and allows dose reduction. *Cancer Med* 4:1003-1015; 2015.

118. Lugade, A. A.; Moran, J. P.; Gerber, S. A.; Rose, R. C.; Frelinger, J. G.; Lord, E. M. Local radiation therapy of B16 melanoma tumors increases the generation of tumor antigen-specific effector cells that traffic to the tumor. *J Immunol* 174:7516-7523; 2005.

119. Dou, Z.; Ghosh, K.; Vizioli, M. G.; Zhu, J.; Sen, P.; Wangensteen, K. J. et al. Cytoplasmic chromatin triggers inflammation in senescence and cancer. *Nature* 550:402-406; 2017.

120. Harding, S. M.; Benci, J. L.; Irianto, J.; Discher, D. E.; Minn, A. J.; Greenberg, R. A. Mitotic progression following DNA damage enables pattern recognition within micronuclei. *Nature* 548:466-470; 2017.

121. Härtlova, A.; Erttmann, S. F.; Raffi, F. A.; Schmalz, A. M.; Resch, U.; Anugula, S. et al. DNA damage primes the type I interferon system via the cytosolic DNA sensor STING to promote anti-microbial innate immunity. *Immunity* 42:332-343; 2015.

122. Wilkins, A. C.; Patin, E. C.; Harrington, K. J.; Melcher, A. A. The immunological consequences of radiation-induced DNA damage. *J Pathol* 247:606-614; 2019.

123. Shevtsov, M.; Sato, H.; Multhoff, G.; Shibata, A. Novel Approaches to Improve the Efficacy of Immuno-Radiotherapy. *Front Oncol* 9:156; 2019.

124. Mattson, K. Interferon gamma and thoracic irradiation in the treatment of unresectable stage IIIA/B non-small cell lung cancer. *Int J Radiat Oncol Biol Phys* 32:271-272; 1995.

125. Kardamakis, D.; Gillies, N. E.; Souhami, R. L.; Bewerley, P. C. Recombinant human interferon alpha-2b enhances the radiosensitivity of small cell lung cancer in vitro. *Anticancer Res* 9:1041-1044; 1989.

126. Gyorki, D. E.; Ainslie, J.; Joon, M. L.; Henderson, M. A.; Millward, M.; McArthur, G. A. Concurrent adjuvant radiotherapy and interferon-alpha2b for resected high risk stage III melanoma -- a retrospective single centre study. *Melanoma Res* 14:223-230; 2004.

127. Picozzi, V. J.; Kozarek, R. A.; Traverso, L. W. Interferon-based adjuvant chemoradiation therapy after pancreaticoduodenectomy for pancreatic adenocarcinoma. *Am J Surg* 185:476-480; 2003.

6

Table S1. Clinical trials

Phase	IFN type	Tumor type	IFN (dose, schedule, duration)	Route	Scheduling*	RTx (total dose, daily, schedule)	Additional treatment	Ref
I	IFN-α	Brain	10-30 MIU/m2, 3 dpw, 3 wks	IV	Before	43 Gy (+17.2 Gy boost) in 7 wks	-	68
I	IFN-α2a	Brain	12 MIU/m2, 3 dpw, weekly or biweekly, 7 wks	SC	After	64.8 Gy, 1.8 Gy/d, 5 dpw	Carmustine	72
I/II	IFN-α2b	Brain	3 MIU, 3 dpw, 2 wks + 5 MIU, 3 dpw, 14 wks	SC	During, after	59.4 Gy, 1.8 Gy/d, 5dpw	-	69
III	IFN-α	Brain	12 MIU/m2, day 1-3, wk 1, 3, 5, 7. Total 6 cycles	SC	After	64.8 Gy, 1.8 Gy/d, 5 dpw	Carmustine	73
II	IFN-α2b	Cervix	5 MIU/m2, 3 dpw	NS	During, after	50 Gy (+boost), variable dose and schedule	-	92
I/II	IFN-α2b	Cervix	5 MIU, 3 dpw	SC	During	45 Gy (+ brachy), 1.8 Gy/d, 5dpw	Cisplatin	91
II	IFN-α2b	Cervix	3 MIU, 3 dpw	SC	During	50 Gy, 2 Gy/d, 5 dpw	Retinoic acid	95
I/II	IFN-α2a	Cervix	6 MIU/d, 3 days + 3 MIU/d, 81 days	SC	During	unknown	Retinoic acid	93
III	IFN-α2b	Cervix	3 MIU/m2, 5 dpw	SC	During	50.4 Gy (+boost), 1.8 Gy/d, 5dpw	-	94
III	IFN-α	HNSCC	6 MIU/d, 4 wks + 6 MIU 3 dpw, 2 months	IM	During, after	30-32 Gy, 2 Gy/d, 5dpw	-	84
II	IFN-α	Lung (NSCLC)	6 MIU, 5 dpw, 12 weeks	IM	Before, during and after	55 Gy, 2x 1.25 Gy/d, 5dpw	Cisplatinum, Vindesine	58
I/II	IFN-α	Lung (SCLC)	800 MIU, 5d + 6 MIU, 3 dpw	IV/IM	Before, during and after	55-30 Gy (20 fractions in 7 wks) + whole brain	-	56

SUPPLEMENTARY MATERIAL

Table S1. Clinical trials (continued)

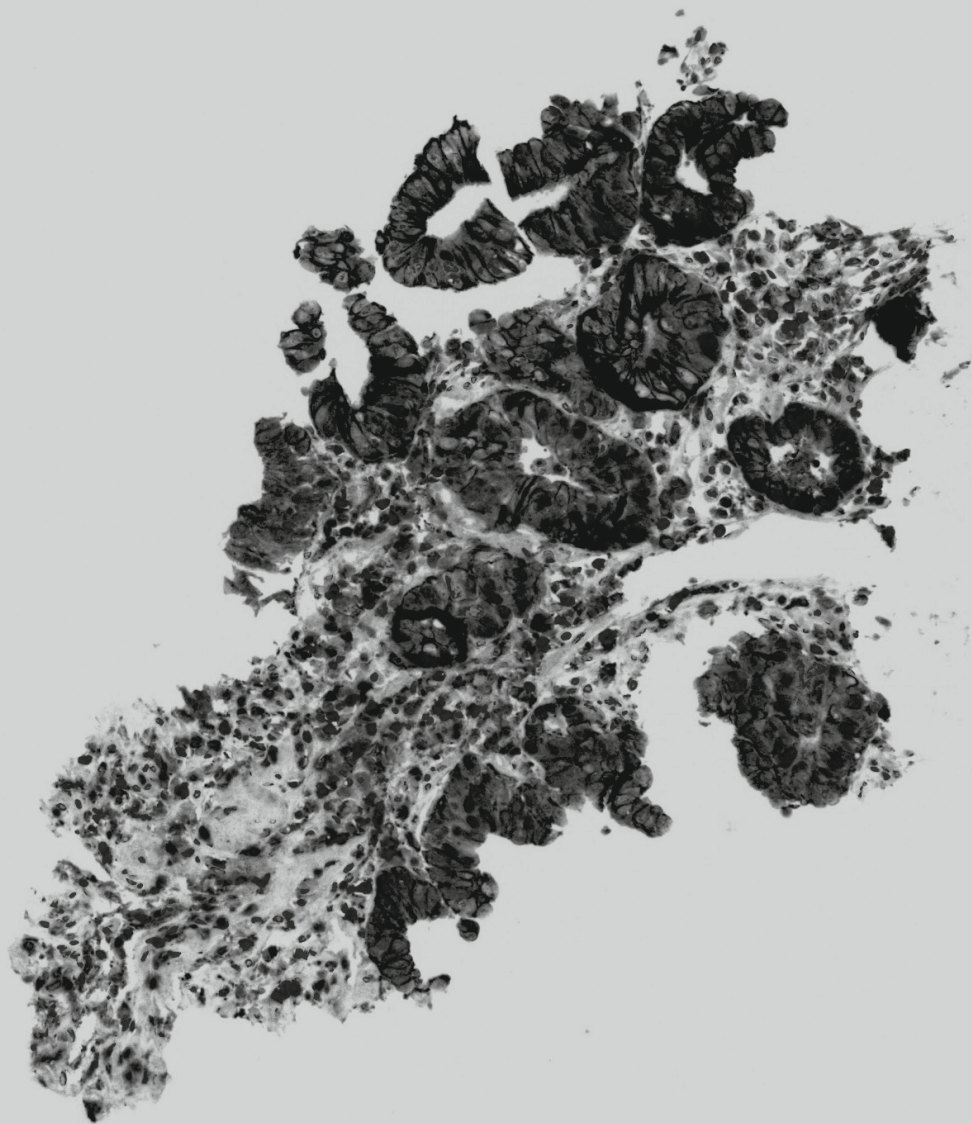| Phase	IFN type	Tumor type	IFN (dose, schedule, duration)	Route	Scheduling*	RTx (total dose, daily, schedule)	Additional treatment	Ref
I/II	IFN-α	Lung (SCLC)	800 MIU, 5d + 6 MIU, 3 dpw or 6 MIU, 3 dpw	IV/IM	Before, during and after	55 Gy (20 fractions in 7 wks) or 44 Gy (40 fractions 4 wks)	-	[57]
I/II	IFN-α	Lung (SCLC)	3 MIU i.m. and 1.5 MIU inh, 5dpw	IM/INH	During	60 Gy, 2x 1.25 Gy/d, 5 dpw	-	[60]
R etrosp.	IFN-α2b	Melanoma	20 MIU/d, 5 dpw, 4 wks + 10 MIU, 3 dpw, 48 wks	IV/SC	Before, during	40-50 Gy in 15 - 25 fractions	-	[126]
I/II	IFN-α	Multiple	3 MIU, 3 dpw	SC	During, after	50-70 Gy, 1.8-2.0 daily	Retinoic acid	[96]
I	IFN-α2a	Multiple	0.5-5 MIU/d, 5 dpw	SC	During	2x 1.25 Gy/d, 5 dpw	Cisplatin	[59]
I	IFN-α	Multiple	2-30 MIU, 3 dpw or 5 dpw	SC	During	unknown	-	[85]
II	IFN-α	Pancreas	3 MIU, 3 dpw, 5 wks	SC	During	45 - 54 Gy in 25 fractions, 5dpw	5-FU, cisplatin	[127]
II	IFN-α	Pancreas	3 MIU, 3 dpw, 6 wks	SC	During	54 Gy, 1.8 Gy/d, 5 dpw + boost 5.4Gy	5-FU, cisplatin	[89]
II	IFN-α2b	Pancreas	3 MIU, 3 dpw, 5.5 wks	SC	During	50.4 Gy, 1.8 Gy/d, 5 dpw	5-FU, cisplatin	[90]
III	IFN-α2b	Pancreas	3 MIU, 3 dpw, 5.5 wks	SC	During	50.4 Gy, 1.8 Gy/d, 5 dpw	5-FU, cisplatin	[87]
II	IFN-α	Pancreas	3 MIU, 3 dpw, 5.5 wks	SC	During	50.4 Gy, 1.8 Gy/d, 5 dpw	5-FU, cisplatin	[86]
I	IFN-α2a	Rectum	3-9 MIU, 3 dpw	SC	During	44 Gy, 2 Gy/d, 5 dpw	-	[83]
I	IFN-β	Brain	3 MIU/m2, once every day + 3 MIU/m2, 4 wks, 6 cycles	IV	During, after	60 Gy, 2.0 Gy/d, 5 dpw	TMZ	[81]

6

Table S1. Clinical trials (continued)

Phase	IFN type	Tumor type	IFN (dose, schedule, duration)	Route	Scheduling*	RTx (total dose, daily, schedule)	Additional treatment	Ref
II	IFN-β	Brain	2 MIU/m2, 5dpw, 8 wks + 2 MIU/m2, biweekly, 2 yrs	IV	During, after	50-60 Gy, 2.0 Gy/d, 5 dpw	Nimustine	79
II	IFN-β	Brain	1 MIU/d, 7 days, 4 wk cycle + 1 MIU biweekly, 3 months	IV	During, after	60 Gy, 2.0 Gy/d, 5 dpw	Ranimustine	78
II	IFN-β	Brain	1-3 MIU/d, 7 days, 6 wk cycles	IV	During	40-60 Gy, variable dose, 5dpw	Nimustine	75
I/II	IFN-β	Brain	1x or 2x 1 MIU/d, 7 days	IV	During, after	60 Gy, 2.0 Gy/d, 5 dpw or 66 Gy, 2x 1.5 Gy/d, 5 dpw	Ranimustine	77
II	IFN-β	Brain	3 MIU, 3 dpw, maintenance 1 dpw, 4 wks	IV	During, after	60 Gy, 2.0 Gy/d, 5 dpw	TMZ	82
II	IFN-β	Brain	6 MIU, 3 dpw, 3 wks, 1 wk rest	IM	After	60 Gy, 2.0 Gy/d, 5 dpw	-	80
II	IFN-β	Brain, pediatric	1-1.5 MIU/d, 7days, 6 wk cycle	IV	During	40-60 Gy, 1.8-2.0 Gy/d, 5 dpw	Nimustine	74
II	IFN-β	Brain, pediatric	12.5-400 MIU/m2, 3 dpw	IV	During, after	72 Gy, 2x 1 Gy/d, 5 dpw	-	76
I	IFN-β	Lung (NSCLC)	1.5-24 MIU/m2, 5 dpw, 6 wks	SC	During	60 Gy, 2 Gy/d, 5 dpw	-	66
I/II	IFN-β	Lung (NSCLC)	10-90 MIU/d, 3 days on wk 1,3 and 5	IV	During	54-59.4 Gy, 1.8 Gy/d, 5dpw	-	65
III	IFN-β	Lung (NSCLC)	16 MIU/d, 3 days on wk 1,3 and 5	IV	During	60 Gy, 2.0 Gy/d, 5 dpw	-	67

*Scheduling relative to radiotherapy treatment. IFN: interferon, RTx: radiotherapy, Retrosp: retrospective study, MIU: million units, dpw: days per week, IV: intravenous, SC: subcutaneous, IM: intramuscular, INH: inhalation, Gy: Gray, TMZ: temozolomide, 5-FU: 5-fluoro-uracil

6

Chapter 7

A phase I open-label clinical trial evaluating the therapeutic vaccine hVEGF$_{26\text{-}104}$/RFASE in patients with advanced solid malignancies

Ruben S.A. Goedegebuure, Madelon Q. Wentink, Johannes J. van der Vliet, Peter Timmerman, Arjan W. Griffioen PhD, Tanja D. de Gruijl, Henk M.W. Verheul

ABSTRACT

Background
Targeting Vascular Endothelial Growth Factor A (VEGF) is a well-established anticancer therapy. We designed a first-in-human clinical trial to investigate safety and immunogenicity of the novel vaccine $hVEGF_{26-104}$/RFASE.

Methods
Patients with advanced solid malignancies with no standard treatment options available were eligible for this phase-I study with a 3+3 dose-escalation design. On days 0, 14 and 28, patients received intramuscular $hVEGF_{26-104}$, a truncated synthetic 3D-structured peptide mimic covering the amino acids 26-104 of human $VEGF_{165}$, emulsified in the novel adjuvant Raffinose Fatty Acid Sulphate Ester (RFASE), a sulpholipopolysaccharide. Objectives were to determine safety, induction of VEGF-neutralizing antibodies and the maximum tolerated dose. Blood was sampled to measure VEGF levels and antibody titers.

Results
Eighteen out of 27 enrolled patients received three immunizations in six different dose-levels up to 1000μg $hVEGF_{26-104}$ and 40mg RFASE. No dose limiting toxicity was observed. Although in four patients an antibody titer against $VEGF_{26-104}$ was induced (highest titer: 2.77 ^{10}log), neither a reduction in VEGF levels, nor neutralizing antibodies against native $hVEGF_{165}$ were detected.

Conclusion
Despite having an attractive safety profile, $hVEGF_{26-104}$/RFASE was not able to elicit seroconversions against native $VEGF_{165}$ and consequently, did not decrease circulating VEGF levels. Deficient RFASE adjuvant activity, as well as dominant immunoreactivity towards neo-epitopes, may have impeded $hVEGF_{26-104}$/RFASE's efficacy in man.

LESSONS LEARNED

- The novel therapeutic vaccine $hVEGF_{26-104}$/RFASE was found to be safe and well tolerated in cancer patients.
- $hVEGF_{26-104}$/RFASE failed to induce seroconversion against native $VEGF_{165}$ and accordingly, neither a decrease in circulating VEGF levels, nor clinical benefit was observed.
- Remarkably, $hVEGF_{26-104}$/RFASE induced $VEGF_{165}$-neutralizing antibodies in a nonhuman primate model. The absence of seroconversion in man calls for caution in the interpretation of efficacy of human vaccines in nonhuman primates.

1. BACKGROUND

Vascular Endothelial Growth Factor-A (VEGF) is an angiogenic growth factor involved in normal physiology (such as embryogenesis) and disease (such as cancer)[1]. VEGF is produced by several cell types in the human body, including cancer cells and megakaryocytes[2]. Four isoforms are detected in the human body, of which $VEGF_{165}$ and $VEGF_{121}$ circulate and are detectable by the VEGF-ELISA as used. VEGF in serum is largely derived from platelets, which secrete VEGF upon wounding and in the tumor vasculature to stimulate angiogenesis, i.e. the growth of new blood vessels from pre-existing capillaries[3]. Upon treatment with the anti-VEGF monoclonal antibody bevacizumab, VEGF is neutralized and no longer exerts biological activity[4].

Anti-angiogenic therapy is mostly combined with cytotoxic agents, although there is mounting interest to combine it with other forms of anti-cancer treatment, such as immunotherapy and radiotherapy[5–7]. Nonetheless, the clinical benefit observed from anti-angiogenic therapy is usually modest and treatment withdrawal has been associated with rebound growth, possibly due to compensatory pathways activated by other pro-angiogenic factors and cytokines[8,9]. Therefore, neutralization of VEGF by active immunization could be an attractive alternative[10]. VEGF inhibition might not only be more durable, but also more pronounced due to the induction of a polyclonal antibody response, resulting in higher avidity binding. Furthermore, tumor-associated plasma cells might ensure that endogenous antibodies have a better tumor-penetrating capacity, as compared to exogenously administered antibodies[11]. In addition, continued VEGF suppression beyond progressive disease might convey a survival benefit, as demonstrated in metastatic colorectal cancer[12,13]. Finally, active immunization could lead to a notable reduction in hospital visits and treatment costs, as compared to monoclonal antibody therapy.

$hVEGF_{26-104}$ is a 3D-structured truncated peptide antigen derived of the endogenous protein $VEGF_{165}$ that perfectly mimics the 3D structure of the cysteine knot motif of $VEGF_{165}$. Immunization with $hVEGF_{26-104}$ is thus expected to result in antibodies that can cross-react with and neutralize $VEGF_{165}$. Biological activity of the (monomeric) peptide $hVEGF_{26-104}$ itself is prohibited by the substitution of two cysteines – vital for the formation of the $VEGF_{165}$ homodimer and consequent receptor binding capacities – for alanines. $hVEGF_{26-104}$ is mixed 1:1 with RFASE adjuvant, a sulpholipopolysaccharide in a squalane-in-water emulsion with polysorbate 80 as emulsifier[14,15]. Immunization of nonhuman primates with $hVEGF_{26-104}$/RFASE resulted in an RFASE dependent antibody titer against $hVEGF_{26-104}$ and cross-reactive antibodies against $VEGF_{165}$ 28 days after primer immunization[16]. Anti-$VEGF_{165}$ antibodies were able to inhibit the binding of bevacizumab with $VEGF_{165}$ in a competition ELISA. Moreover, the biological activity of $VEGF_{165}$ could be inhibited by the addition of immunized monkey serum in a VEGF specific bioassay[17]. Here, we describe the results of a phase-I trial of the novel therapeutic vaccine $hVEGF_{26-104}$/RFASE[16,18] in patients with advanced solid malignancies.

2. METHODS

2.1 Trial design

Patients with advanced solid malignancies with no standard treatment options available were eligible for this phase I study with a 3+3 dose-escalation design. Patients were enrolled in six different dose-levels (**Table S6**). The study medication consisted of 1.0 mL hVEGF26-104 (in escalating doses of 62.5 µg, 125 µg, 250 µg, 500 µg, 1000 µg, 2000 µg and 4000 µg) combined with 1.0 mL RFASE (20 mg in dose-levels 1, 2 and 3A and 40mg in dose-levels 3B, 4 and 5). The total volume that was administered was therefore 2.0 mL. Injections were administered in a split-dose contra-lateral fashion, in either the left and right deltoid- or gluteal muscles. The starting dose of 62.5 µg $hVEGF_{26-104}$ equaled ⅛ of the maximal dose given in animals. The starting dose of 20 mg RFASE equaled ½ of the maximal dose given in animals. On days 0, 14 and 28, patients received $hVEGF_{26-104}$/RFASE intramuscularly, followed by an observation period of six weeks. To assess potential toxicity of RFASE, three patients enrolled in the first cohort of the study received 1.0 mL RFASE (20 mg) as a single agent 14 days prior to the first immunization with $hVEGF_{26-104}$/RFASE. Another booster injection could be administered to patients showing response or stable disease on imaging without (prior) VEGF neutralization in serum at first evaluation (10 weeks).

2.2 Study endpoints

The co-primary outcome measures of this study were the safety and tolerability profile of $hVEGF_{26-104}$/RFASE and the effective dose of $hVEGF_{26-104}$/RFASE required to neutralize VEGF in serum. Secondary outcome measures were the anti-$VEGF_{165}$ and anti-$VEGF_{26-104}$ antibody titers induced by $hVEGF_{26-104}$/RFASE immunization and clinical benefit, defined by at least no signs of progression at first evaluation.

2.3 Safety profile

Toxicity was graded by the NCI Common Terminology Criteria for Adverse Events (CTCAE) version 4.0 and recorded using electronic case record forms (eCRFs). Serious adverse events (SAE) were reported to the Dutch Central Committee on Research Involving Human Subjects (CCMO) through the web portal "ToetsingOnline". Dose-limiting toxicity (DLT) was defined as any one of the following toxicities considered by the investigator to be related to $hVEGF_{26-104}$/RFASE and occurring during the DLT assessment window (day 0 of week 0 – day 7 of week 9): any grade ≥ 3 hematological toxicity or any grade ≥ 3 non-hematological toxicity that was not attributable to disease progression or another clearly identifiable cause, excluding grade 3 diarrhea that responded to standard-of-care therapy, grade 3 nausea or vomiting, in the absence of premedication, that responded to standard-of-care therapy or grade 3 infusion reaction, in the absence of premedication that responded to standard-of-care therapy. Patients were observed for DLTs for a minimum of 42 days after their last dose of $hVEGF_{26-104}$/RFASE before any patient in the next higher dose cohort received treatment, except in

198

cases in which there was no VEGF neutralization observed 14 days after the third and last dose of hVEGF26-104/RFASE.

2.4 VEGF serum levels

VEGF protein concentration was measured in serum, frozen at the day the material was received and stored at −80°C until analysis, using a commercially available human ELISA kit (Quantikine, R&D Systems, Abingdon, UK) according to manufacturer's instructions. Absorbance was measured using a BioTek Synergy HT plate reader with an optical density (OD) of 450 nm. VEGF levels were measured every 2 weeks in the DLT period and VEGF neutralization was defined as a VEGF level below 9 pg/mL.

2.5 VEGF serological responses

Anti-hVEGF antibody titers were measured in serum, frozen the day the material was received and stored at −80°C until analysis, using an in-house developed ELISA. Microplates were coated with 100 μL recombinant $hVEGF_{165}$ (1 μg/mL; Biolegend, San Diego, USA). After washing, the plates were blocked with 200 μL 4% horse serum (SIGMA-ALDRICH, St. Louis, MO). Hereafter, the plates were incubated with 100 μL 1:30 diluted serum. HRP conjugated rabbit anti-human IgG antibodies (1:8000 dilution; Sigma, St. Louis, USA) were applied to detect bound antibodies in the microplate wells. In the presence of chromogenic substrate TMB (R&D Systems, Abingdon, UK) color was developed by the enzymatic reaction of HRP. Absorbance was measured using a BioTek Synergy HT plate reader at an optical density (OD) of 450 nm. If the OD was above a pre-determined cut-off (mean + 3 standard deviations of all patient serum baseline OD levels) a relevant antibody response was suspected and a dilution series was performed. The antibody titer was defined as the [10]logarithm of the highest dilution which resulted in a signal above the pre-determined cut-off. A similar ELISA was performed on all samples to measure antibodies recognizing $hVEGF_{26-104}$.

2.6 Tumor response assessment

Tumor response was assessed according to RECIST 1.1 at baseline, ten weeks after start of treatment and every eight weeks during the follow-up period in case of response and/or a repeated booster administration.

2.7 Cytokine release assay

Peripheral blood mononuclear cells (PBMCs) from healthy donors were isolated by standard Ficoll-Hypaque density centrifugation. Cells were cultured for 24 hours (1×10^6 cells/mL per well) with LPS (1μg/mL) or RFASE (1μg/mL) (without squalene-in-water component, originally tested in a range from 0.5 to 5μg/mL) in culture medium (Iscove's Modified Dulbecco's Media, 10% Fetal Calf Serum, pen/strep). Dimethyl sulfoxide (DMSO) 0.1% served as negative control. A cytokine release assay for IL-1beta, IL-6, IL-10, IL-8 and TNF-alpha (CBA Human Inflammatory Cytokines Kit, Becton Dickinson, CA, USA) was performed following the manufacturer's instructions with cell culture

7

supernatants collected after 24 hours and temporarily stored at -20°. Data acquisition was performed on a FACS-Calibur flow cytometer (Becton Dickinson, CA, USA). Quantity (pg/mL) of the respective cytokines was calculated using FCAP array software (Soft Flow Hungary Ltd.).

2.8 Statistical analysis

Statistical analyses were performed using IBM SPSS Statistics for Windows (Version 25.0. Armonk, NY: IBM Corp.). Kaplan-Meier analysis was performed to determine overall survival and progression free survival. Means of cytokine release assays were compared with a student t-test. Median CRP and WBC levels were compared using a Wilcoxon matched-pairs signed rank test. A p-value of <0.05 was considered statistical significant.

3. RESULTS

In the current phase I clinical trial, 18 out of 27 enrolled patients received all three immunizations and completed the DLT observation period; reasons for not completing treatment are listed in **Supplementary Table S5**. Baseline characteristics of 27 enrolled patients are presented in **Supplementary Table S1**. Dose-limiting toxicities, including related grade≥3 adverse events (AEs), were not observed (**Supplementary Table S2 and S3**); none of the AEs could be associated with VEGF inhibition. In 44% of all administrations a grade 1 local reaction was observed, mostly warmth,
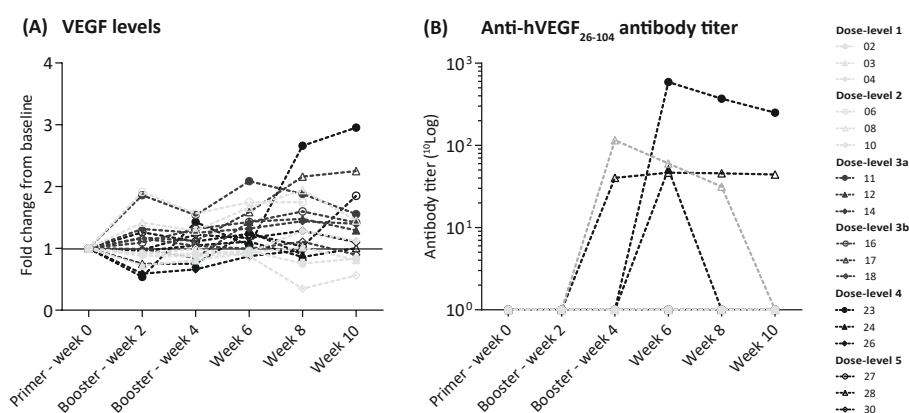

Figure 1. VEGF levels and anti-VEGF$_{26-104}$ antibody titers, shown per patient, per dose-level. VEGF levels in serum are shown relative to baseline in (**A**). Antibody titers measured in serum are shown for hVEGF$_{26-104}$ in (**B**). Titers are in ^{10}log scale: 2.06 for patient 08, 2.77 for patient 23, 1.71 for patient 24 and 1.67 for patient 28, respectively.

pain and swelling (**Supplementary Table S4**). No significant reduction in serum VEGF levels was found (**Figure 1A**). Interestingly, in four patients an antibody titer against hVEGF$_{26-104}$ was measured (highest titer: 2.77 ^{10}log), peaking four to six weeks after the first immunization (**Figure 1B**). Nevertheless, cross-reactive antibodies against native VEGF$_{165}$ were not detected. Comparison of median difference in C-reactive protein (CRP) and White Blood Cell (WBC) count before and after vaccination suggests a possible, but very weak, innate immune response (**Figure 2**). In four patients a body temperature of 38.5°C or higher was observed (Fig 2); in only one of these patients an antibody titer against hVEGF$_{26-104}$ was detected. However, a correlation between dosage and these parameters was not observed.

At a first evaluation by CT-scan, stable disease (SD) was observed in five patients. Nevertheless, four of these patients had clinical progression (PD) and went off-study. One patient in the first dose-level received an additional booster vaccine after 10 weeks (optional for patients with SD and no signs of VEGF suppression); she progressed at evaluation 10 weeks later. In total, 13 patients showed progressive disease (PD). Four patients succumbed before first evaluation; three due to malignant disease and one because of pneumonia. Finally, four patients were not assessable. Median overall survival (OS) was 157 days (95%CI: 117-197) and median progression free survival (PFS) was 70 days (95%CI: 69-71) (**Supplementary Table S5**).
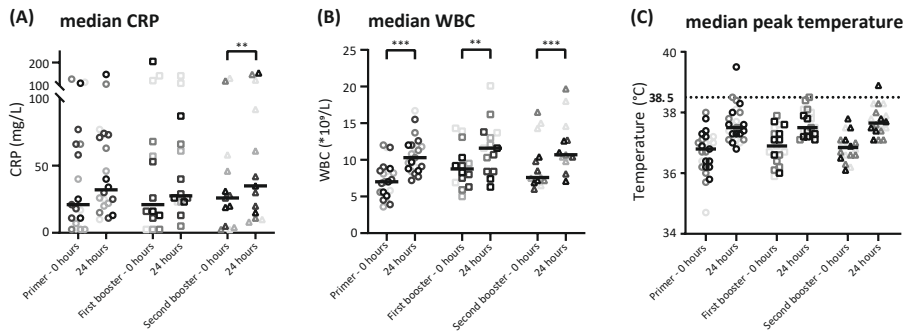
Figure 2. Median rise in CRP **(A)** and WBC **(B)** 24 hours after vaccination as compared to baseline was 7.91 mg/l (95%CI: 0.78 − 11.55, p = 0.030) and 2.87*10^9/l (95%CI: 2.30 − 3.83, p < 0.001), respectively. Median peak body temperature within 24 hours after vaccination **(C)** was 0.90°C (95%CI: 0.67 − 1.22), 0.50°C (95%CI: 0.32 − 1.07) and 0.95°C (95%CI: 0.52 − 1.28) higher as compared to baseline, for primer, first- and second booster, respectively. In four cases a body temperature of 38.5°C or higher was observed.

7

201

4. DISCUSSION

Despite the encouraging results in nonhuman primates, hVEGF$_{26\text{-}104}$/RFASE did not elicit the formation of VEGF$_{165}$-cross-reactive antibodies in patients with cancer. The lack of seroconversion against native VEGF calls for caution in the interpretation of human vaccine efficacies in nonhuman primates. There might be several explanations for the apparent poor antigenicity of hVEGF$_{26\text{-}104}$/RFASE in man. First, the capped N- and C-terminal sequence of VEGF$_{165}$ and the dimerization-domain (in which two cysteines were replaced by alanines) that became solvent-exposed in the monomeric hVEGF$_{26\text{-}104}$, represent potential neo-epitopes. These epitopes could conceivably elicit dominant immunoreactivity and thereby interfere with reactivity to native VEGF. The fact that cross-reactivity to native VEGF was observed in cynomolgus monkeys[16] may be related to inter-species B- or T-cell receptor repertoire differences. Second, lower VEGF levels in nonhuman primates might make them more susceptible to breaking self-tolerance. The hVEGF$_{26\text{-}104}$ dose in man might still have been below the threshold for breaking immune tolerance, since antigen-dosing in vaccination strategies is generally not linearly correlated with the desired immune response, but rather has an "on-off' effect. Finally, RFASE adjuvant might not have been sufficiently potent to induce an immune response against a self-antigen like VEGF, especially in the context of cancer-related immunosuppression.

In order to break immunosuppression and self-tolerance a powerful adjuvant is a key component of any cancer vaccine. Most cancer peptide vaccines have relied on adjuvants such as Incomplete Freund's Adjuvant (IFA) or Montanide ISA-51, both water-in-oil emulsions with the antigen forming a depot for slow release purpose. RFASE is an oil-in-water emulsion designed to function as an antigen depot and to induce local inflammation and activation of Toll Like Receptor 4 (TLR4) signaling. Interestingly, evidence is emerging that Toll Like Receptor ligands, such as CpG oligonucleotides (TLR9 agonist)[19] and Poly I:C (polyinosinic:polycytidylic acid; TLR3 agonist)[20] used as vaccine adjuvants, show more effective immune responses after peptide vaccination as compared to IFA or Montanide ISA-51[21–23]. In our *in vitro* models, stimulation of healthy control human Peripheral Blood Mononuclear Cells (PBMCs) with Lipopolysaccharide (LPS) showed a significant increase in (inflammatory) cytokine release, whereas stimulation with RFASE failed to induce any detectable cytokine release over background levels (**Figure 3**). This is a clear indication that RFASE, which is related to LPS, does not have the capacity for induction of an immune response in man. However, adjuvant substitution would not only require altering the drug composition, but also additional preclinical testing for drug-combination safety, as well as conducting a new phase-I trial. In view of these considerable hurdles it was decided to terminate further development and testing of the vaccine at this point.

Notwithstanding promising activity in nonhuman primate studies, hVEGF$_{26-104}$/RFASE did not elicit cross-reactive neutralizing antibodies against native VEGF and did not show any hint of clinical activity in patients with advanced solid malignancies. We propose that in future studies addition or substitution of RFASE by an alternative adjuvant with proven efficacy should be considered in order to break self-tolerance, induce cross-reactive antibodies against VEGF$_{165}$ and consequently, decrease VEGF serum levels.
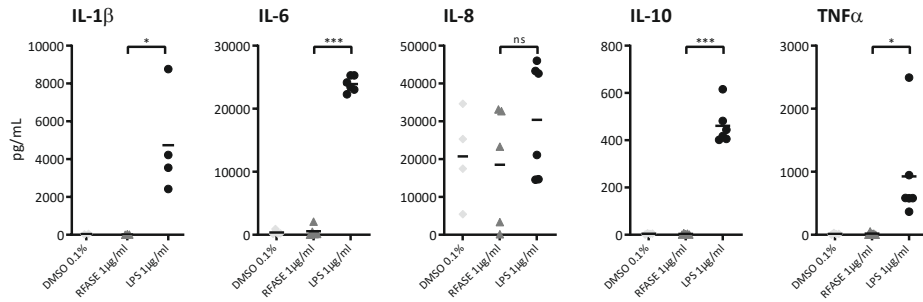

Figure 3. Cytokine levels of Interleukin 1-beta (IL-1β), Interleukin-6 (IL-6), Interleukin-8 (IL-8), Interleukin-10 (IL-10) and Tumor Necrosis Factor-alpha (TNFα) in human Peripheral Blood Mono-nuclear Cell (PBMC) supernatants of healthy controls are shown after incubation for 24 hours with either RFASE (1 μg/mL) or LPS (1 μg/mL). DMSO 0.1% served as negative control.

7

REFERENCES

1   Griffioen AW, Molema G. Angiogenesis: potentials for pharmacologic intervention in the treatment of cancer, cardiovascular diseases, and chronic inflammation. Pharmacol Rev 2000;52:237–68.

2   Möhle R, Green D, Moore MA et al. Constitutive production and thrombin-induced release of vascular endothelial growth factor by human megakaryocytes and platelets. Proc Natl Acad Sci U S A 1997;94:663–668.

3   Verheul HM, Hoekman K, Luykx-de Bakker S et al. Platelet: transporter of vascular endothelial growth factor. Clin Cancer Res 1997;3:2187–2190.

4   Verheul HMW, Lolkema MPJ, Qian DZ et al. Platelets take up the monoclonal antibody bevacizumab. Clin cancer Res an Off J Am Assoc Cancer Res 2007;13:5341–5347.

5   Goedegebuure RSA, De Klerk LK, Bass AJ et al. Combining radiotherapy with anti-angiogenic therapy and immunotherapy; A therapeutic triad for cancer? Front. Immunol. 2019;10:3107.

6   Ramjiawan RR, Griffioen AW, Duda DG. Anti-angiogenesis for cancer revisited: Is there a role for combinations with immunotherapy? Angiogenesis 2017;20:185–204.

7   Dings RPM, Vang KB, Castermans K et al. Enhancement of T-cell-mediated antitumor response: angiostatic adjuvant to immunotherapy against cancer. Clin cancer Res an Off J Am Assoc Cancer Res 2011;17:3134–3145.

8   Haemmerle M, Bottsford-Miller J, Pradeep S et al. FAK regulates platelet extravasation and tumor growth after antiangiogenic therapy withdrawal. J Clin Invest 2016;126:1885–1896.

9   Griffioen AW, Mans LA, de Graaf AMA et al. Rapid angiogenesis onset after discontinuation of sunitinib treatment of renal cell carcinoma patients. Clin cancer Res an Off J Am Assoc Cancer Res 2012;18:3961–3971.

10   Rahat MA. Targeting Angiogenesis With Peptide Vaccines. Front Immunol 2019;10:1924.

11   Wentink MQ, Huijbers EJM, de Gruijl TD et al. Vaccination approach to anti-angiogenic treatment of cancer. Biochim. Biophys. Acta - Rev. Cancer. 2015;1855:155–171.

12   Grothey A, Sugrue MM, Purdie DM et al. Bevacizumab beyond first progression is associated with prolonged overall survival in metastatic colorectal cancer: results from a large observational cohort study (BRiTE). J Clin Oncol Off J Am Soc Clin Oncol 2008;26:5326–5334.

13   Bennouna J, Sastre J, Arnold D et al. Continuation of bevacizumab after first progression in metastatic colorectal cancer (ML18147): a randomised phase 3 trial. Lancet Oncol 2013;14:29–37.

14   Blom AG, Hilgers LAT. Sucrose fatty acid sulphate esters as novel vaccine adjuvants: effect of the chemical composition. Vaccine 2004;23:743–54.

15   Hilgers LAT, Blom AG. Sucrose fatty acid sulphate esters as novel vaccine adjuvant. Vaccine 2006;24:S81–S82.

16   Wentink MQ, Verheul HMW, Griffioen AW et al. A safety and immunogenicity study of immunization with hVEGF 26-104 /RFASE in cynomolgus monkeys. Vaccine 2018;36:2025–2032.

17   Wentink MQ, Broxterman HJ, Lam SW et al. A functional bioassay to determine the activity of anti-VEGF antibody therapy in blood of patients with cancer. Br J Cancer 2016;115:1–9.

18   Wentink MQ, Hackeng TM, Tabruyn SP et al. Targeted vaccination against the bevacizumab binding site on VEGF using 3D-structured peptides elicits efficient antitumor activity. Proc Natl Acad Sci 2016;113:12532–12537.

19   Valmori D, Souleimanian NE, Tosello V et al. Vaccination with NY-ESO-1 protein and CpG in Montanide induces integrated antibody/Th1 responses and CD8 T cells through cross-priming. Proc Natl Acad Sci U S A 2007;104:8947–8952.

20   Ammi R, De Waele J, Willemen Y et al. Poly(I:C) as cancer vaccine adjuvant: Knocking on the door of medical breakthroughs. Pharmacol Ther 2015;146:120–131.

21   Bonam SR, Partidos CD, Halmuthur SKM et al. An Overview of Novel Adjuvants Designed for Improving Vaccine Efficacy. Trends Pharmacol Sci 2017;38:771–793.

22   Dubensky TW, Reed SG. Adjuvants for cancer vaccines. Semin Immunol 2010;22:155–61.

23   Khong H, Overwijk WW. Adjuvants for peptide-based cancer vaccines. J Immunother cancer 2016;4:56.

7

SUPPLEMENTARY MATERIAL

Table S1. Baseline characteristics

Dose-Level	Sex	Age	ECOG status	Prior systemic therapies	Tumor type	Enrolled	Completed DLT period
1	F	51	1	2	Urothelial	Yes	No
1	M	77	1	3	NET* of pancreas	Yes	Yes
1	F	49	1	3	SCC** of unknown primary	Yes	Yes
1	M	70	1	2	Salivary duct	Yes	Yes
2	M	56	NA	7	NET* of unknown primary	No	Screen failure
2	F	56	1	4	Ovarian	Yes	Yes
2	F	59	NA	1	Pancreas	No	Screen failure
2	M	69	1	0	Colorectal	Yes	Yes
2	M	59	NA	0	Gastric	No	Screen failure
2	M	70	1	4	Gastric	Yes	Yes
3A	F	67	1	3	Pleiomorphic adenoma	Yes	Yes
3A	F	68	1	4	Metaplastic carcinoma	Yes	Yes
3A	M	68	2	3	Glioblastoma	Yes	No
3A	M	67	1	3	Tongue base	Yes	Yes
3B	F	59	1	2	Colorectal	Yes	No
3B	M	60	1	6	Colorectal	Yes	Yes
3B	F	78	1	2	Colorectal	Yes	Yes
3B	M	55	1	3	Tonsil	Yes	Yes
4	M	54	1	1	Colorectal	Yes	No
4	M	64	2	3	Oropharynx and esophageal	Yes	No
4	F	62	1	1	Ovarian	Yes	No
4	M	66	1	6	Hepatocellular	Yes	No
4	M	70	1	1	Colorectal	Yes	Yes
4	M	63	1	1	Hypopharynx	Yes	Yes
4	F	40	1	3	Breast	Yes	No
4	M	77	1	5	Esophageal	Yes	Yes
5	M	69	1	9	Hepatocellular	Yes	Yes
5	M	60	0	2	Colorectal	Yes	Yes
5	M	71	1	3	Prostate	Yes	No
5	F	72	1	3	Breast	Yes	Yes

*Neuroendocrine tumor. ** Squamous cell carcinoma

Table S2. Adverse events

Adverse Event*	Grade 1	Grade 2	Grade 3	Grade 4	Grade 5	Total	NC/NA**
Injection site reaction	16	0	0	0	0	16	38.5%
Fatigue	8	3	0	0	0	11	57.7%
Fever	7	2	0	0	0	9	65.4%
Nausea	1	2	0	0	0	3	88.5%
Flu like symptoms	3	0	0	0	0	3	88.5%
Weight loss	1	1	0	0	0	2	92.3%
Malaise	1	1	0	0	0	2	92.3%
Anorexia	1	1	0	0	0	2	92.3%
Pain in extremity	2	0	0	0	0	2	92.3%
Neck pain	1	0	0	0	0	1	96.2%
Bone pain	0	1	0	0	0	1	96.2%
Erythema	1	0	0	0	0	1	96.2%
Aspartate aminotransferase increased	0	1	0	0	0	1	96.2%
Dyspnea	1	0	0	0	0	1	96.2%
Myalgia	0	1	0	0	0	1	96.2%
Rash	1	0	0	0	0	1	96.2%
Dizziness	1	0	0	0	0	1	96.2%
Edema limbs	1	0	0	0	0	1	96.2%
Alkaline phosphatase increased	1	0	0	0	0	1	96.2%
Venous stasis	1	0	0	0	0	1	96.2%
Blood bilirubin increased	1	0	0	0	0	1	96.2%
Diarrhea	1	0	0	0	0	1	96.2%
Headache	1	0	0	0	0	1	96.2%
Total	51	13	0	0	0	64	

*Listed adverse events are possible, probable or certainly related.
**NC/NA: no change from baseline/no adverse event

7

Table S3. Serious adverse events

SAE*	Grade 1	Related	Grade 2	Related	Grade 3	Related	Grade 4	Related	Grade 5	Total
Fever	1	*Probable*	2	*Possible*	0		0		0	3
Pain in extremity	0		0		2	*Unlikely 1x* *Unrelated 1x*	0		0	2
Tumor pain	0		0		1	*Unrelated*	0		0	1
Anemia	0		0		1	*Unrelated*	0		0	1
Confusion	0		1	*Unrelated*	0		0		0	1
Urinary tract infection	0		0		1	*Unrelated*	0		0	1
Sepsis	0		0		0		1	*Unrelated*	0	1
Somnolence	0		0		1	*Unrelated*	0		0	1
Thromboembolic event	0		0		1	*Unrelated*	0		0	1
Abdominal pain	0		1	*Unlikely*	0		0		0	1
Upper GI hemorrhage**	0		0		1	*Unrelated*	0		0	1
Malaise	0		1	*Possible*	0		0		0	1
Nausea	0		1	*Possible*	0		0		0	1
Vomiting	0		1	*Unrelated*	0		0		0	1
Total	1		7		8		1		0	17

* Serious Adverse Event
** Upper gastrointestinal hemorrhage

Table S4. Local injection site reactions

	Dose-level 1	Dose-level 2	Dose-level 3a	Dose-level 3b	Dose-level 4	Dose-level 5	All dose-levels
Reactions*	3	6	6	9	3	1	28 (44%)
Primer	1	1	3	3	2	0	10 (40%)
1th booster	1	2	3	3	0	1	10 (50%
2nd booster	1	3	0	3	1	0	8 (42%)
Type**							
Abscess	0	0	0	0	0	0	0 (0%)
Cellulitis	0	0	0	0	0	0	0 (0%)
Nodule	0	0	1	0	0	0	1 (4%)
Induration	0	4	0	2	0	0	6 (21%)
Swelling	2	4	1	5	0	0	12 (43%)
Pain	2	0	3	7	1	1	14 (50%)
Erythema	1	1	0	0	1	0	3 (11%)
Warmth	1	4	4	6	2	0	17 (61%)

*Number of local injection site reactions observed in 64 vaccine administrations in 26 patients.
**Specification of local reaction type (multiple reaction types possible per reaction).

7

Table S5. Response evaluation

	Dose-level 1	Dose-level 2	Dose-level 3a	Dose-level 3b	Dose-level 4	Dose-level 5	All dose-levels
Screened	4	6	4	4	8	4	30
Enrolled	4	3	4	4	8	4	27
Evaluable for toxicity	4	3	4	4	7*	4	26
Evaluable for efficacy	4	3	4	4	7*	4	26
Stable disease**	2	0	1	2	0	0	5
Progressive disease**	1	2	2	1	4	3	13
Other**	1	1	1	1	3	1	8
Median PFS (days)	140	70	70	NA	68	69	70 (95% CI: 69-71)
Median TTP*** (days)	112	68	70	69	62	69	69 (95% CI: 55-85)
Median OS (days)	146	151	500	125	137	174	157 (95% CI: 117-197)
Median response duration (days)	NA	NA	NA	NA	NA	NA	NA
Median treatment duration (days)	84	70	69	74	34	77	70

* One patient in dose-Level 4 did not commence treatment because of pulmonary embolism and was therefore excluded from efficacy- and toxicity evaluation.
**First response evaluation (week 10) using RECIST 1.1
***Other category specified per dose-level:
DL 1:   Early death from malignant disease (1x)
DL 2:   Not assessable (rapid clinical deterioration) (1x)
DL 3A: Early death from malignant disease (1x)
DL 3B: Not assessable (withdrew consent) (1x)
DL 4:   Early death from malignant disease (1x), early death from other cause (1x), not assessable (off-study after infections) (1x)
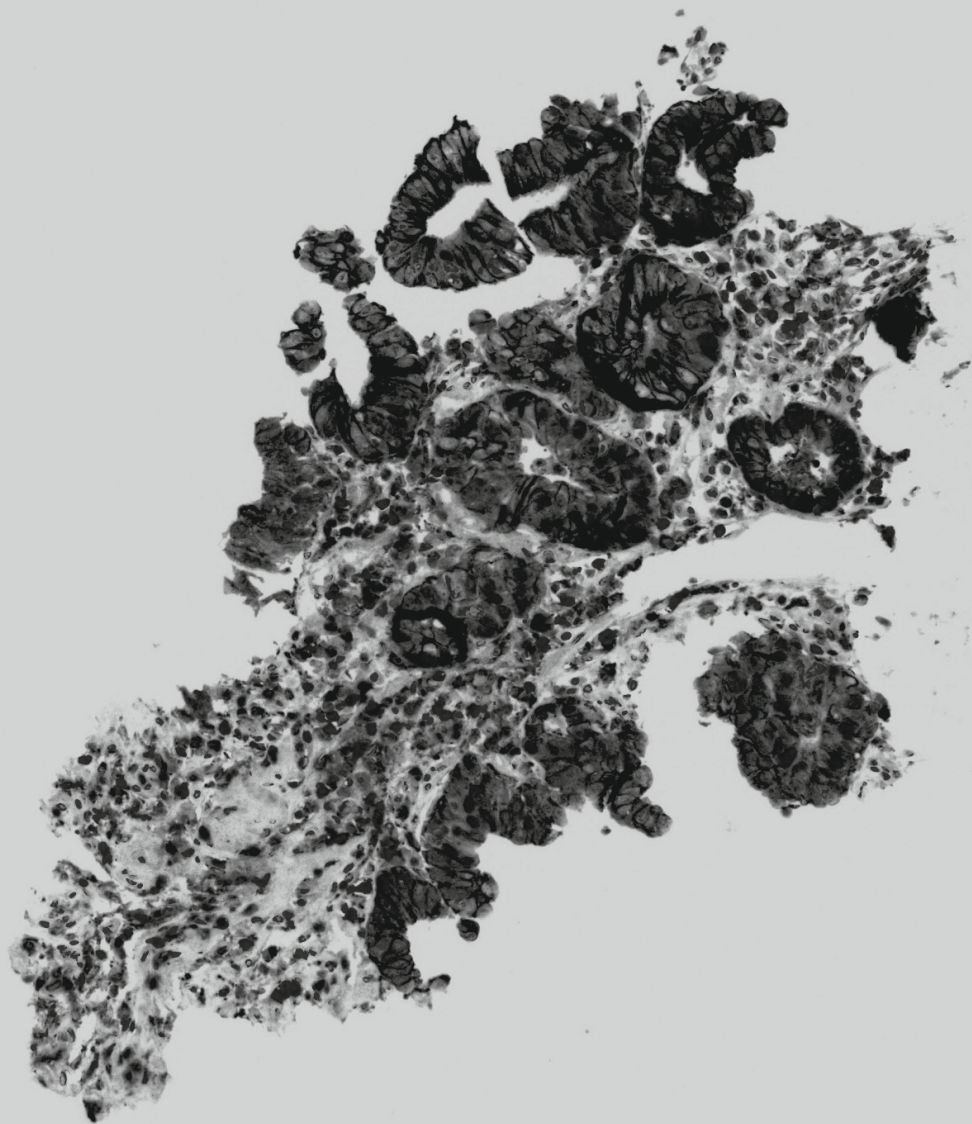DL 5:   Not assessable (withdrew consent) (1x)

95%CI = 95% confidence interval. PFS = progression free survival. TTP: time to progression. OS: overall survival. NA: not available

Table S6. Dose-levels

	hVEGF$_{26\text{-}104}$ (µg)	RFASE (mg)
Dose-Level 1*	62.5	20
Dose-Level 2	125	20
Dose-Level 3A	250	20
Dose-Level 3B	250	40
Dose-Level 4	500	40
Dose-Level 5	1000	40

* The patients in dose-level 1 received a first immunization with 20 mg RFASE alone to study the potential adverse effects of the adjuvant.

7

Chapter 8

Summarizing discussion and future perspectives

Esophageal cancer (EC) is a disease with a poor treatment outcome. Localized disease is often treated with neoadjuvant chemoradiotherapy (fractionated irradiation combined with paclitaxel and carboplatin) followed by surgical resection, but response to chemoradiotherapy (CRT) varies greatly. Patients with residual disease in the resection specimen have a higher risk of disease recurrence and worse prognosis. The overarching goal of this thesis was to gain insights in biological processes influencing the treatment outcome of patients with localized EC. The first aim (**part I**) was to identify molecular and immunological mediators of response to neoadjuvant chemoradiotherapy (CRT) in EC. The second aim (**part II**) was to elucidate molecular and immunological effects of fractionated radiotherapy, which might be exploited for novel treatment strategies.

PART I. Identifying molecular and immunological mediators of response to neoadjuvant chemoradiotherapy in esophageal cancer

Genomic features do not predict response to CRT
In **chapter 2** a targeted DNA sequencing approach, with 243 genes commonly mutated in gastroesophageal cancer, was used to identify molecular differences between patients with a favorable and poor pathological response to neoadjuvant CRT using DNA extracted from pretreatment tumor biopsies. It was found that in esophageal adenocarcinoma (EAC) *CSMD1* deletion and *ETV4* amplification were associated with a favorable histopathological response, while *SMURF1* amplification and S*MARCA4* mutation occurred most frequently in tumors that lacked tumor regression after neoadjuvant treatment. However, as these alterations are only low-prevalent in EAC (between 5.3 to 8%) it is unlikely they can be used for screening purposes. Unfortunately, none of the more prevalent and/or targetable genetic alterations such as amplification of *ERBB2 (HER2), EGFR*, *KRAS* or *GATA4* were enriched in either one of the response groups. In esophageal squamous cell carcinoma (ESCC), *TP63* amplification and *TFPI2* gene promoter methylation were associated with an unfavorable histopathological response, and shorter disease-free survival (DFS) (*TP63*) and overall survival (OS) (*TFPI2*), whereas *CDKN2A* deletion was associated with prolonged OS. Although these alterations were more prevalent (between 10.0% to 25.0%), the number of ESCC cases was to low (n=16) to draw definitive conclusions, and validation in an independent cohort is required.

Based on these findings we conclude that targeted sequencing using a single tumor biopsy will neither help to predict treatment response, nor contribute to personalized treatment in EAC. These results are in agreement with a study by Pectasides *et al.*[1], which reported that EACs show abundant intratumoral genomic heterogeneity and that sampling of one tumor area does not provide a full representation of the molecular makeup of the disease. The authors sequenced multiple areas from the primary tumor and metastases to come to that conclusion. They did not only identify substantial discrepancy within the primary tumor, but also between the primary tumor and distant

214

metastases[1]. Of note, also targetable alterations such as amplification of *ERBB2 (HER2), VEGFA* and *EGFR* were often discordant. This heterogeneity may not only complicate representative tumor sampling, but might also compromise a uniform treatment response[2–5].

There are multiple strategies to overcome this problem. First, multiple region DNA sequencing will likely give a more reliable representation of the molecular drivers and targets of the total tumor burden and thereby increase the chance to respond to specific molecule or pathway targeting therapies. This hypothesis was recently tested in the PANGEA trial[6]. Within this trial both primary and metastatic lesions were sequenced at baseline, and subsequently at the moment of disease progression. A patient-tailored treatment strategy was applied using monoclonal antibodies added to chemotherapy for up to three lines of sequential therapy. With this approach, the researchers confirmed discordant treatment assignments in 28 of 80 (35%) patients based on the molecular profile of primary tumor and metastasis separately. The study showed that when treatment was based on the molecular profile of both tumor sites, the median overall survival was 15.7 months[6], which was superior to historical controls and should be further explored in a phase III randomized trial.

Although this is a promising strategy, repeated biopsies and sequencing costs are clear drawbacks of such an approach. Assessment of circulating tumor DNA (ctDNA), which is shed by tumor cells, may provide an alternative and minimally invasive method for genomic characterization, aiming for personalized treatment strategies. In divergent primary and metastatic lesions, 87.5% concordance for targetable alterations in metastatic tissue and ctDNA was reported[1], suggesting the potential for ctDNA to provide a representative overview of the molecular profile of the entire tumor burden. Nonetheless, ctDNA analyses depend on shedding of DNA in the circulation which is observed in 76.1% of metastatic cancers, and in only 33.3% of localized disease using current sequencing strategies[7]. Improvements in ctDNA sequencing technology to enhance sensitivity and reduce costs are urgently warranted for more accurate detection of alterations in localized disease. For example, CyclomicsSeq, which is based on Oxford Nanopore sequencing of concatenated copies of single DNA molecules, represents a platform that could be cheap, fast and reliable in clinical practice; adequate detection and monitoring of tumor burden during chemoradiotherapy in Head and Neck Squamous Cancer (HNSCC) patients was recently demonstrated using this platform[8].

In conclusion, genomic heterogeneity imposes an important barrier for personalized medicine in esophageal cancer. Currently, the most promising strategy to circumvent this problem is by sequencing either ctDNA or multiple tumor regions to find predictive and prognostic biomarkers and adequately detect druggable targets in individual patients. Positron emission tomography (PET) with radiolabeled isotopes, such as

8

[89]ZR-trastuzumab in HER2 positive disease[9], might represent an interesting upcoming technique for in vivo imaging of molecular targets in patients.

Modulating the tumor microenvironment

It is increasingly acknowledged that besides cancer cells also other cells in the tumor microenvironment (TME), e.g., immune cells, vascular cells and stromal cells, influence the biology of the disease and potentially also the response to CRT[10–12]. Therefore, in **chapter 3**, the role of the tumor immune microenvironment (TME) of EACs was explored in relation to the response to neoadjuvant CRT. Multiplex immunohistochemistry, flowcytometry and mRNA expression analysis were used to study the TME in relation to treatment outcome in pre-treatment biopsies from EAC patients.

In this study it was found that localized immunity, and activation of tumor infiltrating T cells in particular, was associated with response to neoadjuvant CRT. Patients with a complete pathological response to CRT had significantly higher tumor-infiltrating T cell levels in their pre-treatment biopsies. Furthermore, non-(complete) responders were characterized by a higher ratio of CD163^{+} myeloid cells over T cells, compared to complete responders. Interestingly, T cells were in closer proximity to tumor cells in complete responders compared to the other response groups. Gene expression analyses revealed that T cells in non-responders were enriched for a Th2-skewed signature, whereas complete responders were enriched for cytotoxic immune cell signatures. Moreover, tumors from non-responders were enriched in genes linked to immune suppression, i.e. *CLEC4A* (encoding for the suppressive C-type Lectin receptor DCIR expressed in dendritic cells upon TLR signaling[13]) and *CXCL8* (promoting angiogenesis and inhibiting CD8^{+} T cell functions[14]). Finally, analysis of circulating immune cells revealed that complete responders were enriched in memory T cells.

The majority of EACs was characterized by a limited number of infiltrating T cells and also residual disease after CRT. These results are in agreement with a previous study within our research group which showed that the TME of CIN gastroesophageal adenocarcinomas is generally immunologically cold when compared to more inflamed subtypes with microsatellite instability or gastric cancers positive for the Epstein Barr Virus[15]. As such, T cell exclusion seems to be a central feature of therapy resistance in EACs. Finding mechanisms to induce T cell infiltration in these cancer will likely improve radiotherapy efficacy and outcome.

Tumor infiltrating t cells influence response to CRT

There are multiple promising strategies to activate the immune microenvironment to enhance the success of CRT[16,17]. For example, immune-checkpoint inhibitors (ICI) might be beneficial in EAC to reinvigorate T cells and obtain a synergistic effect with CRT. Indeed, combined modality approaches with checkpoint inhibition have been tested to increase radiotherapy efficacy in several cancer types. For example, in early-stage non-

small cell lung cancer (NSCLC) durvalumab (anti-PD-L1) preceded by a short course of stereotactic radiotherapy was associated with higher pathological response rates[18] and in unresectable stage III NSCLC, durvalumab after CRT similarly resulted in prolonged survival rates[19]. For EC, the PERFECT study investigated the feasibility and efficacy of neoadjuvant CRT combined with atezolizumab (anti-PD-L1) in resectable EACs[20]. Although feasible, no additional benefit in pathological response or survival was found compared to a propensity matched cohort. Interestingly, in an underpowered subgroup analysis responders seemed to have an additional survival benefit from atezolizumab compared to non-responders. Transcriptomic analysis showed a higher interferon-y signature in responders compared to non-responders, indicating that pre-treatment immune activation predisposes for tumor clearance in this study.

However, the most impressive results come from the Checkmate-577 trial. In this study adjuvant nivolumab was given to patients with EC or gastroesophageal junction cancer (GEJC) with residual disease in their resection specimen after neoadjuvant CRT. This resulted in an impressive doubling of the disease-free survival (DFS) (22.4 compared to 11.0 month) compared to placebo-treated patients[21]. Of note, DFS in the control group was lower than reported by the Dutch CROSS trial[22], which might be explained by the exclusion of patients with a complete pathological response. Interestingly, patients with ESCC and patients with a complete pathological response of the primary tumor (ypT0N+) seem to benefit most from adjuvant nivolumab. In light of our previous study and the PERFECT trial, it could be hypothesized that patients with a complete pathological response after CRT might also benefit from adjuvant ICIs.

As the ratio of CD163+ Tumor Associated Macrophages (TAMs) to T cells was higher in non-complete responders, targeting macrophages might be an alternative strategy. For example, targeting M2 macrophages through colony-stimulating factor-1 (CSF1)[23] or CXCR2 blockade[24] might shift the balance to less immunosuppression; CSF1/CSF1 receptor blockade has been shown to improve immunotherapy efficacy in pre-clinical models and is currently being investigated in clinical trials[23]. Various other strategies to potentiate, repolarize and inhibit macrophage or dendritic cell (DC) functions are also being explored (pre)clinically, as extensively reviewed elsewhere[25,26]. Of interest, in esophageal cancer a CD40 agonist (sotigalimab) is currently being tested in combination with CRT to enhance cancer specific T cell responses via DC activation (NCT03165994).

Since non-responders were enriched for a Th2-skewed signature, another approach might be to shift the anti-inflammatory immune state towards a pro-inflammatory microenvironment by altering the Th2/Th1 T cell balance. A potential strategy is blocking Notch signaling, since notch receptors and ligands are an important regulator of Th2 cell differentiation[27]. Blocking notch signaling with a y-secretase inhibitor has shown to inhibit Th2 responses and restore Th1/Th2 imbalance in an asthma mouse model[28] and PBMCs from tuberculosis patients[29]. Yet, the universal expression of Notch

8

receptors and ligands on many cell types makes clinical application of Notch targeting challenging[30].

Finally, oncolytic viruses and adoptive cell therapy represent interesting upcoming immunomodulatory strategies to turn "cold" tumors "hot"[31,32]. Oncolytic viruses are viruses that preferentially target cancer cells, either naturally or through genetic modification; selective replication of the virus within the tumor cell will result in cell killing, thus stimulating the immune system through the induction of immunogenic cell death[33]. In addition, oncolytic viruses can be "armed" with (for example Th1-skewing) cytokines for intratumoral delivery[34]. Adoptive cell therapy, such as T cells with engineered chimeric antigen receptors (CAR-Ts), might induce tumor regression by transferring specific immune cells to the tumor-bearing host[35]. It should however be noted that while CAR-T cell therapy caused a paradigm shift in the treatment of hematological malignancies, thus far successes in solid malignancies have been limited, also due to a lack of infiltration into the TME[36].

Due to the complex interplay between different cell types and cytokines within the TME, the effects of targeting a specific immune cell subset might be limited and context dependent. As none of the cell subsets function in a vacuum but depend on each other, it is important to understand how cancer cells, immune cells and stromal cells influence each other within the same microenvironment. Integrating genomic- and transcriptomic data within a detailed map of the TME is needed to provide further insight into the complex interplay between different cells. New technical improvements such as spatial transcriptomics has made these analyses possible.

For EC patients, a major step forward has been made with the recent introduction of nivolumab in patients with residual disease after CRT. Nevertheless, the majority of patients still has limited or incomplete response to CRT. These outcomes could be improved by detailed upfront TME analysis and selection of patients with immunosuppressive traits for pre-CRT immunomodulation. Thus, future research should validate possible immunological hallmarks of (non)response reported by us and others, and further explore patient-tailored pre-CRT immunomodulation.

PART II. Elucidating molecular and immunological responses occurring upon fractionated radiotherapy; towards novel and improved combination treatments

Radiotherapy effects in the tumor microenvironment
To further enhance radiotherapy efficacy, we mined the literature for information regarding the complex interplay between tumor cells, the tumor vasculature and the tumor immune response in the context of radiotherapy. In **chapter 4** we report that fractionated radiotherapy 1) leads to immunogenic cell death of tumor cells, which enhances specific anti-tumor T cell priming and 2) induces a pro-angiogenic response

via induction of Vascular Endothelial Growth Factor A (VEGF), resulting in enhanced perfusion of the tumor, and 3) may improve the extravasation of immune cells into the tumor tissue via induction of chemokines and adhesion molecule expression on endothelial cells, but it can also induce upregulation of immune checkpoint molecules in the TME, hampering effective tumor clearance. Consequently, both immunotherapy and anti-angiogenic therapy have the potential to augment radiotherapy efficacy, but careful dosing and scheduling of these treatment modalities is key.

Interestingly, *VEGF* is amplified in 20-30% of gastroesophageal adenocarcinomas[37], which does not only have angiogenic effects but potentially also immune-suppressive properties, i.e. suppression of antigen presenting cells, inhibition of T cell effector function and attraction of MDSCs, TAMs and Tregs[38]. Anti-angiogenic therapy with either monoclonal antibodies or Tyrosine Kinase Inhibitors (TKIs) potentially counteracts these immune suppressive mechanisms[39]. Interestingly, there is a growing interest in combining anti-angiogenic therapy with ICIs to overcome resistance to immune checkpoint blockade. This has led to successful first-line treatment strategies in hepatocellular carcinoma[40] and renal cell carcinoma[41]. In advanced GC/GEJC the VEGFR multi-TKIs regorafenib[42], lenvatinib[43] and apatinib[44] have been evaluated in combination with ICIs in phase I/II trials and showed promising objective response rates of 44%, 69% and 16%, respectively. In addition, encouraging results with ramucirumab (currently, second line therapy with paclitaxel) in combination with several ICIs were reported[45-47]. To our knowledge, in localized EC no studies have been undertaken to combine CRT with anti-angiogenic therapy. Nonetheless, promising results have been reported in other tumor types[48,49]. For example, improved complete pathological response rates have been reported in rectal cancer with the addition of bevacizumab to neoadjuvant therapy (in different combinations of chemotherapy and chemoradiotherapy)[49].

Given all of the above, in localized EC a short course of anti-angiogenic therapy prior to- or during-CRT is a conceivable strategy that has the potential to augment both radiotherapy and immune effector cell trafficking to the tumor. A clinical trial studying the effects of anti-angiogenic therapy in addition to CRT on immunomodulation and treatment outcome would be of great interest.

An intrinsic type I interferon response in tumor cells
To gain additional insights into radiotherapy effects on tumor cells that might be exploited for new treatment strategies, the molecular and immunological responses occurring during clinically applied fractionated irradiation schedules were investigated (daily fractions of 2Gy for 5 days per week, multiple weeks). In **chapter 5** it is demonstrated that fractionated irradiation induces an intrinsic type I interferon (IFN) response in tumor cells that is characterized by an increased expression of interferon stimulated genes (ISGs). The response peaks within 2 to 3 weeks of treatment and coincides with a convergence to a steady state in clonogenic survival *in vitro* and

8

treatment resistance *in vivo*. While colon cancer and glioblastoma cells were used as model systems, the type I IFN response was also observed in an EC cell line as well as in tumor tissues from esophageal cancer patients during CRT.

Interestingly, the type I IFN response can be induced independently of a specific type I IFN or of Stimulator of Interferon Genes (STING)-mediated signaling; STING is activated upon recognition of double-stranded DNA (dsDNA) via cytosolic DNA sensors such as cyclic GMP-AMP Synthase (cGAS), and is an important regulator of immunogenic cell death[50–53]. Former studies reported that innate immune sensing of cancer is principally mediated via STING[53], but our data suggests it is not the complete story when it comes to radiation-induced type I IFNs and accompanied immune activation. In line with this, Feng et al. demonstrated that besides STING also Mitochondrial Antiviral-Signaling protein (MAVS) signaling plays a role in radiation induced type I IFN response[54]. Like STING, MAVS is an adaptor molecule occupying a central position in the production of type I IFNs and signaling via MAVS is initiated by cytosolic RNA detection as opposed to DNA detection[55]. Whether MAVS signaling played a role in our observation is as yet unknown, but represents a plausible explanation which is currently under investigation.

The consequences of cGAS/STING -and possibly also MAVS- activation in cancer are likely context dependent[56]. In near-diploid tumors, activation might exhibit an anti-tumor effect through the induction of type I interferon signaling and consequently T cell-mediated immunity. When advanced tumors become increasingly chromosomally instable, they adapt to tolerate chronic cGAS/STING signaling in response to accumulating cytosolic DNA resulting from chromosome segregation errors and replication stress during mitosis[57,58]. This adaptation can result in downregulation of downstream IFN signaling. Indeed, in CIN gastric cancer, reductions in STING mRNA and -protein expression levels correlate with increased tumor stage[59]. These observations have led to the proposition that the loss of these proteins is a possible route for cancer cells to escape immune recognition[60]. Likewise, defects in cancer cell IFN signaling have also been linked to resistance to ICI therapy[61,62].

The exact role of type I IFN signaling in the response to radiotherapy in EC patients should be further explored. Besides elucidating the role of MAVS compared to STING, another outstanding question relates to the role of CIN in type I IFN signaling and treatment response. In particular, one could hypothesize that the degree of CIN and the (tolerability of) levels of pre-treatment type I IFN signaling inversely correlate with the capacity of radiotherapy to elicit anti-tumor T cell activation.

Type I interferon signaling; a therapeutic target?
To further improve radiotherapy efficacy, we explored whether IFNs and type I IFN response genes induced by radiotherapy might be exploited as a therapeutic target. First, we reviewed the literature on both intrinsic and extrinsic effects of type I IFNs in

the tumor in **chapter 6**. This literature analysis showed that type I IFNs can inhibit cell growth and migration, induce apoptosis and senescence and activate T cell mediated immunity. As such, the induction of a type I IFN response during fractionated irradiation could be beneficial and provides a rational for combining interferons and radiotherapy in the clinic. Yet, lack of clear survival benefit and increased grade ≥3 toxicity often led to negative recommendations for this treatment approach. Possibly, this is related to inadequate dose-scheduling of both treatment modalities as radiation dose and scheduling have been shown to affect the immunostimulatory activity[63]. Our findings in **chapter 5** also suggest that there is no rational for prolonged administration of IFNs or STING agonists during radiotherapy, particularly if this results in increased toxicity. At the same time, to enhance anti-tumor immune responses, IFNs or STING-agonists might be beneficial when administered briefly, i.e., in the first weeks of fractionated radiotherapy.

Sustained cGAS/STING activation can also lead to therapy resistance. Host STING-induced chronic type I IFN signaling during prolonged exposure to fractionated radiation therapy promotes tumor radioresistance in transplanted MC38 colon tumors, possibly mediated via mobilization of myeloid-derived suppressor cells[64]. In addition, the expression of ISGs and upstream transcription factors like STAT1 (Signal Transducer and Activator of Transcription 1) are associated with resistance to radiotherapy and poor survival[65–67]. In addition, attenuating the duration of ISG responses with GM-CSF has been reported to be beneficial in patients with localized melanoma treated with the immunomodulatory drug CpG-β[68]. Thus, although induction of IFN signaling will boost anti-tumor immunity at first, prolonged IFN signaling could lead to therapy resistance and immune escape. This provides a rational for further studies into counteracting such a response. Nevertheless, neither blocking a specific IFN, nor the regulator protein STING, resulted in diminished induction of ISG expression or clear changes in radiosensitivity (**chapter 5**). As discussed before, this might result from activation of alternative pathways, like MAVS signaling, which requires further research.

Given the observed uncoupling of cGAS/STING and interferon expression on one hand and the induction of ISGs on the other hand, an alternative approach might be targeting of a specific ISG, or interfering with ISG functions. For example, ISG15 is noticeably induced upon irradiation and a key regulator of IFN signaling. It has also been suggested to play a role in in chemosensitivity in EC cell lines by regulating autophagy and survival[69]. Ubiquitin-specific protease 18 (USP18) cleaves ISG15 from substrates and is negative regulator of the IFN pathway[70]. Interestingly, deletion of the USP18 enhances tumor cell antigenicity and radiosensitivity[71]. Thus, ISG15 and other ISGs might represent interesting targets to enhance radiotherapy efficacy and their role could be further explored.

8

221

Lessons learned from a novel VEGF targeting vaccine

As discussed in **chapter 4**, radiotherapy efficacy might be improved via anti-angiogenic therapy, which provides a rational to combine VEGF blocking agents with radiotherapy. In **chapter 7** we describe the lessons learned from developing and testing a novel VEGF targeting peptide vaccine, hVEGF$_{26-104}$/RFASE, that might be applied in such a therapeutic strategy. In a phase I clinical trial, this vaccine was not able to elicit seroconversions against native VEGF. Systemic immune suppression in heavily pre-treated patients with advanced cancer stages, deficient RFASE adjuvant activity and dominant immunoreactivity towards neo-epitopes may have contributed to the lack of efficacy in the study participants. Remarkably, hVEGF$_{26-104}$/RFASE induced VEGF-neutralizing antibodies in a nonhuman primate model[72]. The absence of seroconversion in this study warrants caution when interpreting efficacy results of human vaccines in nonhuman primates.

The outcome of this clinical trial displays one of the central challenges in cancer vaccine development; how to overcome immune suppression? Unfortunately, despite FDA approval of sipuleucel-T (a dendritic cell-based vaccine) in 2010, no other therapeutic cancer vaccine has been approved since[73]. It is now recognized that the efficacy of cancer vaccines can be compromised by tumor cell intrinsic resistance and local or systemic immunosuppressive mechanisms[74]. Vaccines are more effective in cancer when disease burden is low and immunosuppression is limited. Careful selection of immunogenic tumor associated antigens or tumor-specific neoantigens in combination with potent adjuvants, such as TLR agonists (i.e., Poly I:C or CpG), are key to elicit an effective immune response. Recently, novel vaccine platforms have been developed, such as mRNA-based vaccines and nanoparticle delivery systems[75]. mRNA-based vaccines have been successfully used to fight the COVID-19 pandemic[76] but were originally developed for cancer treatment in which they have recently also shown promise[77]. To enhance efficacy, cancer vaccines can be combined with chemotherapy, radiotherapy and ICIs[74]. Despite progress made, further research on overcoming immunosuppressive mechanisms in the TME is mandatory for successful implementation in clinical practice.

Concluding remarks

Esophageal cancer is a disease characterized by a substantial genomic- and immunological heterogeneity and dismal treatment outcomes. In this thesis, several molecular and immunological factors influencing the treatment outcome of patients with localized EC were identified, with a key role for T cell mediated immunity and a type I IFN response. Treatment outcomes of localized EC might be further improved by comprehensive upfront TME analysis and selection of patients with immunosuppressive traits for pre-CRT immunomodulation.

8

REFERENCES

1. Pectasides E, Stachler MD, Derks S, et al. Genomic Heterogeneity as a Barrier to Precision Medicine in Gastroesophageal Adenocarcinoma. *Cancer Discov*. January 2017:CD-17-0395. doi:10.1158/2159-8290.CD-17-0395

2. Murugaesu N, Wilson GA, Birkbak NJ, et al. Tracking the genomic evolution of esophageal adenocarcinoma through neoadjuvant chemotherapy. *Cancer Discov*. 2015;5(8):821-831. doi:10.1158/2159-8290.CD-15-0412

3. Findlay JM, Castro-Giner F, Makino S, et al. Differential clonal evolution in oesophageal cancers in response to neo-adjuvant chemotherapy. *Nat Commun*. 2016;7(1):11111. doi:10.1038/ncomms11111

4. Dagogo-Jack I, Shaw AT. Tumour heterogeneity and resistance to cancer therapies. *Nat Rev Clin Oncol*. 2018;15(2):81-94. doi:10.1038/nrclinonc.2017.166

5. Burrell RA, McGranahan N, Bartek J, Swanton C. The causes and consequences of genetic heterogeneity in cancer evolution. *Nature*. 2013;501(7467):338-345. doi:10.1038/nature12625

6. Catenacci DVT, Moya S, Lomnicki S, et al. Personalized antibodies for gastroesophageal adenocarcinoma (Pangea): A phase ii study evaluating an individualized treatment strategy for metastatic disease. *Cancer Discov*. 2021;11(2):308-325. doi:10.1158/2159-8290.CD-20-1408

7. Kato S, Okamura R, Baumgartner JM, et al. Analysis of Circulating Tumor DNA and Clinical Correlates in Patients with Esophageal, Gastroesophageal Junction, and Gastric Adenocarcinoma. *Clin Cancer Res*. 2018;24(24):6248-6256. doi:10.1158/1078-0432.CCR-18-1128

8. Marcozzi A, Jager M, Elferink M, et al. Accurate detection of circulating tumor DNA using nanopore consensus sequencing. *NPJ genomic Med*. 2021;6(1):106. doi:10.1038/S41525-021-00272-Y

9. O'Donoghue JA, Lewis JS, Pandit-Taskar N, et al. Pharmacokinetics, biodistribution, and radiation dosimetry for 89 Zr-trastuzumab in patients with esophagogastric cancer. *J Nucl Med*. 2018;59(1):161-166. doi:10.2967/jnumed.117.194555

10. Wang Z, Zhang S, Siu TL, Huang S. Glioblastoma multiforme formation and EMT: role of FoxM1 transcription factor. *Curr Pharm Des*. 2015;21(10):1268-1271.

11. van der Most RG, Currie A, Robinson BWS, Lake RA. Cranking the Immunologic Engine with Chemotherapy: Using Context to Drive Tumor Antigen Cross-Presentation towards Useful Antitumor Immunity. *Cancer Res*. 2006;66(2):601-604. doi:10.1158/0008-5472.CAN-05-2967

12. Arina A, Beckett M, Fernandez C, et al. Tumor-reprogrammed resident T cells resist radiation to control tumors. *Nat Commun*. 2019;10(1). doi:10.1038/s41467-019-11906-2

13. Uto T, Fukaya T, Takagi H, et al. Clec4A4 is a regulatory receptor for dendritic cells that impairs inflammation and T-cell immunity. *Nat Commun*. 2016. doi:10.1038/ncomms11273

14. Lin C, He H, Liu H, et al. Tumour-associated macrophages-derived CXCL8 determines immune evasion through autonomous PD-L1 expression in gastric cancer. *Gut*. 2019;68(10):1764-1773. doi:10.1136/gutjnl-2018-316324

15. Derks S, de Klerk LK, Xu X, et al. Characterizing diversity in the tumor-immune microenvironment of distinct subclasses of gastroesophageal adenocarcinomas. *Ann Oncol Off J Eur Soc Med Oncol*. 2020;31(8):1011-1020. doi:10.1016/j.annonc.2020.04.011
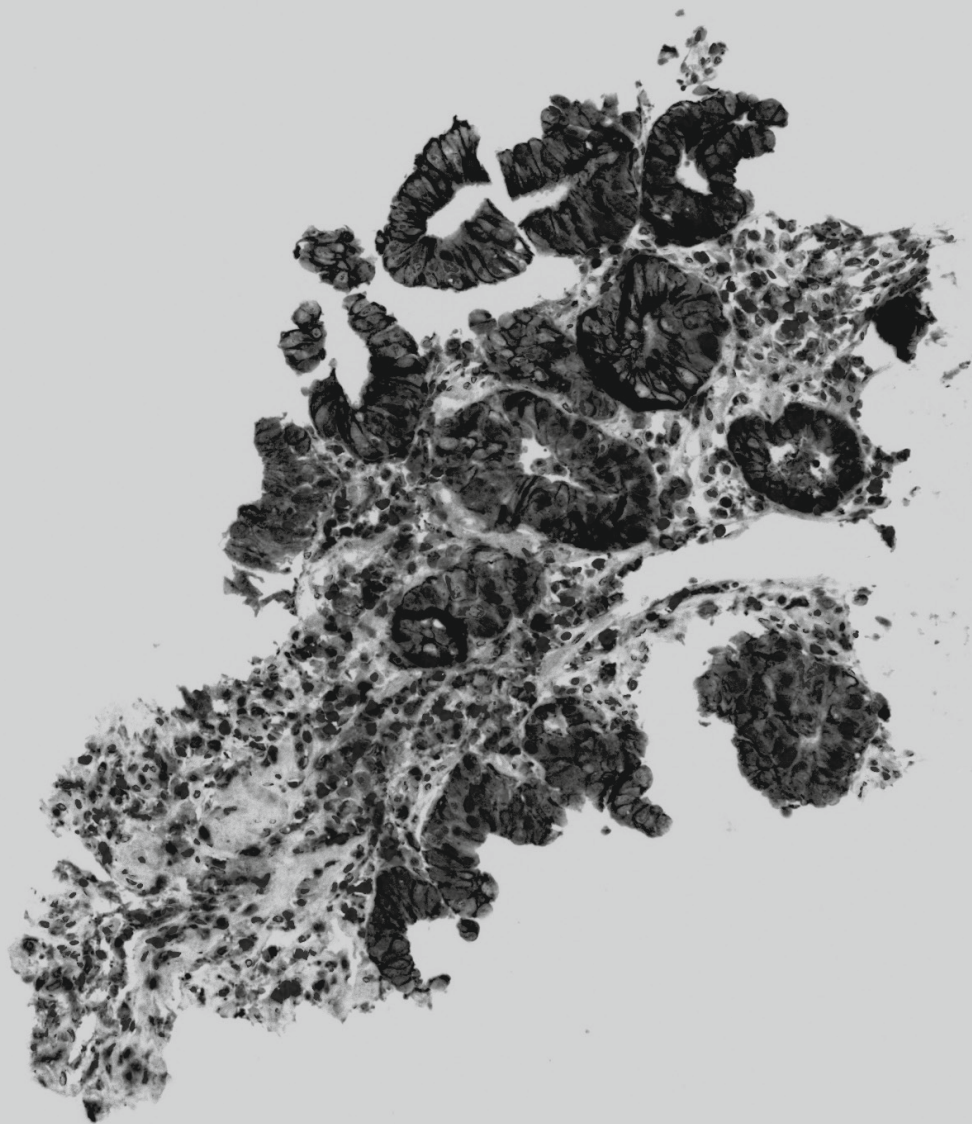
16. Wang Y, Deng W, Li N, et al. Combining Immunotherapy and Radiotherapy for Cancer Treatment: Current Challenges and Future Directions. *Front Pharmacol*. 2018;9(March):1-11. doi:10.3389/fphar.2018.00185

17. Jagodinsky JC, Harari PM, Morris ZS. The Promise of Combining Radiation Therapy With Immunotherapy. *Int J Radiat Oncol Biol Phys*. 2020;108(1):6-16. doi:10.1016/j.ijrobp.2020.04.023

18. Altorki NK, McGraw TE, Borczuk AC, et al. Neoadjuvant durvalumab with or without stereotactic body radiotherapy in patients with early-stage non-small-cell lung cancer: a single-centre, randomised phase 2 trial. *Lancet Oncol*. 2021;22(6):824-835. doi:10.1016/S1470-2045(21)00149-2

19. Antonia SJ, Villegas A, Daniel D, et al. Overall Survival with Durvalumab after Chemoradiotherapy in Stage III NSCLC. *N Engl J Med*. 2018;379(24):2342-2350. doi:10.1056/NEJMOA1809697/SUPPL_FILE/NEJMOA1809697_DATA-SHARING.PDF

20. van den Ende T, de Clercq NC, van Berge Henegouwen MI, et al. A phase II feasibility trial of neoadjuvant chemoradiotherapy combined with atezolizumab for resectable esophageal adenocarcinoma: The PERFECT trial. *J Clin Oncol*. 2019. doi:10.1200/jco.2019.37.15_suppl.4045

21. Kelly RJ, Ajani JA, Kuzdzal J, et al. LBA9_PR Adjuvant nivolumab in resected esophageal or gastroesophageal junction cancer (EC/GEJC) following neoadjuvant chemoradiation therapy (CRT): First results of the CheckMate 577 study. *Ann Oncol*. 2020;31:S1193-S1194. doi:10.1016/j.annonc.2020.08.2299

22. van Hagen P, Hulshof MCCMC, van Lanschot JJBJ, et al. Preoperative chemoradiotherapy for esophageal or junctional cancer. *N Engl J Med*. 2012;366(22):2074-2084. doi:10.1056/NEJMoa1112088

23. Cannarile MA, Weisser M, Jacob W, Jegg AM, Ries CH, Rüttinger D. Colony-stimulating factor 1 receptor (CSF1R) inhibitors in cancer therapy. *J Immunother Cancer*. 2017;5(1):53. doi:10.1186/S40425-017-0257-Y

24. Di Mitri D, Mirenda M, Vasilevska J, et al. Re-education of Tumor-Associated Macrophages by CXCR2 Blockade Drives Senescence and Tumor Inhibition in Advanced Prostate Cancer. *Cell Rep*. 2019. doi:10.1016/j.celrep.2019.07.068

25. Duan Z, Luo Y. Targeting macrophages in cancer immunotherapy. *Signal Transduct Target Ther*. 2021;6(1):1-21. doi:10.1038/s41392-021-00506-6

26. Xiang X, Wang J, Lu D, Xu X. Targeting tumor-associated macrophages to synergize tumor immunotherapy. *Signal Transduct Target Ther 2021 61*. 2021;6(1):1-12. doi:10.1038/s41392-021-00484-9

27. Tu LL, Fang TC, Artis D, et al. Notch signaling is an important regulator of type 2 immunity. *J Exp Med*. 2005;202(8):1037-1042. doi:10.1084/jem.20050923

28. Hu C, Li Z, Feng J, et al. Glucocorticoids Modulate Th1 and Th2 Responses in Asthmatic Mouse Models by Inhibition of Notch1 Signaling. *Int Arch Allergy Immunol*. 2018;175(1-2):44-52. doi:10.1159/000485890

29. Li Q, Zhang H, Yu L, et al. Down-regulation of Notch signaling pathway reverses the Th1/Th2 imbalance in tuberculosis patients. *Int Immunopharmacol*. 2018;54:24-32. doi:10.1016/j.intimp.2017.10.026

30. Christopoulos PF, Gjølberg TT, Krüger S, Haraldsen G, Andersen JT, Sundlisæter E. Targeting the Notch Signaling Pathway in Chronic Inflammatory Diseases. *Front Immunol*. 2021;12:1194. doi:10.3389/fimmu.2021.668207

8

31. Duan Q, Zhang H, Zheng J, Zhang L. Turning Cold into Hot: Firing up the Tumor Microenvironment. *Trends in cancer*. 2020;6(7):605-618. doi:10.1016/J.TRECAN.2020.02.022

32. Haanen JBAG. Converting Cold into Hot Tumors by Combining Immunotherapies. *Cell*. 2017;170(6):1055-1056. doi:10.1016/J.CELL.2017.08.031

33. Lawler SE, Speranza M-C, Cho C-F, Chiocca EA. Oncolytic Viruses in Cancer Treatment: A Review. *JAMA Oncol*. 2017;3(6):841-849. doi:10.1001/jamaoncol.2016.2064

34. De Gruijl TD, Janssen AB, Van Beusechem VW. Arming oncolytic viruses to leverage antitumor immunity. *Expert Opin Biol Ther*. 2015;15(7):959-971. doi:10.1517/14712598.2015.1044433

35. Kirtane K, Elmariah H, Chung CH, Abate-Daga D. Adoptive cellular therapy in solid tumor malignancies: Review of the literature and challenges ahead. *J Immunother Cancer*. 2021;9(7):e002723. doi:10.1136/jitc-2021-002723

36. Morotti M, Albukhari A, Alsaadi A, et al. Promises and challenges of adoptive T-cell therapies for solid tumours. *Br J Cancer*. 2021;124(11):1759-1776. doi:10.1038/s41416-021-01353-6

37. Kim JJ, Bowlby R, Mungall AJ, et al. Integrated genomic characterization of oesophageal carcinoma. *Nature*. 2017;541(7636):169-174. doi:10.1038/nature20805

38. Fukumura D, Kloepper J, Amoozgar Z, Duda DG, Jain RK. Enhancing cancer immunotherapy using antiangiogenics: opportunities and challenges. *Nat Rev Clin Oncol*. 2018;15(5):325-340. doi:10.1038/NRCLINONC.2018.29

39. Saeed A, Park R, Sun W. The integration of immune checkpoint inhibitors with VEGF targeted agents in advanced gastric and gastroesophageal adenocarcinoma: a review on the rationale and results of early phase trials. *J Hematol Oncol*. 2021;14(1):1-11. doi:10.1186/s13045-021-01034-0

40. Finn RS, Qin S, Ikeda M, et al. Atezolizumab plus Bevacizumab in Unresectable Hepatocellular Carcinoma. *N Engl J Med*. 2020;382(20):1894-1905. doi:10.1056/nejmoa1915745

41. Rini BI, Plimack ER, Stus V, et al. Pembrolizumab plus Axitinib versus Sunitinib for Advanced Renal-Cell Carcinoma. *N Engl J Med*. 2019;380(12):1116-1127. doi:10.1056/nejmoa1816714

42. Fukuoka S, Hara H, Takahashi N, et al. Regorafenib plus Nivolumab in Patients with Advanced Gastric or Colorectal Cancer: An Open-Label, Dose-Escalation, and Dose-Expansion Phase Ib Trial (REGONIVO, EPOC1603). *J Clin Oncol*. 2020;38(18):2053-2061. doi:10.1200/JCO.19.03296

43. Kawazoe A, Fukuoka S, Nakamura Y, et al. Lenvatinib plus pembrolizumab in patients with advanced gastric cancer in the first-line or second-line setting (EPOC1706): an open-label, single-arm, phase 2 trial. *Lancet Oncol*. 2020;21(8):1057-1065. doi:10.1016/S1470-2045(20)30271-0

44. Xu J, Zhang Y, Jia R, et al. Anti-PD-1 Antibody SHR-1210 Combined with Apatinib for Advanced Hepatocellular Carcinoma, Gastric, or Esophagogastric Junction Cancer: An Open-label, Dose Escalation and Expansion Study. *Clin Cancer Res*. 2019;25(2):515-523. doi:10.1158/1078-0432.CCR-18-2484

45. Herbst RS, Arkenau HT, Santana-Davila R, et al. Ramucirumab plus pembrolizumab in patients with previously treated advanced non-small-cell lung cancer, gastro-oesophageal cancer, or urothelial carcinomas (JVDF): a multicohort, non-randomised, open-label, phase 1a/b trial. *Lancet Oncol*. 2019;20(8):1109-1123. doi:10.1016/S1470-2045(19)30458-9

46. Hara H, Shoji H, Takahari D, et al. Phase I/II study of ramucirumab plus nivolumab in patients in second-line treatment for advanced gastric adenocarcinoma (NivoRam study). *J Clin Oncol*. 2019;37(4_suppl):129-129. doi:10.1200/jco.2019.37.4_suppl.129

47. Bang YJ, Golan T, Dahan L, et al. Ramucirumab and durvalumab for previously treated, advanced non–small-cell lung cancer, gastric/gastro-oesophageal junction adenocarcinoma, or hepatocellular carcinoma: An open-label, phase Ia/b study (JVDJ). *Eur J Cancer*. 2020;137:272-284. doi:10.1016/j.ejca.2020.06.007

48. Yang H, Zhang Y, Liu C, et al. The integration of bevacizumab improves tumor response and survival in patients with refractory cervical cancer treated with radical chemoradiotherapy. *Ann Transl Med*. 2021;9(14):1184-1184. doi:10.21037/ATM-21-3521

49. Zhou Y, Guo Z, Wu Z, et al. The efficacy and safety of adding bevacizumab in neoadjuvant therapy for locally advanced rectal cancer patients: A systematic review and meta-analysis. *Transl Oncol*. 2021;14(1):100964. doi:10.1016/J.TRANON.2020.100964

50. Burnette BC, Liang H, Lee Y, et al. The efficacy of radiotherapy relies upon induction of type I interferon-dependent innate and adaptive immunity. *Cancer Res*. 2011;71(7):2488-2496. doi:10.1158/0008-5472.CAN-10-2820

51. Deng L, Liang H, Xu M, et al. STING-dependent cytosolic DNA sensing promotes radiation-induced type I interferon-dependent antitumor immunity in immunogenic tumors. *Immunity*. 2014;41(5):843-852. doi:10.1016/j.immuni.2014.10.019

52. Durante M, Formenti SC. Radiation-Induced Chromosomal Aberrations and Immunotherapy: Micronuclei, Cytosolic DNA, and Interferon-Production Pathway. *Front Oncol*. 2018;8(May). doi:10.3389/fonc.2018.00192

53. Woo SR, Fuertes MB, Corrales L, et al. STING-dependent cytosolic DNA sensing mediates innate immune recognition of immunogenic tumors. *Immunity*. 2014;41(5):830-842. doi:10.1016/j.immuni.2014.10.017

54. Feng X, Tubbs A, Zhang C, et al. ATR inhibition potentiates ionizing radiation-induced interferon response via cytosolic nucleic acid-sensing pathways. *EMBO J*. 2020;39(14). doi:10.15252/embj.2019104036

55. Ren Z, Ding T, Zuo Z, Xu Z, Deng J, Wei Z. Regulation of MAVS Expression and Signaling Function in the Antiviral Innate Immune Response. *Front Immunol*. 2020;11. doi:10.3389/fimmu.2020.01030

56. Bakhoum SF, Cantley LC. *The Multifaceted Role of Chromosomal Instability in Cancer and Its Microenvironment*. Vol 174. Cell Press; 2018:1347-1360. doi:10.1016/j.cell.2018.08.027

57. Creemers A, Ebbing EA, Pelgrim TC, et al. A systematic review and meta-analysis of prognostic biomarkers in resectable esophageal adenocarcinomas. *Sci Rep*. 2018;8(1):13281. doi:10.1038/s41598-018-31548-6

58. MacKenzie KJ, Carroll P, Martin CA, et al. CGAS surveillance of micronuclei links genome instability to innate immunity. *Nature*. 2017;548(7668):461-465. doi:10.1038/nature23449

59. Song S, Peng P, Tang Z, et al. Decreased expression of STING predicts poor prognosis in patients with gastric cancer. *Sci Rep*. 2017;7. doi:10.1038/srep39858

60. Xia T, Konno H, Ahn J, Barber GN. Deregulation of STING Signaling in Colorectal Carcinoma Constrains DNA Damage Responses and Correlates With Tumorigenesis. *Cell Rep*. 2016;14(2):282-297. doi:10.1016/j.celrep.2015.12.029

61. Kalbasi A, Tariveranmoshabad M, Hakimi K, et al. Uncoupling interferon signaling and antigen presentation to overcome immunotherapy resistance due to JAK1 loss in melanoma. *Sci Transl Med*. 2020;12(565):152. doi:10.1126/SCITRANSLMED.ABB0152

62. Kalbasi A, Ribas A. Tumour-intrinsic resistance to immune checkpoint blockade. *Nat Rev Immunol 2019 201*. 2019;20(1):25-39. doi:10.1038/s41577-019-0218-4

8

63. Gandhi SJ, Minn AJ, Vonderheide RH, Wherry EJ, Hahn SM, Maity A. Awakening the immune system with radiation: Optimal dose and fractionation. *Cancer Lett*. 2015;368(2):185-190. doi:10.1016/j.canlet.2015.03.024

64. Liang H, Deng L, Hou Y, et al. Host STING-dependent MDSC mobilization drives extrinsic radiation resistance. *Nat Commun*. 2017;8(1). doi:10.1038/s41467-017-01566-5

65. Duarte CW, Willey CD, Zhi D, et al. Expression signature of IFN/STAT1 signaling genes predicts poor survival outcome in glioblastoma multiforme in a subtype-specific manner. *PLoS One*. 2012;7(1). doi:10.1371/journal.pone.0029653

66. Weichselbaum RR, Ishwaran H, Yoon T, et al. An interferon-related gene signature for DNA damage resistance is a predictive marker for chemotherapy and radiation for breast cancer. *Proc Natl Acad Sci U S A*. 2008;105(47):18490-18495. doi:10.1073/pnas.0809242105

67. Pitroda SP, Wakim BT, Sood RF, et al. STAT1-dependent expression of energy metabolic pathways links tumour growth and radioresistance to the Warburg effect. *BMC Med*. 2009;7(Cc):1-10. doi:10.1186/1741-7015-7-68

68. Koster BD, de Jong TD, van den Hout MFCM, et al. In the mix: the potential benefits of adding GM-CSF to CpG-B in the local treatment of patients with early-stage melanoma. *Oncoimmunology*. 2020;9(1). doi:10.1080/2162402X.2019.1708066

69. Falvey CM, O'Donovan TR, El-Mashed S, Nyhan MJ, O'Reilly S, McKenna SL. UBE2L6/UBCH8 and ISG15 attenuate autophagy in esophageal cancer cells. *Oncotarget*. 2017;8(14):23479-23491. doi:10.18632/oncotarget.15182

70. Sandy Z, da Costa IC, Schmidt CK. More than meets the isg15: Emerging roles in the dna damage response and beyond. *Biomolecules*. 2020;10(11):1-30. doi:10.3390/biom10111557

71. Pinto-Fernandez A, Salio M, Partridge T, et al. Deletion of the deISGylating enzyme USP18 enhances tumour cell antigenicity and radiosensitivity. *Br J Cancer*. 2021;124(4):817-830. doi:10.1038/s41416-020-01167-y

72. Wentink MQ, Verheul HMW, Griffioen AW, et al. A safety and immunogenicity study of immunization with hVEGF 26-104 /RFASE in cynomolgus monkeys. *Vaccine*. 2018;36(15):2025-2032. doi:10.1016/j.vaccine.2018.02.066

73. PW K, CS H, ND S, et al. Sipuleucel-T immunotherapy for castration-resistant prostate cancer. *N Engl J Med*. 2010;363(5):411-422. doi:10.1056/NEJMOA1001294

74. Hollingsworth RE, Jansen K. Turning the corner on therapeutic cancer vaccines. *npj Vaccines 2019 41*. 2019;4(1):1-10. doi:10.1038/s41541-019-0103-y

75. Jou J, Harrington KJ, Zocca M-B, Ehrnrooth E, Cohen EEW. The Changing Landscape of Therapeutic Cancer Vaccines—Novel Platforms and Neoantigen Identification. *Clin Cancer Res*. 2021;27(3):689-703. doi:10.1158/1078-0432.CCR-20-0245

76. Casadevall A. The mRNA vaccine revolution is the dividend from decades of basic science research. *J Clin Invest*. 2021;131(19). doi:10.1172/JCI153721

77. Sahin U, Oehm P, Derhovanessian E, et al. An RNA vaccine drives immunity in checkpoint-inhibitor-treated melanoma. *Nature*. 2020;585(7823):107-112. doi:10.1038/s41586-020-2537-9

8

Addendum

Nederlandse samenvatting
Dankwoord
Curriculum vitae
List of publications
List of coauthors

NEDERLANDSE SAMENVATTING

Slokdarmkanker is een moeilijk behandelbare vorm van kanker. Deels komt dit doordat de ziekte vaak pas laat klachten geeft, waardoor hij vaak pas ontdekt wordt als hij al vergevorderd is. Een andere reden is dat de resultaten van behandelingen met medicijnen zoals chemotherapie tegenvallen. Alhoewel de afgelopen decennia de overleving wel flink verbeterd is, is de vijfjaarsoverleving beperkt. Van de mensen waarbij de ziekte zich beperkt tot de slokdarm, is de helft na 5 jaar nog in leven. Wanneer de ziekte zich heeft uitgebreid naar de lymfeklieren rondom de tumor, is dat een kwart. Wanneer er uitzaaiingen in andere organen zijn, is na 5 jaar nog maar 1 op 20 patiënten in leven. Er is dus dringend behoefte aan betere behandelmethoden om de prognose van patiënten te verbeteren.

Er zijn twee vormen van slokdarmkanker. *Plaveiselcelcarcinoom* ontstaat uit plaveiselcellen. Dit zijn dezelfde soort cellen als je huid, behalve dat ze geen hoornlaag hebben. *Adenocarcinoom* ontstaat uit kliercellen. Dit zijn cellen die het grootste deel van je maagdarmkanaal bekleden. In de Westerse wereld zien we de afgelopen decennia een sterke toename van het adenocarcinoom van de slokdarm (in Nederland zelfs een verdubbeling). Dit is vervelend omdat juist deze vorm minder goed op behandeling met bestraling reageert.

De behandeling van de slokdarmkanker is afhankelijk van het stadium. Indien er sprake is van uitzaaiingen naar andere organen, is genezing niet meer mogelijk en bestaat de behandeling hoofdzakelijk uit chemotherapie, waarbij het doel is het ziekteproces te vertragen. Wanneer de ziekte zich beperkt tot de slokdarm en omliggende lymfeklieren, dan richt de behandeling zich op genezing. Hiervoor krijgen mensen eerst vijf weken lang een voorbehandeling met *chemoradiatie*: een combinatie van bestraling (radiotherapie) op werkdagen met wekelijks twee verschillende vormen van chemotherapie in het infuus. Daarna wordt de resterende tumor met een grote operatie verwijderd.

Bij een deel van de patiënten zien we dat de chemoradiatie zo goed aanslaat dat er bij de operatie geen kankercellen meer worden teruggevonden. Dit is erg gunstig voor de prognose van de patiënt (er wordt zelfs onderzocht of zo'n grote operatie dan niet veilig achterwege gelaten kan worden). Helaas heeft de chemoradiatie bij een ander deel van de patiënten weinig tot geen effect. Deze mensen zou je het liefst een andere, of aanvullende behandeling aanbieden. Op dit moment kunnen we niet van te voren voorspellen welke patiënten wel, en welke patiënten geen baat van chemoradiatie hebben.

Het doel van dit proefschrift is om inzicht te krijgen in verschillende biologische factoren die invloed hebben het effect van chemoradiatie. In **deel I** onderzochten we of het genetisch profiel (de bouwtekening) van de tumor en de samenstelling van afweercellen

rondom de tumor van invloed zijn op de uitkomst van de behandeling. In **deel II** verdiepten we ons in de effecten die optreden tijdens radiotherapie, met als doel om nieuwe aangrijpingspunten te vinden die de behandeling effectiever kunnen maken.

Deel I

In het verleden zijn alle DNA-veranderingen in kankercellen van slokdarmkanker patiënten uitgebreid in kaart gebracht door "The Cancer Genome Atlas" (een samenwerking van onderzoekers). Het resultaat hiervan zou je kunnen zien als een blauwdruk van het DNA van slokdarmkanker. Ruim 250 van de meest voorkomende DNA-veranderingen hebben wij in **hoofdstuk 2** onderzocht in biopten van patiënten die in het Amsterdam UMC zijn behandeld met chemoradiatie. Hierbij probeerden wij te ontdekken of er DNA-veranderingen zijn die voorspellend zijn voor het aanslaan van de behandeling. Dit bleek niet het geval. Inmiddels weten we dat de tumor erg heterogeen is, wat wil zeggen dat de DNA-veranderingen binnen een tumor (en zelfs tussen de oorspronkelijke tumor en verschillende uitzaaiingen) sterk kunnen verschillen. Aangezien je met biopten maar een klein stukje van de tumor in kaart brengt, is het mogelijk dat we een onvolledig beeld hebben gekregen. In de toekomst zou het interessant zijn om deze studie te herhalen met *cell free DNA*. Dit zijn kleine stukjes DNA die rondzweven in het bloed en deels afkomstig zijn van de tumor. Door steeds betere technieken kunnen we op deze manier mogelijk een vollediger DNA-profiel van de tumor maken uit bloed dan uit biopten. Een bijkomend voordeel is dat dit patiëntvriendelijker is.

Omdat we inmiddels weten dat het menselijk afweersysteem kankercellen al vroeg herkent en probeert op te ruimen (net als met virussen en bacteriën), hebben we in **hoofdstuk 3** onderzocht of de afweercellen in en om de tumor voorspellend zijn voor het aanslaan van een behandeling met chemoradiatie. Het bleek dat patiënten met veel *T-cellen* (een bepaald type afweercel) in de tumor inderdaad vaker een complete respons op chemoradiatie hadden. Niet alleen het aantal, maar ook de locatie lijkt hierbij een rol te spelen. Het effect was namelijk het grootst wanneer de T-cellen in direct contact stonden met kankercellen. Dit konden we goed beoordelen door een techniek die *multicolor immunohistochemistry* heet. Hierbij worden verschillende kleuringen van kankercellen en afweercellen gecombineerd onder de microscoop bekeken. De omslag van dit proefschrift is hier een voorbeeld van (de kankercellen zijn groen en de T-cellen zijn paars en oranje).

Deel II

In **hoofdstuk 4** hebben we in de literatuur onderzocht wat er allemaal bekend is over de rol van afweercellen in de tumor bij het wel of niet aanslaan van radiotherapie. Daarnaast hebben we het ook gekeken naar de rol van bloedvaten. Afweercellen, bloedvaten en kankercellen vormen samen een micromilieu, ook wel de *tumor micro environment* genoemd. Het blijkt dat de samenstelling van dit micromilieu een

A

belangrijke rol speelt bij de effectiviteit van radiotherapie. Daarnaast kan onder invloed van radiotherapie de samenstelling van het micromilieu veranderen. Of deze effecten positief of negatief zijn, is afhankelijk van de dosis en duur van bestraling, en niet voor iedere vorm van kanker hetzelfde. Het is mogelijk om met *immunotherapie* (een behandeling met eiwitten die de lichaamseigen afweer tegen de tumor versterkt) de effecten van bestraling te versterken. Daarnaast is het mogelijk de groei van bloedvaten naar de tumor (*angiogenese*) te remmen met medicijnen. Ook deze behandeling blijkt de effecten van radiotherapie te kunnen versterken. Op basis van al deze gegevens denken wij dat radiotherapie, immunotherapie en angiogeneseremmers slimmer gecombineerd zouden kunnen worden in de behandeling van slokdarmkanker.

In **hoofdstuk 5** onderzochten we wat er precies gebeurd met de machinerie van de kankercel wanneer deze meerdere weken achter elkaar wordt bestraald, zoals bij chemoradiatie het geval is. Dit heet *gefractioneerde bestraling*: je knipt een hoge dosis op in kleine stukjes en verspreidt deze in de tijd. Je kan zo veilig (zonder te veel schade aan gezonde cellen) een hogere dosis straling aan kankercellen geven. We hebben het behandelschema van patiënten nagebootst in het lab en kwamen er achter dat kankercellen na gemiddeld twee weken een reactie vertonen die erg lijkt op een reactie die cellen vertonen wanneer ze geïnfecteerd raken met een virus. Een virus bevat kleine stukjes DNA (of RNA), waarop de cel reageert met de productie van eiwitten die de afweer op gang brengen, de zogenoemde *type I interferon respons*. Door bestraling ontstaan er foutjes in het DNA van de cel (waarbij je hoopt dat een kankercel steeds meer foutjes oploopt en onherstelbaar beschadigt, terwijl een gezonde cel de foutjes in het DNA repareert). Door deze DNA-schade komen er kleine fragmentjes DNA vrij in de cel; dit is voor de cel niet te onderscheiden van een virus. Aan de ene kant worden door radiotherapie dus afweercellen (via de interferon respons) gestimuleerd om kankercellen op te ruimen. Dit is uiteraard een gunstig effect. Aan de andere kant zagen we ook een nadelig effect. Bij langdurige blootstelling aan interferon werden de kankercellen (in ieder geval tijdelijk) minder gevoelig voor bestraling. We weten nog niet goed hoe dit werkt. Een andere opvallende bevinding is dat de type I interferon respons ook optreedt in afwezigheid van een eiwit (STING). Men dacht dat dit eiwit essentieel was voor deze reactie. Waarschijnlijk zijn er dus 1 of meerdere eiwitten betrokken die de rol van STING kunnen overnemen.

In het verleden is type I interferon als medicijn regelmatig gecombineerd met radiotherapie, met als doel de effecten van radiotherapie te versterken door meer afweercellen tegen de tumor te activeren. In **hoofdstuk 6** hebben we de literatuur naar deze combinatiebehandelingen bestudeerd. Hiervan zijn geen grote successen te melden, omdat er vaak ernstige bijwerkingen optraden na toediening van interferon. Met de kennis van nu zou er slimmer gecombineerd kunnen worden (waardoor je mogelijk minder bijwerkingen krijgt). Daarnaast zijn er tegenwoordig ook medicijnen

die STING stimuleren of juist remmen. Deze medicijnen moeten nog verder onderzocht worden in combinatie met radiotherapie.

Tot slot beschrijven we in **hoofdstuk 7** de resultaten van een fase I studie. Dit is een vroege fase van onderzoek in de kliniek, met als doel het vaststellen van de veiligheid en verdraagzaamheid van een medicijn. We onderzochten een nieuw vaccin tegen *VEGF*, een eiwit dat angiogenese stimuleert. Het remmen van VEGF is al een bestaande antikankerbehandeling, waarbij de tumor minder voedingstoffen krijgt doordat er minder bloedvaten worden gevormd. Echter, deze behandeling vereist regelmatige toediening van eiwitten via een infuus en is relatief duur. De productie van een vaccin is over het algemeen goedkoper en patiënten hoeven minder vaak (en lang) naar het ziekenhuis te komen. Ook werken antistoffen die door het lichaam zelf gevormd worden over het algemeen beter dan een fabricaat. Eerder hebben we al aangetoond dat muizen en apen na vaccinatie antistoffen tegen VEGF maakten. Helaas bleek dit bij kankerpatiënten niet te lukken. Hiervoor zijn verschillende verklaringen mogelijk, waarbij het gebruik van een relatief zwakke hulpstof (RFASE) de meest waarschijnlijke is. Aan een vaccin wordt over het algemeen een hulpstof toegevoegd die afweercellen stimuleert om antistoffen te maken. Bij gezonde mensen hoeft dit niet zo'n sterke hulpstof te zijn, maar bij kankerpatiënten is er een flinke stimulus nodig omdat ze over het algemeen een verzwakt afweersysteem hebben. Helaas bleek het moeizaam om de samenstelling van het vaccin te veranderen en is het onderzoek om deze reden gestaakt.

Concluderend blijkt slokdarmkanker een heterogene ziekte, waarbij de samenstelling van het micromilieu belangrijk lijkt voor het slagen van een behandeling met chemoradiatie. Om deze behandeling nog effectiever te maken, zou er slimmer gecombineerd kunnen worden met andere behandelingen, zoals vormen van immunotherapie en angiogeneseremmers. Door de samenstelling van het micromilieu van te voren zorgvuldig in kaart te brengen, valt mogelijk vooraf beter in te schatten of een behandeling met chemoradiatie zinvol is. Daarnaast zou je patiënten met een "ongunstig" micromilieu wellicht vooraf met medicijnen kunnen behandelen om een "gunstig" micromilieu te creëren. Hier moet meer onderzoek naar plaatsvinden.

A

DANKWOORD

"Een boekje is om te schrijven, niet om te lezen", grap ik altijd. Je bent nu echter beland bij het meest gelezen hoofdstuk. Dit is een moment om terug te blikken op een periode die niet mogelijk zou zijn geweest zonder de inbreng van vele personen aan wie ik dank verschuldigd ben.

Allereerst wil ik alle **patiënten** en hun naasten hartelijk danken voor hun bijdrage aan dit onderzoek. Zonder hun belangeloze deelname, bijvoorbeeld door het afstaan van extra bloed of biopten, of door deelname aan de vaccinatiestudie, hadden wij al deze inzichten niet kunnen verkrijgen.

Beste **Henk**, begin 2017 kwamen wij in contact via Haiko Bloemendaal, destijds internist-oncoloog in het Meander. Ik had de ambitie om oncoloog te worden en wilde mij verdiepen in de tumorbiologie en -immunologie middels promotieonderzoek. Hoewel ik dacht dat klinisch onderzoek voor mij was weggelegd, haalde jij mij over om het lab in te gaan. Met een fase I studie met translationele arm had je het ideale project voor mij, en na een gesprek met Tanja en Arjan hoefde ik er niet lang meer over na te denken. Ik verruilde het Utrechtse voor het Amsterdamse en begon in mei 2017 aan een van de onderzoeksprojecten die uiteindelijk heeft geleid tot het proefschrift dat ik op 1 november 2022 verdedig. Gaandeweg bracht je me in contact met Victor en Sarah, waardoor de rest van mijn boekje vorm kreeg. Ik denk dat dat jouw grote kracht is, je weet mensen samen te brengen en uit te dagen het beste uit zichzelf te halen. Terugkijkend op dit proefschrift kan ik bevestigen dat dit gelukt is.

Beste **Tanja**, al snel werd ik door jou opgenomen binnen de immunotherapie groep in het CCA. Met jouw huiselijke kamer inclusief dito vloerkleedje, (zwartgallige) humor en klassieke muziek die regelmatig door de gangen schalde, deed jij het CCA zo nu en dan even als een tweede thuis voelen. Je bent altijd erg betrokken bij alle projecten en ik kon altijd even binnenlopen voor overleg; dat heb ik erg gewaardeerd. Ondanks al onze inspanningen lukte het helaas niet een doorstart te maken met CpG in de vaccinatiestudie; eeuwig zonde, want ik ben erg benieuwd of hier inderdaad de sleutel tot succes lag. Dank voor alle scherpe discussies, immunologische verdieping en prettige begeleiding.

Beste **Victor** en **Sarah**, jullie waren een gouden combinatie qua begeleiding! Jullie enthousiasme, gedrevenheid en gezelligheid hebben in belangrijke mate bijgedragen aan het succes van mijn proefschrift. Nog waardevoller was het begrip en de ruimte die ik van jullie kreeg op de momenten dat mijn gezin mijn aandacht 100% nodig had; heel veel dank hiervoor. **Sarah**, jij hebt een grenzeloze ambitie en durft groot te denken. Het was bijzonder om jouw ontwikkeling van junior PI naar groepsleider binnen Oncode van dichtbij mee te maken. Dank voor alle zinvolle en kritische discussies waarin je mij

altijd weer wist te stimuleren om mezelf verder te ontwikkelen. "Every lab should have a **Victor"**; een integere, zorgzame en kritische onderzoeker waar je als promovendus op kan terugvallen wanneer je uitleg of advies nodig hebt. Ik kon altijd bij je binnenlopen om te brainstormen over een experiment of data, en als ik eindelijk (na lang ploeteren) een versie van een manuscript naar je gestuurd had (en dacht even iets anders te kunnen doen) had jij het binnen een dag alweer geredigeerd. Qua schrijfstijl en figuren ben je een stylist pur sang; het was een genoegen om van je te mogen leren.

Geachte leden van de leescommissie, dear **prof. dr. N.C.T. van Grieken, prof. dr. A.W. Griffioen, prof. dr. J.M. de Vries, prof. dr. A.L. Harris, dr. B. Mostert** and **dr. R.E. Pouw**, thank you for your time and effort to critically review my thesis. Beste **Nicole,** daarnaast veel dank voor jouw inbreng als patholoog waarbij wij samen regelmatig coupes van patiëntmateriaal hebben beoordeeld. Beste **Arjan**, mijn speciale dank gaat uit naar je grote betrokkenheid bij de vaccinatie studie. Dear **Adrian**, I really enjoyed your input and our lively discussions regarding radiotherapy effects and type I interferons, both face-to-face during the AACR, as well as via zoom.

Tijdens mijn promotietijd heb ik mogen samenwerking met vele gezellige collega's in verschillende groepen. Het is onmogelijk om iedereen bij naam te noemen, maar laat ik beginnen met **mijn paranimfen, Tessa** en **Bram**, dank dat jullie mij op 1 november willen bijstaan! **Tessa**, ik leerde je als piepjonge bachelor student kennen, waarbij je al opviel als een collegiale harde werker. Het was natuurlijk top dat je ons team als mede PhD-student kwam versterken en ook buiten het werk om zorgde jij voor veel gezelligheid, zoals tijdens de spelletjesavond bij jou thuis of ons congres in Praag. **Bram**, wat een genot om samen met jou over de zin en onzin van onderzoek, het CCA en over het leven in het algemeen te discussiëren. Samen met **Dennis** en **Lenka** maakten we een onvergetelijke roadtrip naar New Orleans. Je bent een mooie vent, alleen een beetje jammer van dat advies van die cryptomunten…

Dear **colleagues from the Thijssen/Derks group**, I have enjoyed seeing this group grow in size, diversity and scientific output. Many thanks for all input, help and a great time! Beste **Kitty**, zonder jou zou ik letterlijk zijn verzopen op het lab! Jouw hulp is van onschatbare waarde geweest voor de data van dit proefschrift en daarnaast was het ook super gezellig met jou als kamergenoot! Beste **Jaap**, ik ben de tel kwijtgeraakt hoeveel clonogenic assays jij de afgelopen jaren hebt uitgevoerd. Gelukkig wist je de kelder van het VUmc vaak genoeg te ontvluchten voor vakanties naar het warme zuiden; hopelijk geniet je daar nu volop van. Beste **Merve**, dank voor je hulp bij de vele kleuringen en uren achter de Vectra en Inform, het heeft een mooi hoofdstuk opgeleverd. Beste **Kris**, op afstand hebben we regelmatig samengewerkt tijdens jouw PhD in Boston. In de tijd ben ik je kritische blik en harde werken enorm gaan waarderen. Dear **Micaela**, we've only worked together in the last year of my PhD, but I really enjoyed our collaboration

A

and your FACS expertise. Dear **Tesfay**, you are so dedicated and have learned so much in the time we worked together. I am sure there is a bright future ahead of you.

Beste **collega's van de Verheul groep,** beste **Cyrillo, Dennis, Elisa, Elske, Erik, Iris, Jessica, Lemonitsa, Lotte, Madelon, Maria, Robin** en **Sophie**, dank voor het mij laten thuis voelen op de afdeling medische oncologie in het VUmc. Helaas viel onze groep uiteen met het vertrek van Henk, maar ik denk met veel plezier terug aan de discussies en croissantjes op vrijdagochtend. Speciale dank aan **Henk Dekker** en **Richard de Goeij**, voor hun hulp bij het uitvoeren van allerlei experimenten, opvangen van biopten en andere hand en spandiensten waarvoor ik altijd bij jullie terecht kon.

Dear **colleagues from the de Gruijl group**, thank you all for your kindness and help in and around the immunotherapy lab. You're a very social group and it has always been a pleasure hopping by at CCA 2.48 for a chat or advise. Beste **Antia, Sienead**, **Joyce, Jana** en **Vinitha,** heel veel dank voor jullie hulp bij alle (FACS) experimenten en strakke organisatie op het lab. Speciale dank aan **Katja** en **Noëlle** voor jullie multicolor immunohistochemistry expertise, en aan **Lisa** voor onze samenwerking tijdens weefseldissociatie van slokdarm patiënten.

Ook studenten vanuit verschillende opleidingen hebben een rol gespeeld bij de totstandkoming van dit proefschrift. Ik heb genoten van de begeleiding van **Luuk, Maeve, Mustafa, Lisa** en **Brigitte,** en wens hen alle geluk in hun toekomstige carrière.

Niet te onderschatten was ook de inzet van verschillende artsen en verpleegkundigen van de afdelingen maag-, darm- en leverziekten, heelkunde en oncologie van het Amsterdam UMC en Noordwest Ziekenhuisgroep Alkmaar. In het bijzonder wil ik **Lia van Huffel, Linda Penninx, Nel de Vries, Roy van Wanrooij, Maarten Jacobs, Roos Pouw, Donald van der Peet, Marc van Berge Henegouwen** en **Anne-Marie van Berkel** bedanken voor hun hulp bij de inclusie van patiënten en de afname van biopten en/ of resectiemateriaal. Daarnaast wil ik **Sophie** en **Mikkjal** bedanken voor hun rol als researchverpleegkundigen bij de vaccinatiestudie, evenals **alle datamanagers** van het trialbureau oncologie.

Graag wil ik ook **Wim Mol** en **Peter Timmerman** van Immunovo hartelijk danken voor de prettige samenwerking tijdens de vaccinatiestudie.

Ik voel me bevoorrecht dat ik momenteel mag werken binnen een enthousiast en gedreven team van **stafartsen en fellows van de afdeling medische oncologie** van het Amsterdam UMC. Veel dank voor de leerzame en gezellige opleidingstijd met jullie.

Lieve **vrienden**, jullie hebben de afgelopen jaren regelmatig de highs en lows meegekregen van mijn promotietraject. Het is fijn dat ik altijd bij jullie terecht kan!

Beste **Arja, Joppe, Francine, Nienke** en **Floor**, wat heerlijk dat ik al 15 jaar van jullie vriendschap mag genieten. Best bijzonder om te beseffen dat wij na het afronden van onze studie nu allemaal een proefschrift hebben mogen verdedigen. Hoewel ik jullie ooit voorging, sluit ik nu de rij. Ik kijk uit naar meer etentjes en weekendjes weg met alle aanhang en de steeds grotere schare kids! Beste **Jasper, Jochem, Ferry** en **Tom,** bij dat roeien hoorde een ploeghap, en die schiet er door alle verhuizingen en COVID steevast bij in. Laten we die traditie snel weer in ere herstellen. Beste **Lennart, Tim, Bas, Christian** en **Ivo**, zèèègh, weer een bakkie doen binnenkort?

Lieve **familie Ter Haar**, dank dat ik me alweer zestien jaar thuis mag voelen in jullie midden en lief en leed met jullie kan delen. Lieve **familie Goedegebuure**, ondanks dat we elkaar minder vaak zien en spreken dan ik zou willen, wil ik jullie bedanken voor de warme band en liefdevolle ondersteuning in deze periode. Beste **Ard**, hoewel je nooit zeker weet wat de rol is van nature en nurture, heb jij ongetwijfeld jouw wetenschappelijke genen aan mij overgedragen, en zie hier het resultaat. Lieve **Jan**, dank voor je niet aflatende steun als vriend en mantelzorger van mijn moeder. Lieve **Jan-David** en **Marijn,** hopelijk kunnen we nu dit proefschrift af is weer tijd vinden om eens vaker af te spreken. Lieve **Barbara**, praten en lezen zijn door de afasie moeilijk geworden, maar jouw liefdevolle opvoeding vormt de basis voor wie ik vandaag ben. Dank je wel hiervoor.

Lieve **Nienke**, het afronden van een proefschrift combineren met een jong gezin en twee drukke banen is topsport. Gelukkig heb ik met jou een topatlete aan mijn zijde en is ons team meer dan de som van twee individuen! Zonder jouw eindeloze geduld, flexibiliteit en luisterend oor was dit proefschrift er niet geweest. Dank je wel voor de ontelbare momenten waarop je me de ruimte hebt geboden, zoals ook nu, wanneer ik tijdens mijn vakantie toch de laptop weer even pak om dit dankwoord te schrijven. Lieve **Amber**, **Thomas** en **Matthijs**, jullie houden mij met beide benen op de grond en laten elke dag weer zien wat werkelijk belangrijk is in het leven. Ik hou van jullie!

A

CURRICULUM VITAE

Ruben Goedegebuure was born on the 5th of February 1986 in Leiden, The Netherlands. He grew up in Losser and Enschede and finished secondary school (Gymnasium) at the Stedelijk Lyceum Zuid in Enschede. Subsequently, he moved to Utrecht in September 2004 to study Medicine at Utrecht University. During his studies, in 2007-2008, he was fulltime chair of the medical student association MSFU "Sams".

After he finished Medicine in January 2012, he started working as an intern (ANIOS) at the Intensive Care Unit of the Meander Medical Center in Amersfoort. Subsequently, he worked at the department of Gastroenterology and Internal Medicine. From January 2014 he started his residency (AIOS) Internal Medicine at the Meander Medical Center in Amersfoort under supervision of dr. Rob Fijnheer, which he continued at the University Medical Center Utrecht under supervision of prof. dr. Karin Kaasjager.

From May 2017 he got involved in several (pre-)clinical research projects in the Cancer Center Amsterdam, supervised by prof. dr. Henk Verheul, prof. dr. Tanja de Gruijl, dr. ir. Victor Thijssen and dr. Sarah Derks, which resulted in this thesis. From November 2020 he continued his residency Internal Medicine at the Amsterdam University Medical Centers, with a fellowship Medical Oncology under supervision of dr. Inge Konings. He will finish in April 2023 and continues to combine patientcare with research focused on (gastro)intestinal malignancies as Medical Oncologist in the Antoni van Leeuwenhoek Hospital / Netherlands Cancer Institute.

Ruben is married to Nienke. They live together in Utrecht and have three children, Amber (5 years old), Thomas and Matthijs (both 3 years old).

LIST OF PUBLICATIONS

1. **Goedegebuure RSA**, Harrasser M, de Klerk LK et al. Pre-treatment tumor-infiltrating T cells influence response to neoadjuvant chemoradiotherapy in esophageal adenocarcinoma. Oncoimmunology 2021;10:1954807.

2. **Goedegebuure RSA**, Kleibeuker EA, Buffa FM et al. Interferon- and STING-independent induction of type I interferon stimulated genes during fractionated irradiation. J Exp Clin Cancer Res 2021;40:161.

3. de Klerk LK, **Goedegebuure RSA**, van Grieken NCT et al. Molecular profiles of response to neoadjuvant chemoradiotherapy in oesophageal cancers to develop personalized treatment strategies. Mol Oncol 2021;15:901–914.

4. **Goedegebuure RSA**, Wentink MQ, van der Vliet HJ et al. A Phase I Open-Label Clinical Trial Evaluating the Therapeutic Vaccine hVEGF26–104/RFASE in Patients with Advanced Solid Malignancies. Oncologist 2021;26:e218–e229.

5. **Goedegebuure RSA**, Vonk C, Kooij LP et al. Combining Radiation Therapy With Interferons: Back to the Future. Int J Radiat Oncol Biol Phys 2020;108:56–69.

6. van den Berg J, Castricum KCM, Meel MH, **Goedegebuure RSA** et al. Development of transient radioresistance during fractionated irradiation in vitro. Radiother Oncol 2020;148:107–114.

7. Voeten DM, den Bakker CM, **Goedegebuure RSA** et al. Non-metastatic oesophageal cancer: diagnosis and treatment. Ned Tijdschr Geneeskd 2019;163.

8. **Goedegebuure RSA**, De Klerk LK, Bass AJ et al. Combining radiotherapy with anti-angiogenic therapy and immunotherapy; A therapeutic triad for cancer? Front Immunol 2019;10:3107.

9. Huijts CM, Werter IM, Lougheed SM, **Goedegebuure RSA** et al. Phase 1 study of everolimus and low-dose oral cyclophosphamide in patients with metastatic renal cell carcinoma. Cancer Immunol Immunother 2019;68:319–329.

10. Janse JA, **Goedegebuure RSA**, Veersema S et al. Hysteroscopic sterilization using a virtual reality simulator: Assessment of learning curve. J Minim Invasive Gynecol 2013;20:775–782.

A

LIST OF COAUTHORS   AMSTERDAM UMC

Jaap van den Berg	Department of Radiation Oncology
Mark I. van Berge Henegouwen	Department of Surgery
Kitty C.M. Castricum	Department of Radiation Oncology
Sarah Derks	Department of Medical Oncology
Merve Eken	Department of Hematology
Micaela Harrasser	Department of Medical Oncology
Nicole C.T. van Grieken	Department of pathology
Arjan W. Griffioen	Department of Medical oncology
Maeve S. Grifhorst	Department of Medical Oncology
Tanja D. de Gruijl	Department of Medical Oncology
Maarten A.J.M. Jacobs	Department of Gastroenterology
Ekaterina S. Jordanova	Department of Obstetrics and Gynecology
Leonie K. de Klerk	Department of Medical Oncology
Laura P. Kooij	Department of Radiation Oncology
Luuk ten Kroode	Department of Radiation Oncology
Hanneke W.M. van Laarhoven	Department of Medical Oncology
Donald L. van der Peet	Department of Surgery
Noëlle Pocorni	Department of Medical Oncology
Roos E. Pouw	Department of Gastroenterology
Arantza F. Sarasqueta	Department of Pathology

Tessa S. van Schooten   Department of Medical Oncology

Iris A. Schulkens   Department of Medical oncology

Ben J. Slotman   Department of Radiation Oncology

Victor L.J.L Thijssen   Department of Radiation Oncology

Johannes J. van der Vliet   Department of Medical Oncology

Christian Vonk   Department of Radiation Oncology

Roy L. J. van Wanrooij   Department of Gastroenterology

Madelon Q. Wentink   Department of Medical oncology

A

243

LIST OF COAUTHORS   OTHER CENTERS

Adam J. Bass

Dana-Farber Cancer Institute, Department of Medical Oncology, Boston, MA USA

Cancer Program, The Broad Institute of MIT and Harvard, Cambridge, MA, USA.

Anne-Marie van Berkel

Noord West Ziekenhuisgroep, Department of Gastroenterology, Alkmaar, The Netherlands.

Francesca M. Buffa

University of Oxford, Department of Molecular Oncology, Oxford, UK.

Annemieke Cats

Netherlands Cancer Institute/Antoni van Leeuwenhoek Hospital, Department of Gastroenterology, Amsterdam, The Netherlands.

Manon van Engeland

Department of Pathology, GROW-School for Oncology and Developmental Biology, Maastricht University Medical Center, Maastricht, The Netherlands.

Syed Haider

University of Oxford, Department of Molecular Oncology, Oxford, UK.

Adrian L. Harris

University of Oxford, Department of Molecular Oncology, Oxford, UK.

Rosa T. van der Kaaij

Department of Gastrointestinal Oncology, Netherlands Cancer Institute/Antoni van Leeuwenhoek Hospital, Amsterdam, The Netherlands.

Esther A. Kleibeuker

UMC Groningen, Department of Medical oncology, Groningen, The Netherlands

Johanna W. van Sandick

Netherlands Cancer Institute/Antoni van Leeuwenhoek Hospital, Department of Surgery, Amsterdam, The Netherlands.

Jurrien Stiekema

Franciscus Gasthuis en Vlietland, Department of Surgery, Rotterdam, The Netherlands.

Aaron R. Thorner   Center for Cancer Genome Discovery, Dana-Farber
                          Cancer Institute, Boston, MA, USA.

Peter Timmerman   Pepscan, Lelystad, The Netherlands

Henk M.W. Verheul   Radboud UMC, Department of Medical Oncology,
                          Nijmegen, The Netherlands

A